

EPA-600/7-81-165
October 1981

FINAL REPORT
FOR
THE CPU-400 PILOT PLANT
INTEGRATION AND OPERATION

by

Combustion Power Company, Inc.
A Weyerhaeuser Company
1346 Willow Road
Menlo Park, Ca 94025

Contract No. 68-03-0143
Program Element No. EHE-624B

Project Officer

Richard A. Chapman

Fuels Technology Branch
Energy Systems Environmental Control Division
Industrial Environmental Research Laboratory
Cincinnati, Ohio 45268

INDUSTRIAL ENVIRONMENTAL RESEARCH LABORATORY
OFFICE OF RESEARCH AND DEVELOPMENT
U.S. ENVIRONMENTAL PROTECTION AGENCY
CINCINNATI, OHIO 45268

REPRODUCED BY
NATIONAL TECHNICAL
INFORMATION SERVICE
U.S. DEPARTMENT OF COMMERCE
SPRINGFIELD, VA 22161

DISCLAIMER

This report has been reviewed by the Industrial Environmental Research Laboratory - Cincinnati, U.S. Environmental Protection Agency, and approved for publication. Approval does not signify that the contents necessarily reflect the views and policies of the U.S. Environmental Protection Agency, nor does mention of trade names or commercial products constitute endorsement or recommendation for use.

FOREWORD

When energy and material resources are extracted, processed, converted, and used, the related pollutional impacts on our environment and even on our health often require that new and increasingly more efficient pollution control methods be used. The Industrial Environmental Research Laboratory-Cincinnati (IERL-Ci) assists in developing and demonstrating new and improved methodologies that will meet these needs both efficiently and economically.

This report discusses the results of Agency's "CPU-400" research program, a program to develop a fluidized bed system for converting solid wastes directly into electric power. The report also discusses using the CPU-400 system to convert wood wastes and coal into power. The information contained herein will be of interest to those involved in the development of moving-media particulate filtration systems, as well as those developing fluidized bed combustion processes for energy recovery. Inquiries and comments regarding the report should be directed to the Fuels Technology Branch of the Energy Systems Environmental Control Division.

David G. Stephan
Director
Industrial Environmental Research Laboratory
Cincinnati

ABSTRACT

A program of research and development was carried out in an effort to demonstrate the feasibility of burning municipal solid waste to generate electrical power in a direct-fired gas turbine. Included in the contract work were the design, construction, and checkout of a solid-waste processing station, integration and checkout of the system with the gas turbine installed; design and construction of a moving-bed granular filter; and a program of corrosion, erosion, and deposition studies. Under other sponsorship, the direct-fired gas-turbine system was tested in 101 hours of wood-waste combustion and 551 hours of burning high-sulfur coal.

Problems with erosion and deposition in the turbine--and resultant loss of surge margin--limited the system's capability for continuous operation. Small inertial separators were found to be susceptible to plugging, and cyclone separators alone were found inadequate for reducing exhaust loading to a point that would permit long-term turbine operation. Based on subscale tests, a moving-bed granular filter showed good promise for removing the fine particulate inherent in the fluid-bed combustion process; a design was developed for the inlet screen of such a filter that effectively prevented buildup of deposition on the screen. Checkout of a full-scale granular filter was not completed, owing to a structural failure of the inlet screen.

In subscale testing, chemical additives were shown to have the capability of combining with aluminum--a serious contributor to deposition in municipal solid wastes--in solid compounds that can be removed in the filtration process. The additives also convert to stable solids the alkali-metal salts that could pass through a granular filter in the vapor phase and condense to undesirable particulate downstream of the filter.

Corrosion of turbine materials was found to impose no serious problems in operating with municipal solid waste.

The fluid-bed combustor was shown to be a highly efficient device for burning low-Btu fuel such as solid waste; combustion efficiency in excess of 99% was readily achieved. Gaseous emissions from solid-waste fuel were well within current environmental standards.

CONTENTS

Section	<u>Page</u>
FOREWORD	iii
ABSTRACT	iv
FIGURES	vii
TABLES	xiii
1 INTRODUCTION	1
2 SYSTEM DESCRIPTION	3
A. Storage and Feed System	5
B. Combustor	9
C. Gas-Cleanup System	12
D. Residue-Removal System	15
E. Turboelectric System	16
F. Control System	18
3 SOLID-WASTE PROCESSING STATION (TASK LP-13)	28
A. Design	29
B. Process Equipment	31
C. Checkout	34
D. Summation	34
4 TURBINE INTEGRATION & CHECKOUT (TASK HP-3)	37
A. Task Objectives	37
B. Turboelectric System Checkout (Phase A)	37
C. Fluid-Bed Combustor on Oil (Phase B)	40
D. Solid-Waste Testing (Phase C)	44
5 WEYERHAEUSER WOOD-WASTE TESTING	55
A. Synopsis of Test Events	55
B. Summary of Results	58
6 THE COAL PROGRAM	65
A. System Configuration	65
B. System Testing	69
C. Hot-Corrosion Program	76

CONTENTS (Continued)

<u>Section</u>	<u>Page</u>
6 (Cont'd)	
D. Pilot Plant Hot-Corrosion Tests	77
E. Operational Summary	82
7	
THE GRANULAR FILTER (TASKS GF-1 & GF-2)	86
A. Background	86
B. Model Tests	88
C. Front-Face Cleaning	105
D. Design of the Pilot Plant GBF	114
E. Installation and Checkout	128
F. Failure Analysis	135
G. Structural Redesign	137
H. Other Modifications	140
8	
CORROSION, EROSION, & DEPOSITION STUDIES (TASK CP-6)	143
A. Purpose	143
B. Chemical Considerations	143
C. Additive Screening	147
D. The Model Combustor	148
E. Model-Combustor Tests	149
9	
SYSTEMS STUDIES (TASK SS-10)	159
A. Background	159
B. Basis of Studies	159
C. Steady-State Operating Solutions	161
D. System Operations	166
10	
CONCLUSIONS	172
REFERENCES	174
CONVERSION TABLE	175

FIGURES

<u>Number</u>		<u>Page</u>
1	CPU-400 Pilot Plant	3
2	Plan View of Pilot Plant	4
3	Flow Diagram	4
4	Storage and Feed Components	6
5	Interior Views of the Atlas Storage Unit	7
6	Thirty-Inch Airlock Feeder Valve.	9
7	Pilot Plant Combustor	10
8	Air Diffusers and Feed Pipes	11
9	Combustor Air Diffuser	11
10	Combustor Exhaust and Backheat Burner Ports	11
11	Vessels of the Gas-Cleanup System	12
12	Second- and Third-Stage Inertial Tubes	13
13	Second-Stage Multicyclone Separator-Tube Assy.	14
14	First-Stage Separator	15
15	Residue-Collection Baghouse and Cyclone	16
16	Ruston TA-1500 Turbine	17
17	Control Room	19
18	Computer-System Block Diagram	20
19	Data-Acquisition System	23
20	Layout of Solid-Waste Processing Station.	29
21	Solid-Waste Processing Station	30
22	Solid-Waste Facility	31

FIGURES (Continued)

<u>Number</u>		<u>Page</u>
23	Loading of Shredder Feed Conveyors by Front Loader	32
24	Shredders	32
25	Air Classifier, Transport Line, and Simulated Material-Recovery System	34
26	Maximum Noise Levels in dB(A) during Shredding and Transport	35
27	Speed-Control System	39
28	Backheat-Mode Temperature	41
29	Compressor Surging during Startup Trials	41
30	First Turbine Operation on the Oil-Fired Fluid-Bed Combustor, 19 March 1973	43
31	Operational Parameters in Test 6 on MSW	48
32	Test 10 on MSW with Water Added	49
33	Test 12 on MSW with Water Injection	49
34	Deposition in Compressor-Turbine Stator	51
35	Deposits on Compressor-Turbine Rotor	51
36	Root Erosion of Second-Stage Stator Blades	52
37	Deposits in Entrance of Vane Tube of 6-Inch Inertial Separator	52
38	CPU-400 Pilot Plant with Injection System	59
40	Direct and Mirror Image, Worst Blade of Second-Stage Compressor-Turbine Stator after Hog-Fuel Test	64

FIGURES (Continued)

<u>Number</u>		<u>Page</u>
41	Coal-Processing System	66
42	Directional-Change Designs for Pneumatic Transport Line	67
43	Coal Dust Vent System	68
44	Flow Diagram for Coal Combustion	69
45	First-Stage Cyclone Separators	70
46	Second-Stage Cyclone	70
47	Ash-Removal Configuration	71
48	Trailing-Edge Erosion of Second-Stage Compressor- Turbine Stator (Inlet is at 258°)	74
49	Test P-203B	75
50	Test P-203C	76
51	System Temperatures, Test P-403	80
52	Turbine Parameters, Test P-403	81
53	Fluid-Bed Ash-Removal System	82
54	Computer Image of the Coal-Burning Pilot Plant .	85
55	Collection of Fine Particulate by Granular Media	86
56	The Dry Scrubber	87
57	Fixed-Bed Test Setup for High Temperature Pressure	88
58	Model Combustor and GBF Flow Diagram	89
59	First Hot-Flow Model GBF	89
60	Louver Types for Model GBF	90

FIGURES (Continued)

<u>Number</u>		<u>Page</u>
61	Hot-Flow Test Setup	91
62	Arrangement of Outlet Louver for Hot-Flow Test H-3	92
63	Cold-Flow Test Segment	94
64	Cold-Flow Test Setup	95
65	GBF Pressure Drop with 7-8 Mesh San Simeon Sand .	97
66	Pneumatic Circulation and Cleanup System	98
67	GBF Pressure Drop with 5-7 Mesh Al_2O_3 as Media	100
68	Pressure Drop and Loadings with Pulsed and Continuous Media Circulation, Test H-13	103
69	Inlet Louver Panel after Test H-16	104
70	Model Setup for Front-Face Cleaning Tests	106
71	Lift-Pipe Calibration	107
72	Rate Effects on Front-Face Spillage	107
73	Front-Face Spillage with Dust Injection and Air at 100 ft/min	108
74	Duos Louver	109
75	Panel Configuration	110
76	Comparative Results for Slotted and Louvered Panels	110
77	Media Retention and Flow	112
78	Slotted Louver Panel after 513 Hours of Hot Operations with Wood Combustion	114

FIGURES (Continued)

<u>Number</u>		<u>Page</u>
79	Particle Loading for Solid-Waste Operation . . .	115
80	Particle Loading for Coal Operation	115
81	Nominal Flows in GBF on Solid Waste	117
82	Moving-Bed Granular Filter	119
83	GBF Control System	127
84	High-Pressure Sampling Probe	128
85	Granular-Filter Pressure Vessel During Installation	129
86	Inner and Outer Louver Panels in Place in GBF Vessel	129
87	GBF Upper Distribution Cone	130
88	Completed GBF Installation with Media- Circulation System	130
89	Granular-Filter Heatup on Fuel Oil	131
90	GBF and Fluid-Bed Pressure Drops	132
91	Fill Pattern in GBF Inlet Cone	134
92	Pressure Loads on Inner Louver Panel	135
93	Redesign of Louver-Panel Support Structures . .	138
94	Media Inventory Reservoir	140
95	Mode-6 Vent	141
96	Model Combustor System	149
97	Model Combustor Flow Schematic	150
98	Model No. 3 Combustor	150

FIGURES (Continued)

<u>Number</u>		<u>Page</u>
99	Deposition in Second-Stage Separator for Test Series CP6M	153
100	Simple-Cycle Gas Turbine	161
101	Cycle Schematic	162
102	Cycle-Analysis Output	163
103	Effect of Ambient Temperature on Commercial Units	167
104	Effect of Ambient Temperature in Component System	168
105	Effect of Exhaust Back Pressure	169
106	Process Schematic	170

TABLES

<u>Number</u>		<u>Page</u>
1	Software Task Outline	25
2	Solid-Waste Processing Data	35
3	Phase-C Tests	45
4	Gas Analyses	50
5	Particle Sampling	50
6	Composition of Ash Deposits	53
7	Summary of Turbine Operations on Wood	56
8	Process Statistics Following Turbine Start 8	62
9	Process Statistics Following Turbine Start 14	62
10	Particle-Separator & Residue-Removal Configurations	71
11	Pilot Plant System Tests	72
12	P-201 System Performance Data	72
13	Exhaust Emissions Data	73
14	Typical P-202 Test Data	73
15	Typical P-203 Test Data	74
16	Coal Test Series - Hot Corrosion	77
17	P-401 Test Data	78
18	P-402 Test Data	79
19	P-403 Test Data	80
20	Results of Fixed-Bed Filtration	88
21	First Hot-Flow GBF Tests	90

TABLES (Continued)

<u>Number</u>		<u>Page</u>
22	Cold-Flow Tests	96
23	Media Spillage Through Outlet Louver	96
24	GBF Outlet Loading with Clean Air	97
25	Inlet and Outlet Loadings	99
26	Loadings in Cold-Flow Test	99
27	Loadings in Cold-Flow Test C-7	101
28	Second Hot-Flow GBF Tests	102
29	Louver-Panel Evaluation Results	111
30	Wood-Waste Verification Tests	113
32	Area, Flow, and Velocity Summary	120
33	Percent Reductions of Water-Soluble Ions	148
34	Summary of Conditions for Test Series CP6M	151
35	Summary of Aluminum-Slag Clinker and Ash Deposits for Test Series CP6M	152
36	Corrosion Specimen Materials	154
37	Results of Analysis of Selected Alloys by Scanning Electron Microscope	154
38	Condensibles from Vapor-Collection Tube for Test Series CP6M	155
39	Solids Analyses for Test Series CP6M	156
40	Comparison of Ash Compositions	157
41	Commercial Turbine Characteristics	160

TABLES (Continued)

<u>Number</u>		<u>Page</u>
42	Computer Program Nomenclature	164
43	CPU-400 Cycle Parameters	165
44	CPU-400 Cycle Summary	165

SECTION 1

INTRODUCTION

Combustion Power Company, Inc. (CPC) of Menlo Park, California has carried out a program of research and development aimed at demonstrating the feasibility of burning municipal solid waste to generate electrical power in a direct-fired gas turbine. The power system, designated the CPU-400, efficiently burns solid waste and other solid or liquid fuels in a fluid-bed combustor at elevated pressure. The testing has been conducted in a 1-MW Pilot Plant designed to consume about 85 tons/day of municipal wastes.

The work described in this report pertains to tasks defined in Contract No. 68-03-0143, and was performed during the period from 20 June 1972 to 31 March 1977. This contract effort was designed as the final stage in the development of the solid-waste-fired turbine system. Earlier phases of the development were conducted at low pressure under Contract No. 68-03-0054. A Final Report for that contract (Ref.1) was written in early 1974, and covers all low-pressure Pilot Plant testing, as well as the design for the integration of the high-pressure Pilot Plant and the turbine.

The following EPA-sponsored tasks are reported here: Task LP-13, covering the design, construction, and checkout of a solid-waste processing station; Task HP-3, integration and checkout of the system with the gas turbine; Tasks GF-1 and GF-2, providing for the design, construction, and checkout of a moving-bed granular filter as the final stage of hot-gas cleanup; Task CP-6, a series of corrosion, erosion, and deposition studies; and Task SS-10, systems studies for full-scale solid-waste-fired gas-turbine systems.

During the contract period, CPC was also actively engaged in developments using the Pilot Plant for the combustion of wood wastes and high-sulfur coal. The work on wood wastes (Ref.2) was sponsored by the Weyerhaeuser Company; that on coal was funded by the United States Energy Research and Development Administration (ERDA) under Contract No. EX-76-C-01-1536. A full discussion of the coal program may be found in Ref. 3.

Because both the wood-waste program and the coal program provide useful extension of the EPA-sponsored work, and serve to verify the solid-fuel-fired gas turbine as a potentially viable system of power

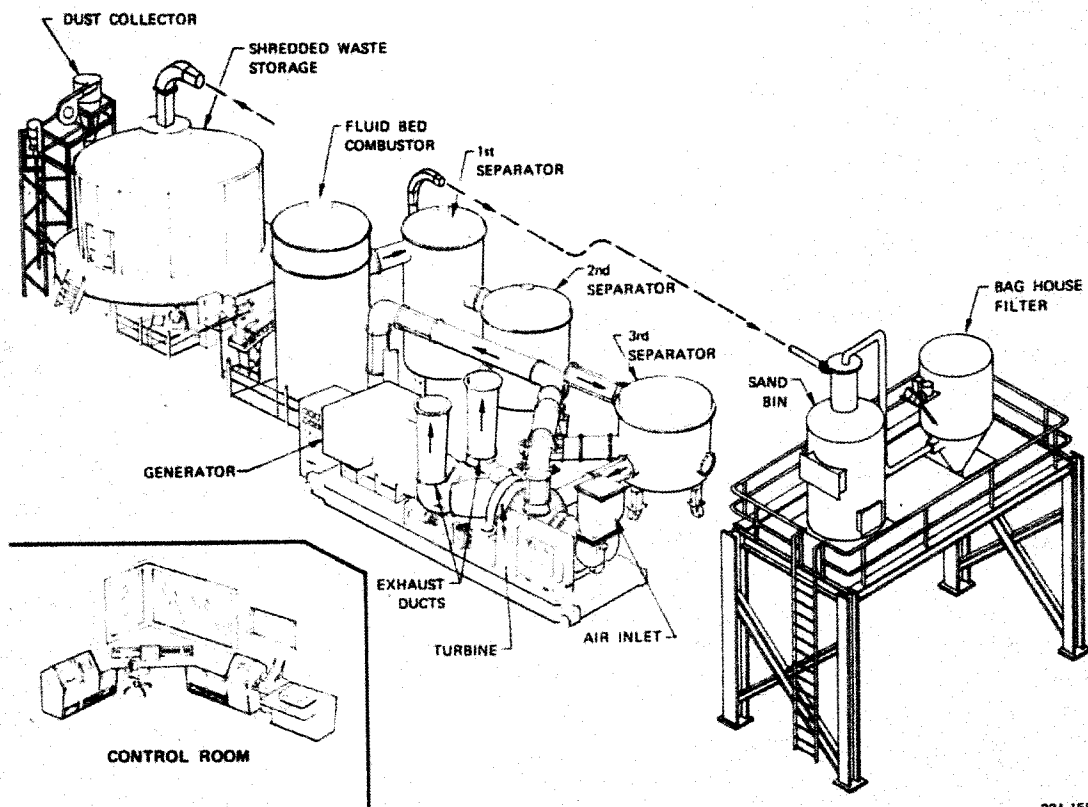
generation, two sections of this report are devoted to summary reports on parts of those programs.

While the concept has been well demonstrated, the full system development remains incomplete. State-of-the-art devices for hot-gas cleanup have proven inadequate for removing fine particulate matter, either to meet established environmental standards or to permit long-duration turbine operation. A moving-bed granular filter, proposed to fill this gap, was installed as a final cleanup stage, but checkout testing was aborted when a louver panel suffered a structural failure. EPA funding was not available to cover rebuilding the filter and conducting a new series of checkout tests. Development of the device is continuing, however, under ERDA sponsorship (installation costs for the unit reported here, as well as the cost of checkout testing, were borne by ERDA).

SECTION 2

SYSTEM DESCRIPTION

Configuration of the CPU-400 Pilot Plant is shown in Figures 1 and 2; Figure 3 is a general flow diagram. The solid-waste processing



221-158

Figure 1 CPU-400 Pilot Plant

station, also part of the overall system, is not shown here inasmuch as its development is fully described in Section 3. With that exception, the system as depicted was used for the tests of Task HP-3, reported in Section 4. Some changes were made to the system prior to and during the course of coal testing; these are described in Section 6. A granular-bed filter, added to the cleanup train just before program termination, is described in Section 7.

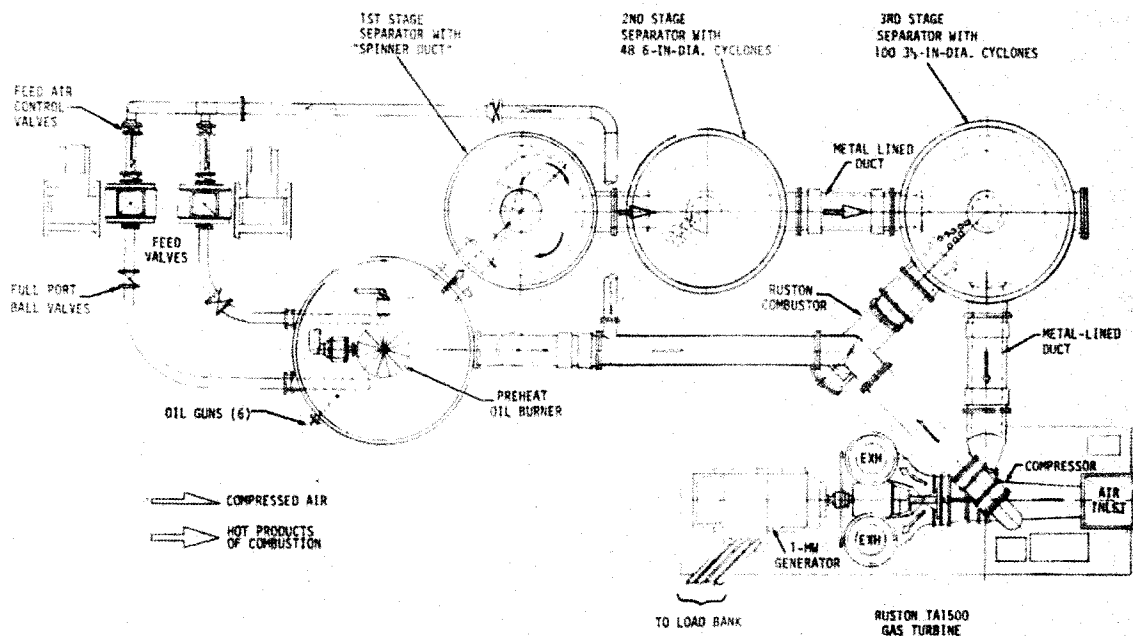


Figure 2 Plan View of Pilot Plant

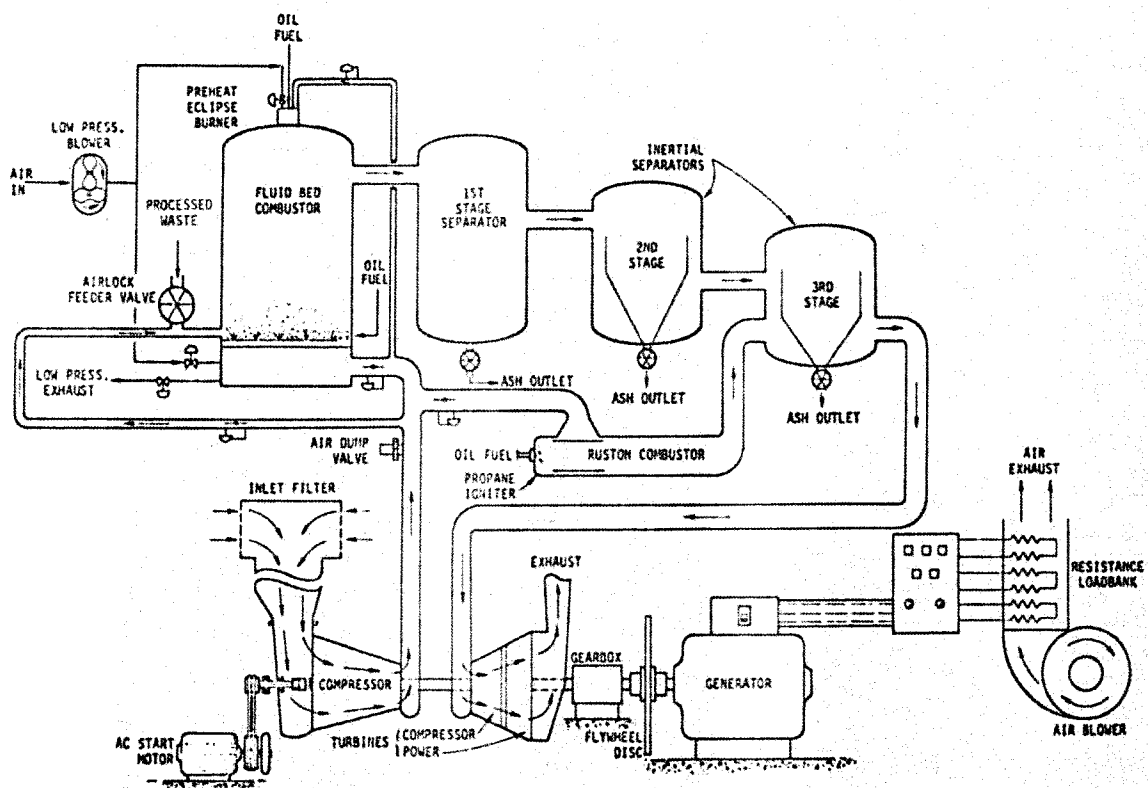


Figure 3 Flow Diagram

That part of the Pilot Plant shown in Figures 1 through 3 divides functionally into six systems: the storage and feed system, the combustor, the gas-cleanup system, the residue-removal system, the turboelectric system, and the control system.

A. STORAGE AND FEED SYSTEM

The storage and feed system, shown in Figure 4, provides storage and automatic retrieval and delivery of the fuel quantity required to satisfy combustor demand. A description of its components follows.

Atlas Storage Unit

This unit is a cylindrical structure 16 ft in diameter and 20 ft * tall, with a capacity for storing 3400 cu ft of shredded waste. Recovery rate can be varied from 100 to 1000 cu ft/hr. The recovery is accomplished by four chains of sweep buckets located on the floor of the cylindrical bin. Each sweep chain is fixed at one end to a powered rotating "pull ring" encircling the storage area, the other end trailing free. As the pull ring rotates around the periphery of the bin, the sweep chains trail toward the center, contacting the stored material at the outside of the pile and filling the buckets, which then drop material onto a single outfeed drag conveyor recessed in the floor (Figure 5).

In earlier testing, the efficiency of the sweeps was improved by adding an extra bucket to each chain and incorporating digger spikes; the circum-cyclone inlet at the top of the Atlas, which had produced unsymmetrical distribution and local compacting, was replaced by a flat stationary splatter plate that evenly distributed material over the atlas floor; and a rotating "clod buster" was added at the end of the outfeed conveyor to break up lumps of packed or composted waste.

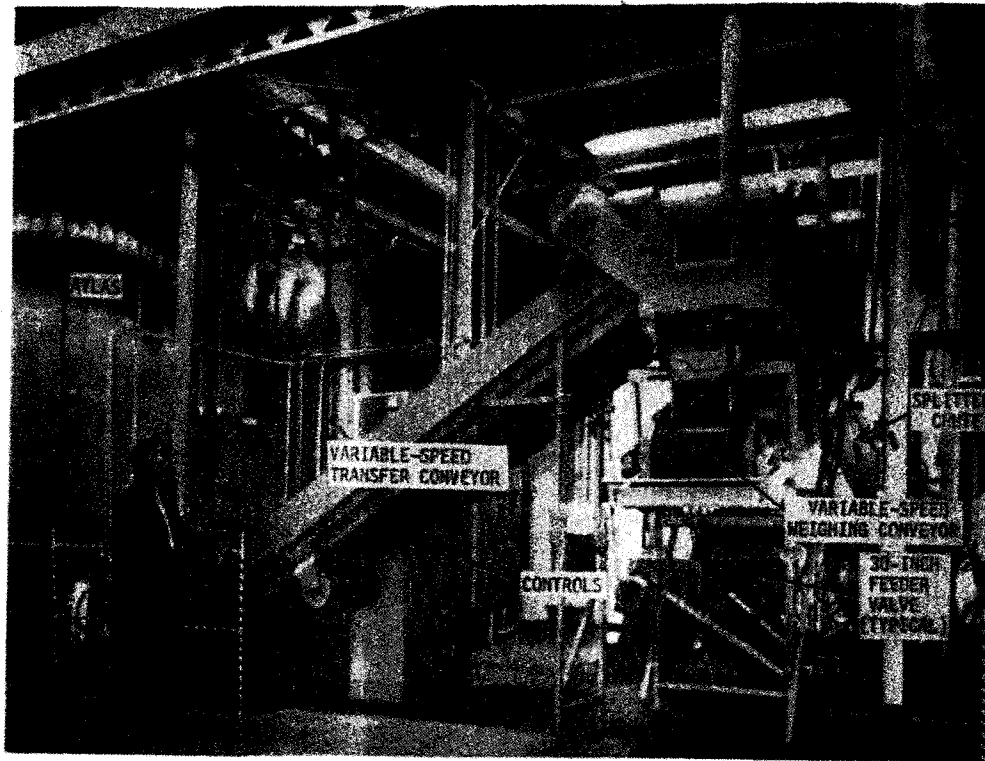
Both the sweeps and the outfeed conveyor are driven by Houdaille fixed-displacement hydraulic motors, the power units consisting of Vickers variable-displacement piston pumps coupled to 1800-rpm, TEFC, a-c electric motors (7½ hp for the sweeps, 5 hp for the conveyor). Conveyor speed can be varied from zero to about 75 ft/min. In use, however, it is generally operated in an on-off mode.

Control System (AVTEK)

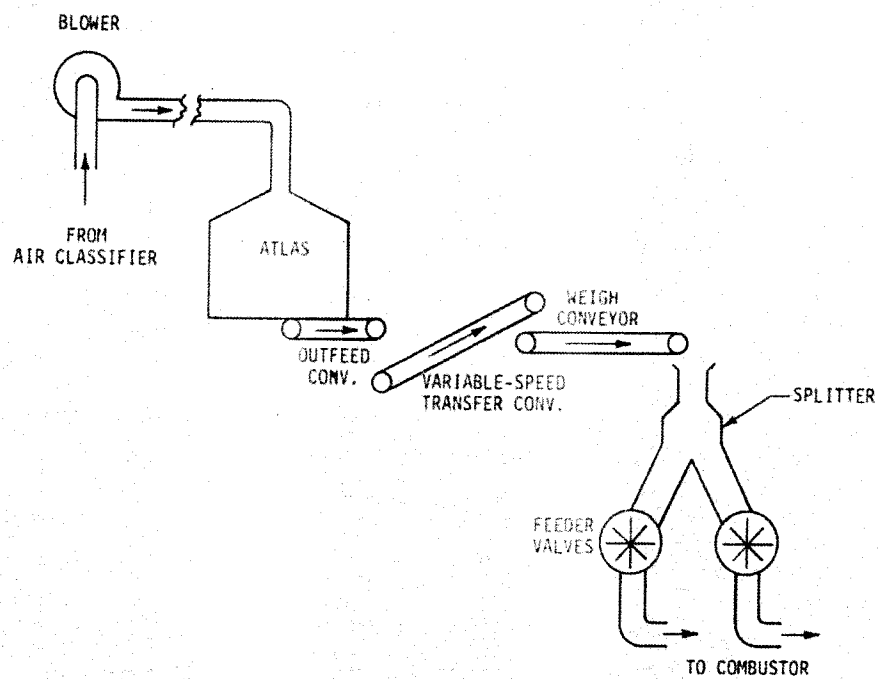
Several modes of operation are available to provide the flexibility required to support large combustor operations or to satisfy lower volume requirements of model combustor tests. Briefly, these modes include:

Mode I Non-production - Maintenance

* U.S. Measurement units are used throughout, to preserve whole numbers adopted at the start of the program; a table of conversions to SI units is included at the back of the report.



GBF Test Set-Up



GBF Controls & Instrumentation

Figure 6-1 GBF Cold-Flow Test Set-Up



Figure 5 Interior Views of the Atlas Storage Unit

- Mode II Manual Speed Control - Direct manual control of sweep drive and outfeed conveyor
- Mode III Manual Volume Demand with Automatic Volume Control - Manually set to desired volume output and then automatically maintained
- Mode IV Process Demand with Automatic Volume Control - The "process demand" signal for volume output is supplied from the fluid combustor operational control source (i.e., fluid-bed and exhaust temperature)

Constant volume output is controlled through a paddle sensor located on the output end of the outfeed conveyor trench. When material level is low in the trench, the paddle sensor signals the volume control system which speeds up the sweeps. As this deficiency is corrected, the sweeps slow down to provide the proper material height in the trench. If, during operation, the stored waste free-flows to fill the trench completely, this condition will stop the sweep system. However, if free-flowing continues, and the trench remains full, the volume outfeed rate will be higher than required. It then becomes necessary to slow the conveyor down to maintain the required volume output; this is done automatically. As soon as free-flow stops, the system will return to normal operation.

Instrumentation provided to monitor Atlas operation includes a pressure indicator located on the side wall of the Atlas bin to measure internal pressure in inches of water; a demand load indicator (demand volume of solid waste required expressed in percentage of feed rate to the combustor); and an actual load indicator (measured output delivered, expressed in percentage feed rate).

Transfer and Weigh Conveyors

The transfer and weigh conveyors carry the material to the feeder-valve inlets. The transfer conveyor, seen in Figure 4, has a 22-foot-long 22-inch belt with 1½-inch cleats at 16-inch spacing. It is chain driven by a 1½-hp gear motor, and is equipped with a paddle-wheel leveler to assist in feedrate control.

The weigh conveyor is a self-contained 3600-lb/hr unit made up of the following standard equipment:

1. 20-inch by 12-foot rubber belt with 1-inch-high flange and full-length skirt boards.
2. Head pulley driven through reducer and drive chain by a 1-hp a-c squirrel-cage reversible induction motor operating on 230/460-volt 60-cycle 3-phase.
3. Merrick Model 440 Weightometer including multiple-idler suspension, temperature-compensated load cell, solid-state millivolt-to-volt amplifier, output indicator, and load-cell-excitation power supply.
4. Running-time meter with thumbwheel reset.
5. Solid-state millivolt-to-volt integrator including rate integrator, seven-digit totalizer, zero and span adjustments, test button, and impulse transmitter.

The Model 440 Weightometer is a mechanical suspension system that transmits the weight on the conveyor idlers to an electronic load cell. The millivolt output from the load cell is proportional to the material weight per lineal foot of conveyor belt. The signal can be amplified directly, or combined with a speed measurement and amplified to produce a rate signal. (At constant speed, the simple weight measurement is proportional to rate).

Feeder Valves

The weigh conveyor delivers the material to a stainless-steel splitter chute that divides the load between two rotary-airlock feeder valves; the valves serve to transfer material from ambient pressure to two 6-inch pressurized pneumatic-transport lines leading to the combustor. The general arrangement is shown in Figure 6. The two ESCO Rotafeeders are 30-inch-diameter cast stainless-steel valves, having 13 feed pockets and 13 sealing edges between. The nominal capacity of each valve is 36 cu ft/min when rotating at 11 rpm. Each valve is driven by a gear motor rated at 20 hp.

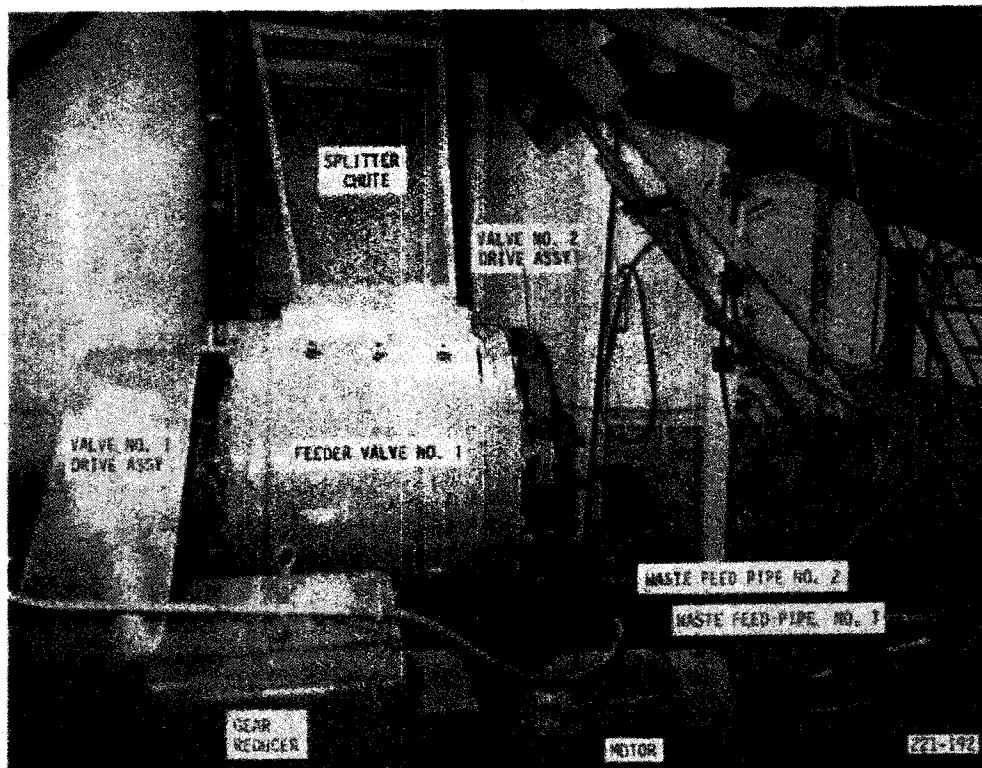


Figure 6 Thirty-Inch Airlock Feeder Valve

The pressure seal is provided by adjustable hardened knife-edge blades; at any time, four on each side of the rotor are in full-width contact with the housing. The high-pressure air that fills the pockets as they pass through the pressure zone is twice released during return to the low-pressure side of the valve, before the final release to atmosphere. Feed-air purge lines assist in blowing solid waste from the pockets as they pass over the valve outlet. To avoid thermal distortion of the valve body--and thus to permit closer running clearances and reduced air loss--it is water-jacketed and kept heated to near the feed-air temperature. Rotor-shaft bearings are graphite-impregnated sleeves, cooled by water at about 9.2 gpm under pressure ranging from 5 to 8 psig.

B. COMBUSTOR

The combustor, shown in Figure 7, is a 22-ft-long by 9½-ft-diameter cylindrical carbon-steel pressure vessel with dished heads. The upper chamber, being exposed to high-temperature gases, is lined with refractory insulation. The cylindrical wall insulation consists of a hard, wear-resistant firebrick inner liner backed up with a liner of insulation brick. A thin layer of packed bulk-kaowool insulation between the brick and the pressure shell protects the shell against stresses induced by the thermal expansion of the refractory brick. The two-foot-deep (when static) fluid bed is supported by a flat carbon-steel plate insulated on top by two layers of castable refractories.

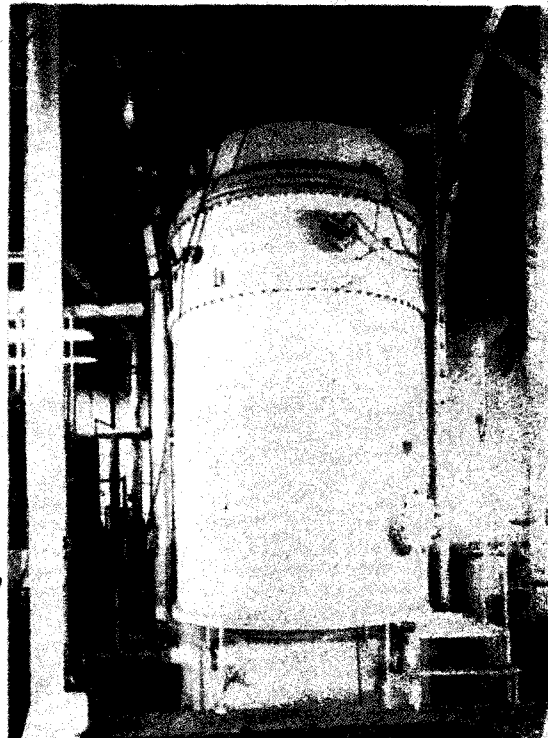
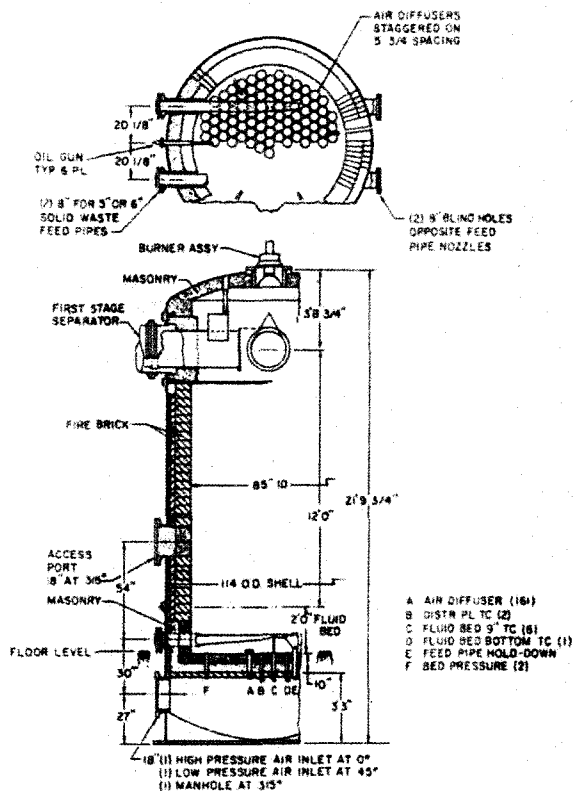


Figure 7 Pilot Plant Combustor

Penetrations through the pressure shell and refractory insulation into the fluid bed provide for two solid-waste feed points and six oil-fuel injection points. Other major penetrations through the pressure shell and liner into the combustor are provided for residue removal, instrumentation, inspection, and entry. The bottom of the combustor is the air plenum chamber below the distributor plate. It is penetrated by three 18-inch ports (high-pressure air supply, low-pressure air supply, and manhole) and three eight-inch-diameter ports (instrumentation, high-pressure backheat, and alternate feedline air supply). Air distribution is achieved through 161 diffusers mounted to standpipes that penetrate the castable insulation on top of the distributor plate (Figure 8). The diffuser screens (Figure 9) are held down by three studs secured with bend-tab lock washers, since experience has shown that ordinary lock washers can work loose after repeated thermal cycling.

An oil burner for use in preheating the sand bed during a cold system start is mounted in the top dome of the fluid-bed combustor (Figure 10). It is a light oil burner rigged for straight-down firing.



Figure 8 Air Diffusers and Feed Pipes

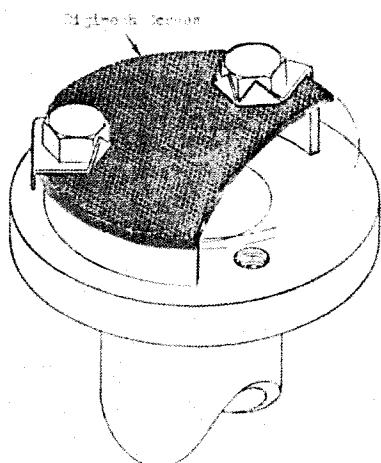


Figure 9 Combustor Air Diffuser

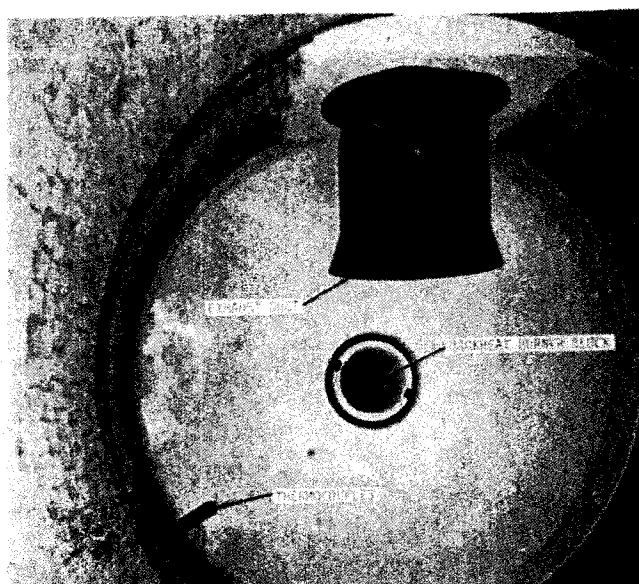


Figure 10 Combustor Exhaust and Backheat Burner Ports

It incorporates an oil-metering valve, a main air valve, manual atomizing-air valves, and manual oil and gas shutoff valves. Burner ignition is a propane pilot system with air and gas valves, mixer, and spark plug. The burner is enclosed in a pressure casing to obviate its removal for high-pressure operation. The backheat air flow for the preheat burner is provided from a Roots type blower of 4750-cfm capacity driven by a 125-hp electric motor. This blower also provides cooling air into the air plenum chamber during preheat operations.

C. GAS-CLEANUP SYSTEM

The hot gas passes through three stages of particulate separation in moving from the combustor to the turbine. The three vessels housing the stages are shown in Figure 11. Construction of the three vessels

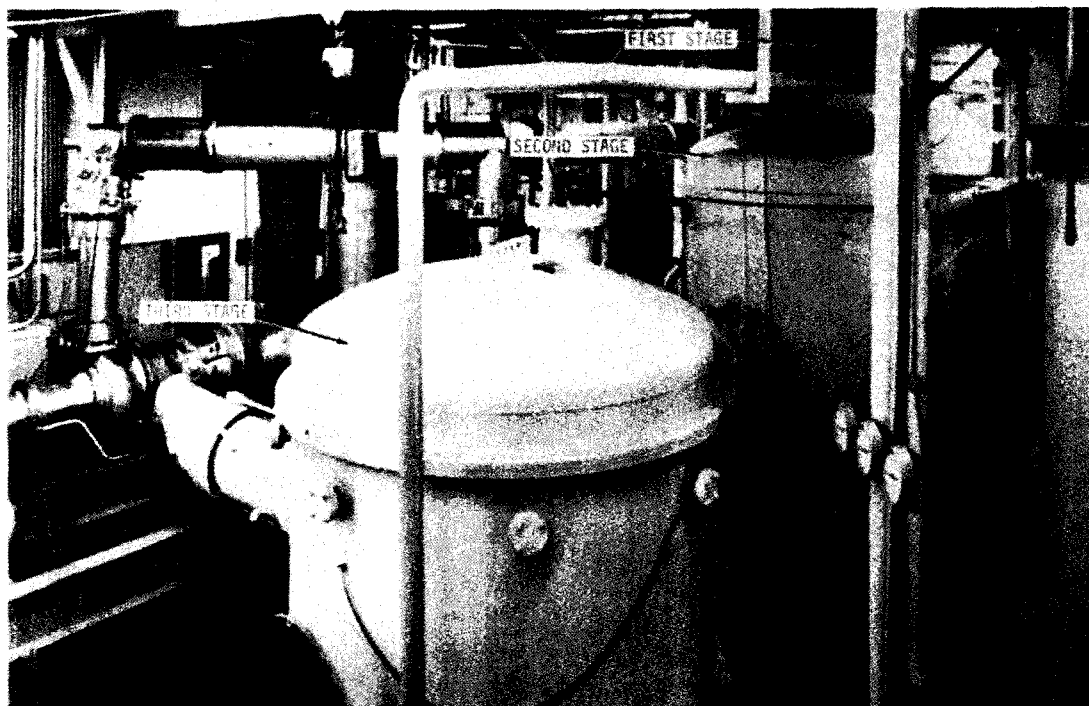


Figure 11 Vessels of the Gas-Cleanup System

is essentially the same: each is a mild-steel pressure vessel insulated by 2 inches of mineral wool and 3 inches of Kaowool. The insulation is protected from the hot gas by a stainless-steel liner. The first vessel is 8 feet in diameter and 16 feet high, the second 8 feet in diameter and 10 feet high, and the third 9 feet in diameter and 9½ feet high.

The separation devices contained in the vessels were designed or selected under the previous EPA contract, which encompassed testing at low pressure only. Reverse-flow inertial tubes were used in the second and third stages. As shown in Figure 12, the dirty gas enters the inlet

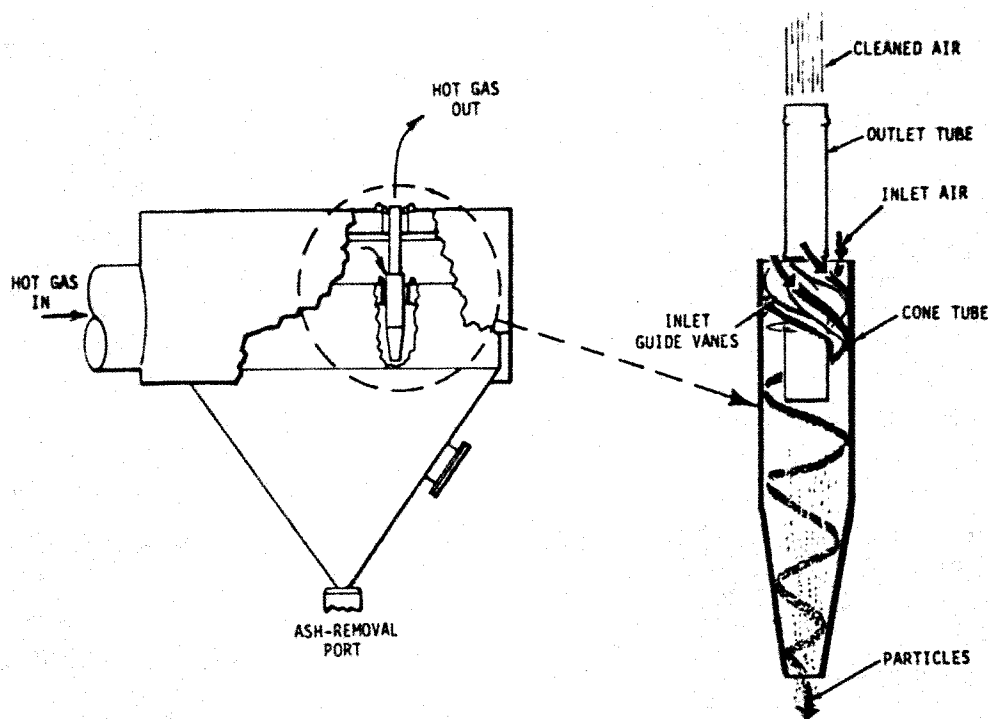


Figure 12 Second- and Third-Stage Inertial Tubes

annular cavity, where helical vanes impart rotational motion to downward-flowing gas, centrifuging particles to the outer wall. The particles spinning along the wall decelerate and fall through the opening in the bottom of the tube to a common collection hopper, while the gas exits upwardly through the center of the finned tube. The general arrangement of the tubes in the second-stage vessel is shown in Figure 13 (the outlet-tube manifold has here been removed). This stage contained 48 6-in.-diameter tubes. A similar arrangement was used in the third stage, but with 100 3½-in. tubes. Design cut points for the tube arrays were 4.5 microns (second stage) and 1.9 microns (third stage).

Prior testing with these inertial separators had indicated that in a solid-waste-fired system they would be functionally impaired by sand and aluminum in the hot gas. These materials would cause heavy loading, excessive wear, and material deposit and removal problems. Use of the fluid-bed combustor is accompanied by elutriation of some fine sand particles from the bed, and small quantities of aluminum (from bits of foil, beverage-can pull tabs, etc.) will usually be present in the fuel. The combustion gas transports the aluminum in the form of molten particles protected by a thin, stable shell of aluminum oxide. The particles are of sufficient mass to separate from the hot-gas stream at

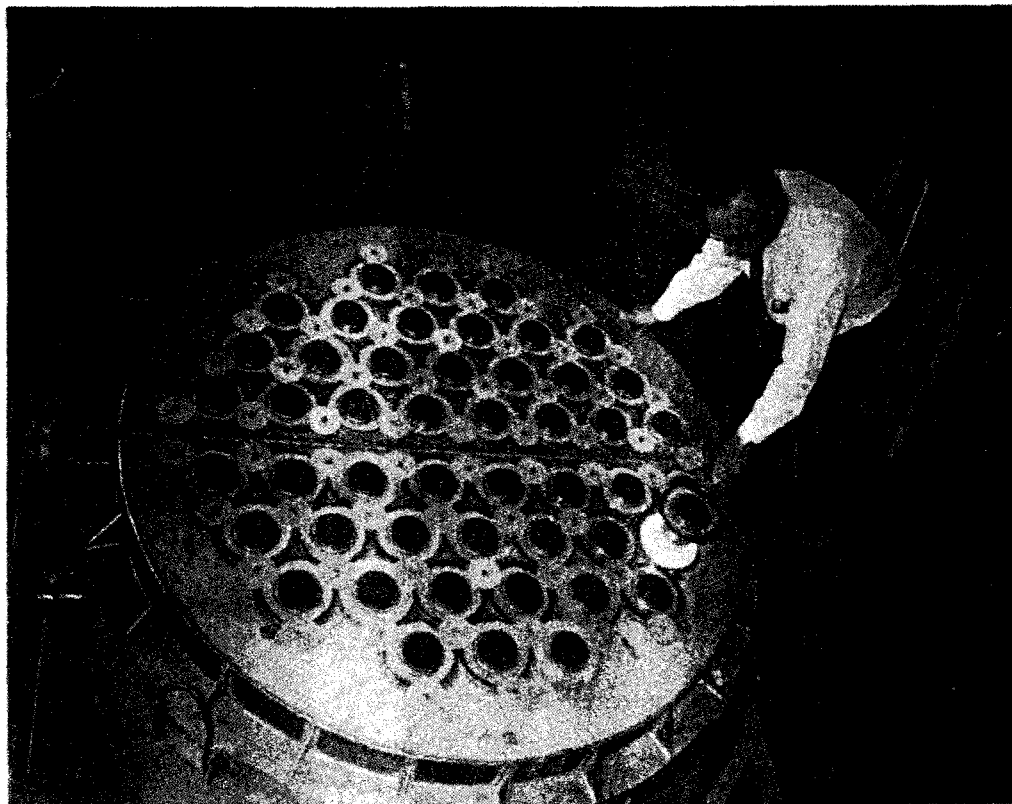


Figure 13 Second-Stage Multicyclone Separator-Tube Assembly

relatively high velocities. On impact with component surfaces, the oxide shell is destroyed and the particle fragmented, but new oxide coatings are immediately formed by virtue of the aluminum's contacting the oxygen-rich hot gas. With time, the repetition of this process results in the formation of large, hard, clinker-type deposits on component surfaces.

The first-stage separator (Figure 14) was designed for the specific purpose of removing sand and aluminum from the hot gas before its entry into the inertial tubes. Hot gas enters through a spinner duct that imparts a low-velocity centrifugal action. Velocities are kept low enough to minimize the impacting of molten-aluminum spheres on separator surfaces, while the sand that is being elutriated from the bed serves to scour the walls and thus minimize buildup of deposits.

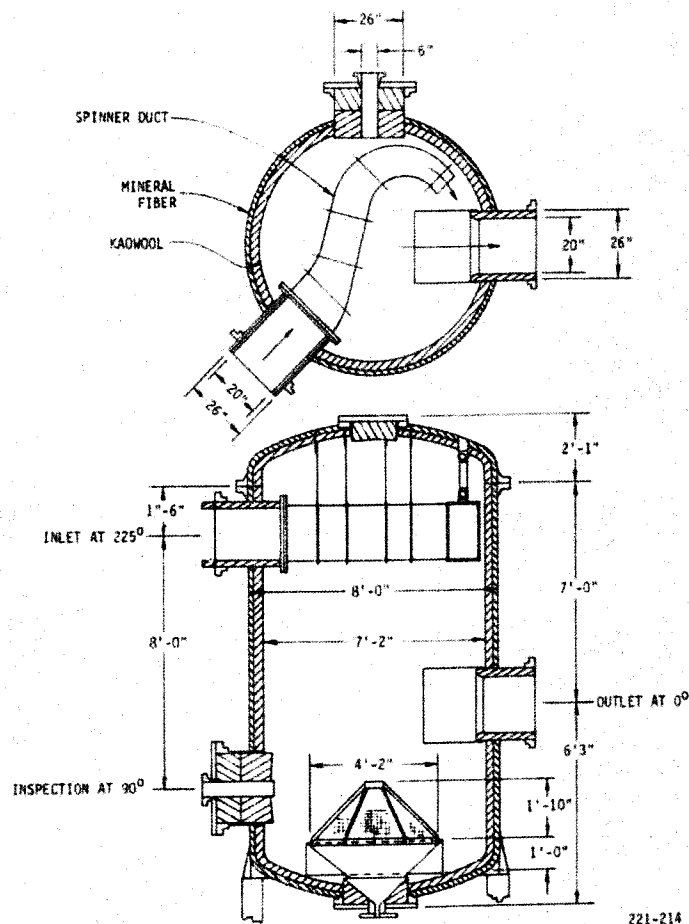


Figure 14 First-Stage Separator

D. RESIDUE-REMOVAL SYSTEM

Separated particulate falls to a hopper in the bottom of each of the pressure vessels. During Task HP-3, removal from the hoppers in each of the first two stages was accomplished through a double-ball-valve airlock that was time-cycled. Residue and gas thus removed were cooled in a water-jacketed transfer pipe. The hopper in the first stage was covered with a conical screen (shown in Figure 14) as a precaution against the entry of any clinkers that might build on the walls of the spinner duct and subsequently spall off. Removal of residue from the third-stage hopper was accomplished through a continuous-bleed orifice.

Material removed from the separator vessels is pneumatically transported by low-pressure blower to the residue-collection system, which consists of a bin with a cyclone inlet that catches most of the heavy residue and a baghouse that retrieves the flyash (Figure 15). The bin



Figure 15 Residue-Collection Baghouse and Cyclone

has no active parts to affect residue collection. The baghouse contains 24 fiber bags which filter the fine particles that carry over with the transport gas. The bags are cleaned by a puffback system that includes a blower and rotating-arm assembly that backflows each bag once per revolution of the arm. At the bottom of the collection hopper is an airlock rotary valve for unloading of the accumulated material into a standard cement trailer.

E. TURBOELECTRIC SYSTEM

The turboelectric system comprises the equipment used for the delivery of compressed air for combustion of oil and solid waste, the generation of electricity from the resultant hot gas, and the dissipation of the generated electric power. Major components of this system are the Ruston Model TA-1500 gas turbine (with relocated Ruston combustor), a 1000-kW a-c generator, electric-power switch gear, electrical load bank, and load-bank switching equipment.

Ruston Turbine

Figure 16 shows the Ruston turbine as installed. Ambient air for the turbine cycle is drawn through an inlet filter and ducting into the compressor. The compressor, rotating at a nominal 11,600 rpm, compresses 22.4 lb/sec of air to 44 psig and delivers it to the compressor-outlet piping manifold.

For operation on the relocated Ruston combustor, propane fuel and a spark igniter are used to establish a flame. Diesel oil is then injected into the combustor and burned in the compressed-air stream. This produces combustion-product gas at 1400 F and 43 psig as delivered to the turbines.

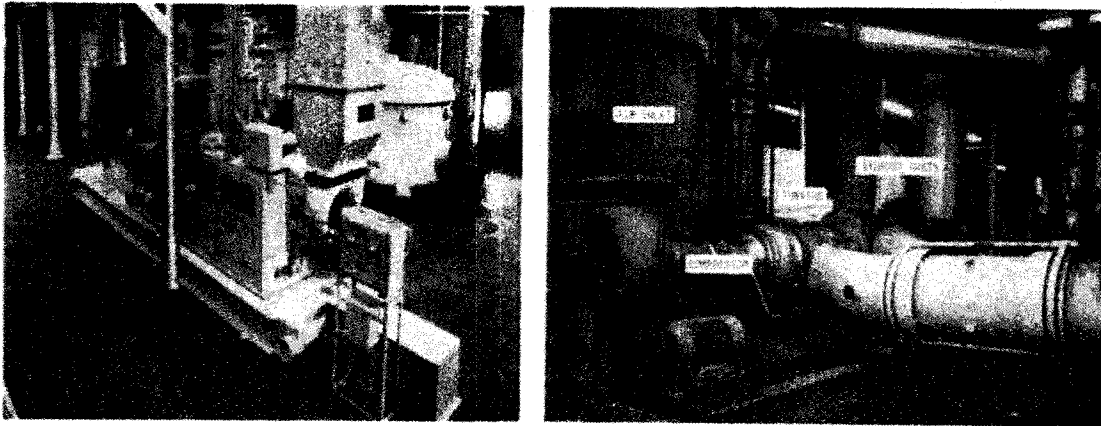


Figure 16 Ruston TA-1500 Turbine

The hot gas is expanded down to 10 psig (at 1100F) through the compressor turbine, which develops the power for driving the compressor. The compressor turbine has two rotor stages of 83 blades and two stator stages of 76 blades each. Further expansion to ambient pressure occurs in the power turbine, which is on a separate shaft from the compressor, rotating at 6000 rpm and delivering about 1450 hp to a speed-reducing gearbox. Like the compressor turbine, the power turbine has two stages, but of larger diameter, with 97 blades in each rotor stage and 92 in each stator stage. Exhaust gas at 940 F is vented to atmosphere through two parallel exhaust ducts with silencers.

Starting energy for the turbine is provided by a 50-hp a-c starter motor and drive system. A fluid coupling mounted on the constant-speed motor absorbs speed slippage between motor and compressor. The output of the coupling is delivered to the shaft through a speed-increasing vee-belt drive, with a self-engaging mechanism and overriding clutch on the compressor shaft; the cranking system is thus disengaged from the compressor shaft when not in use.

Electrical System

The generator coupled to the gearbox output shaft is driven at 1800 rpm. It has a maximum rating of 1250 kW, but in this installation generates a nominal 1000 kW. The output power is 3-phase a-c at 480 volts. To dissipate this power, a resistance load bank with switching equipment and a cooling blower are used. This permits load selections from zero to 1150 kW in minimum increments of 25 kW.

The switchgear unit utilizes power from the generator and is therefore independent of facility power problems. The unit provides monitoring means for the power system and includes, for each power

phase, a current monitor, a 1600-ampere trip, and a voltage transducer. In addition, a wattmeter and a watthour meter are installed in the panel along with the generator exciter servo. On the face of the panel, meters display generator voltage, current wattage, power factor, frequency, and winding temperature.

From the switchgear, the power is routed to the load bank for dissipation. This is accomplished through fourteen 75-kW resistors and four 25-kW resistors. The load is selectively applied to these resistors by 14 fused, latching, lighting contactors, and four fused nonlatching, lighting contactors. The contactors are operated by control relays either by manual switches or through the automatic generator-speed control unit. The load-bank blower motor, which is interlocked to plenum doors and a flow switch, will generate a system shutdown if inoperative.

F. CONTROL SYSTEM

The control system interacts with the other Pilot Plant systems to control their respective outputs in response to commanded setpoints, supervises the acquisition of data from various instrumentation channels, and reduces the data into a form suitable for test evaluation. It includes a manual control system and a computer (automatic) control system (Figure 17). The manual control system is composed of signal transmitters, analog process controllers, manually operated toggle switches and relay logic networks. The computer (automatic) control system, basically a Texas Instruments Model 960A digital computer, includes the main frame, operator terminals, and computer input/output and storage devices. The automatic control system is the primary control mode used for Pilot Plant operations.

The manual control system provides for direct operator control of the various system elements. Relay logic networks are incorporated to prevent the operator from implementing unsafe system configurations and to reduce the number of manual operations required during change-over from one configuration to another.

The operational mode is selected by the test conductor's actuating one of eleven mode switches located on the operator's console. These switches are for:

1. Backheat
2. Fluidized operation on diesel fuel (low pressure)
3. Fluidized operation on diesel fuel and solid waste (low pressure)
4. Fluidized operation on solid waste (low pressure)
5. Fluidized operation without fuel (low pressure)
6. Fluidized system heating (low pressure)
7. Operation on Ruston combustor (high pressure)
8. Fluidized operation on diesel fuel (high pressure)

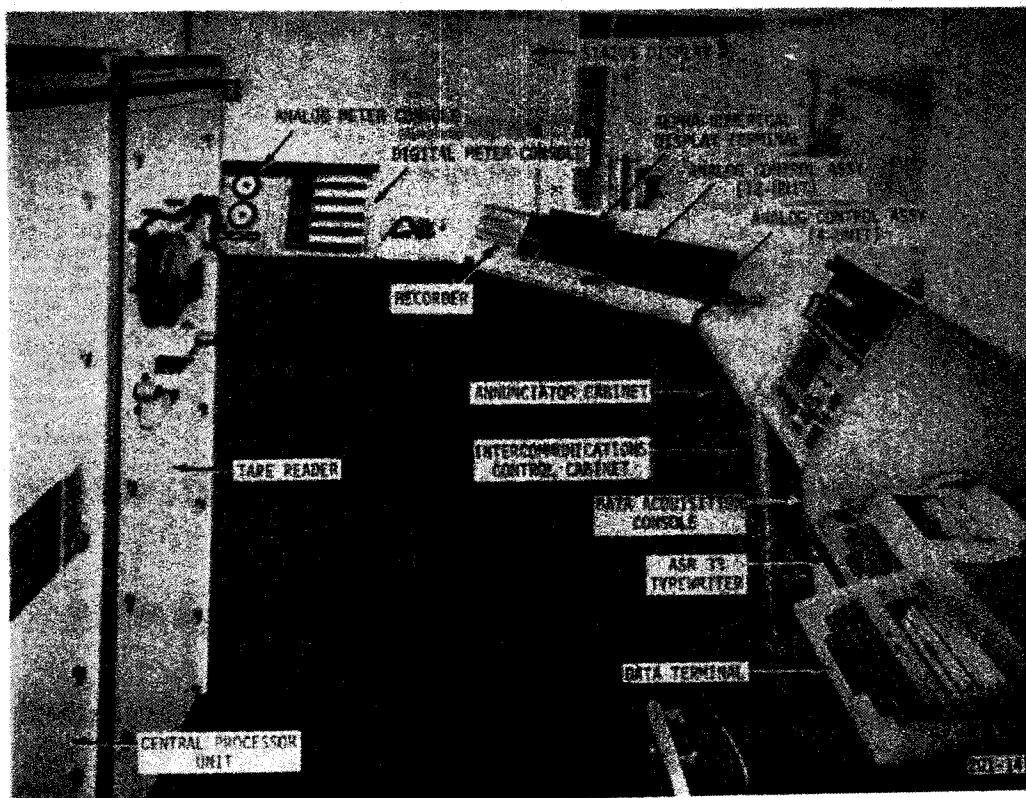


Figure 17 Control Room

9. Fluidized operation on diesel fuel and solid waste (high pressure)
10. Fluidized operation on solid waste (high pressure)
11. Fluidized operation without fuel (high pressure)

The switches are interlocked such that operation of any single mode will cause the system to operate in the associated mode only if predefined constraints are met. If the mode is acceptable, the mode switch will be magnetically held in the ON position and any previously selected mode switch will be magnetically released to the OFF position. If the mode is unacceptable, the system will continue to operate in the prior mode and the mode switch selected will spring back to the OFF position when released.

Manual control of the proportional valves (valves whose position is proportional to an input signal) and of the solid-waste feed system is provided by analog process controllers. These controllers provide for operation or control of the associated devices from the control room or for automatic control based upon system measurements. In the manual mode, the test conductor actuates a thumb wheel to increase or decrease the signal sent to the associated controller. A meter on

the front of each controller provides an indication of the signal being sent to the controlled unit.

In the automatic mode, the process controller compares a signal from measurement of a preselected system parameter to an operator-selected level or setpoint. The controller then increases or decreases the signal to the controlled unit based upon the difference between the measurement and the setpoint. Each controller has provisions for adjusting the system gain. The controllers also have integral circuits where the controller output is a function of the time integral of the error.

In cases where the measured parameter for control purposes is a temperature, thermocouples are used and transmitters provide signal amplification and conditioning. Pressures are measured using pressure transmitters directly coupled to the system and providing a current signal.

Process Control Computer

The process-control computer provides control, data collection, and monitoring functions for the process. The basic system schematic is illustrated in Figure 18. The following paragraphs provide a brief description of each major element of this system.

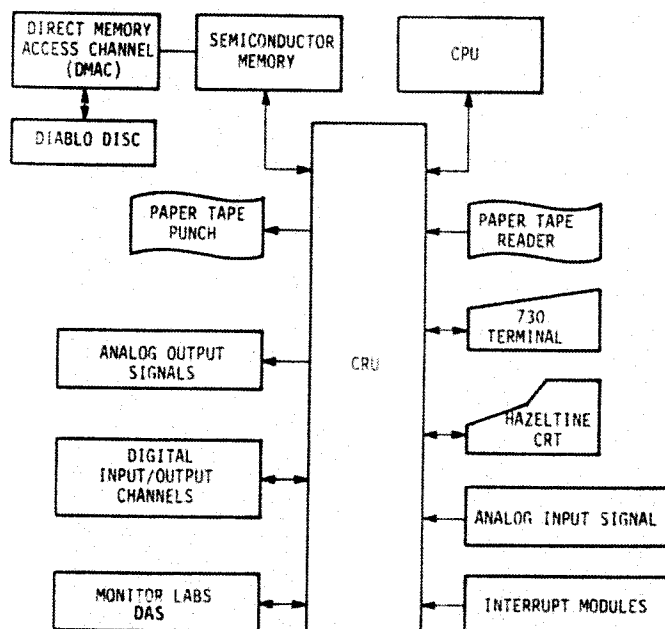


Figure 18 Computer-System Block Diagram

Central Process Unit (CPU)--

The heart of the system is a minicomputer with 28,672 16-bit words of semiconductor main memory, a battery pack for continuous memory refreshing, memory parity, variable-length memory protect, power-failure interrupt, extended arithmetic option, expanded internal communications register unit (CRU) providing for computer/process interfacing, and a control panel with keylock.

Mass Data Storage Unit--

The mass storage unit, a moving-head Diablo disc pack with controller, handles 1.14 million 16-bit words. It interfaces directly with the CPU through a direct memory-

access channel (DMAC). It has an average access time of 100 ms, and is used for process program compilation, process task storage, process data storage, task overlay operations, systems generation, and storage of overall process-control programs.

Teletypewriter--

The Silent 730 typewriter is a 30-character-per-second teletype that is used as the system's main data-logging device and the primary programmer's interface.

Alpha-Numeric Display Terminal (CRT)--

The cathode-ray-tube display terminal has a maximum data-transfer rate of 2400 baud; it serves as the primary process operator's interface.

Paper-Tape Punch Unit (PTP)--

The eight-column paper-tape punch unit is a 60-character-per-second device that is used for permanent storage of process source programs and process data.

Paper-Tape Reader (PTR)--

The eight-column reader unit is a 300-character-per-second device that is used to load memory from source tapes and from stored data tapes.

Interval Timer--

The interval timer, with 1-ms resolution, provides controller/process synchronization, and provides the system with real-time clock capability for time-of-day acquisition and recording.

Lo-Level Differential Analog-Input Subsystem--

The lo-level A/D subsystem provides 30 channels of low-level analog inputs, accurate to 0.05%, for measurement of process temperatures with thermocouples.

Hi-Level Single-Ended Analog-Input Subsystem--

The hi-level A/D subsystem provides 80 channels of high-level analog inputs, accurate to 0.05%, for measurement of process transducer outputs (e.g., pressure, speed, position, voltage, flow rate, weight).

Hi-Level Single-Ended Analog-Output Subsystem--

The high-level analog-output subsystem provides 18 channels of high-level analog outputs, accurate to 0.05%, for generation of process setpoints.

Discrete Contact Closures--

The 160 sets of isolated, buffered contact closures are used to control the energizing and de-energizing of numerous process-control relays and contactors for programmed sequential plant operation.

Discrete Contact Sense--

The 160 channels of this subsystem are used to monitor numerous process contact closures, to ensure correct sequential plant operation, and to indicate urgent and semi-urgent process alarm conditions.

Digital-Input Subsystem--

Thirty-two bits of the 96-bit digital-input subsystem are used to monitor the modes of operation of the various process controllers. The remaining 64 bits are used in conjunction with the 64-bit digital-output subsystem to interface the computer system with the process data-acquisition system.

External-Interrupt Subsystem--

The 16-channel external-interrupt subsystem is used to sense process alarm conditions and generate immediate remedial action, to permit supervisor control for certain peripheral devices, and to permit immediate operator control of the process under predefined conditions. Each external interrupt will cause the computer to trap to predefined memory locations for programmed servicing of the particular interrupt.

Annunciation and Alarm--

Indications of status and out-of-tolerance conditions are provided to the test conductor during all test operations. For manual operation, lights behind a schematic display panel provide indication of those units that are activated; an annunciator panel blinks a preselected light when a measured parameter goes out of tolerance. In automatic operation, these signals are additional to status advice provided through the CRT; alarm conditions are also recorded--and time-tagged--on the teletypewriter terminal.

Data-Acquisition System--

The data-acquisition system is used to read the various measurement devices, convert the measurements to engineering units, and record the data. The stand-alone data-acquisition system can be used during either manual or computer operations.

The system is shown schematically in Figure 19. The scanner transfers multiple analog input signals sequentially under internal control, to a common set of output lines. Numbered front-panel pushbutton switches permit skipping unwanted channels. To notify the operator of the scanner's position, the pushbuttons are illuminated during the scan cycle.

Switches are enclosed in a guard shield to assure accurate switching of d-c and a-c signals in the presence of common-mode noise. The unit is configured to switch input-signal guard to preserve the guard through the scanner. To reduce interchannel cross talk, each 10-channel switch module contains one "output decoupling" relay. The relay isolates all nonactive 10-channel modules, resulting in reduced coupling and higher common-mode rejection.

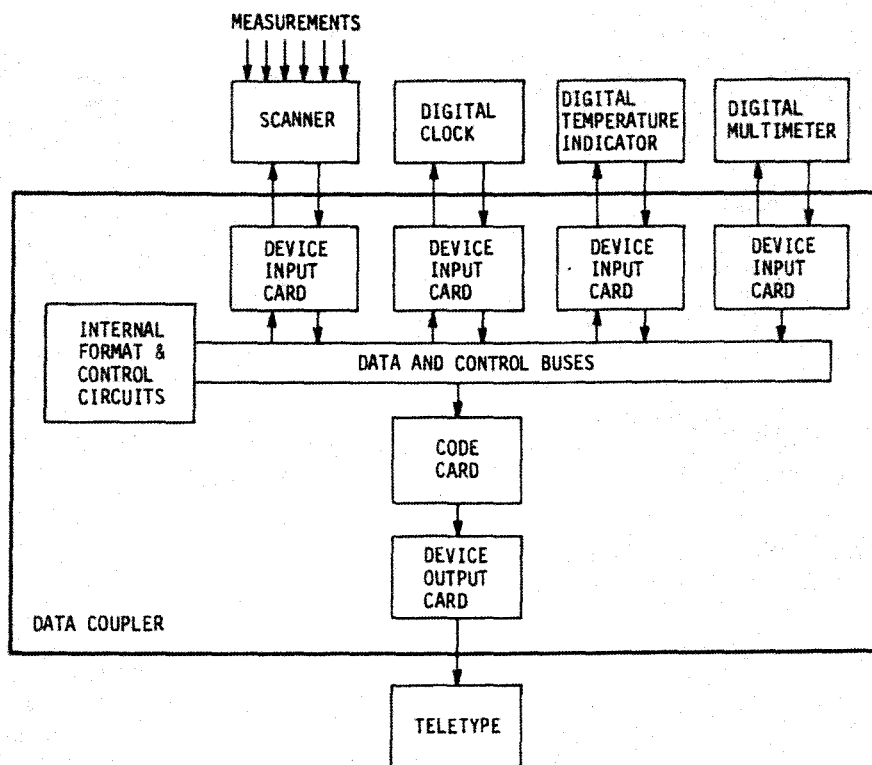


Figure 19 Data-Acquisition System

The digital clock controls the scan process through 63 different selectable time intervals. It also provides a time heading for the data prior to each scan.

The data coupler resembles a small, hard-wired processor, consisting of a mainframe, data-control buses, device input cards, device output cards, code cards, and formatting matrices. This unit couples the digital output devices (multimeter, thermometer, or clock) to a teletype unit. It also allows for formatting the data (i.e., provides the capability to include engineering units in the record).

The teletype unit is a standard ASR 33 unit with paper-tape punch and reader.

Thermocouple measurements are converted from millivolts to temperature via the digital temperature indicator. This unit provides linearization for the thermocouples (type K) along with a reference-junction compensation. Voltage and resistance measurements are made via the digital multimeter. This unit is capable of autoranging and having the mode externally selectable.

Process-Computer Software

Software for the TI 960A computer is written primarily in PCL

(process control language), a FORTRAN-like language extended to work with digital and analog input/output signals. The communication between computer and process thus afforded is handled by the CRU channels. The further addition of WAIT statements enables the computer to work in a real-time environment.

PCL programs are compiled in a single pass to source-assembly-language (SAL) statements. The SAL program is next processed in a two-pass assembler to object code. If subroutines are employed, a third step known as linking is required to obtain a complete object for the program (also known as a "task") which may be loaded for execution by the computer. In special cases SAL statements may be interspersed with PCL statements to achieve economies or extend PCL capabilities.

The computer manufacturer supplies a monitor system (known as PAM/D for process automation monitor with disc) that supervises the execution of many such tasks on a priority basis. PAM/D uses an interval timer with a 0.1-sec polling period and uniquely assigned priority numbers to service individual task requirements.

The multiple-task capability of PAM/D has been exploited in the design of CPU-400 Pilot-Plant software. The functions of major tasks in the complete inter-related set are outlined in Table 1. One of the advantages of this structure is the flexibility afforded; changes to a particular task can be made without disturbing any of the others. Additionally, two versions of a given task can be available and selectively used without impacting others.

A key aspect of the overall structure is a memory-resident common data base that is accessible to all tasks. This data base provides the chief mechanism for inter-task communication. Certain tasks, particularly those controlled by executive Task 12 (see Table 1), act to refresh numbers stored in the data base. Others utilize the values (e.g., temperatures, pressures, valve positions, etc.,) for supervisory control purposes, alarm messages, display, and logging. The common data base consists of four major sections:

1. An executive section with clock registers, elapsed-time registers, bid-frequency codes for sampling and logging tasks, and zero-level readings for certain process transducers.
2. An index section which relates CRU addresses and parameter numbers to a process variable and signal-numbering system (primarily to facilitate computer/operator communication).
3. A parameter section where control and monitoring numbers (e.g., setpoints, gain terms, alarm levels), most recent system measurements, and other saved numbers (e.g., calibration constants) are stored.

TABLE 1
SOFTWARE TASK OUTLINE

TASK NO.	DESCRIPTION
10	Controlling Executive Task <ul style="list-style-type: none"> • Always present in memory • Starts most other tasks in proper sequence • Responds to operator commands at CRT for parameter display and modification, task control, etc.
A2	Fills Common Data Base with Initial Values
A4	Real-Time Clock, including Two Elapsed-Time Registers <ul style="list-style-type: none"> • Counts weighing-conveyor signal pulses, computes rate
12	Analog Input Signal Sampling Executive <ul style="list-style-type: none"> • Periodically bids 10 worker tasks that sample process transducers, convert measurements to engineering units, store result in common data base • Bid intervals are individually adjustable
17	Disc Logging Executive <ul style="list-style-type: none"> • Periodically bids 13 worker tasks that log disc records (14 real values each) from the common data base, or smooth noisy measurements by difference equations • Bid intervals are individually adjustable
30	Controller Initialization and Transducer Readiness
31	Pilot Plant Valve Exercise
33	Bed Preheat Control and Monitoring (Mode 1)
34	Separator-Vessel Preheat Control and Monitoring (Mode 6)
35	Turbine Starting and Operation on Ruston Combustor (Mode 7)
36	Mode 7-Mode 8 Transition
50	Fluidized Operation Control (Modes 8-11)
51	Fluidized Operation Monitoring and Display (Modes 8-11)
52	System Shutdown Sequence Completion
54	Residue-Removal System Control
64	Memory-Resident Parameter Array Maintenance (Adjustable Frequency)
61/62/63	Selectable Real-Time Displays
66	Real-Time Statistics Analysis and Display

4. A real-time display array where 25 time records of 14 key system variables are maintained.

Many of the tasks in Table 1 are involved in preliminary operations and the two modes of preheat using the low-pressure blower. Thus, only one of Tasks 30, 31, 33, and 34 is in memory (under control of Task 10) at a given time. Tasks 35 and 36 then are used to implement a fully automatic turbine-start sequence and the transition from one combustor to the other by suitable valve sequencing. The last function of Task 36 is to "unsuspend" Tasks 50 and 51 so that these may supervise high-pressure fluidized operations.

As indicated in Table 1, the activities are split between Tasks 50 and 51 in all fluidized operating modes. Task 50 handles the following duties:

1. Refreshes bypass-valve position command every 1.0 second.
2. Services feedline valve logic and air-flow commands every 1.0 second.
3. Conducts all mode-change sequence operations.
4. Monitors fuel feed system for malfunction indications every 1.0 second.
5. Updates bed-temperature controller setpoint based on an outer supervisory loop every 5.0 seconds.
6. Updates freeboard-temperature controller setpoint based on an outer turbine-inlet-temperature control loop every 5.0 seconds.
7. Updates generator-speed and voltage controller setpoints every 5.0 seconds using an outer supervisory loop.

Meanwhile, Task 51:

1. Monitors many system variables for out-of-tolerance conditions, writing appropriate CRT messages depending on status.
2. Monitors certain key parameters such as bed temperature and generator and compressor speed to determine if shut-down conditions exist, and initiates same if required.
3. Monitors certain key discrete inputs as in item 2 above.

4. Produces a periodic display on the CRT for operator information.

Whenever fluidized operation is terminated, Task 52 assumes control to bring the Pilot Plant safely and systematically to a rest condition.

In addition to the CRT terminal, the operator is able to use the operator interface panel to communicate with the computer and exercise software options. The customized operator interface panel consists of several switches and lights interfaced with the computer through the CRU channels. The panel enables the operator to perform the following operations:

1. Select slow or fast display option.
2. Initiate feedline airflow.
3. Select feedline high or low airflow options.
4. Initiate a software emergency shutdown.
5. Acknowledge certain digital alarms.
6. Check status of sampling and logging operations.
7. Check the mode of fluidized operation that Task 50 is executing.

SECTION 3

SOLID-WASTE PROCESSING STATION (TASK LP-13)

To satisfy the solid-waste feed rate of the CPU-400 Pilot Plant for the projected long-duration tests (100 hours or longer) of Task HP-4, it was required to expand the solid-waste storage and processing capability to handle at least 85 tons per day of as-received residential solid waste. Coupled with this provision was a requirement to transport the shredded and air-classified fuel fraction from the processing area to a solid-fuel storage and feed system serving the Pilot Plant fluid-bed combustor.

To meet this requirement, trade-off studies were conducted to evaluate the alternatives of expanding the existing storage and shredding facility, as installed in the main Pilot Plant building under previous EPA contract, versus the various siting options for a completely separate processing building.

It was determined that the existing facilities did not provide sufficient indoor holding area to support a 24-hour operation. Further, attempts to increase the output of the single 75-hp shredder and air classifier failed to produce the fuel quantities required to meet projected combustor feed rates of 100 lb/min on a continuous basis. The objectives of Task LP-13 therefore resolved to the design and development of a separate solid-waste processing station incorporating the following:

- Solid-waste receiving (tipping area) and covered storage.
- Shredding of residential solid waste at rates to sustain continuous operation of the Pilot Plant for 120 hours.
- Air classification capable of delivering a combustible fuel fraction comprising 80-85% of the as-received solid waste.
- Pneumatic transportation of the fuel fraction from the processing station to the Pilot Plant fuel-storage silo (Atlas).
- Provision for disposal of reject material from the air classifier.
- Adequate lighting for 24-hour operation.
- Fire protection for stored solid waste.
- Retention of wind-borne solid waste.
- Protection of personnel from noise generated by shredding of solid waste.
- Vector control and other health considerations.

The following paragraphs describe the design, construction, and check-out of this solid-waste processing station.

A. DESIGN

Solid-Waste Receiving and Storage Building

Conceptual designs of this facility were developed by CPC to meet the criteria specified above. Potential siting and land-lease arrangements were simultaneously reviewed, resulting in an approved location for the new building approximately 100 feet from the main Pilot Plant building. A final conceptual drawing and cost estimate of the complete facility, including installed equipment, was approved by the EPA Project Officer and go-ahead given to initiate final design, construction, and procurement of equipment.

A consulting civil engineering firm was engaged to develop detail facility designs and specifications; arrange for required soils investigation; handle all municipal use and building permits; prepare bid packages for candidate General Contractors; and assist in the award of the sub-contract and supervision of construction.

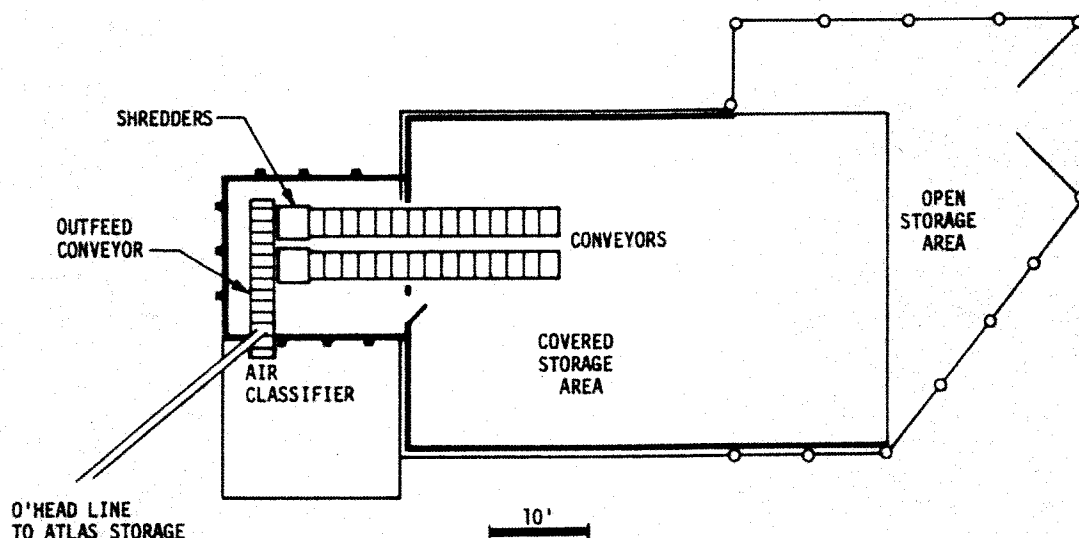


Figure 20 Layout of Solid-Waste Processing Station

The final facility design (a general layout is shown in Figure 20; Figure 21 is an isometric view of the arrangement) incorporates a 2500-sq-ft pad that provides tipping area for approximately 85 tons of solid waste. This amounts to approximately 20 packer trucks per day, delivering over a period of 6 to 8 hours (routine pickup). Two shallow pits are provided for individual shredder-feed conveyors, allowing solid waste to be pushed onto the conveyors from ground level. An adjoining roofless concrete-block acoustic wall (12 ft high) encloses an area for the two mini-mill Eidal shredders and their in-feed and out-feed conveyors. An adjacent external pad provides a working area for the air classifier and reject-handling equipment. The tipping area, beyond the building proper, is enclosed by a 12-ft-high, slatted

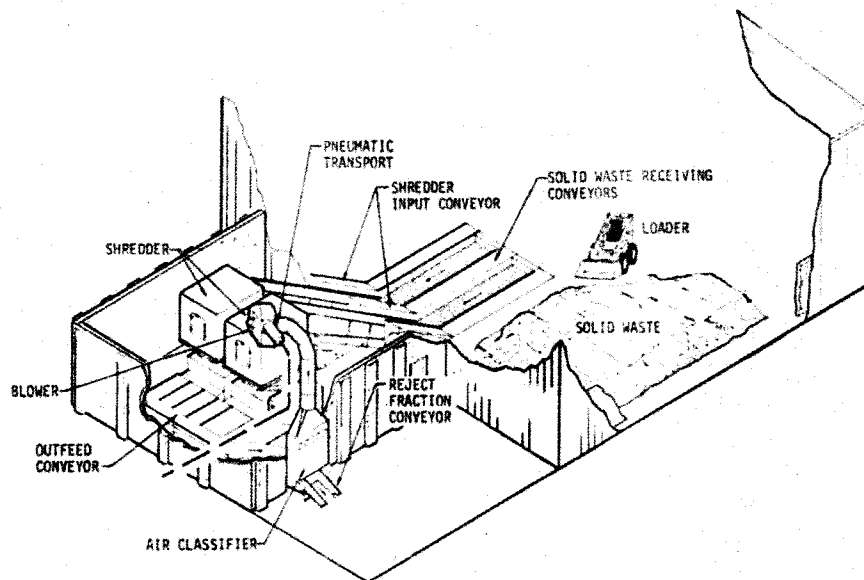


Figure 21 Solid-Waste Processing Station

cyclone fence and gate to contain blowing solid waste. The high water table at the site precluded the use of deep conveyor pits and conventional sewage and drain hook-up; portable sump pumps were therefore specified as a cost-effective means to handle drainage and wash-down operations.

Fire Protection

On inspection of the facility drawings and specifications, the local Bureau of Fire Prevention directed the installation of specific fire-protection equipment. A separate subcontract to a licensed fire-protection contractor provided design and installation of a dedicated water service, alarm system, and sprinkler heads over solid-waste storage areas, conveyors, and shredders. The system as installed was tested and approved by the Fire Department and insurance carrier.

Controls, Instrumentation, and Utilities

The facility is equipped with its own 400-amp, 600-V service line, and a motor-control center at the site. Communication lines are also provided between the Processing Station and the Pilot Plant control center in the main building. Air and service-water systems are also provided.

Health Considerations

Particular attention was given in the design to the development of construction details that minimize accumulation and retention of solid waste in corners, under equipment, etc. Provision is made for full wash-down of tipping area, shredder area, reject-collection area, and conveyor pits, with sumps and pumps to collect and remove the wash water. The facility has been approved by the County Health Department.

B. PROCESS EQUIPMENT

Shredder Infeed Conveyors

Two horizontal/inclined steel-belt conveyors are set in a pit to receive solid waste from the tipping floor and convey it to the shredders; conveyor belts are 4 ft wide and 37 ft long. Conveyor speed can be manually controlled; in usual operation, however, it is automatically controlled--in an on-off mode--according to current drawn by the shredder motors. This method of control assures a fairly constant volumetric output from the two shredders, while avoiding any inadvertent shutdown triggered by the thermal overload switches on the motors.

A portion of the conveyors can be seen in the view taken across the tipping floor, Figure 22; the manner in which the conveyors are fed is illustrated in Figure 23.

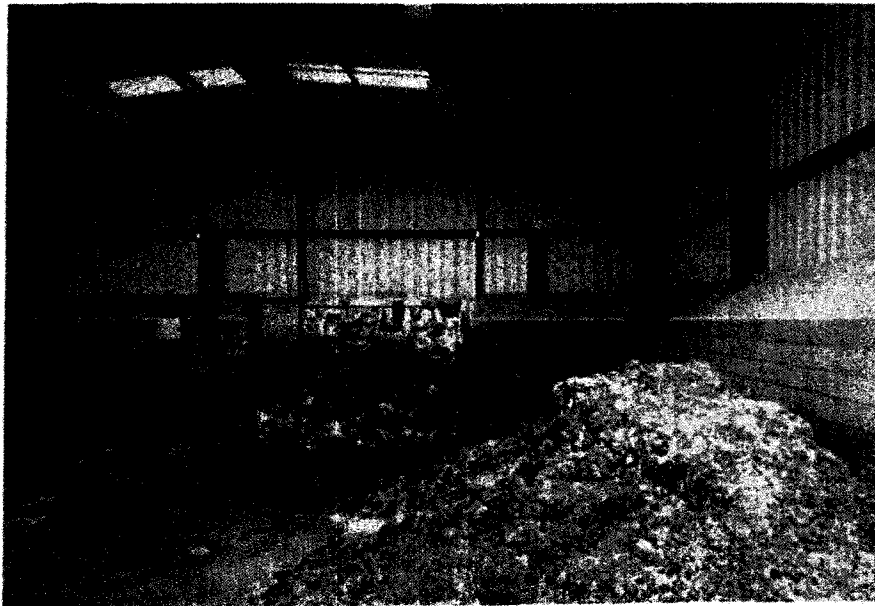


Figure 22 Solid-Waste Facility

Shredders

The tests that were planned for the CPU-400 Pilot Plant would require feeding up to 6000 lb/hr of solid fuel. Thus, to maintain fuel supplies and provide for the possibility of unscheduled maintenance on one of the shredders, it was predicted that a combined capacity of 4 tph would be desirable. To provide this, the existing 75-hp Eidal shredder, nominally rated at 2 to 2½ tph, was supplemented with another, similar unit. Trade-off studies led to a decision to purchase a somewhat improved version with a 100-hp motor. This new shredder was nominally rated at 3 to 4 tph of "wet domestic garbage." The combined output of the two units, shown in Figure 24, thus substantially exceeded burn-rate requirements and provided a substantial reserve capability.



Figure 23 Loading of Shredder Feed Conveyors by Front Loader

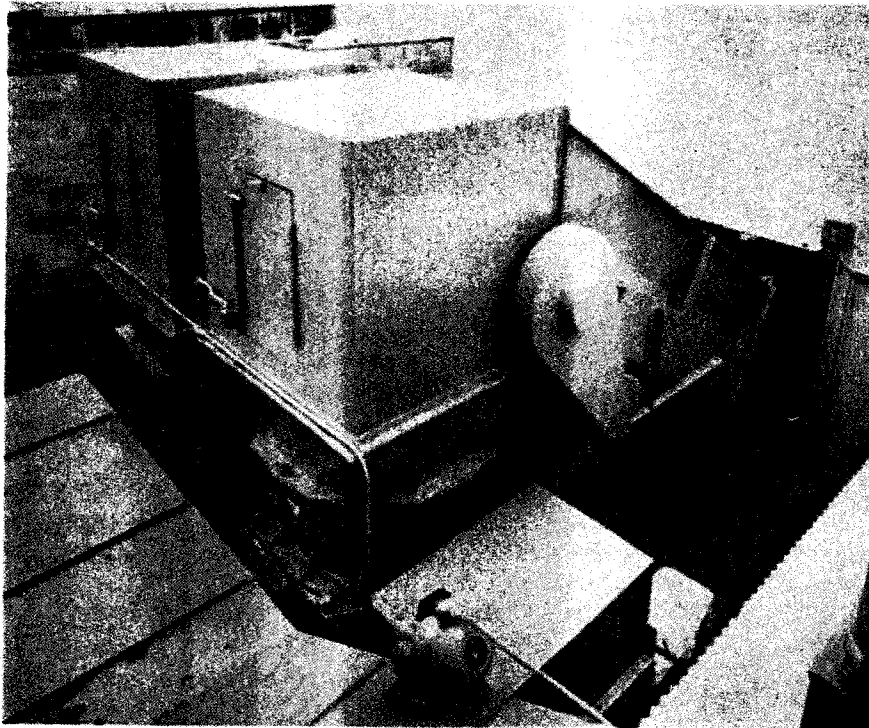


Figure 24 Shredders

No in-depth study of other makes of shredders was made, since the existing unit had already processed more than 250 tons of solid waste without requiring maintenance or replacement parts, and the identical outward geometry of the two similar units simplified the design of the associated hardware.

Outfeed Conveyor

Air classifiers developed during prior EPA contracts were designed to be close-coupled to the shredder exhaust. Experience revealed that such a configuration could not compensate for surges and slugs of high-density material without plugging completely or markedly reducing efficiency and throughput. Prior to and during the design of the Solid-Waste Processing Station, a series of subscale and full-scale tests with various air-classifier and feed-control devices resulted in a concept that provided consistent and predictable performance regardless of variations in shredder output. The design solution provides a horizontal/inclined outfeed conveyor with a surge box, on which the material is maintained at a depth of about 8 inches by rotating paddle-style load levelers. Rate of feed to the air classifier is controlled by varying conveyor speed, to compensate for variations in density, moisture content, and combustion characteristics of the material being classified.

It was found with residential solid waste that a setpoint could be found by trial and error that would provide a consistent and controllable throughput. The single steel-belt conveyor--like the infeed conveyors, 4 ft wide--receives the output from both shredders. The surge bin and conveyor are provided with a dust cover, a corner of which is seen at the lower left in Figure 24.

Air Classifier and Pneumatic Transport

The air classifier (Figure 25), fabricated of sheet steel, is 5 ft wide, 7 ft high, and 1 ft deep, and serves to separate the light combustible material from the heavy non-combustibles. It is fitted with a 7600-cfm industrial blower (Buffalo Forge Type OW, size 50) powered by a 60-hp 440-V 3-phase motor. Air entering the bottom of the unit is drawn up past a series of baffles, intercepting and dispersing the incoming solid waste. The baffles serve to create turbulence that assists in the separation of heavy and light materials.

The air classifier typically drops out about 16 percent of the material (heavy fraction) and about 78 percent (light fraction) is pneumatically transported to the storage silo; the remaining 6 percent is accounted for as moisture lost in shredding. The separation by this means into combustibles and non-combustibles is adequate, since the fluid-bed combustor is extremely tolerant of fuel composition, although about 12 percent of the light fraction is inert material in the form of glass, sand, metal foils, and ash (about 28 percent of the heavy fraction is combustible).

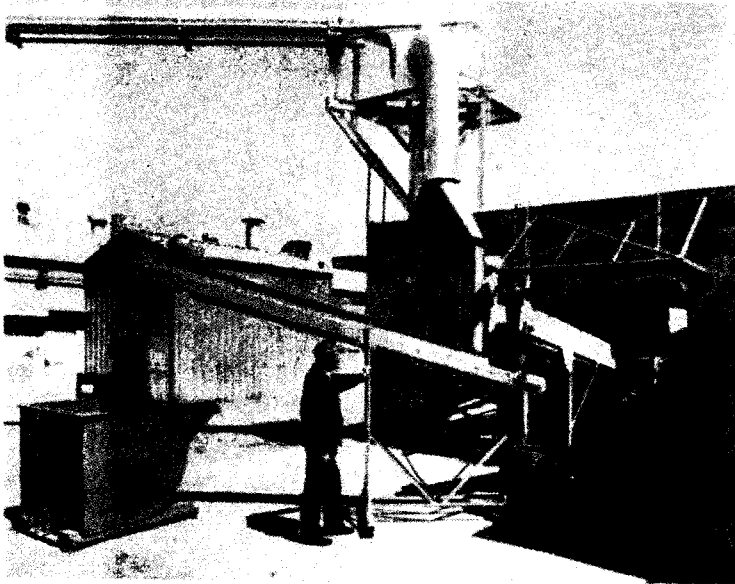


Figure 25 Air Classifier, Transport Line, and Simulated Material-Recovery System

The transport line is a 16-inch-diameter pipe about 275 ft. long. A conveyor moves the heavy fraction to a reject hopper; the hoppers are periodically hauled to the city's disposal site.

C. CHECKOUT

Checkout of the Solid-Waste Processing Station was conducted with two truckloads of weighed residential solid waste which were delivered to the tipping area and separately processed. Measured data and calculated results of the operation are shown in Table 2.

All parts of the system functioned as intended, and a total of 14,371 lb of air-classified combustibles was pneumatically transported to the Atlas storage facility; this amounted to 80.7% of the initial solid-waste input. One minor interruption occurred near the end of the operation, when a ragball caused a minor jam in the 75-hp shredder. Problems of this kind were later found to be characteristic of this type shredder, particularly with solid waste containing a high proportion of fabric and fibrous material. Corrective action consisted of requiring scheduled shutdowns to inspect the shredders and remove any accumulation of material that might restrict shredder output.

Sound-level measurements taken during processing are shown in Figure 26. Both OSHA and the California Administrative Code establish a sound level of 90dB(A) as the maximum allowable for 8-hour-a-day exposure. It is thus seen from Figure 26 that ear protection is needed in the shredder enclosure. The same codes allow 92 dB(A) for 6-hour-a-day exposure, and the pit area is seen to be acceptable without ear protection if the front loader does not operate more than 75 percent of the time. It is marginal, however, so ear protection has been called for in this area as well.

D. SUMMATION

In summary, the design, construction, and operation of the Solid-Waste Processing Station fulfilled all design requirements for supplying a continuous flow of processed solid-waste fuel for CPU-400 Pilot

TABLE 2
SOLID-WASTE PROCESSING DATA

	S/W Weight (lb)	Process Time (min)	Process Rate (tph)	Total Rejects (lb)	Organic Rejects (lb)	Ferrous Rejects (lb)
Truck #7	10,240	57	5.39	1983 (19.4%)	1505 (14.7%)	478 (4.7%)
Truck #5	7,560	43	5.28	1446 (19.1%)	1029 (13.6%)	417 (5.5%)
Total Avg.	17,800	100	5.34	3429 (19.3%)	2534 (14.2%)	895 (5.0%)
Density (lb/ft ³)	6				37	44

Con- dition	Vol. Air (cfm)	Blower Inlet Pressure (IW)	Blower Outlet Pressure (IW)	Blower Current	Atlas Pressure (IW)
No Load	6820	1.9	5.8	32.5 A	+.01
Load	-	1.7	6.0	32.5 A	-.02

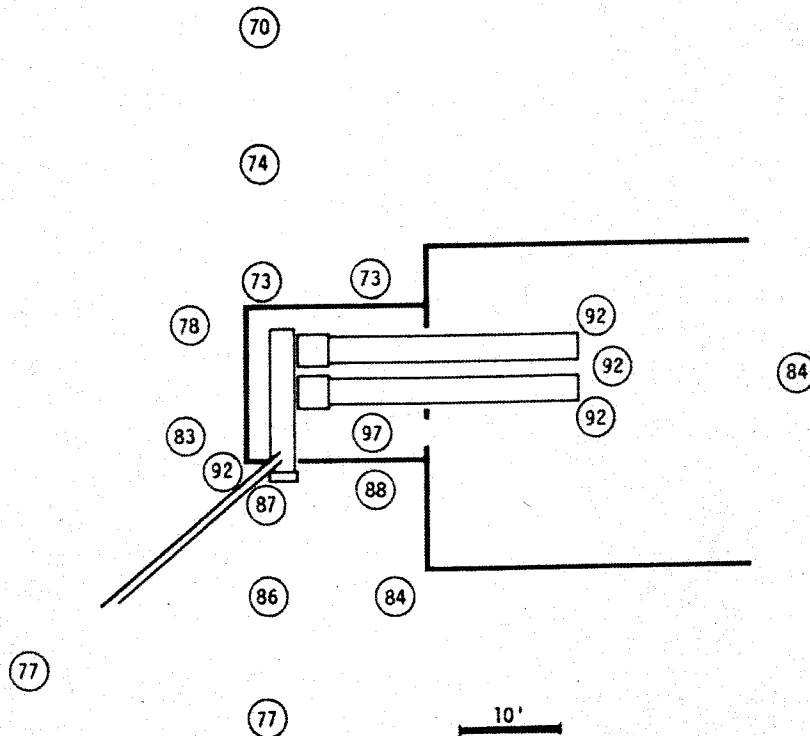


Figure 26 Maximum Noise Levels in dB(A) During Shredding and Transport

Plant consumption. The facility and its equipment were designed, installed, and checked out in time to meet the test schedule of Task HP-3. The full intended use of the facility (i.e., Task HP-4) was not carried out, but sufficient operating experience was accumulated to engender confidence that it could have supported all the long-duration tests originally planned without difficulty.

SECTION 4

TURBINE INTEGRATION AND CHECKOUT (TASK HP-3)

A. TASK OBJECTIVES

The overall objective of this task was to integrate the various Pilot Plant subsystems and verify operational capability of the completed Pilot Plant. To accomplish this, the task was divided into four test phases, as follows:

1. Phase A--Installation and checkout of the turboelectric system prior to integration with the fluid-bed combustor.
2. Phase B--Integration of the turboelectric system and operation with the fluid-bed combustor on auxiliary fuel (oil).
3. Phase C--Checkout operation of the completed Pilot Plant on solid-waste fuel, culminating with two-hour continuous operation under fully automatic control.
4. Phase D--Continuous operation of the Pilot Plant for 48 hours, under automatic control and burning solid-waste fuel.

The above Phases A and B were completed essentially as planned. Phase C was also completed, and met most of its stated objectives. The testing, however, uncovered problems with deposition and erosion of a magnitude sufficient to rule out completion of Phase D with the system in its then-existing configuration. The overall program plan was at that time revamped to include the design, fabrication, and installation of a granular filter (Tasks GF-1 and GF-2) and a program of corrosion, erosion, and deposition studies to be carried out in a model combustor (Task CP-6). Phase D was postponed pending those developments; and ultimately, the schedule did not permit its being carried out at all. Since Task HP-4 was dependent upon completion of Phase D, that work was also omitted.

B. TURBOELECTRIC SYSTEM CHECKOUT (PHASE A)

The special objective of this phase was to evaluate the turbine's as-delivered performance, to familiarize operating personnel with the

machinery, and to establish actual turbine baseline performance as a basis for analytical math models.

Commissioning tests were first carried out on the as-received turbine and turbine electrical system. Any initial difficulties that were encountered were worked out with the Ruston personnel who were on hand at the installation, and all components ultimately proved to be reliable and functional. A number of changes were then made in the turbine configuration to facilitate its integration into the Pilot Plant.

The fluid-bed combustor and separator vessels contain a large reservoir of pressurized hot gas when the system is operating, and release of this gas through the turbine would result in severe overspeed conditions for the power-turbine/generator shaft in the event of an electrical load shed. Unrestrained, the high rotational speed could cause great physical damage--if not the actual destruction of the generator. To forestall such a situation, a 1400-lb disc flywheel with a dual-redundant caliper braking system was added to the generator coupling.

The method for controlling speed under an electrical load also required some modification. While the turbine is operating on its own oil-fired combustor, the speed of the power turbine and generator is regulated by a governor that controls fuel flow. For reasons implicit in the foregoing, this system would not be effective for operation of the turbine on the fluid-bed combustor, and an alternative control had to be devised.

The system that was developed is completely unique, and relies primarily on using changes in electrical load to control turbine speed; it is diagrammed in Figure 27. As depicted there, the power turbine's speed is sensed by a magnetic speed pickup (SY 244), which produces a pulsating voltage signal whose frequency is directly proportional to the rotating frequency of the power turbine's shaft. The speed transmitter (ST 244) transmits this speed signal to the process-control computer (C/I 244), to a speed indicator (SI 244A), and to a speed-indicating proportional controller (SIC 244). SOC 244 receives its setpoint directly from the process-control computer (C/O 054). SIC 244 compares this speed setpoint to the turbine's speed signal and then generates an appropriate output error signal, which is used to correct the actual speed to the desired setpoint speed.

The error signal is fed to two different speed-control systems, one of which is for fine, and the other for coarse, speed control. The fine speed-control system consists of a servo-driven system called the exciter-voltage controller, which physically positions the wiper on the potentiometer (VAR) to provide generator-exciter potential control. (The output of SIC 244 is limited internally by an anti-reset windup module to insure that the exciter control maintains the generator's output voltage very close to the desired 480 V a-c. Coarse speed

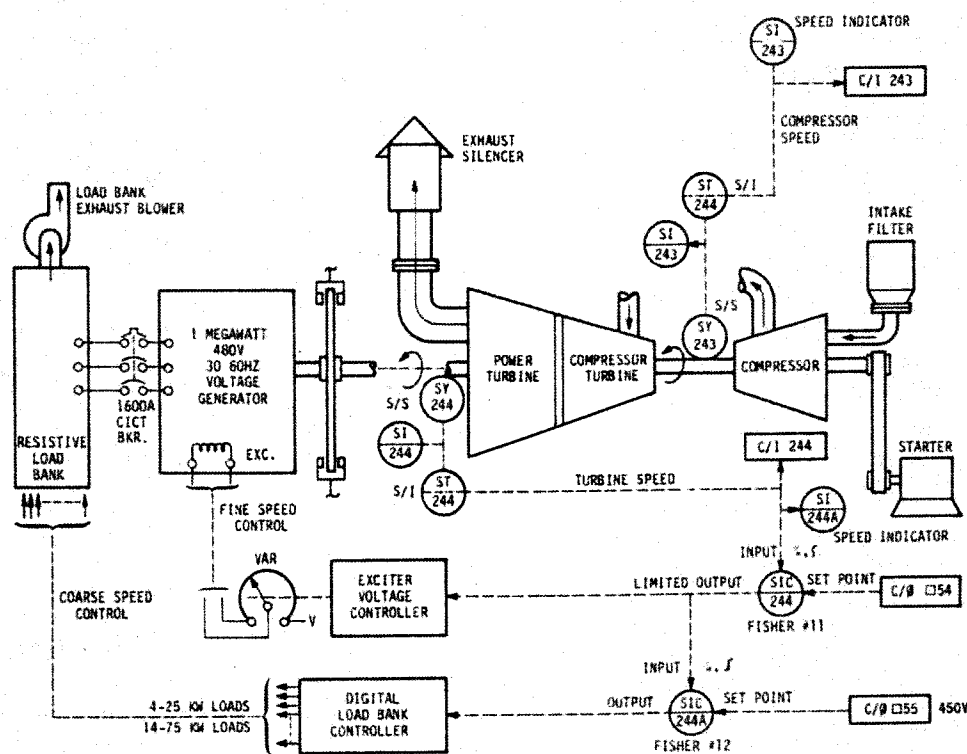


Figure 27 Speed-Control System

control is accomplished by the employment of a second proportional controller (SIC 244A) which also receives its setpoint from the process-control computer (C/O 055), but whose process-variable input comes from the limited output of the initial controller (SIC 244). The output of SIC 244A is the input signal to a digital load-resistance selector system, called the load-bank controller. The load-bank controller takes a 1-5 V d-c input signal, and in turn provides 18 digital outputs that are used either to apply load or to remove load from the voltage generator in discrete 25-kW increments, using the fourteen 75-kW and four 25-kW resistors available in the load bank.

The process-control computer actively senses the compressor-turbine speed (C/I 243), the power-turbine speed (C/I 244), and the total load applied to the generator, and by manipulating its setpoint outputs (C/O 054 and C/O 055) in software, exercises total speed control of the entire turbine-generator set to control startup overshoot, 3% and 10% overspeed conditions, compressor surge, and combustor-to-combustor transition.

These control loops provide effective fast-response speed control; the much slower response to changing fuel feed is called upon only when the desired load has been reached.

The turbine as delivered was equipped with a 20-hp d-c starting motor, with a mechanical clutch coupling it to the compressor shaft. The battery-powered motor was intended to operate infrequently and for periods on the order of one minute per startup. Starting the turbine in conjunction with the fluid-bed combustor would clearly require more sustained operation. A 30-hp a-c starting motor was therefore installed, connected through a fluid coupling and a speed-increasing vee-belt drive to the compressor's starter shaft.

The remaining major change was the relocation of the Ruston combustor, to put it in parallel with the fluid-bed combustor, and installation of the hot-gas piping leading from the third-stage separator to the power-turbine inlet.

Following these changes, trials were conducted with the revised starter configuration. A series of startup runs was made with varying turn ratios between the fluid coupling and starter-shaft sheaves and with varying amounts of oil in the fluid coupling; none was successful in attaining a speed sufficient to fluidize the combustor bed or to start the turbine if coupled to its own combustor. Whenever the sheave ratio was high enough to produce the desired speed, the trial would be quickly aborted by motor overload.

A 50-hp motor was then installed to replace the 30-hp one, and resistors were added to permit starting at a reduced voltage. The new arrangement was found adequate both to start the turbine on its own combustor and to fluidize the bed in the Pilot Plant combustor. This completed the initial checkout of the turboelectric system.

C. FLUID-BED COMBUSTOR ON OIL (PHASE B)

The objectives of this phase were to demonstrate system stability and controllability burning auxiliary fuel (oil), to evaluate system performance during startup, normal operation, and shutdown, and to evaluate the system of speed control by modulating voltage and load.

The initial testing consisted of a series of attempts to start the turbine in conjunction with the preheated fluid-bed combustor. For such an operation, the combustor bed is first back-heated from the oil burner in the combustor dome, the combustion gas passing through the bed and plenum and exhausting to atmosphere (passage from third stage to turbine is blocked during this operation). The freeboard and bed temperature histories of Figure 28 are typical for this operational mode. For the first 50 minutes, the bed temperature remains at the cold-sand level because the combustion-gas energy is given up to the upper sand layers; then the bed temperature rises at about 25 F/min.

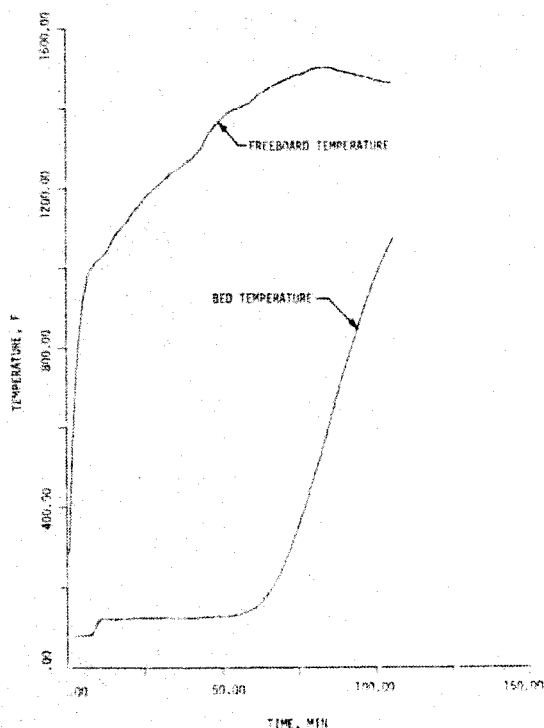


Figure 28 Backheat-Mode Temperatures

Backheating is generally continued until the temperature at the base of the bed reaches 1250 F.

The first startup attempts were by the simplest possible procedure, the output from the compressor being used to fluidize the bed and support oil combustion there. The results were, to say the least, disappointing. The thermal input at the combustor was completely dissipated in the long passage through cold vessels before the combustion gas reached the compressor turbine, with the result that the compressor turbine contributed essentially no net driving torque. Under these conditions the compressor -- driven by the starter motor only--could not develop a mass flow commensurate with the back pressure from the fluid bed, and surge ensued. At the outset,

as seen in Figure 29, compressor surge would take place at intervals of 30 to 40 seconds.

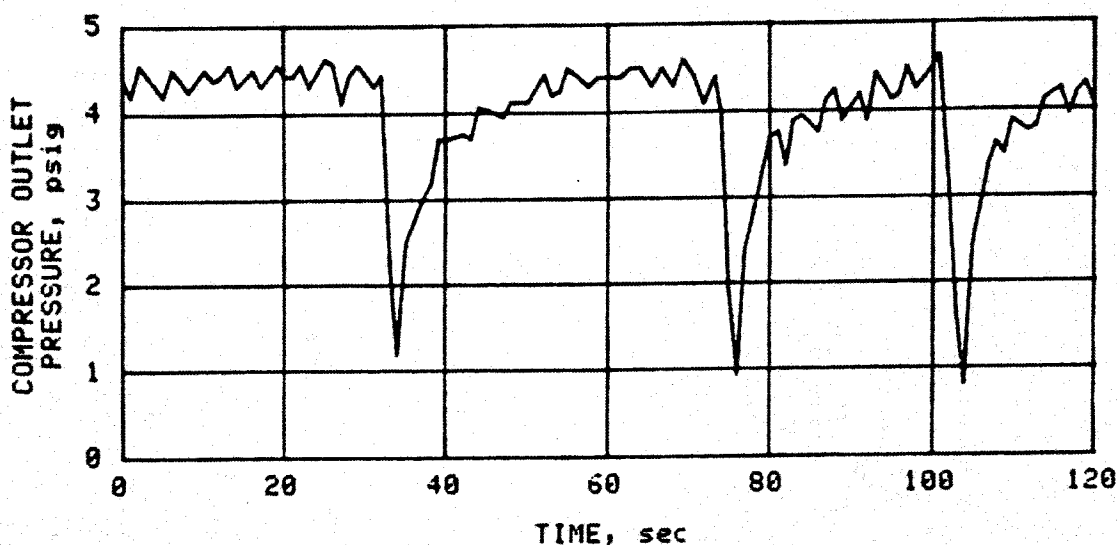


Figure 29 Compressor Surging During Startup Trials

To increase mass flow through the compressor and decrease back pressure, subsequent attempts were made with the exhaust valve from the plenum cracked open to bleed a part of the air to the atmosphere. This approach, of course, was to some extent self-defeating, since it reduced the mass flow available to the compressor turbine. Repeated attempts were made to find the minimum acceptable valve opening, such that compressor surge would be avoided while enough hot gas could still be generated at the turbine inlet to accelerate the compressor. The attempts were of themselves unsuccessful, but they did eventually produce a turbine-inlet temperature of 1200 F.

It was at this point concluded that higher turbine speeds would be required in order to initiate self-sustaining operation. The next series of trials was therefore made by starting the turbine on its own combustor, applying electrical load to bring up the turbine speed, switching the turbine air to the fluid-bed combustor, and firing that combustor as soon as fluidization was accomplished. A series of trials using varying levels of load eventually resulted in a successful transition with a starting load of 446 kW. Parametric data for this first operation of a turbine on a fluid-bed combustor are shown in Figure 30.

The crisis, so to speak, was passed about 130 seconds after the oil supply to the Ruston combustor was stopped. At that point, the pressure had dropped to 19 psig and compressor speed was down to 7950 rpm--very close to surge conditions. Pressure and speed began rising thereafter, however, and routine operation was established.

Turbine-inlet temperature is seen to have undergone a sharp drop immediately after the transition was started. This occurred because the separator vessels had been cooling during the several preceding trials, while temperature at the turbine inlet had been maintained close to 1200 F by the operation of the Ruston combustor. Some of the heat of the combustion gas was consequently dissipated in these vessels until they had been reheated.

The curve for generator rpm (note the expanded scale) shows very successful operation of the speed-control system. Variation around the mean value was only about $\pm 0.5\%$.

The maximum attained power level of just over 600 kW represents the limit of the oil pump fueling the fluid-bed combustor (a larger pump was subsequently installed). Once that level had been reached, a routine shutdown was carried out. It is worth noting that the shutdown was not in response to any operational difficulty: it was simply done because it was by then midnight of what had been a long and trying day.

This run established a startup procedure that was continued in use for much of the testing of Phase C, as follows:

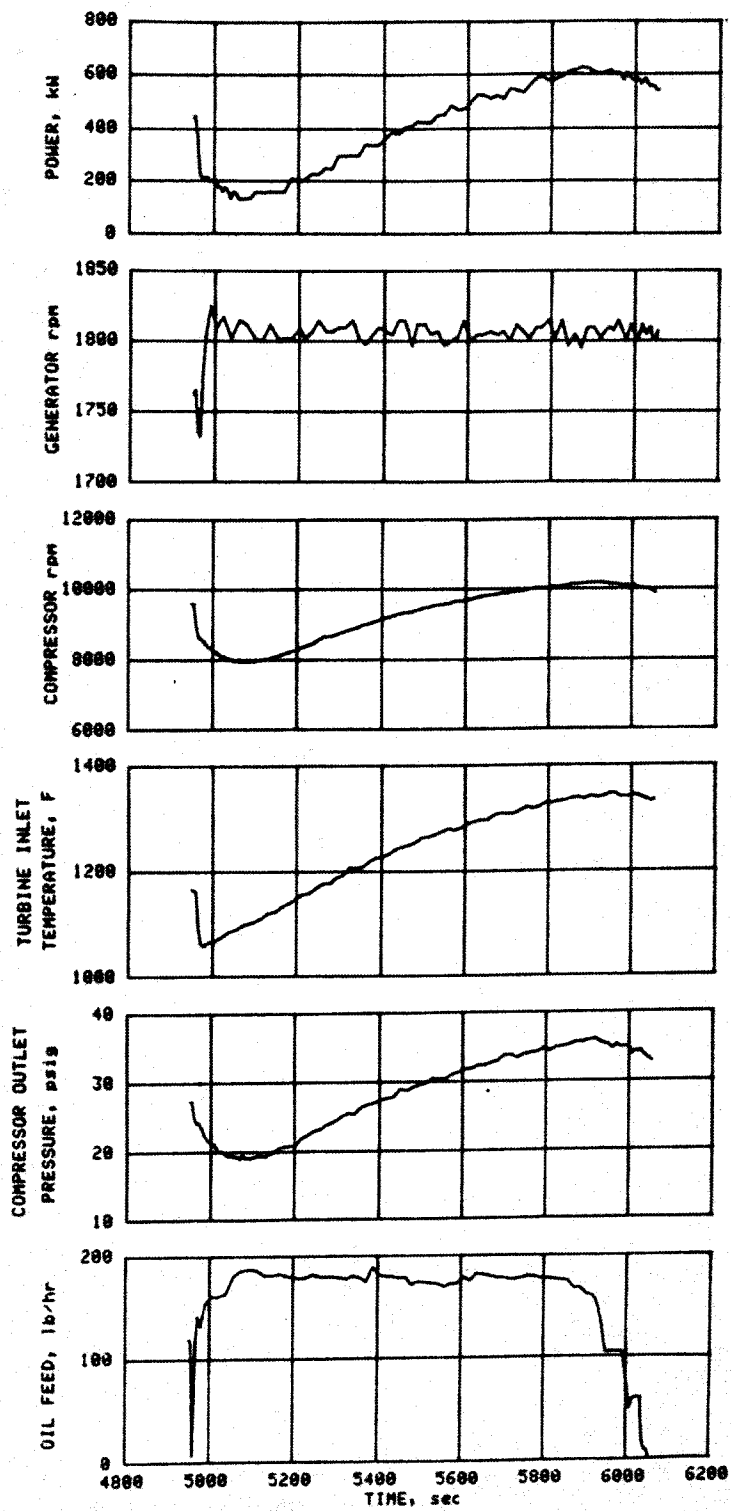


Figure 30 First Turbine Operation on the Oil-Fired Fluid-Bed Combustor, 19 March 1973

1. Combustor-bed backheat.
2. Preheating of the hot-gas system with the turbine driven by the starter and some of the compressor output being bled to atmosphere to prevent surge.
3. Shutdown when turbine-inlet temperature reaches 1200 F.
4. Startup of the turbine on its own combustor, followed by application of electrical load to increase turbine speed.
5. Transition by diverting flow of compressor air and oil from the turbine combustor to the fluidized-bed combustor.

D. SOLID-WASTE TESTING (PHASE C)

Objectives

The testing of Phase C marked the first introduction of solid fuel. The objective of this phase was to demonstrate system stability and controllability burning solid waste under fully automatic control. Initial tests were designed to evaluate system performance during transition from oil to solid waste, during full and reduced power outputs, under transient conditions, and during shutdown. Also to be evaluated were gaseous and particulate emissions.

Automatic startup, operation at full power for two hours, and a normal controlled shutdown were the final objectives of Phase C.

Chronology

The series of tests conducted within the scope of Phase C began as a straightforward effort to meet the stated objectives, but underwent a change of emphasis as the magnitude of problems posed by particulates in the exhaust gas became apparent; ultimately, it led to changes in the direction of the whole program here reported.

Table 3 lists the tests chronologically, along with some of the more significant information pertaining to each test. It will be helpful to consider briefly the sequence of events and decisions represented by the table, as background for the more extended discussion of specific areas of interest that follows.

The first test, run under manual control, served only to show that the outfeed conveyor from the Atlas storage vessel was not fast enough to meet the fuel requirements of full-power operation in Mode 10 (although 6 minutes of operation were in that mode); the conveyor

TABLE 3
PHASE-C TESTS

TEST	DATE(S)	FUEL	HOURS	MAX kW	REMARKS	PROBLEMS
1	4/13/73	oil/MSW	.75	650	Supplemented by oil.	Atlas outfeed inadequate to support Mode 10.
2	4/23/73	oil/MSW	.5	1100	Supplemented by oil.	Feeder valves ran rough and stopped from overload. Feed inadequate for Mode 10.
3	5/11/73	MSW	1.75	700	Computer control through Mode 8. Planned shutdown at end of day.	Some lesser mechanical problems, but both feeder valves functioned well.
4	5/17/73	MSW	1.0	1000	Computer control through Mode 8. Full power for 15 min.	Second-stage residue-removal line plugged.
5	5/24-25/73	MSW	.55	800	Computer control through Mode 10.	Minor mechanical problems. Test stopped when control computer dropped out.
6	5/31, 6/1/73	MSW	2.6	1000	Continuous run of 1.8 hr, with 1 hr at or near full power.	No serious problems; readiness for 2-hr test appeared confirmed.
7	6/6-7/73	MSW	1.7	850	First try at 2-hr run.	Temp. of 100 F prevented transition to Mode 8 on first day. Power limited by malfunction of one feeder valve. Trouble with plugging of residue-removal orifices.
8	7/2-3/73	MSW	5.25	750	Airlocks for residue removal from second and third stage. Two runs of 1.65 and 3.6 hr.	Inertial separators suffered plugging. Power severely limited by deposition in turbine.
9	7/19/73	MSW	1.6	900	Sand injection between second and third stage; water added to feed.	Solid-waste plug in one feedline after first 34 min.
10	7/20/73	MSW	3.5	1000	Sand injection and water added. Longest continuous run: 1.7 hr, with 19 min at full power.	Leveler jam on feed conveyor. Surge margin decayed as a result of deposition in turbine.
11	8/15/73	oil	1.7	650	Trial of water injection with turbine inlet at 1100 F.	Inadvertent closure of bypass valve caused compressor surge.
12	8/17/73	MSW	2.35	1000	Water injection, 1100 F TIT. Longest continuous run: 1.9 hr, with 50 min at full power.	One shutdown for inadequate feed, one for computer freeze-up. Serious deposition in turbine.
13	8/24/73	MSW	2.0	(a)	Water injection, 1050 F TIT.	Decaying surge margin caused shutdown.
14	8/30/73	wood	5.0	1000	1360 F TIT. Continuous run of 3.0 hr with average power of 900 kW.	Shutdown because fuel exhausted. Some deposition in turbine.
15	9/5/73	oil	4.0	900	Particulate check on oil.	Still some deposition.
16	9/11/73	oil	4.0	900	New sand bed.	None.
17	9/13/73	wood	2.6	900	First use of L.P. blower for pre-heat (manual control).	Some deposition, but no operating problems.
18	9/24/73	oil/wood	3.8	(a)	Wood at 5% normal feed. Computer-controlled preheat.	Mild deposition.

(a) Not recorded

- Mode 1: Combustor-bed preheat
- Mode 6: System preheat
- Mode 7: Operation on turbine combustor
- Mode 8: Operation on fluid bed (oil)
- Mode 9: Operation with oil & MSW
- Mode 10: Operation on fluid bed (MSW)

would need to be geared up. Then, in Test 2, difficulties were encountered with the feeder valves, and operation was again limited by inadequate fuel feed.

Tests 3, 4, and 5 showed a decreasing reliance on manual control, as computer software was being developed and checked out for system control of all operational modes from initial fluid-bed backheat through routine operation on MSW. After Test 6, which featured a 1.8-hr period of continuous Mode-10 operation--with an hour at or very near full power--it seemed the objective of two hours at full power under computer control would not be particularly difficult to attain.

Test 7, however, again experienced difficulties with the feeder valves. Additionally, plugging of residue-removal orifices gave some hint of the problem that was soon to overshadow all others: deposition. Airlocks were added to the residue-removal system for Test 8, but deposition in the turbine was beginning to limit the power that could be generated, and plugging of inertial separators became a problem. In Tests 9 and 10, sand was injected between the second and third separation stages to combat plugging by scouring the inertial tubes. The effect of adding water to the fuel was also explored, preparatory to running the tests to follow, wherein a reduced turbine-inlet temperature was used by way of exploring the nature of the deposition problem by ruling out the presence of molten aluminum in the gas stream.

Test 11 was run in Mode 8 (oil only) to establish baseline operating parameters for running with water injection and reduced turbine temperature. Test 12 came close to meeting the original objective; but in that test, and in the following Test 13, although aluminum deposits were significantly reduced, non-aluminum deposits formed. It was at this point that the program took on a new direction: plans were made for the development of a granular-bed filter (Tasks GF-1 and GF-2).

The remaining tests in the Pilot Plant were aimed at isolating some of the deposition-controlling factors, especially the role of aluminum in the solid waste. Test 13, using wood wastes as fuel, gave reduced but still significant deposition, as did the following Test 15 on oil. Residuals in the bed were shown to be the cause in the latter case: oil was burned in a new sand bed in Test 16, and no difficulties were experienced. Further quantitative information was sought in Tests 17 and 18, the one using wood as fuel, the other using oil supplemented by a small amount of wood. The last two tests saw the final steps in the evolution of the process-control system. In 17, the low-pressure blower used for backheat replaced the turbine's compressor (running on the starter motor) as the source of combustion and fluidizing air for system preheat (Mode 6); in 18, this revised operation was put under computer control.

Performance

The CPU-400 Pilot Plant is a totally new kind of power system. Its "shakedown cruise" understandably encountered numerous electrical and mechanical difficulties. But these were and are amenable to correction, and those tests that were successfully completed did demonstrate the feasibility of this kind of power system, provided that deposition (and the closely related phenomena of corrosion and erosion) can be eliminated as a limiting factor. Sections VII and VIII point the way to accomplishing that.

At the completion of Test 6, solid waste had been burned in the Pilot Plant for just under 6 hours; accumulated deposition had not yet reduced performance levels by any appreciable amount. Figure 31 shows parametric data for the run of 1.8 hours that was completed in Test 6, under fully computerized control. Note that the voltage modulation employed in the speed-control loop is over a very narrow range. Overall control was good, in spite of fairly wide swings in system pressure, caused primarily by variations in fuel composition.

Tests 10 and 12 featured continuous runs of 1.7 and 1.9 hours, respectively. Test 10 was a first trial of adding water to increase the mass flow through the turbine, prior to fabrication of a system for water injection. The total MSW burn time was 3.5 hours, average feed rate over that time span was 100 lb/min, and average moisture content of the fuel was 27.6%. Water was sprayed on the MSW passing along the transfer conveyor at a rate of 8.4 lb/min, bringing effective moisture content to an average value of 30.2%. The result was an increase of about 50 kW in power output for otherwise like conditions. Figure 32 shows the results during the 1.7-hr run.

Test 10 was actually terminated when a load leveler at the transfer conveyor jammed, but a decaying surge margin, also shown in Figure 32, indicates that deposition in the turbine was becoming increasingly troublesome.

In Test 12, water was injected into the hot-gas system, both in the bed and downstream of the combustor (half at each location). Total water addition was at 110 lb/min, resulting in a turbine-inlet temperature of 1100 F, and a 10-percent increase in the fuel rate. Figure 33 shows the power generated (and the generator speed) during the 1.9-hr run. The full-power capability under these operating conditions is evident--momentary peaks above 1100 kW were attained.

In this instance, water injection was used to increase mass flow through the turbine, in compensation for the reduced turbine-inlet temperature used to freeze out aluminum. The fact of its success in that regard reveals this as a potentially powerful means of system control; the turbine responded well to the added mass flow so generated.

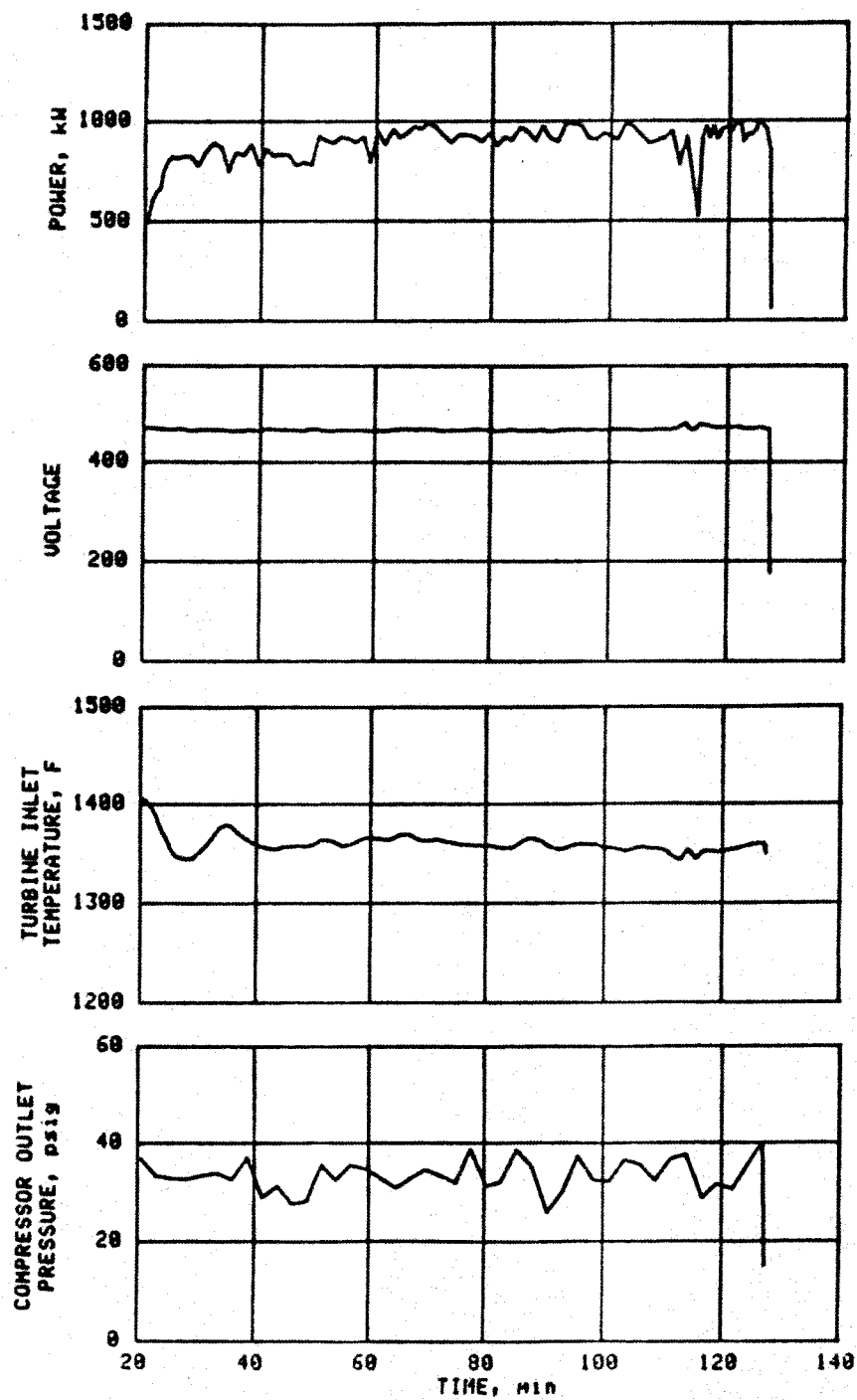


Figure 31 Operational Parameters in Test 5 on MSW

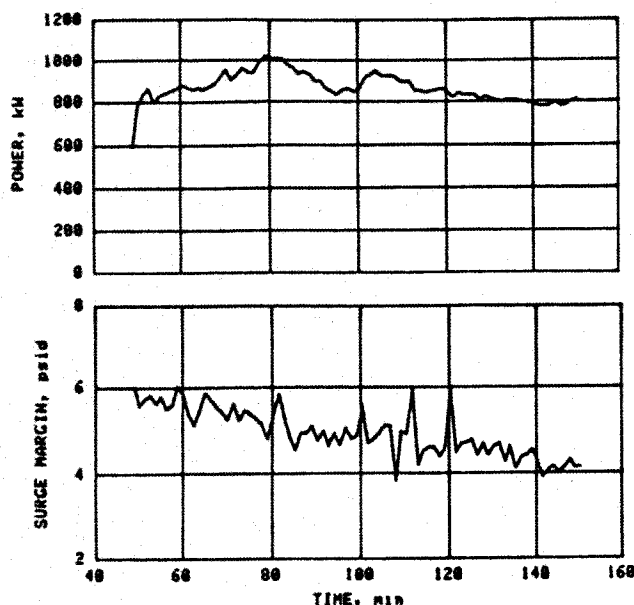


Figure 32 Test 10 on MSW with Water Added

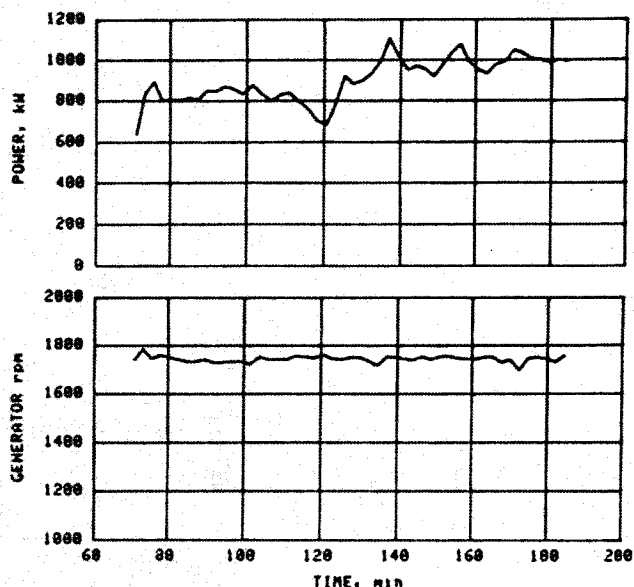


Figure 33 Test 12 on MSW with Water Injection

The success of the system for controlling speed by adjusting load is also evident in Figure 33.

One further comment on performance is in order: the failure, in the first attempt at Test 7, to transition from the turbine combustor to the fluid bed on a hot day does not represent any real system limitation. On that particular day, there had been extended delays after the preheat of the hot-gas system. The combination of the partially cooled system and the high temperature of intake air caused the difficulties. Procedures were instituted to assure adequate system preheat, and the problem did not recur.

Exhaust Constituents

Results of exhaust-gas sampling during the tests here reported are shown in Table 4. The uniformly high levels of O_2 --and the low levels of CO_2 --reflect the fact that the fluid-bed combustor is operated at 300% excess air. As a result of the intimate mixing in the fluid bed of hot sand particles with the fuel, high combustion efficiency is obtained, as evidenced by the very low levels of CO and CH_x .

Precise conversions of ppm to lb/million Btu is dependent, among other things, on the heating value of the fuel being fed when the sample is taken. A

TABLE 4						
GAS ANALYSES						
Test	O ₂ %	CO ₂ %	CO ppm	CH ₄ ppm	SO ₂ ppm	NO _x ppm
4	15.8	2.5	50	3	50	110
10	16.2	2.7	50	2	35	92
12	14.4	3.8	40	7	15	135
14 (wood)	16.0	6.3	50	3	14	106

rough rule of thumb, however, is that 150 ppm corresponds to about 0.7 lb/million Btu. It is thus seen that SO₂ presents no problem in combusting either solid waste or wood. The levels of NO_x are somewhat closer to the standard, but seem not to be any real cause for concern.

Table 5 shows results of particle sampling. Except for the single low value recorded in Test 4, the total loadings recorded for solid-waste combustion would exceed the applicable standard if corrected for 12% CO₂. As will be seen below, however, there is a far more compelling reason for developing improved methods of filtration; i.e., the loading is excessive as regards continuous turbine operation. Comparison of total loadings with the inerts content of the fuel indicates that the separators employed had overall collection efficiencies ranging from 90 to 99% (since bed growth was minimal, it may be assumed that most of the inerts were still present in the exhaust). However, they are evidently unable to remove the very fine fraction (note that very little of what comes through is larger than 5 microns). A much larger proportion of the fines must be removed to provide a viable system; it is that fact that gives impetus to the development of the granular-bed filter.

TABLE 5		
PARTICLE SAMPLING		
Test	Total Ldg. gr/scf	Ldg. >5µm gr/scf
4	.028, .013	.00026, .00005
5	.100	-
6	.162, .126	.00020, .00020
7	.034	.00040
8	.070, .110	.00013, .00015
9	.094	-
10	.067, .124, .161, 0.79, .165	-
14 (wood)	.007	.00005

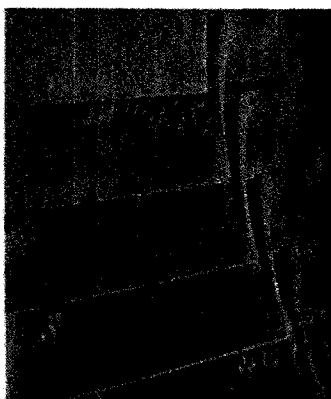
Deposition and Erosion

Deposition first showed up as a critical problem between Tests 4 and 5: during a brief checkout of new computer software, it was found that the second-stage residue-removal line was plugged. When the plugging was cleared, Test 5 was conducted without incident, although post-test inspection revealed some ash accumulation at the outlets of the second- and third-stage separators. During system heatup for Tests 6 and 7, plugs developed in the residue-removal lines of both the second and third stages. The nature of the plugs showed that hard deposits were developing in the ash hoppers of the separator vessels, and then flaking off during later cooldown and heatup. Double-ball-valve airlocks were added beneath both vessels to provide for removal of chunks such as these that could not pass through the bleed orifices.

One of the airlocks (second stage) plugged during heatup for Test 8; that plug, however, was cleared by simultaneous opening of both airlock valves. All inertial separators had been cleaned before starting Test 8; post-test inspection revealed that 16 of the third-stage cones were partially plugged and three completely so. In the second stage, two were partially and one completely plugged. A rising system pressure also indicated some restriction of flow area in the turbine.

The turbine was cleaned out before starting Test 9. A decaying surge margin during Tests 9 and 10 (this was shown in Figure 32) indicated, though, that flow area was again being restricted. Inspection at this time revealed the worst deposition experienced at any time in the Phase C testing--and the situation was now complicated by severe erosion.

Deposits in the compressor turbine were as much as 1/8 in. thick. Most of the deposition was relatively loose, but there was also a development of quite hard deposits on the blades, as seen in the two views in Figure 34. Even some of the "loose" material was sufficiently coherent to remain attached to the inlet volute cowl, as can be seen particularly on the left side of Figure 35.



(a) As First Revealed (b) After Removal of Loose Flyash
Figure 34 Deposition in Compressor-Turbine Stator

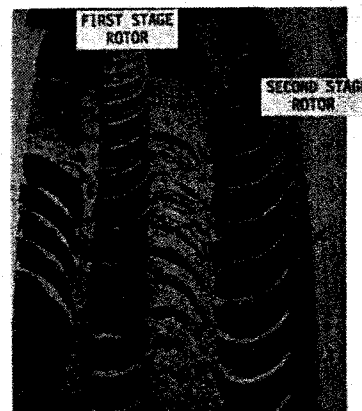


Figure 35 Deposits on
Compressor-Turbine Rotor

The hard deposits that adhered to the blades required thermal shock with an oxy-acetylene torch and sandblasting to effect their removal.

There was pitting--of a type that was probably caused by particle impingement--on the leading edges of blades in the first-stage stator. Potentially catastrophic erosion, however, was in evidence on the blade roots of the second-stage stator (Figure 36). There was evidence of spalling of the buildup on the first row of rotor blades. Thus the severe erosion in the second stage can be laid to a sequence of deposition, agglomeration, and re-entrainment as relatively large chunks. The pitting of the first stator stage nevertheless gives evidence that the unaltered gas-borne particulate could present an erosion problem in the long term.



Figure 36 Root Erosion of Second-Stage Stator Blades

Inspection of the first-stage separator revealed a two-inch hole in the spinner duct, doubtless a contributing factor in the high loadings experienced.

Inspection of the second-stage separator revealed deposits on the outsides of the outlet tubes. The vane areas were mostly clean, but all inlet tubes had heavy (up to $\frac{1}{4}$ ") deposits on the first eight inches of the inside surface at the tube entrance (Figure 37). A large crack was found in the weld at the top of the hopper, so situated as to provide a direct passage for re-entrainment of separated particulate.

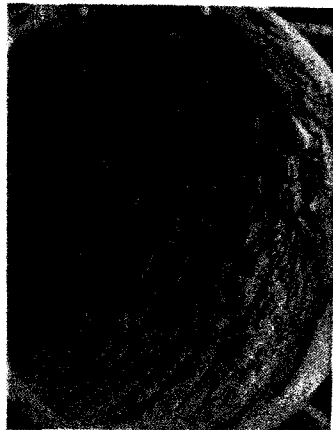


Figure 37 Deposits in Entrance of Vane Tube of 6-inch Inertial Separator

Samples of deposits were subjected to analysis by emission spectrography (a semi-quantitative method). Results are shown in Table 6.

The high level of aluminum, and particularly the ratio of aluminum to silicon, indicates that significant amounts of aluminum metal remained after three separation stages. Silicon is present as silicates from paper pigments, soil, and the bed sand. The relatively high levels of calcium, sodium, potassium, and magnesium are probably derived

TABLE 6
COMPOSITION OF ASH DEPOSITS

Element	Inertial-Separator Outlet (3rd Stage)	Inertial-Separator Wall (3rd Stage)	Stator Blades
Silicon (Si)	25 %	25 %	17.5 %
Aluminum (Al)	40	25	Principal
Calcium (Ca)	10	10	1.25
Sodium (Na)	4	12.5	0.75
Iron (Fe)	4.5	7	1.5
Titanium (Ti)	2.5	3.5	0.85
Potassium (K)	3.5	7.5	1.0
Magnesium (Mg)	1.75	1.5	1.25

Note: Minor constituents omitted

from common bottle glass or soda lime glass, which may contain the following percentages of the several oxides:

SiO ₂	72%	MgO	3%
K ₂ O+Na ₂ O	15%	Al ₂ O ₃	1%
CaO	9%		

Other glasses may contain different proportions of these elements, as well as boron oxide and lead oxide. Potassium may also be introduced in foodstuffs, and could react with kaolin (in paper pigments, say) to be present in the ash as feldspar.

Alkali-metal oxides are fluxes that reduce the melting or softening points of Al₂O₃ and SiO₂. The presence of the alkali metals can reduce the softening point of alumina, iron oxide, and silica mixtures appreciably. The possibility exists that fluxed Al₂O₃/SiO₂ forms a soft sticky ash that deposits and agglomerates on system walls and turbine blades.

Low-melting glasses are also potential binders. Common soda-lime glass may soften at 1300 F and lead-silicate glasses at 1100 to 1200 F.

Additional analysis showed that the turbine-blade deposits contained a large amount of elemental aluminum as well as Al₂O₃. Since the melting point of aluminum is 1220 F, it would be molten in the gas stream. It would be protected against complete oxidation by an oxide skin, but that skin would be easily ruptured by impingement, and the molten aluminum released would be an effective binding agent.

Glasses and aluminum provide the most reasonable sources of agglomeration in the deposits found. If either were responsible, then a temperature reduction could be expected to render them inoperative.

Operation with turbine-inlet temperatures of 1050 and 1100 F would not provide an overall system capable of meeting the original CPU-400 goals. Tests 12 and 13, which employed those temperatures, were there-

fore run not as an effort to reach the original task goals, but to shed additional light on the nature of the deposition problem. The deposit problem, in those tests, was not totally eliminated, but it was drastically reduced. Some hard deposits were found after Test 12, but only in the form of a light bead along the leading edge of compressor-turbine stator blades. There were no hard deposits following Test 13, although there was some soft ash accumulated on the concave sides of the stator blades.

The remaining tests were conducted to further isolate causes by using a fuel that was virtually aluminum-free. Tests 14 on wood (Ponderosa pine) and 15 on oil still developed both hard and soft deposits. These were shown by the final three tests, run with a new sand bed, to have arisen because of residuals in the old bed. Test 16 on oil generated some very minor deposits, all soft; Test 17 on wood produced some slight deposition, but none of it hard. Test 18, using oil plus wood at 5% normal feed, resulted in almost no deposition. There was some hard deposition, but only in the form of a hairline bead along stator-blade leading edges.

This closed out the testing in the Pilot Plant. Study of deposition--along with erosion and corrosion--was carried out thereafter in the Model Combustor, as Task CP-6.

SECTION 5

WEYERHAEUSER WOOD-WASTE TESTING

Because the fluid-bed concept is adaptable to the combustion of a wide variety of low-grade fuels, the Weyerhaeuser Company was actively interested in the CPU-400 concept, and considering development of a prototype system for generating electrical power by burning wood wastes (hog fuel). It was proposed that a 100-hour test be conducted in the Pilot Plant. Since wood wastes and municipal solid waste are virtually interchangeable with respect to system operation, and since the proposed test would add useful data and operating experience to the ongoing EPA program at no additional cost to that agency, their permission was sought and obtained for carrying out the testing. (The conduct of Task HP-3 had already been postponed pending installation of the granular filter).

The program will be briefly recounted here; a full discussion may be found in Reference 2.

A. SYNOPSIS OF TEST EVENTS

The testing program was divided into three phases as follows:

1. A system preheat and checkout that involved only 10 minutes of wood combustion.
2. Test Sequence A, comprising 18.8 hours of wood combustion.
3. Test Sequence B, comprising 82.0 hours of wood combustion.

Seventeen separate starts of the turbine were made in accumulating the total of 101 hours of wood combustion. As seen in the summary, Table 7, three of these included multiple periods of wood operation separated by intervals of operation on oil, during which problems were resolved.

Checkout Test

System preheat was completed with only one untoward incident: midway in the operation, the process-control computer tripped with a parity error in one of the semiconductor memory boards, and the preheat was completed under manual control. The board was replaced in time for

TABLE 7
SUMMARY OF TURBINE OPERATIONS ON WOOD

Turbine Start	Wood-Burning Segments (hr)	Reason for Termination of Wood Combustion
System Checkout		
1	0.17	Feed-system adjustment problems
Test Sequence A		
2	0.10	Low setting on load-bank current Monitor
3	0.72	Fouling of storage-tank sweeps
4	4.80	Plugged wood feedlines
5	0.51 6.01 1.20 4.21 1.22	Transfer-conveyor leveler needing adjustment Plugged wood feedlines Jammed transfer-conveyor leveler Jammed transfer-conveyor leveler Planned Shutdown
Test Sequence B		
6	8.75	First-stage ash outlet plugged
7	1.76	Third-stage ash outlet plugged
8	24.48	Feeder-valve electrical problems
9	2.67 0.10 8.83	Storage-tank outfeed conveyor stalled Unresponsive outfeed conveyor Procedural error cleared computer data base
10	3.75	Cracked water jacket, second-stage ash outlet
11	2.26	Turbine-annunciator malfunction
12	1.19	Turbine-annunciator malfunction
13	1.36	Turbine-annunciator malfunction
14	9.11 5.07 0.19	Low bed temperature Faulty conveyor control Low bed temperature
15	6.21	Generator Overspeed
16	0.24	Procedural error
17	6.10	Planned shutdown
Total	101.01	

the computer to participate in all subsequent operations, and no further computer-hardware problems occurred in the entire test program.

Although the checkout involved only 10 minutes of wood-burning operation, it was sufficient to show that load levelers on the transfer conveyor would need adjustment in order to develop a sufficiently low rate of feed, and that the high moisture content of the fuel would require that some of the combustion air be bypassed to the turbine in order to keep both bed temperature and mass flow through the turbine sufficiently high.

Test Sequence A

This test was planned as a single 24-hour operation on wood combustion, after which the system would be cooled to permit compressor-turbine inspection. As shown in Table 7, however, four separate turbine starts contributed to a cumulative 18.77-hour duration. The test was intentionally terminated short of 24 hours because the surge margin was repeatedly dropping below 1 psid.

The most significant incidents during the test were the fouling of the sweep buckets in the storage tank and jamming or plugging in the feed system from tank to combustor. The first of these occurred when the sweeps tended to climb on top of the wood in storage and jam in the tank framework; it was remedied by removing two buckets from each sweep. The second kind of problem showed that the system as configured could not consistently handle some of the larger pieces of wood; such problems were totally eliminated in sequence B by manual removal of oversize pieces. For more extended operation, of course, they could be prevented by appropriate pre-processing and/or screening.

Turbine start No. 5 resulted in 14.75 hours of continuous fluid-bed operation, of which 13.15 hours, or 89%, were run with wood as fuel. During this--and the previous start--there was a plug in one of the feedlines, and the entire run was carried out with only one feedline operative. No difficulties resulted from the single-point feeding.

Following that test sequence, an inspection of the turbine revealed a heavy buildup of soft, porous, light-green material on the first stage of compressor-turbine stator blades. Heavy deposits of tan ash were found distributed from the second stage of the compressor turbine through the power turbine. Only a small amount of hard deposit was found, all in the stator root area. Turbine-blade erosion appeared negligible, so the stages were all cleaned and reassembled for Test Sequence B.

Test Sequence B

To prevent the buildup of turbine-blade deposits, a blade-cleaning system was incorporated for Test Sequence B. The cleaning medium consisted of ground (12-20 mesh) walnut shells, having a bulk density of

35.5 lb/cu ft. (The material was locally available, and had been successfully employed by others). As shown in Figure 38, an airlock system was used to feed the shells at a nominal rate of a one-pound batch each hour. This technique was successful in markedly reducing the overall rate of surge-margin decay.

Turbine starts 6 and 7 were both terminated by plugging of ash-removal lines; in each case, the plugs developed out of conditions attendant on the preceding shutdown. The chief operational problem with the removal system is the maintaining of satisfactory conditions during start and stop transients and in standby periods.

The run following turbine start 8 (Table 7) was the longest continuous run achieved. Satisfactory operation of the temperature-control systems, in the fully automatic mode, is demonstrated by the following statistics recorded for 25 samplings during a 48-minute period.

	<u>Mean</u>	<u>Std.</u> <u>Deviation</u>	
Bed Temperature, F	1350.6	5.4	(Setpoint, 1350)
Freeboard Temperature, F	1475.5	5.6	
Turbine-Inlet, Temp. F	1319.1	5.3	(Setpoint, 1320)

With minor perturbations, the surge-margin history for turbine start 8 was well represented by three straight line segments, as follows:

0-4 hr, increase from 5.3 to 6.5 psid
4-20 hr, decrease to 6.1 psid
20-24 hr, decrease to 5.3 psid

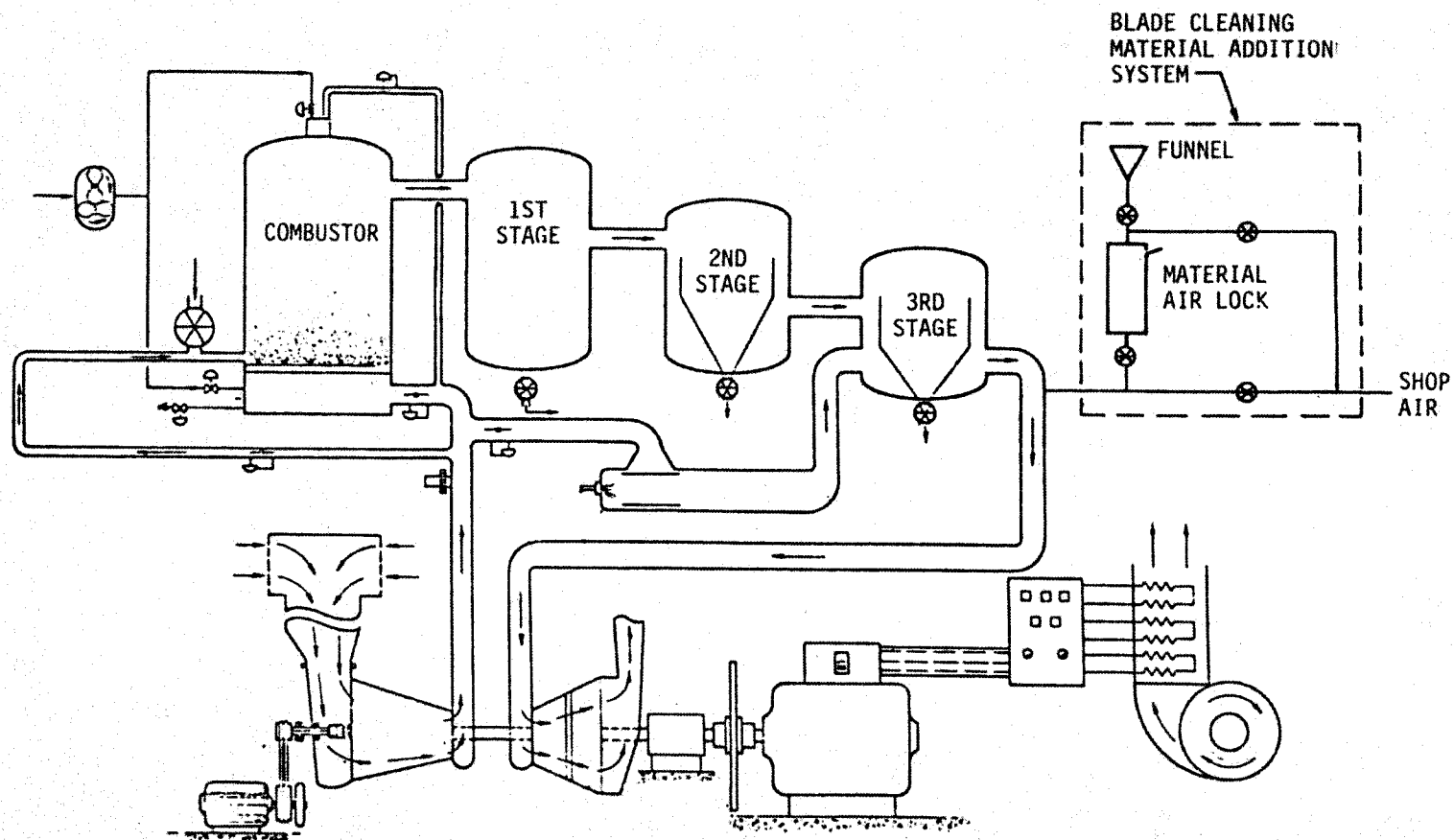
For the remaining 47 hours of testing (turbine starts 9 through 17), the surge margin continued to behave in much the same fashion as indicated by the above observations.

By comparison with other test periods, start 14 was troubled with relatively poor temperature regulation. Difficulty in maintaining bed temperature was encountered several times, apparently due primarily to abrupt changes in wood moisture content. The first interruption of wood combustion was for 20 minutes of oil operation to recover from a sudden drop in bed temperature to 1050 F; a later sudden plunge of bed temperature to 900 F concluded with an automatic system shutdown.

B. SUMMARY OF RESULTS

Fuel Consumption

A review of weighing-conveyor records showed that 283.67 tons of material were processed over the total test period; 1.65 tons were in the



1A 221-331

Figure 38 CPU-400 Pilot Plant with Injection System

form of makeup sand for the bed. Fuel consumption thus breaks down as follows:

	<u>Weight (tons)</u>	<u>Flow Rate (tons/hr)</u>
System C/O	0.35	2.10
Sequence A	48.55	2.59
Sequence B	<u>233.12</u>	<u>2.84</u>
Overall	282.02	2.79

Bed Makeup

Over the 101-hr test, 3300 lb of sand was added, for a final average rate of 0.54 lb/min. Bed pressure drop at the conclusion of the test was 30.85 IWD, compared with an initial value of 33.87 IWD; to maintain a constant bed depth, therefore, the rate of addition would have had to be about 0.66 lb/min (just under one-half ton per day).

Fuel Analysis

Periodic samplings during the test enable a good characterization of the hog-fuel properties as conveyed into the combustor. Mean values were as follows:

Wet-Basis Composition

Moisture fraction	0.4262
Combustible fraction	0.5570
Inerts fraction	0.0168

Dry-Basis Composition

Combustible fraction	0.9708
Inerts fraction	0.0292

Higher Heating Value:	8575 Btu/lb
Lower Heating Value:	8020 Btu/lb

By way of providing perspective, the addition of sand to the bed at 0.66 lb/min is equivalent to increasing the inerts fraction of the fuel (dry basis) from 2.92% to 4.10%.

Combustion Efficiency

Two performance intervals in Test Sequence B were selected for combustion-efficiency calculations, one of 6 hours and one of 10. The results gave 99.76% for the first period and 99.74% for the second.

System Performance

Tables 8 and 9 provide performance statistics for two steady operational periods separated by 45 hours. Both periods are from Test Sequence B, so the surge margin shows the expected very low linear-regression rate, a slow increase indicated in one instance and a slow decrease in the other.

High fuel moisture presented some temporary problems, but these were well handled by bypass control. The direct effect of high moisture is to shift more of the combustion reaction and heat release from bed to freeboard. Maintenance of a fixed bed temperature of 1350 F in the presence of this afterburning requires that a significant airflow be diverted from the bed and bypassed to mix with the hotter exhaust gases before turbine entry. For wood of 40 to 50% moisture content, a bypass of 15 to 25% of the air is required. By comparison, bypass ratios under 10% are sufficient for moisture contents of 20 to 35%, such as are typically encountered with municipal solid waste.

Gaseous Emissions

The average exhaust-gas compositions for Test Sequences A and B are compared below.

	<u>CO</u> <u>(ppm)</u>	<u>CH_x</u> <u>(ppm)</u>	<u>SO₂</u> <u>(ppm)</u>	<u>NO_x</u> <u>(ppm)</u>	<u>CO₂</u> <u>(%)</u>	<u>O₂</u> <u>(%)</u>
Sequence A	165	2.0	12.1	48.5	5.0	14.4
Sequence B	45	1.6	0.0	66.0	5.8	14.1

The difference in CO level between the two sequences probably reflects the use of a single feedline in A, as against the normal two in B. Somewhat less uniform fuel distribution and slightly lower combustion efficiency are to be expected with the single feedline, particularly since it is displaced to one side of the bed. The higher CO₂ and lower O₂ readings in Sequence B are due to the higher average power level and fuel flowrates in that sequence.

The difference in SO₂ between the two sequences is most likely a simple instrumentation error. The low indicated level is near the instrument threshold, and it is considered likely that a zero shift occurred in mid-test. The NO_x level in Sequence B converts to 0.264 lb/million Btu, well below the EPA standard of 0.7.

Particulate Emissions

Two stack samples, each of one-hour duration, showed total-loading levels of 0.11 gr/sdcf, as corrected to 12% CO₂. Eight-sample averages for size distribution are plotted in Figure 39. The indication is that 97 percent of the total particulate is smaller than 5 microns, and

TABLE 8
PROCESS STATISTICS FOLLOWING
TURBINE START 8

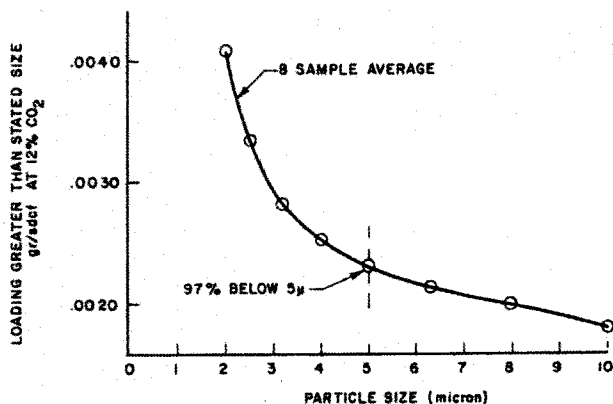
BASED ON 25 SAMPLES IN FOLLOWING ETS RANGE:
738.46 TO 786.46

PARAMETER	MEAN VALUE	STANDARD DEVIATION	MAX VALUE	MIN VALUE	LINEAR REGRESSION RATE
BED TEMPERATURE	1250.6	5.40	1281.2	1241.6	.025
BED STANDARD DEV.	12.2	1.90	15.1	11.7	-.006
FREEBOARD TEMP.	1474.5	5.52	1484.4	1461.5	-.057
TURBINE IN TEMP.	1119.1	5.33	1131.7	1109.6	.153
AH TRANSPORT TEMP	252.8	1.31	271.2	236.5	.044
FUEL LB/MIN	35.1	3.41	101.0	24.2	-.012
POWER, KW	221.7	16.05	422.0	54.5	.333
COMPRESSOR RPM	10814.7	42.3	10905.0	10710.0	1.32
GENERATOR RPM	1759.2	2.03	1775.0	1742.5	.068
GENERATOR VOLTAGE	430.57	1.327	431.47	429.94	-.0497
COMPRESSOR PSIG	45.10	1.494	46.37	43.95	.0103
CURGE MARGIN, PSID	5.27	1.245	6.75	3.68	.0047
BED DROP, IN	30.23	1.53	30.34	29.67	.031
INERTIAL DROP, IN	12.96	1.544	20.23	18.04	.0112
BURNER AIRFLOW, LB/MIN	52.33	13.73	92.71	42.60	-.363
DR AIRFLOW, LB/MIN	281.36	20.30	373.33	229.72	-.732
FEEDLINE #1 FLOW, LB/MIN	155.91	1.09	157.43	154.94	.010
FEEDLINE #2 FLOW, LB/MIN	153.10	.72	154.91	153.27	-.033
BYPASS AIRFLOW, LB/MIN	217.44	4.30	221.72	211.15	-.233
COMP. IN FLOW, LB/MIN	1366.3	3.29	1377.5	1357.9	.155
BED SUPER VEL, FT/SEC	5.76	.22	5.76	5.00	-.005
FRBD SUPER VEL, FT/SEC	6.23	.24	6.45	5.95	-.006
PLENUM PRESSURE, PSIG	42.36	.34	42.91	42.74	.019

TABLE 9
PROCESS STATISTICS FOLLOWING
TURBINE START 14

BASED ON 25 SAMPLES IN FOLLOWING ETS RANGE:
730.15 TO 814.15

PARAMETER	MEAN VALUE	STANDARD DEVIATION	MAX VALUE	MIN VALUE	LINEAR REGRESSION RATE
BED TEMPERATURE	1375.7	24.13	1411.2	1331.2	-.031
BED STANDARD DEV.	13.4	1.21	15.7	10.7	.043
FREEBOARD TEMP.	1429.5	2.00	1501.0	1472.0	-.351
TURBINE IN TEMP.	1069.2	4.26	1113.7	1000.3	.144
AH TRANSPORT TEMP	277.4	1.53	291.5	273.6	.002
FUEL LB/MIN	100.9	5.63	111.9	91.0	-.697
POWER, KW	222.1	23.21	295.0	95.5	-2.218
COMPRESSOR RPM	10751.7	22.7	11040.0	10635.0	-7.29
GENERATOR RPM	1761.3	7.34	1775.0	1747.5	-.401
GENERATOR VOLTAGE	430.27	1.042	430.39	430.20	.0049
COMPRESSOR PSIG	45.90	1.773	47.53	44.41	-.0773
CURGE MARGIN, PSID	5.20	1.345	5.75	4.95	-.0052
BED DROP, IN	32.33	1.025	32.344	32.313	-.003
INERTIAL DROP, IN	21.99	1.703	22.32	21.07	-.0614
BURNER AIRFLOW, LB/MIN	102.29	4.52	103.15	95.25	-.530
DR AIRFLOW, LB/MIN	530.68	10.31	602.02	521.96	-.584
FEEDLINE #1 FLOW, LB/MIN	155.94	2.29	157.50	153.33	.151
FEEDLINE #2 FLOW, LB/MIN	160.42	1.43	159.93	160.13	-.036
BYPASS AIRFLOW, LB/MIN	214.74	7.16	223.09	210.23	-.575
COMP. IN FLOW, LB/MIN	1364.4	7.62	1373.2	1357.0	-.632
BED SUPER VEL, FT/SEC	5.06	.05	5.12	5.03	.004
FRBD SUPER VEL, FT/SEC	6.15	.07	6.23	6.09	-.004
PLENUM PRESSURE, PSIG	42.36	.43	44.35	43.55	-.036



NOTE: ASSUMED VALUE AT ZERO PARTICLE SIZE IS 0.088 gr/sdct AT 12% CO₂

Figure 39 Averaged Turbine-Exhaust Particle-Size Distribution

94 percent smaller than 2 microns. This result further demonstrates the inability of inertial-type separators to remove fine particulate, and once again demonstrates the need for a separator like the granular filter.

Deposition and Erosion

Sequence A showed that deposition can be a serious problem in wood combustion. Although hard deposits, such as those that plagued MSW testing, were not much in evidence, the softer deposits that did occur resulted in rapidly decreasing surge margin. The soft, green-

colored deposits were shown in analysis to be largely a potassium sulfate/phosphate complex, along with relatively small amounts of sodium; the green coloration resulted from the presence as well of significant amounts of sodium.

Earlier feasibility tests with wood had not produced this kind of deposit, having been run with Ponderosa pine, which has a potassium-to-silicon ratio of about 1:5; the white fir used in these tests has a ratio of about 5:1. Massive deposits were eliminated in Sequence B by the blade-cleaning system, but erosion became a factor in that sequence. The worst blade found on post-test inspection is shown in Figure 40. Two distributional phenomena are evident in the erosion pattern that developed:

- (1) Leakage past the tip clearance of the first-stage rotor allows a particle-laden jet of gas to impinge on the convex leading-edge root fillet of the subsequent blade row. This is the very localized deep erosion seen in the photograph.
- (2) Particles in the gas stream are concentrated toward the outside by centrifugal force. The large-radius scallop in the trailing edge of the blade shown illustrates this well-defined concentration.

It is again made evident that improved particle separation is a "must" for a viable power system.

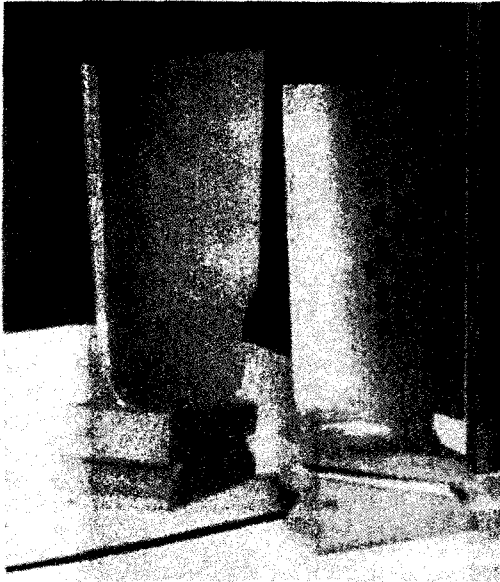


Figure 40

Direct and Mirror Image, Worst Blade of Second-Stage Compressor-Turbine Stator after Hog-Fuel Test

Computerized Control

Generally good performance of the process-control computer was a feature of this test. A memory-board parity error was encountered almost at the outset, but timely replacement of the board produced a configuration that functioned without failure for the remainder of the test program. Some idea of the duty cycle completed in the test program can be obtained from the fact that (among other things) the computer (1) sampled over 2.5 million temperature readings; (2) loaded from the disc and executed a pressure-sampling task approximately 430,000 times; (3) updated analog-controller setpoints approximately 86,000 times; and (4) logged on disc files some 20,000 records each of 14 parameters.

Some improvements in overall system were naturally identified during this test, and subsequently incorporated. These included the following:

1. A step was added to operator-keyed commands for parameter changes, in which the new value is displayed and the operator given a final opportunity to accept or reject it before it becomes effective.
2. The warning-message structure was modified to be more explicit and concise, and to repeat out-of-tolerance messages periodically.
3. The list of analog input signals monitored for warning messages was expanded, particularly in the residue-removal area and for preheat modes.
4. Additional software was written to implement a virtually endless data-logging mechanism, using periodic paper-tape punch cycles to clear memory for re-use.

SECTION 6

THE COAL PROGRAM

A second departure from the basic EPA program arose out of an interest in using high-sulfur coal for the generation of electrical power. Since the Pilot Plant had ceased to be actively involved in the EPA program--pending development of the granular filter--plans were worked out with the then Office of Coal Research (OCR) for using it in a coal-combustion program. With the cooperation of the EPA, the OCR--and its successor, the Energy Research and Development Administration (ERDA)--awarded a contract to CPC to conduct research and development tasks in the combustion of high-sulfur coal using CPU-400 technology.

Many of the problems--and solutions--that are associated with the operation of a direct-fired gas turbine on solid fuel are common to all such fuels. It will be useful, therefore, to include here a review of parts of the coal program that bear on the general objective of turbine operation, particularly the 526 hours of Pilot Plant operation that were accumulated. A more detailed discussion of these program elements--and others not reviewed here--may be found in Reference 3.

A. SYSTEM CONFIGURATION

The general arrangement of combustor, separator vessels, and turbine remained unchanged from the configuration used for the combustion of municipal solid waste and hog fuel. It was necessary, however, to provide a new system for fuel preparation and feeding. Changes were also made--in an evolutionary fashion--in the particle-separation devices employed and in the methods for removing residue from the system.

Fuel-Processing System

The fuel processing system, shown in Figure 41, contained the equipment necessary for reducing the coal lump size to less than 1/4 inch* and moving it to storage; for moving the SO₂-suppressing additive to storage; for providing dust control while processing; for providing an inert atmosphere while in storage; and for metering and pneumatically transporting the coal and additive to the fluid-bed combustor in the correct proportions and at the correct rate.

* A size determined to be suitable by a series of parametric tests in the Model Combustor.

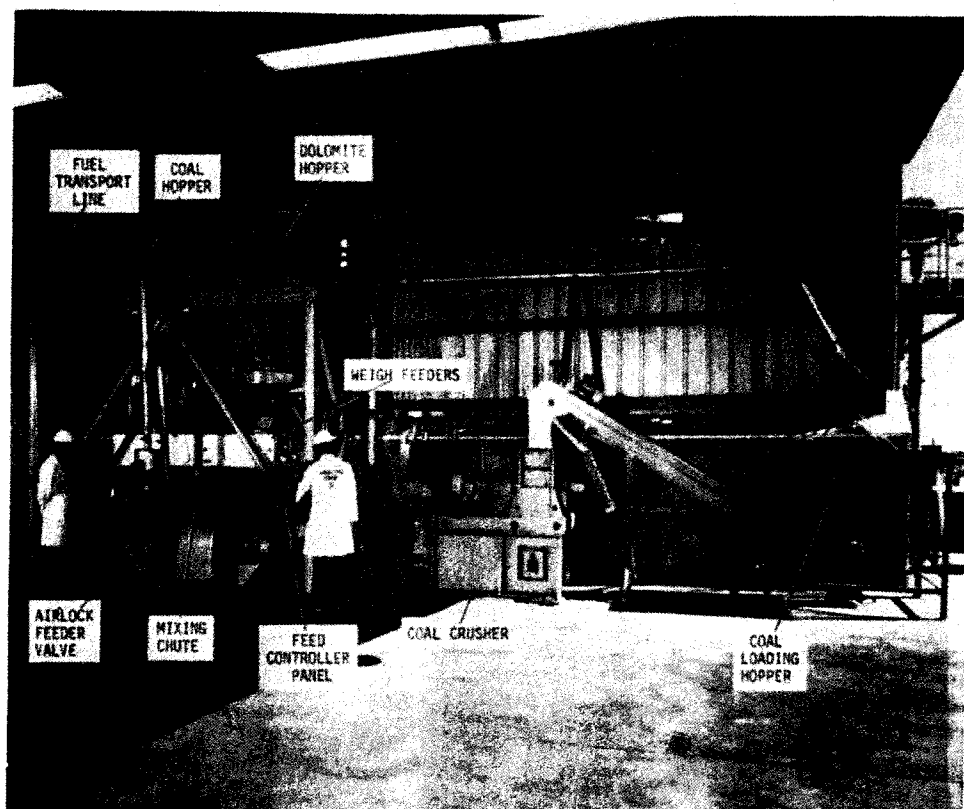
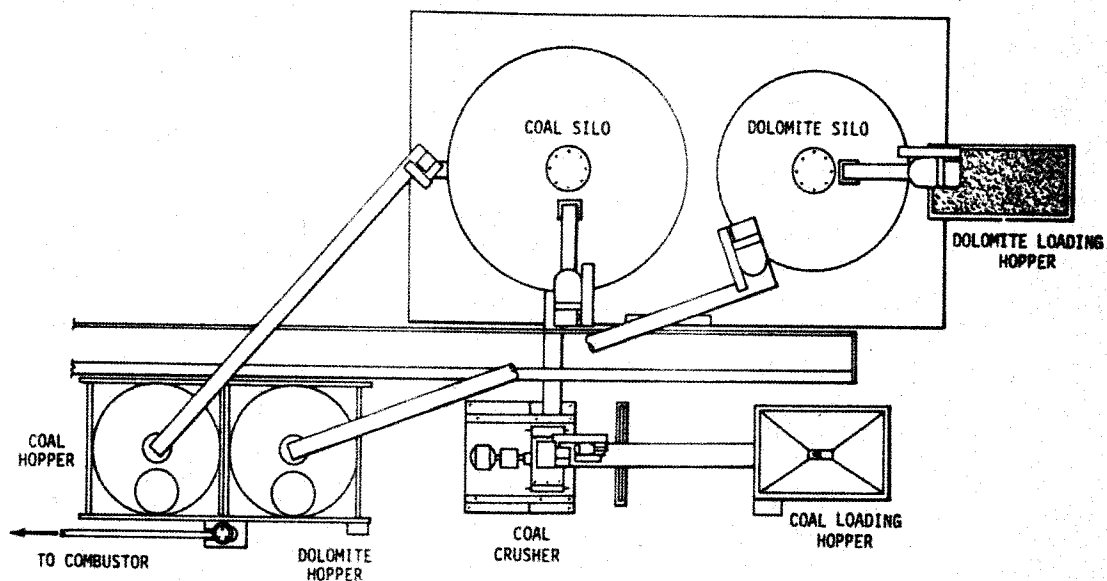


Figure 41 Coal-Processing System

The coal and dolomite (or limestone) were first loaded into separate loading hoppers. A series of screw conveyors moved the already sized dolomite directly into a storage silo; the coal was first crushed to size and then moved to its own storage silo. The storage silos had respective capacities of 480 cu ft (36,000 lb of dolomite) and 1150 cu ft (60,000 lb of coal); they provided a 24-hour supply of coal and additive.

From the storage silos, the coal and additive were conveyed as required to two 110-cu-ft feed hoppers. Twelve level-indicating controls supervised the action of conveyors and vibrating bin bottoms to keep materials moving as needed. Two K-Tron weigh feeders metered and ratioed the coal and additive into a six-inch close-fitting screw conveyor, from which it was dropped into a rotary-airlock feeder valve for transfer to the high-pressure transport line.

The single pneumatic-transport line was of 1-1/2-inch pipe, and carried the coal/additive mix directly into the fluid bed of the combustor, a distance of some 300 feet. Several turns had to be negotiated along the way, and these initially presented problems in design. Originally, all directional changes were accommodated with bends of 48-inch radius, but these failed by erosion after little more than four hours of operation. Installation of a series of "dead boxes" (Figure 42a) to retain some of the transported material to serve as expendable impact surfaces brought only small improvement; the pipe still wore through at the junctions between adjacent pockets. The design solution finally adopted employed right-angle turns using dead-ended tees, as shown in Figure 42b. Transport-line failure ceased to be a problem after this final modification.

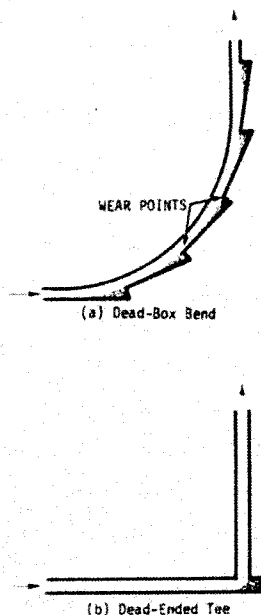


Figure 42 Directional-Change Designs for Pneumatic-Transport Line

Included in the system were a dust-collecting unit and an inert-gas purge system. Dust was collected in the areas of the coal crusher and the airlock feeder. The dust (about 6% by weight of the total feed) was pneumatically injected into the transport line downstream of the feeder valve through a sequenced double-valve airlock. The general arrangement is shown in Figure 43.

A flow diagram for the Pilot Plant as configured for coal combustion is shown in Figure 44.

Hot-Gas Cleanup

As the coal-burning program got underway, the arrangement of the

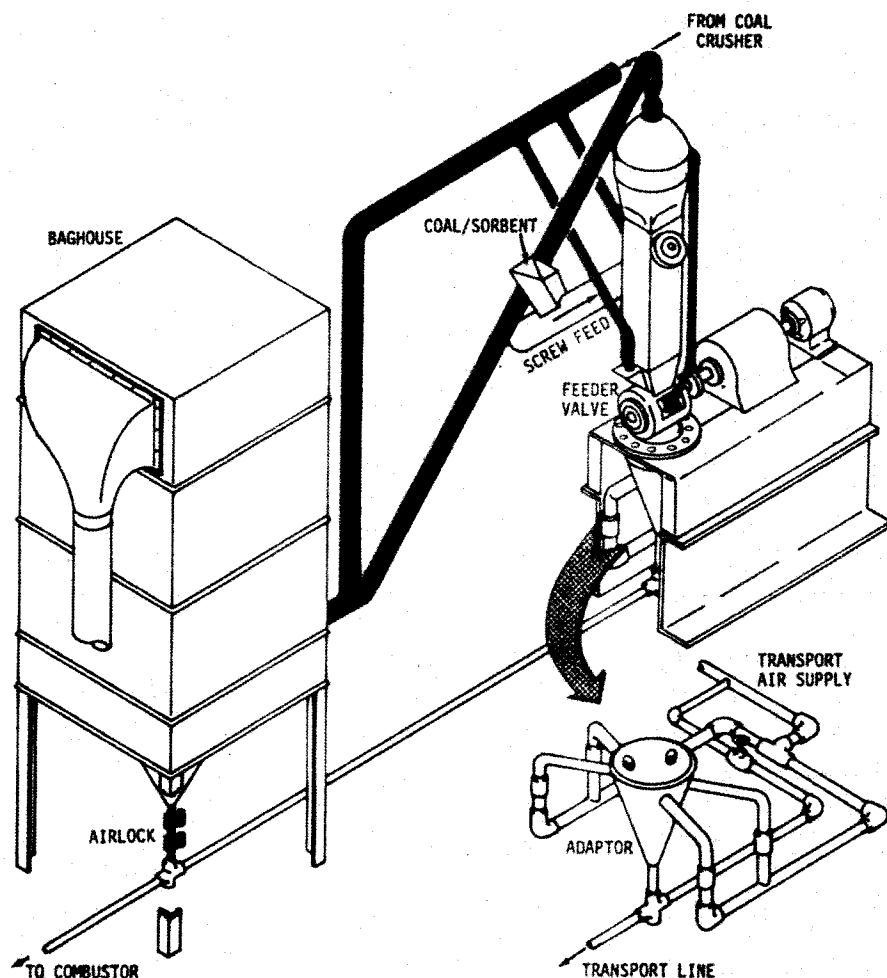
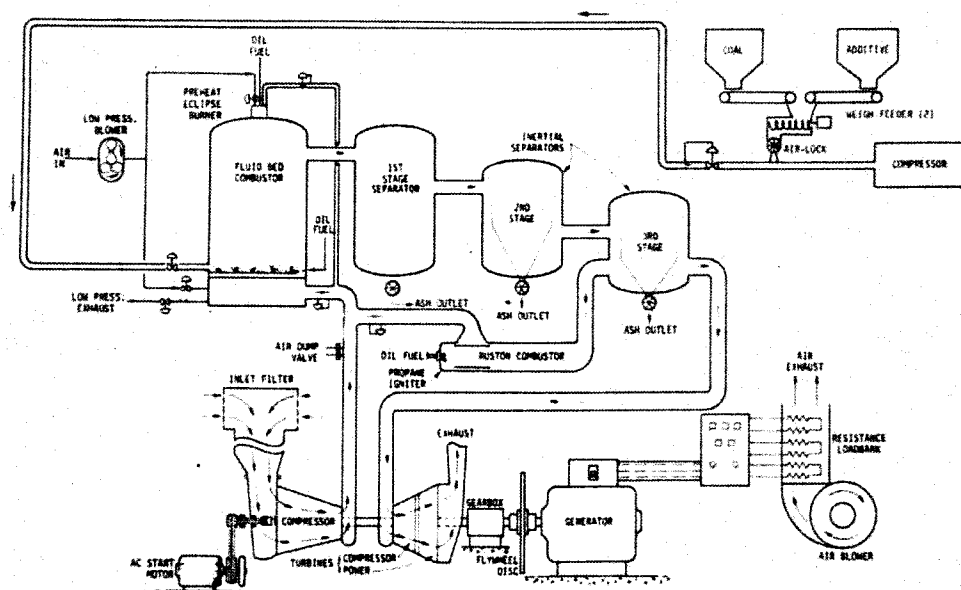


Figure 43 Coal Dust Vent System

particle separators was the same as that used in the EPA and wood-waste programs. The first change, made early in the program, involved the installation of twin cyclone separators (Figure 45) in the first-stage vessel, replacing the spinner duct previously installed there. Later twin separators of the configuration shown in Figure 46 were installed in the second-stage vessel, and the original array of six-inch inertial tubes was removed.

The system for removal of collected residue from the vessels also underwent changes during the program, in an effort to eliminate plugging problems. Table 10 lists, for general reference, the various particle-separator and residue-removal configurations that were used for the several tests; Figure 47 shows the residue-removal configuration that existed just prior to the final test run. A quenched



1A-221-326

Figure 44 Flow Diagram for Coal Combustion

fluid-bed system for residue removal used in the final test segment will be described in the discussion on that segment.

B. SYSTEM TESTING

The Pilot Plant was operated in two distinct test series, the first series having as its primary goal a general evaluation of system performance, suppression of noxious gases, and control of particulate in the exhaust gas, and the second series being aimed at a broader understanding of the potential for hot corrosion. Table 11 summarizes the tests conducted in the first series.

Test P-201

The checkout and preliminary test phase, designated P-201, included a total of 20 hours of operation of the coal-fired combustor, with the longest continuous operation on coal being 4.3 hours. Dolomite was fed with the coal at a calcium-to-sulfur mole ratio of 1.28. Overall performance data for the 4.3-hour period are shown in Table 12, and data on exhaust emissions are given in Table 13. It is seen that neither the SO_2 suppression nor the particulate removal was adequate to meet standards.

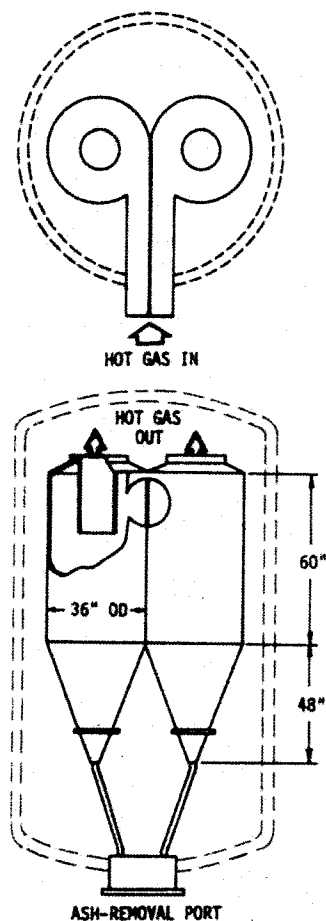


Figure 45 First-Stage Cyclone Separators

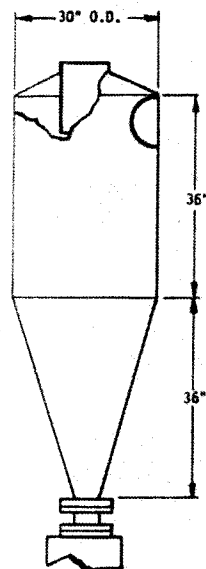


Figure 46 Second-Stage Cyclone

Test P-202

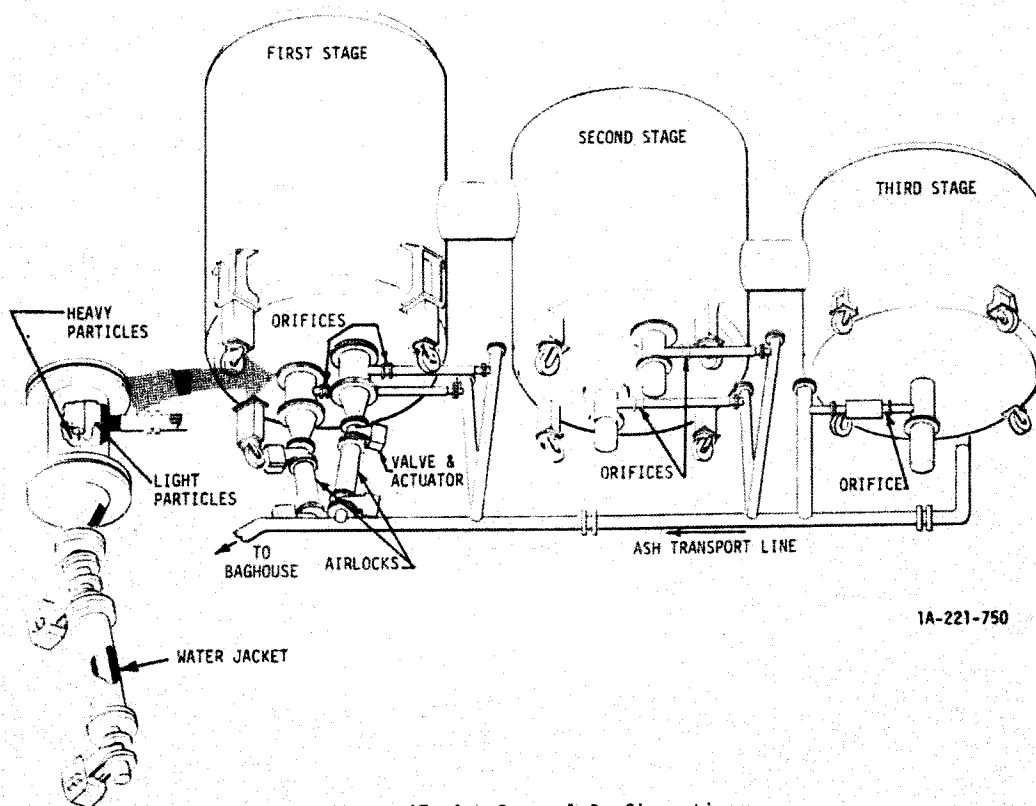
For this test, two 30-inch-diameter by 72-inch-long cyclones were installed in the combustor freeboard to evaluate the possibility of improving SO_2 suppression by recycling unspent additive to the bed. Also, the two 36-inch tangential cyclones were installed in the first-stage vessel, replacing the spinner duct. Test P-202 logged 29.4 hours of coal-burning operation, the first 3 hours as

baseline without dolomite. Table 14 contains representative data. Several changes in calcium-sulfur ratio were made in the course of the test, but satisfactory suppression of SO_2 was never achieved. Post-test inspection revealed that the diplegs through which the internal cyclones were to have returned fines to the bed had not performed that function but had remained plugged; the reason for the failure was the too-short dipleg, constrained by space limitations within the combustor. The internal cyclones were removed for all subsequent testing.

A frequent cause of shutdowns during this test was plugging of the ash-removal lines from the first- and third-stage separators. Post-test inspection of the turbine revealed that the high particle loadings had resulted as well in extensive erosion and deposition; both are visible in Figure 48.

TABLE 10
PARTICLE-SEPARATOR AND RESIDUE-REMOVAL CONFIGURATIONS

TEST	COMBUSTOR	FIRST STAGE	SECOND STAGE	THIRD STAGE
P-201	None	Spinner duct, single ash airlock	48 6-in. inertial tubes, single ash airlock	100 3½-in. inertial tubes, continuous-bleed orifice
P-202	2 30-in.-dia cyclones for recycle	2 36-in. dia cyclones, single ash airlock	↓	↓
P-203	None	2 36-in.-dia cyclones, dual airlocks on vessel c, 2 continuous-bleed orifices	↓	↓
P-401	↓	2 36-in.-dia cyclones, dual vertical outlets & airlocks, 2 continuous-bleed orifices	2 30-in.-dia cyclones, 2 continuous-bleed orifices	None
P-402	↓	↓	↓	↓
P-403A	↓	Same as P-401, but with enlarged orifice downcomers	↓	↓
P-403B	↓	Quenched fluid beds added ahead of orifices	↓	↓



1A-221-750

Figure 47 Ash-Removal Configuration

TABLE 11				
PILOT PLANT SYSTEM TESTS				
Test Series	Bed Temp. F	V _{sf} fps	Duration hr	Primary Objective
P-201	1450	6.7	20.0	System checkout: Evaluate SO ₂ & NO _x suppression.
P-202	1450	6.5	29.4	Same as P-201, with recycle cyclones in combustor.
P-203	1450-1550	6.7	131.6	SO ₂ suppression in extended operation.

TABLE 12		
P-201 SYSTEM PERFORMANCE DATA		
Parameter	Mean Value	Standard Deviation
Combustor Outlet Temperature, F	351	1.3
Bed Temperature (Ave. of 6), F	1438	5.9
Freeboard Temperature, F	1468	3.4
Turbine Inlet Temperature, F	1270	2.4
Turbine Exhaust Temperature, F	851	1.5
Ash Transport Temperature, F	280	3.6
Fuel Transport Inlet Pressure, psig	65.0	0.59
Compressor Outlet Pressure, psig	41.5	0.13
Freeboard Pressure, psig	39.9	0.18
Turbine Inlet Pressure, psig	38.1	0.16
Computed Surge Margin, psid	9.9	0.18
Bed Pressure Drop, IWD	32.3	0.77
First-Stage Pressure Drop, IWD	6.6	0.46
Second-Stage Pressure Drop, IWD	16.9	0.27
Third-Stage Pressure Drop, IWD	21.7	0.32
Compressor Inlet Airflow, lb/min	1361	2.8
Fuel Transport Airflow, lb/min	37.3	0.37
Coal Flow, lb/min	34.6	0.37
Dolomite Flow, lb/min	11.2	0.23
Compressor Speed, rpm	10,863	17.5
Generator Speed, rpm	1740	6.2
Generator Voltage	473.9	0.48
Power, kW	869	6.6

TABLE 13		
EXHAUST EMISSIONS DATA		
SO ₂	4.19 lb/10 ⁶ Btu	537 ppm
NO _x	0.415 lb/10 ⁶ Btu	74 ppm
CO	0.140 lb/10 ⁶ Btu	41 ppm
CH _x	0.013 lb/10 ⁶ Btu	3.6 ppm
CO ₂		3.5%
O ₂		16.0%
Particle Loading	1.82 lb/10 ⁶ Btu	0.27 gr/scf
Amount > 5 microns	0.0061 lb/10 ⁶ Btu	0.0009 gr/scf

TABLE 14										
TYPICAL P-202 TEST DATA										
Test Segment	A	B	C	D	E	F	G	H	I	J
Coal-Burning Time (hr)	3.0	2.0	0.4	1.9	4.3	2.4	1.4	2.8	6.7	3.6
Type Coal	Illinois No. 6									
Type Dolomite (Kaiser)	CBM									
Ca/S (mol ratio)	0	1.53	3.47	1.45	3.33	1.46	3.30	1.65	1.56	1.53
Superficial velocity (fps)	6.5	6.9	6.9	6.4	6.5	6.4	6.6	6.7	6.6	6.4
Fluid Bed Temp (F)	1394	1460	1440	1407	1470	1465	1467	1474	1470	1462
Coal Feed (lb/min)	39.9	37.7	37.9	37.3	37.7	36.8	39.1	36.9	37.5	37.0
Dolomite Feed (lb/min)	0.0	12.7	28.9	12.0	27.6	11.8	28.2	13.4	13.0	12.6
Gas Analysis										
SO ₂ (lb/10 ⁶ BTU)	5.26	4.21	3.27	4.71	2.28	2.52	2.78	3.14	3.17	(a)
NO _x (lb/10 ⁶ BTU)	(a)	0.94	0.78	0.23	0.325	0.19	0.31	0.36	0.38	0.65
Particle Loading (lb/10 ⁶ BTU)	(a)	1.61	(a)	1.28	3.50	1.50	8.57	2.88	3.20	3.71
Loading >5μ (lb/10 ⁶ BTU)	(a)	(a)	(a)	(a)	0.018	0.027	(a)	(a)	(a)	(a)
SO ₂ Suppression (%)	29.5(b)	43.5	56.1	38.1	69.4	66.2	69.5	57.9	57.5	---
Combustion Efficiency (%)	99.7	99.8	99.8	99.6	99.8	99.8	99.8	99.8	99.8	99.8
Excess Air (%)	244	286	282	317	310	329	299	318	297	316

Secondary inlets added to combustor cyclones

Cyclones raised and diplegs shortened
2000# CBM dolomite added to bed

(a) Not recorded

(b) SO₂ suppression is calculated from a comparison of theoretical and actual emissions; theoretical value assumes all sulfur converted to SO₂, but sulfidation of calcium and potassium in the coal, along with some conversion to SO₃, produce some suppression in the absence of any additive.

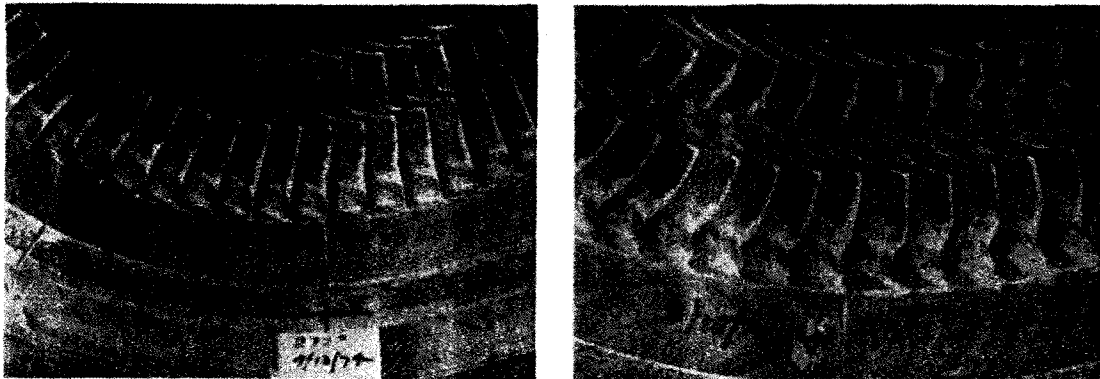


Figure 48 Trailing-Edge Erosion of Second-Stage Compressor-Turbine Stator
(Inlet is at 258°)

Test P-203

Typical data for various periods of Test P-203 are shown in Table 15. This test developed into three rather distinct segments, in which the role of temperature in the sulfur-suppression process became apparent. The test used a starter bed of dolomite instead of a sand bed. The first segment, P-203A, comprised 29.8 hours of coal-burning operation. Most of this was at a calcium-sulfur mole ratio

TABLE 15					
TYPICAL P-203 TEST DATA					
Test Segment	P-203A		P-203B	P-203C	
Coal-Burning Time (hr)	6.1	4.1	9.2	6.5	9.8
Type Coal	← Illinois No. 6 →				
Type Dolomite	← Kaiser No. 6 →				
Ca/S (mol ratio)	1.50	1.54	1.55	1.75	2.00
Fluid-bed Temp (F)	1456	1450	1557	1543	1555
Coal Feed (lb/min)	37.9	37.3	40.6	38.4	39.0
Dolomite Feed (lb/min)	12.9	12.8	13.9	10.4	15.9
Gas Analysis:					
SO ₂ (lb/10 ⁶ Btu)	2.78	2.84	1.25	1.86	0.95
NO _x (lb/10 ⁶ Btu)	0.50	0.68	0.48	0.19	0.60
Particle Loading (lb/10 ⁶ Btu)	1.54	1.40	2.08	1.44	2.24
Loading >5μ (lb/10 ⁶ Btu)	.012	.005	.291	(a)	(a)

(a) Not recorded

of 1.5; the final 2.4 hours, however, were at a ratio of 3.0. Nominal bed temperature was 1450 F, and freeboard temperature varied between 1410 and 1460 F; the lowest SO_2 level achieved was 2.36 lb/million Btu.

The second segment, P-2038, logged 54.7 hours of coal burning, and demonstrated a significant effect of increased bed temperature. A period when bed temperature was raised to and maintained at a nominal 1550 F is illustrated by the graph of Figure 49. A dramatic improvement in sulfur suppression followed; final levels were from 1.25 to 1.3 lb/million Btu.

Bed temperature was at this time still being controlled by modulation of a valve in a bypass line from combustor plenum to freeboard. To raise bed temperature, an increased amount of air would be bypassed to the freeboard, resulting in a freeboard temperature often lower than that of the bed. The significance of this fact in sulfur suppression became clearly evident in post-test plotting of data from Test P-203C.

This final segment began with a calcium-sulfur mole ratio of 1.25, and subsequent increases were made to 1.5, 1.75, and 2.0. Figure 50 is a plot for the portion of the segment that was carried out with a ratio of 1.75. Examination of the plot shows that, without significant exception, SO_2 suppression improved whenever the freeboard temperature rose above 1510 F, and deteriorated whenever it dropped below that level (the low point in the SO_2 level corresponds to about 1 lb/million Btu).

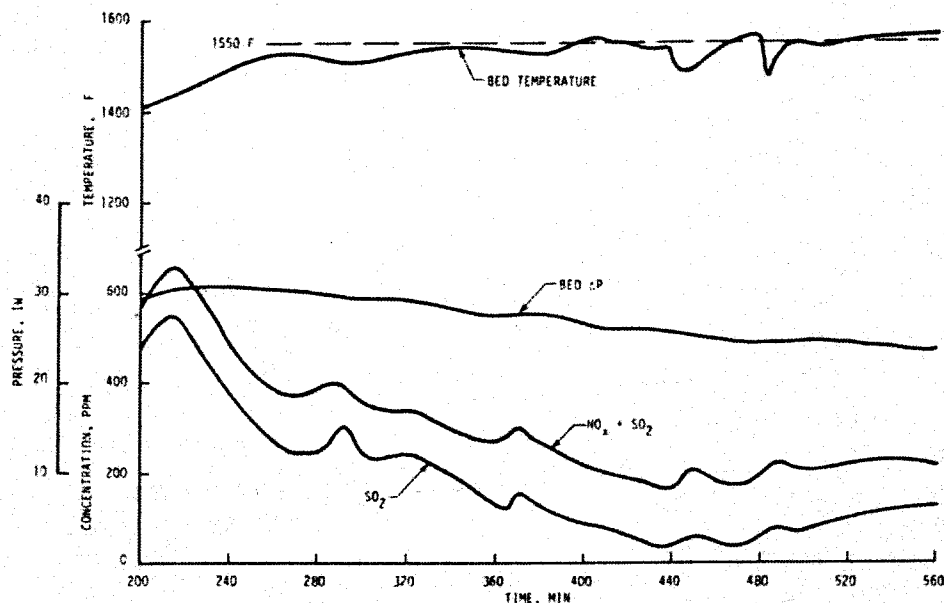


Figure 49 Test P-2038

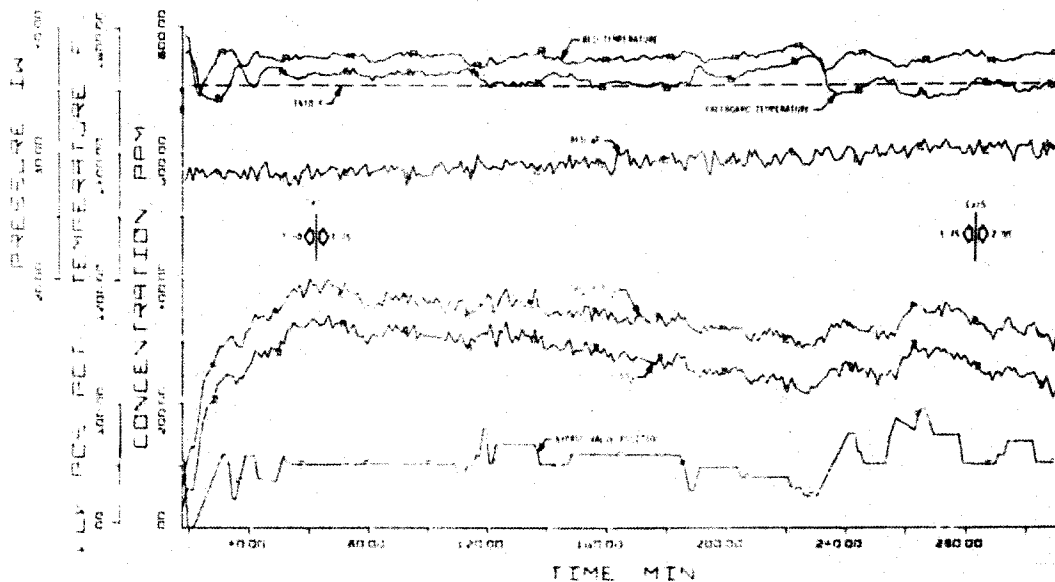


Figure 50 Test P-203C

During the segment shown, pressure drop through the bed rose from about 28 IWD to 31 IWD. For more than six hours thereafter, however, it remained steady at 31 IWD, indicating that a stable condition is possible in which neither bed makeup nor bed removal is required.

Exhaust loading during this segment rose from an initial 1.4 lb/million Btu to a final 2.6, and problems with plugging in inertial separators and ash-removal ports continued to plague operations; the longest uninterrupted period of coal burning was 11 hours.

C. HOT-CORROSION PROGRAM

Hot corrosion--or sulfidation--is an accelerated attack on metal alloys caused by the presence of liquid alkali sulfates, and is characterized by the migration of sulfur into the metal ahead of visible surface damage. The quantity of liquid needed to promote this type of attack is miniscule and, since turbine fuels all contain sufficient sulfur for the formation of alkali sulfates, the amounts that can form are usually determined by the amount of alkalis present.

Preliminary exposures of metal alloys in the Model Combustor had given definite evidence of sulfidation after less than 300 hours. The extent of the damage, however, was orders of magnitude less than might be expected by extension from oil-burning experiments, based on the amounts of alkalis present. Some inhibiting mechanism was evidently at work.

The hot-corrosion program that was developed was aimed at exploring mechanisms that can inhibit sulfidation, and testing additives in the combustion process capable of enhancing the inhibition. By far the majority of the testing (over 2800 hr) was carried out in the Model Combustor, and the Pilot Plant was operated primarily as a means of confirming results in full-scale operation. In the process, of course, additional operating experience was gained, and for that reason the Pilot Plant tests are of interest here and will be briefly described.

(A full discussion of the hot-corrosion results will be found in Reference 3. In brief, it was found that the Illinois No. 6 coal that was used contains enough available aluminum silicate in the ash to suppress the alkali materials as stable feldspars at a temperature of 1600 F; oxidation, rather than sulfidation, is the mechanism controlling corrosion rates at temperatures below 1670 F. Based on corrosion as the only limiting factor, a turbine life of 14,000 hours could be projected at 1600 F, 50,000 hours at 1550 F).

D. PILOT PLANT HOT-CORROSION TESTS

Pilot Plant testing in support of the hot-corrosion program comprised three main segments: an 85-hour baseline test without corrosion inhibitor, an 85-hour baseline test in which calcium-aluminum silicate in the form of Johns-Manville "Zelie" was fed with the coal as corrosion inhibitor, and a 175-hour test using aluminum silicate in the form of Burgess No. 10 clay pigment for that purpose; a summary is shown in Table 16.

TABLE 16						
COAL TEST SERIES - HOT CORROSION						
Test Series	Bed Temp.	Vsf	Additive	Additive % of Coal Wt.	Test Duration(hr)	Objective
P-401	1600F	6 fps	none	---	84.5	Establish baseline parameters with no corrosion inhibitors.
P-402	1600	6 fps	Zelie	0.5	85.6	Evaluate Zelie as corrosion additive during 80 hours of high-pressure operations.
P-403	1600	6 fps	Burgess No. 10	0.4	175	Evaluate Burgess #10 as corrosion additive during extended high-pressure operation.

The use of multiple inertial separators was abandoned for these tests. The 6-inch tubes in the second stage were replaced by the twin 30-inch cyclones described earlier, and the 3½-inch tubes were removed from the third-stage vessel, leaving it to serve only as a plenum chamber for exposure of specimens and mixing of combustion gas with bypass air.

Test P-401, Baseline

This test was used to check out limestone (Pfizer No. 69 grits) as a sulfur suppressant, and to determine to what extent suppression continued to occur downstream of the combustor freeboard. Significant test parameters are listed in Table 17.

Initially, limestone was introduced at a calcium-sulfur mole ratio of 1.65; the resultant SO₂ level in the exhaust was 4 lb/million Btu. Increases were made in the course of the test but, as seen in Table 17, satisfactory suppression was never achieved. Measurements of SO₂ in the combustor freeboard, the third-stage vessel, and the turbine exhaust indicated that all suppression occurred before the exhaust gas left the combustor freeboard; observed differences in the levels corresponded directly to the dilution-air ratio used to maintain a turbine-inlet temperature of 1400 F.

Revised systems of temperature control were activated in Test P-401; the bypass used to control turbine-inlet temperature was automated, and bed temperature was controlled by modulation of the coal feed (bypassing of a portion of the combustion air to the freeboard was discontinued).

TABLE 17
P-401 TEST DATA

Coal-Burning Time, hr	84.6		
Bed Temperature, F	1560-1580		
Freeboard Temperature, F	1590		
Generator Output, kW	350-950		
Ave. Coal Feedrate, lb/min	40.9		
Ave. Limestone Feedrate, lb/min	10.0		
Total coal consumed, lb	207,869		
Total limestone consumed, lb	51,281		
Ca/S Ratio	1.8	2.2	2.4
SO ₂ , lb/10 ⁶ Btu	2.98	2.43	2.42
NO _x , lb/10 ⁶ Btu	0.47	0.53	0.59

It is of interest that no measurable increase in exhaust loading was encountered as a result of the removal of third-stage internals. At the low initial limestone feedrate, the average of four loading samples was 1.6 lb/million Btu; at the high final rate, it was 1.98.

Test P-402

Significant parameters for Test P-402 are listed in Table 18. The first 14 hours used limestone still resident in the feed system as sulfur-suppressant. A switch back to dolomite was made when that supply was exhausted.

Exhaust-gas data were again obtained at three system locations, and again indicated that virtually all suppression of SO_2 occurs within the combustor. Nine total loading samples averaged 2.58 lb/million Btu, with a slight tendency toward a decrease as the test progressed.

Test P-403

A parametric summary of Test P-403 is given in Table 19. A significant result of this test was the achievement of one 30-hour period of continuous operation. Some of the parameters for that run are plotted in Figures 51 and 52. the computer-controlled turbine-inlet temperature is seen in Figure 51 to have been held within ± 4 of the 1400 F setpoint; computer-control of bed temperature is not quite so precise because there is always a time lag before a change in feedrate can be felt as a change in temperature.

TABLE 18
P-402 TEST DATA

Total Coal-Burning Time, hr	85.6
Bed Temperature, F	1560-1580
Freeboard Temperature, F	1590
Cascade Temperature, F	1675
Generator Output, kW	750-800
Ave. Coal Feedrate, lb/min	28.9
Ave. Dolomite Feedrate, lb/min	13.6
Total Coal Consumed, lb	199,795
Total Limestone/Dolomite Consumed, lb	69,899
Ave. Ca/S Ratio	1.97
Ave. SO_2 , lb/ 10^6 Btu	2.31
Ave. NO_x , lb/ 10^6 Btu	0.60

TABLE 19
P-403 TEST DATA

Compressor Inlet Temperature, F	73
Bed Temperature, F	1561
Freeboard Temperature, F	1561
Turbine-Inlet Temperature, F	1400
Turbine-Exhaust Temperature, F	992
Compressor Discharge Pressure, psig	40.3
Turbine-Inlet Pressure, psig	35.8
Bed Pressure Drop, lWd	32.8
Coal Flowrate, lb/min	38.8
SO ₂ -Sorbent Flowrate, lb/min	9.8
Corrosion-Inhibitor Flowrate, lb/min	0.2
Generator Average Voltage,	480.0
Generator Speed, rpm	1762
Generator Output Power, kW	753
Turbine-Exhaust SO ₂ , ppm (v/v dry)	382
Turbine-Exhaust NO _x , ppm (v/v drv)	52
Turbine-Exhaust Average Total Loading, gr/sdcf	0.415

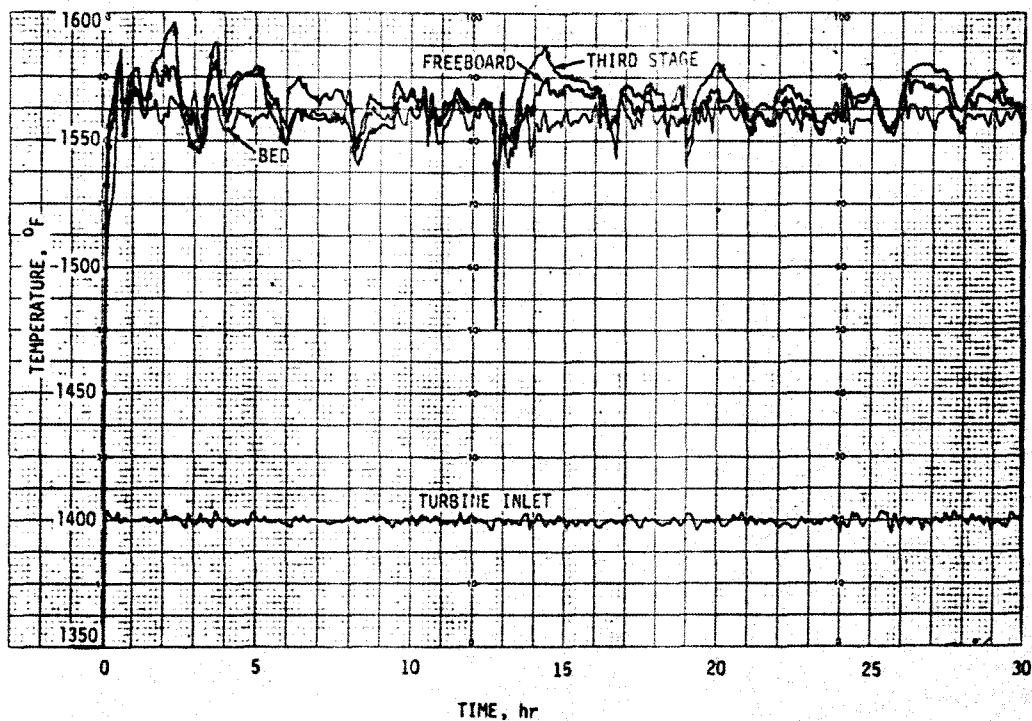


Figure 51 System Temperatures, Test P-403

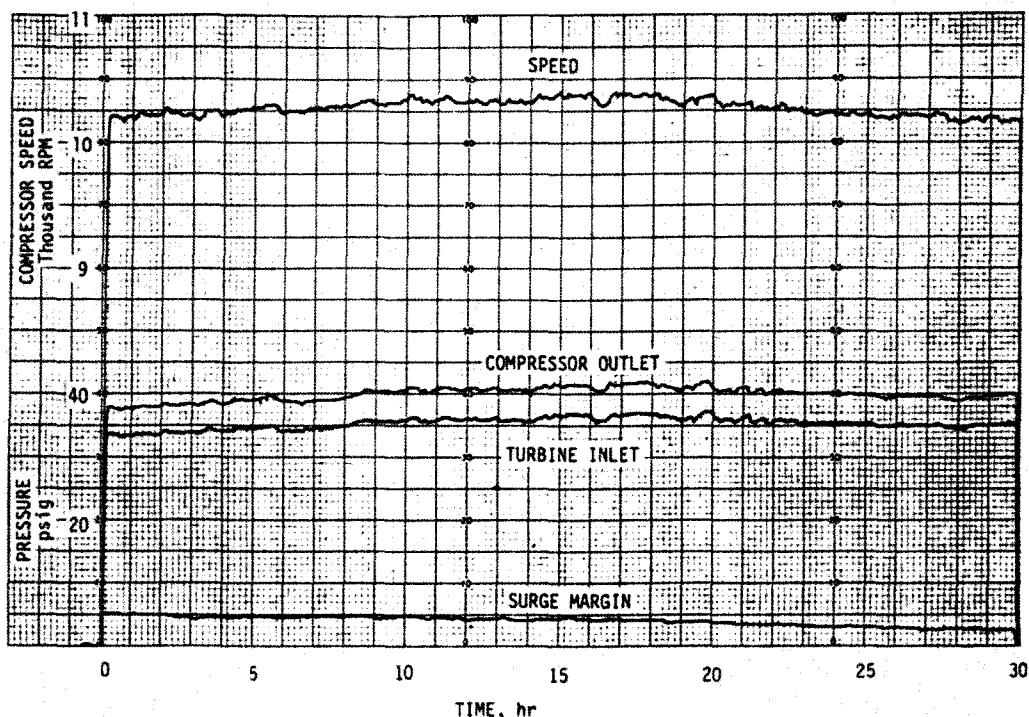


Figure 52 Turbine Parameters, Test P-403

It can be seen in Figure 52 that a gradual reduction in surge margin was taking place as a result of deposition in the turbine. Pressure drop across the fluid bed began at 31 lwd, increased to 32.5 within five hours and 33.5 after 15, but remained steady thereafter, once again indicating the possibility of running for extended periods without any addition or removal of bed material.

A significant modification to ash-removal hardware was made midway through this test. The lighter portion of the ash collected by the first-stage separator had hitherto been removed through a horizontal line with an orifice-controlled bleed flow of hot gas (See Figure 47, page 70) and the ash moved from this line into a vertical downcomer before entering the main flow to the baghouse. With this system, a buildup of ash where the bleed flow impinged on the far wall of the downcomer had frequently been sufficient to choke off this route of ash removal.

The arrangement was replaced during Test P-403 by an ash-removal device employing a quenching fluid bed in a pressurized environment; the system is illustrated in Figure 53. A water jacket is used to cool the ash rapidly in the fluid bed to about 300 F (i.e., well below the 700-1100 F range within which the ash displays a characteristic stickiness).

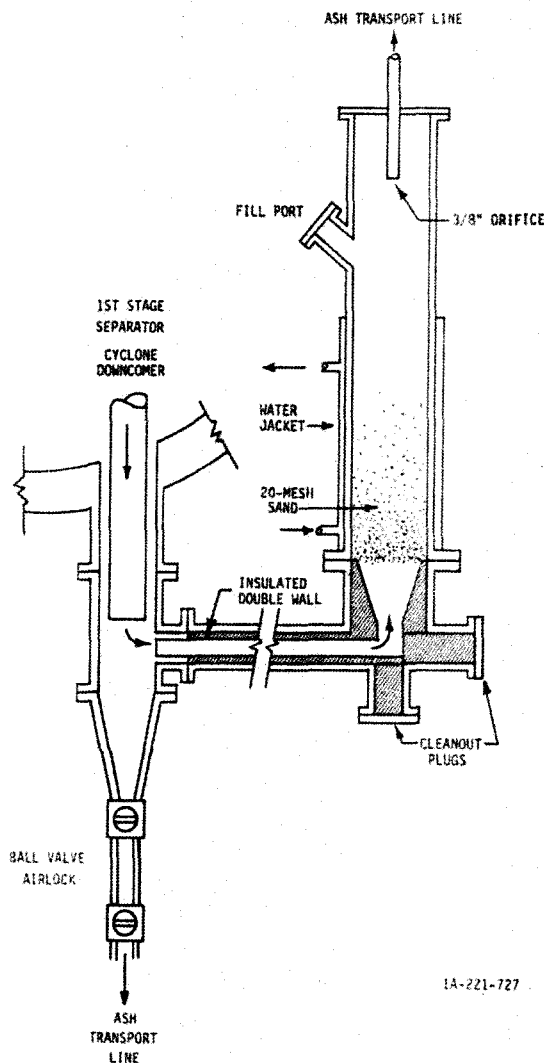


Figure 53 Fluid-Bed Ash-Removal System

The success of the device was apparent both during and after the test. After it was made operational, there were no interruptions because of bleed-flow stoppage, and post-test inspection showed no hard deposits in the exit orifice or downstream of it. There was also a complete absence of wear or deposition in the fluid-bed enclosure.

E. OPERATIONAL SUMMARY

Significant advances were made during the coal program with respect to the operation of a direct-fired gas turbine on solid fuel; significant problem areas still remain. Some of the gains made and some of the problems are discussed in the following paragraphs.

Feed System

The transfer of solids from ambient conditions to the pressurized feedline presented problems that were not fully solved during this program. A rotary-airlock feeder valve was used, and was a not-infrequent cause for test interruptions. When clearances between rotor and housing were sufficiently large for rotation without excessive torque requirements, they were also large enough to admit particles of

coal and dolomite, which were extremely abrasive. The valve had to be returned to the manufacturer for rework on a number of occasions, the first one after about 200 hours of operation. Design solutions to incorporate positive drum-to-housing clearance along with positive sealing are probably possible, but constraints of test schedules and other commitments precluded any such action during this program.

Once the fuel has been put into the feedline, there appear to be no serious problems. Use of dead-end tees for directional changes eliminated feedline erosion as a problem, and with a single point of feed into the fluid bed, combustion efficiencies in excess of 99% were routinely observed.

Particulate Control

Coal combustion presents difficulties in particulate removal quite similar to those seen in burning MSW, somewhat aggravated here by the inerts added in the interest of sulfur suppression. At no time during the program was the exhaust loading low enough either to meet environmental standards or to permit long-term turbine operation. A decaying surge margin showed the influence of deposition in the turbine, and turbine-blade erosion was severe.

Small (3½-in. and 6-in.) inertial separators were found to be ineffectual after brief periods of operation and prone to plugging with the very sticky ash. As in the MSW testing, it appears that for coal, too, the granular filter will be an essential element in any viable system.

Ash Removal

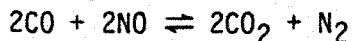
Plugging of residue-removal lines was a frequent cause for stoppage. Only in the final test did it appear that a cure had been found for this difficulty. The use of a quenched fluid bed to cool the ash below the temperatures at which it exhibited extreme stickiness ended the problem of deposition buildup at and beyond bleed orifices.

Noxious Gases

The original promise of the fluidized-bed combustor in the area of suppressing gaseous pollutants was in large measure fulfilled. A corollary to the high combustion efficiency is the very low concentration of unburned hydrocarbons and carbon monoxide. Measured turbine-exhaust hydrocarbon levels did not exceed 3 ppm, and carbon-monoxide levels were only about 10 ppm; both are at least an order of magnitude below applicable standards.

Because of their recognized contributions to atmospheric pollution, oxides of nitrogen could pose a serious potential emission problem. The fluidized bed minimizes fixation from atmospheric nitrogen as a possible source of the original compound (NO is the only oxide of concern in the 1400-1800 F range) by eliminating zones of very high temperature, where favorable equilibrium conditions for the reaction exist. However, it is known that concentrations of NO well above equilibrium levels can be generated from nitrogen contained in the fuel. At atmospheric pressure, coal combustion in the Model Combustor often produced NO_x emissions well above the EPA standard of 0.7 lb/10⁶.

Fortunately, decomposition kinetics are favored by pressure. In addition, local partial pressure of carbon monoxide in bed combustion zones is believed to assist oxide suppression according to the reaction:



The net combination of these effects accounts for measured stack concentrations for the pressurized combustor of 0.4 to 0.5 lb/million Btu, well within the standard.

With high-sulfur coal, the dominant problem emission is, of course, sulfur dioxide. For nominal operation on coal with 4 percent sulfur, 84-percent suppression is required to meet a standard of 1.2 lb SO₂ per million Btu. The highest utilization observed here was 51 percent. In tests in the Model Combustor, however, 90 percent utilization was routinely attained. Those tests used a recycle cyclone to separate unspent fines and return them to the bed. Use of a cyclone in the Pilot Plant combustor was hampered by geometric limitations of the system; it is felt that a system designed for the inclusion of recycle cyclones would successfully meet standards for SO₂ emissions.

Computerized Control

As anticipated, "bugs" in computer software and hardware showed up occasionally in the EPA program and the subsequent hog-fuel tests; but the system may be said to have come of age during the coal program. The experience gained shows that the Pilot Plant is readily controlled in all modes by a process controller featuring analog controllers under the supervisory control of a digital process computer.

An innovation to the computer software that became effective with the start of the P-400 series was a system for generating images of parts of the system with real-time data superimposed. Figure 54 shows a permanent record of one such image, this one providing parametric information over virtually the entire system.

85

Figure 54 Computer Image of the Coal-Burning Pilot Plant

SECTION 7

THE GRANULAR FILTER (TASKS GF-1 & GF-2)

A. BACKGROUND

In Section 4 (Task HP-3), it was seen that inertial separators could not adequately remove the large proportion of fine particulate that is generated by the combustion of municipal solid waste; some other device would have to be found. There was experimental evidence, as in Ref. 1, to show that when a particle-laden gas is passed through a granular media, the particulate contacts the media surfaces by impaction (Figure 55) and is held to the surface of the media.

Earlier attempts to commercialize such a process, however, had not met with success.

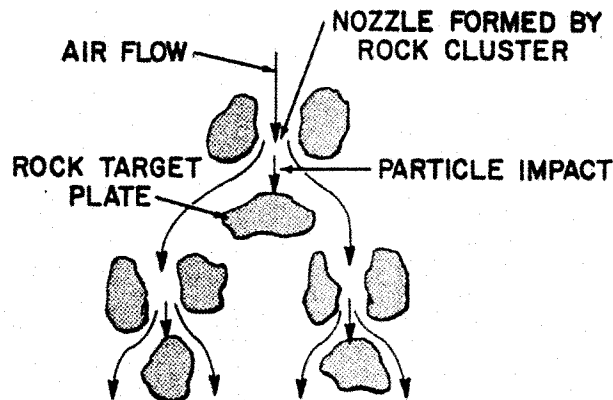


Figure 55 Collection of Fine Particulate by Granular Media

Interest in such a filtration device had nevertheless remained high at CPC. At the time of aborting Task HP-3, plans were in fact underway for the first commercial Dry Scrubber. In this unit, illustrated in Figure 56, a granular media (sand or gravel) is contained between two cylindrical louvered panels. Hot dirty gas

enters the annular space between the vessel and the outer panel and passes through the media to be cleaned, exhausting through the central cylindrical opening. Saturation of the media is prevented by drawing it off at the bottom, passing it through a vibratory screener for clean-up, and returning the cleaned media to the top of the unit. The proven efficacy of the Dry Scrubber gave impetus to the idea of developing a similar device suitable for incorporation into the Pilot Plant.

In preliminary investigations immediately following the HP-3 testing, a small fixed bed of sand was placed in the third-stage vessel, and tests were conducted in which about one percent of the combustion gas (from MSW) was bled off to pass through the bed and exit through a

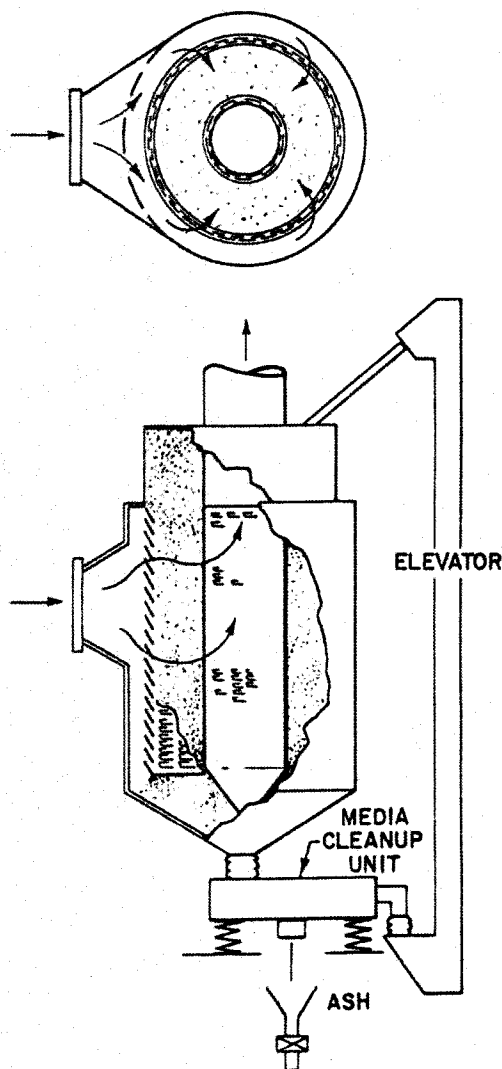


Figure 56 The Dry Scrubber

turbine-blade cascade and flow-control orifice to atmosphere. The arrangement is shown in Figure 57.

Following a baseline test with no media in the bed, a run was made with a 6-inch bed of 16-mesh sand as filter media. The test was relatively brief, since the pressure drop through the bed rose from 0.55 psi after 3 minutes to 3.3 psi after 15. It did have encouraging results, however, since only light and soft flyash deposits were found on the blades in the cascade while hard deposits again built up on the leading edges of blades in the turbine.

Additional tests were then run with a 9-inch bed of 6-8 mesh sand and a 10-inch bed of 1/8" x 16-mesh sand. Increase in pressure drop with time was not so drastic as in the preceding test, but still sufficient to keep the tests to a limited duration. Post-test inspection of the beds revealed that a substantial portion of the fines retained

there actually consisted of pulverized media. In spite of that fact, a decided reduction in exhaust loading was achieved, as shown in Table 20.

The comparison of turbine and cascade blades was essentially the same in all tests: hard leading-edge deposits in the turbine and only light deposits of soft flyash in the cascade.

It was decided on the basis of these results to proceed with testing of models in support of the design of a granular filter for the Pilot Plant.

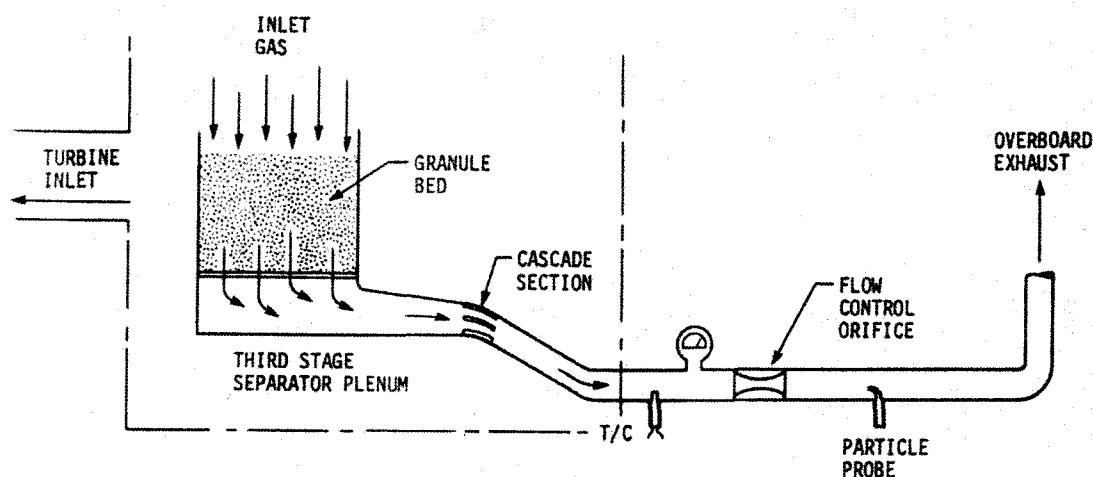


Figure 57 Fixed-Bed Test Setup for High Temperature and Pressure

TABLE 20		
RESULTS OF FIXED-BED FILTRATION		
	Loading at Turbine Exhaust (gr/scf)	Loading at Cascade Exhaust (gr/scf)
None	0.0474	0.0289
9" of 6-8 mesh	.0127	.0005
10" of 1/8 x 16-mesh	-	.0004
10" of 1/8 x 16-mesh	.153	.0005
10" of 1/8 x 16-mesh	.130	.0023

B. MODEL TESTS

Hot-flow testing was conducted in conjunction with a model-combustor system employing a 2.2-sq-ft fluid bed (1/18 the area of that in the Pilot Plant). The complete system is described under Task CP-6, in Section 8 following; a general flow diagram for operation on coal is shown in Figure 58. Hot gas from the combustor passes through two stages of centrifugal separation before entering the granular-bed filter (GBF); a bleed to atmosphere from the second stage provides control of entrance velocity at the filter.

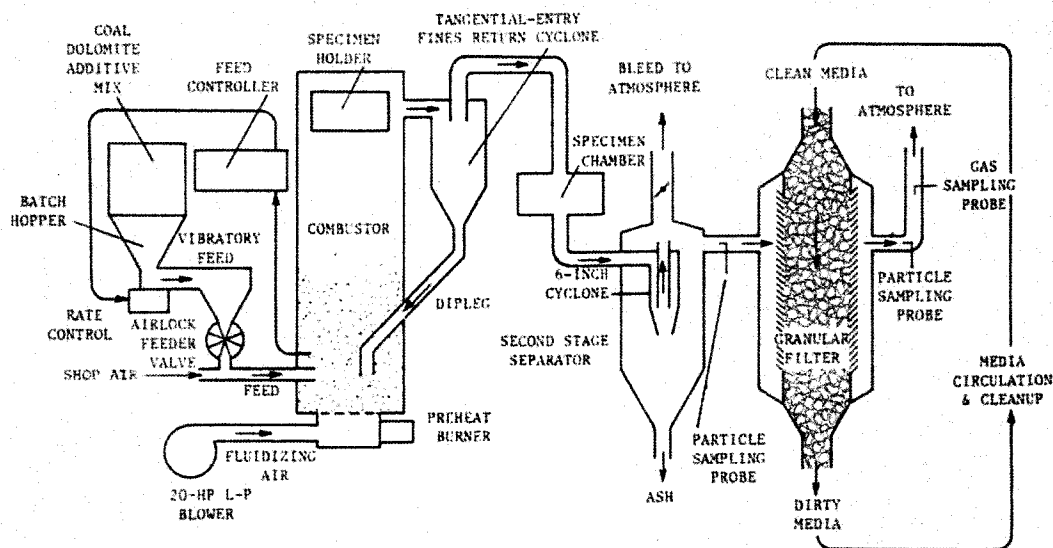


Figure 58 Model Combustor and GBF Flow Diagram

Configuration of the first model GBF, a stainless-steel unit, was as shown in Figure 59. Ribbing was placed along the interior faces of both sides of the unit in an effort to prevent edge effects that could otherwise occur because of the freer gas-flow path that would exist

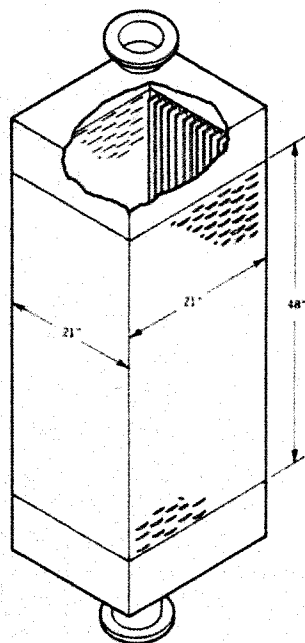


Figure 59 First Hot-Flow Model GBF

along the side walls. In this model, the inlet louver was made of "sunshade" expanded-metal screening, while the outlet side had a louver with flatter and narrower openings; nominal dimensions are shown in Figure 60.

A few media trials were made prior to undertaking the hot-flow testing, with an aim of achieving an entrance velocity of at least 100 ft/min. With 6-12 mesh Monterey sand, it was found that the velocity could not be run above 50 ft/min without encountering excessive spillage of media through the outlet louver. The media was screened to 6-8 mesh, which changed the spillage-governed velocity limit to 73 ft/min. The final try, with 1/8 x 1/4 pebbles, made possible an entrance velocity of 135 ft/min. Accordingly, that was the media selected for the first series of hot-flow tests.

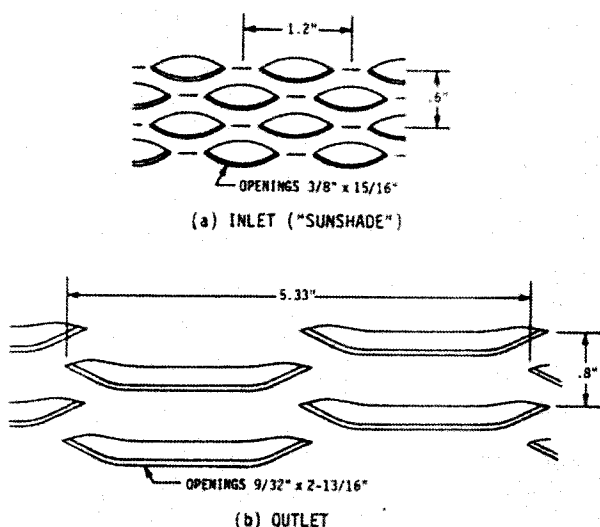


Figure 60 Louver Types for Model GBF

First Hot-Flow Tests

The general arrangement for these initial hot flow tests is shown in Figure 61. Media circulation was intermittent, accomplished by a single tilt-bucket lift. Media, cleaned by a vibrator screener, was returned to the top of the GBF whenever the bucket became full. A cascade of turbine blades was installed at the outlet from the GBF chamber, sized to provide a gas velocity of 575 ft/sec at the minimum area for a front-face velocity to the GBF of 100 ft/min.

Additionally, to prevent media spillage, a perforated-metal screen (1/32" holes, 195 holes per sq. in., 22% open area) was installed in front of the outlet louver.

The several tests in the first hot-flow series are summarized in Table 21. The first test was conducted with municipal solid waste (MSW) as fuel; thereafter, testing was done with coal (dolomite added to suppress sulfur) because that fuel required fewer personnel to operate the system.

TABLE 21							
FIRST HOT-FLOW GBF TESTS							
Test	Media Size	Fuel	Duration (hr)	Media Circ. (lb/min)	GBF Delta-p (IW)	Inlet Loading (gr/scf)	Outlet Loading (gr/scf)
H-1	1/8x1/4	MSW	10.9	1.2	1-4.5	0.09	0.13
H-2	6-8 mesh	Coal	4.4	10	12-18	-	-
			6.4	12	4-10	.50	.09
			3.2	7	7-28	-	-
			6.3	10	6-34	.89	.28
			2.7	2-8	4-30+	-	-
			4.7	20 max	15-60	.26	.04
			6.6	4-6.5	7-10	.37	.06
			4.5	2.5-4.5	8-14	.25	.15
H-3	16-20 mesh		13.0	4-5	39-52	.44	.10

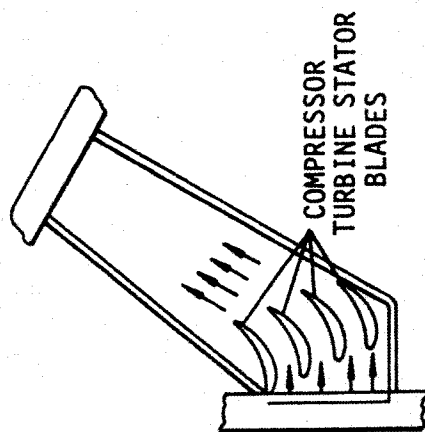
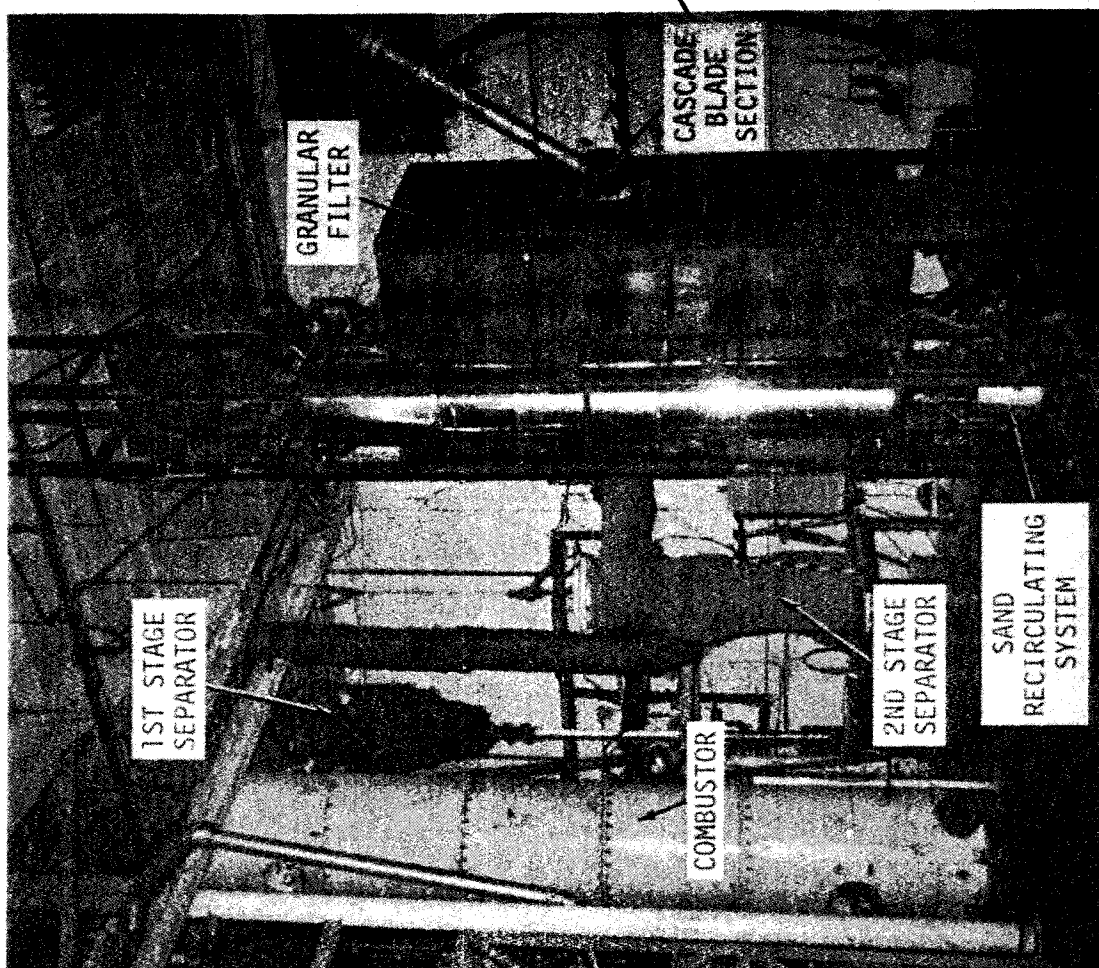


Figure 61 Hot-Flow Test Setup

The testing was begun with the optimistic objective of verifying the granular-filter concept with a 100-hour run. Test H-1, however, was terminated when spillage at the outlet screen became excessive (media had worked around the inner screen at places where it had not been welded because of inaccessibility). Even without this problem, however, the test would soon have terminated because of the buildup in pressure drop through the cascade section; this drop had risen from 60 to 100 Iwd during the 10.9 hours of testing, and post-test inspection showed heavy--though soft--deposition on the turbine blades. The anomaly of an outlet loading greater than that at the inlet probably represents only an initially faulty technique in measurement. Regardless of technique, however, the deposition in the cascade section made it very clear that particulate removal was inadequate.

To improve filtration, a slightly finer cut of media was used in Test H-2. A total of eight starts were made, but periodic loading measurements continued to show inadequate filtration. One problem was that the vibrator/screener was not properly cleaning the dirty media before it was returned to the top of the GBF; in the final four starts, therefore, the used media drained at the bottom was simply discarded and replaced with clean 6-8 mesh sand. This operational change was still not sufficient, however, to produce consistently small enough outlet loadings. (For the model system burning coal, a loading of 0.04 gr/scf, when corrected to 12% CO₂, is roughly equivalent to the environmental standard of 0.1 lb/million Btu). One problem whose full significance was not then appreciated was fragmentation of the media itself, a phenomenon that was adding to the outlet loading. At the time, it

was hoped that this sort of attrition would ultimately run its course, and that a steady state might be attained in which no further attrition would occur.

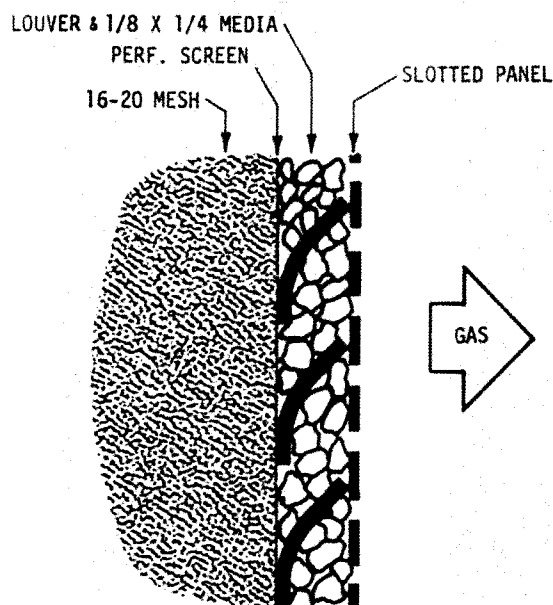


Figure 62 Arrangement of Outlet Louver for Hot-Flow Test H-3

Test H-3 was the final attempt in this series to achieve adequate filtration --this time by use of smaller media. Monterey sand at 16-20 mesh was used, its retention within the filter bed being facilitated by the arrangement illustrated in Figure 62. A perforated-metal panel (1/32-inch slots) was added on the downstream face of the louver panel, and the space between it and the

interior perforated screen was filled with 1/8 x 1/4 media. A number of starts were made. On the first day, with a filter approach velocity of 100 ft/min, the media drain rate was varied from 1/2 to 10 lb/min in an attempt to stabilize the pressure drop through the filter; pressure drop, however, continued to increase at about 0.5 IW/min, regardless of drain rate.

Next, the filter approach velocity was lowered to 80 ft/min, and drain rate was maintained at 4 lb/min. Pressure drop increased at half the earlier rate for the next hour, then suddenly dropped 13 IW, and stayed at 30 IW for 2-1/4 hours. The only significant change during this period was a decreasing filter outlet temperature. On the following day, the same test conditions were imposed, but the pressure drop continued to climb. A final attempt was made in which the media drain was pulsed, a method that had seen some success in previous tests; in this case, however, it had no apparent effect.

At this point, hot-flow testing was temporarily halted to await completion of a series of cold-flow tests then underway, aimed at developing a better parametric understanding of filtration phenomena.

Cold-Flow Tests

At the time of initiating cold-flow testing, design of the Pilot Plant GBF had become firm enough that the model filter could be made more representative of the ultimate design. Configuration for the cold-flow testing was as shown in Figure 63; the model represents a 31° segment of the annular Pilot Plant filter. The test setup is shown in Figure 64.

A summary of the tests is given in Table 22. Test C-1 consisted of a set of parameter variations, using clean air and 7-8 mesh San Simeon sand as media; significant results are shown in Table 23 and Figure 65. The tabulated data on spillage led to the selection of 8 lb/min for the media drain rate and 125 ft/min as the approach velocity. These values provided an initial pressure drop through the GBF of just under 6 IW (Figure 65).

Test C-2 also used clean air, since it was run to establish baseline values for outlet loading. Results are shown in Table 24. All measured loadings were sufficiently low to be an insignificant factor in terms of the measurements for dust-laden air.

Test C-2 also saw the introduction of an experimental pneumatic system for circulation and cleanup of the media, shown schematically in

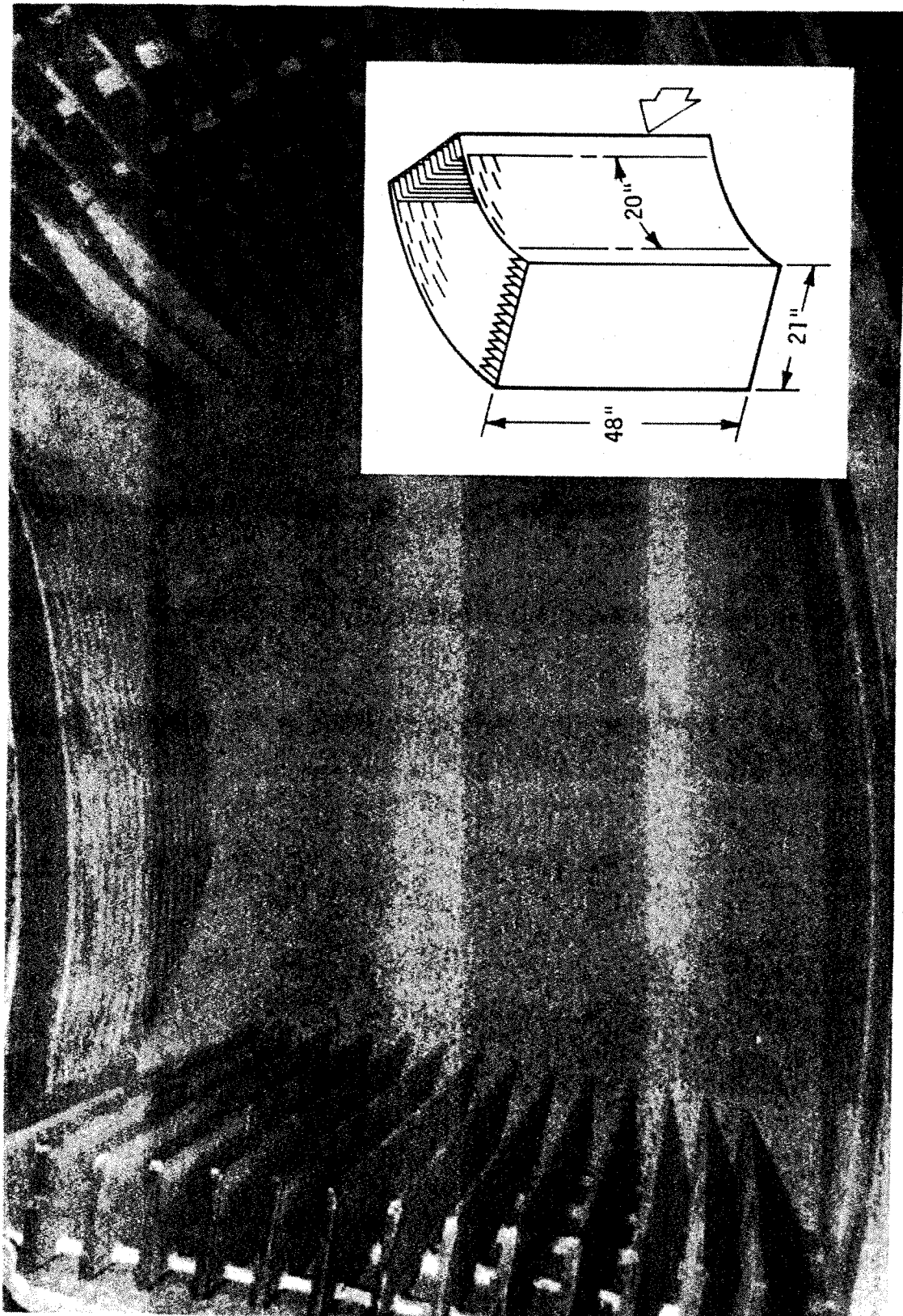


Figure 63 Cold-Flow Test Segment

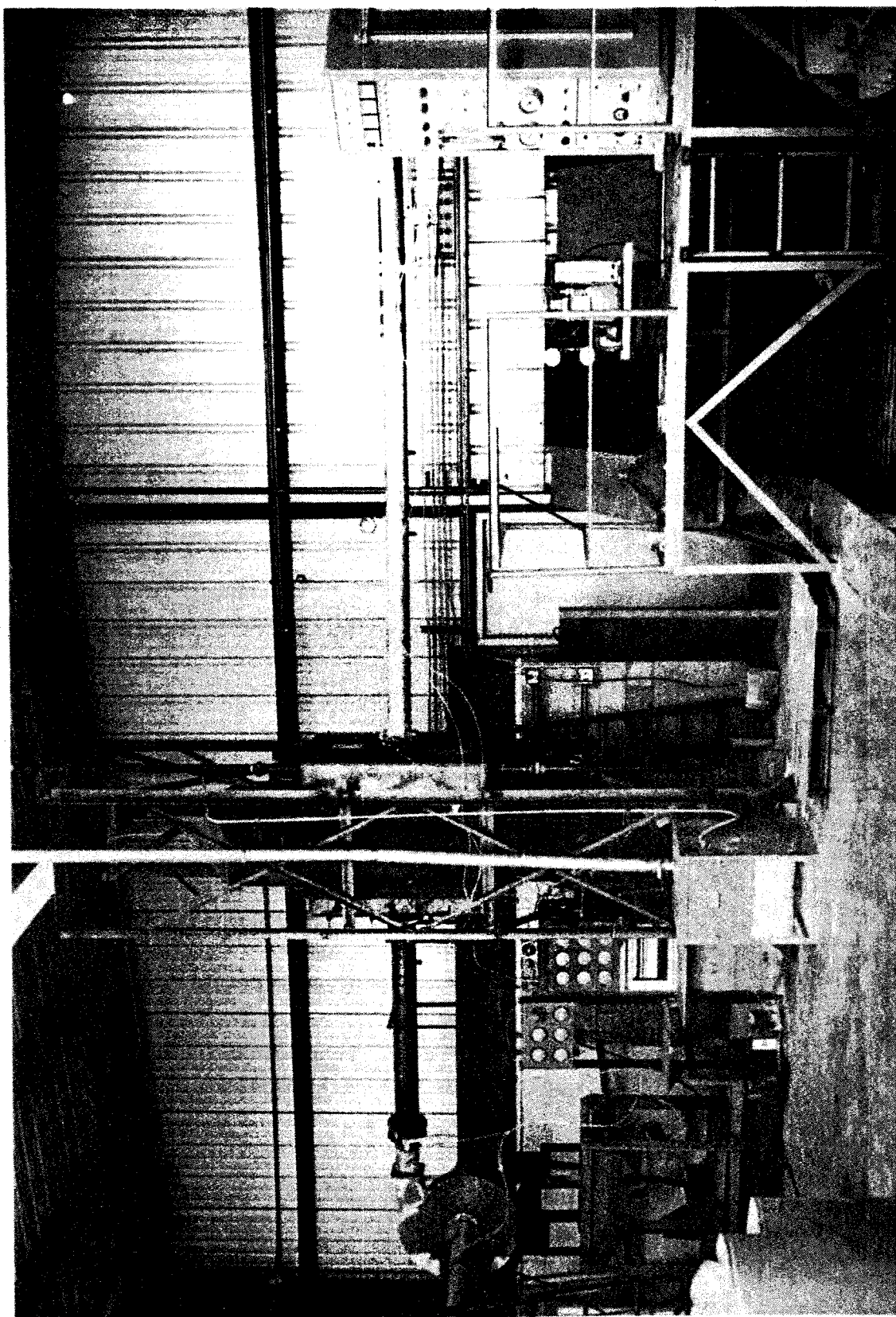


Figure 64 Cold-Flow Test Setup

TABLE 22
COLD-FLOW TESTS

Test	Media	Media Circulation (lb/min)	Approach Velocity ft/min	Description
C-1	7-8 mesh sand	variable	variable	Parametric study
C-2	↓	variable	variable	Baseline loading
C-3	↓	8	125	Evaluation of filtering
C-4	↓	8	↓	New baseline for cleaned media
C-5	↓	9	↓	Evaluation of filtering
C-6	5-7 mesh Al ₂ O ₃	13	variable	Baseline loading
C-7	↓	11	125	Evaluation of filtering

TABLE 23
MEDIA SPILLAGE THROUGH
OUTLET LOUVER

Media Drain Rate, lb/min	Time of Operation, min	Approach Velocity, ft/min		
		0	100	200
		Spillage, grams		
0	12	-	4.6	261
8	6	.8	18.6	1369
16	3	.9	18.1	1159

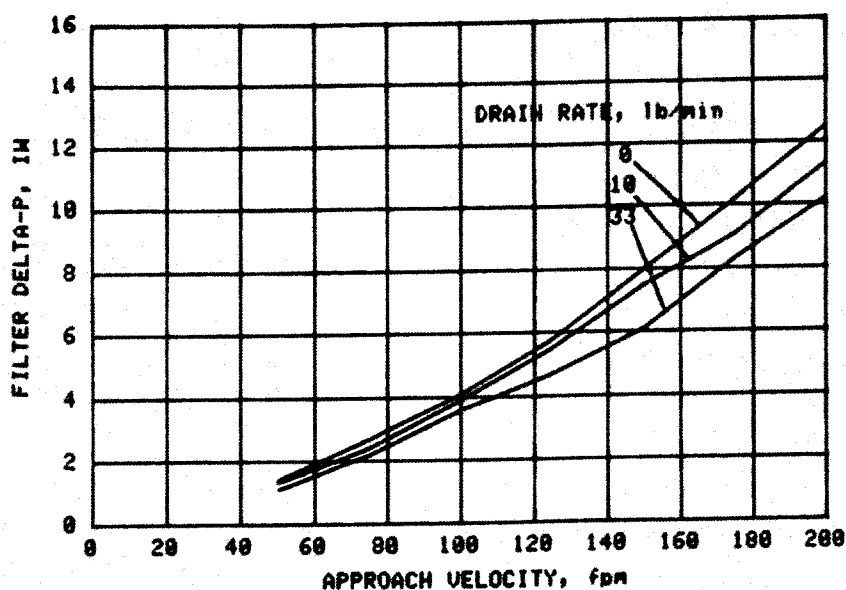


Figure 65 GBF Pressure Drop with 7-8 Mesh San Simeon Sand

TABLE 24		
GBF OUTLET LOADING WITH CLEAN AIR		
Approach Velocity, ft/min	Media Drain Rate, lb/min	
	0	8
Outlet Loading, gr/scf		
100	.00230	.00015
125	.00008	.00120
150	.00001	.00070

Figure 66. Cleanup of the media was accomplished by agitation in the process of being transported to the top of the system, by impact as the media fell through a series of baffles, and by further agitation and impact in a fluid bed. From this upper fluid bed, it fell back into the top of the GBF. The dust-laden transport air and the fluidizing air for the upper fluid bed exhausted to the baghouse.

A second fluid bed was incorporated at the lower end of the system, in an attempt to avoid an adverse pressure gradient in the downcomer from the GBF. There was concern that the gradient might tend to force dust back up into the filter. This lower bed, however, never functioned as planned, since replenishment of media

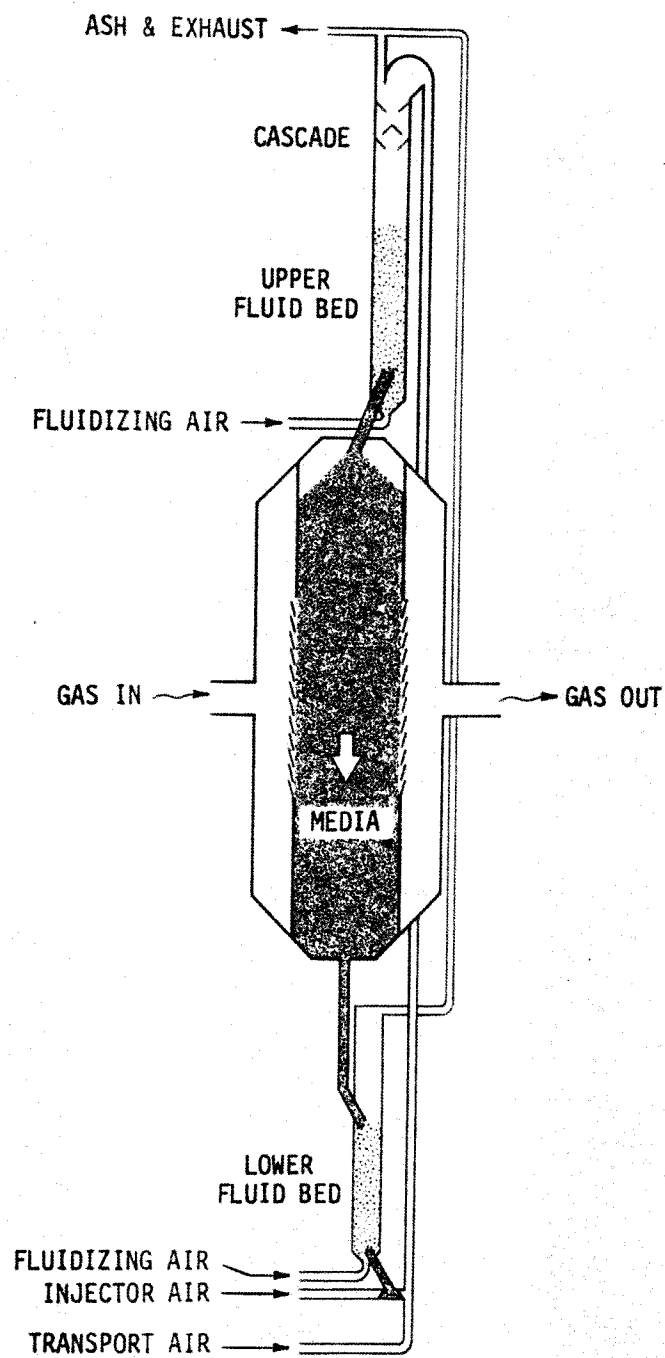


Figure 66 Pneumatic Circulation and Cleanup System

by gravity feed from the filter was always rapid enough to keep the "freeboard" in a packed state; augmenting the fluidizing air only succeeded in transporting quantities of media to the baghouse.

Test C-3 was the first try at operating the filter with simulated ash carried by the throughput air. Burgess #10 clay pigment, with an average particle size of about one-half micron, was injected into the air upstream of the filter. The test comprised some 27 hours of operation, divided into three segments, with three different pigment-injection rates. Results are shown in Table 25.

TABLE 25 INLET AND OUTLET LOADINGS		
Pigment Injection Rate (lb/hr)	Inlet Loading (gr/scf)	Outlet Loading (gr/scf)
10	2.32	.012
5.6	.82	.008
3.8	.52	.006

Tests C-4 and C-5 were run for repeatability. The media was first circulated for several hours to clean it for the C-4 baseline. This had somewhat limited success, in that outlet loadings of 0.0082 and 0.0045 gr/scf were recorded in Test C-4; these compare with a high of 0.0023 during C-2. (A part of the increase is attributable to progressive fragmentation of the media).

Good gas cleanup was achieved nonetheless in Test C-5. During some 23 hours, with media being circulated at 9.3 lb/min and pigment being injected at 3.25 lb/hr, the loadings of Table 26 were recorded; the readings were reasonably consistent, and showed no evidence of any deterioration during the progress of the test.

TABLE 26 LOADINGS IN COLD-FLOW TEST C-5		
Elapsed Time (min)	Inlet Loading (gr/scf)	Outlet Loading (gr/scf)
100	.6074	.0052
419	.5658	.0142
556	.5490	.0038
785	.5010	.0063
1070	.3993	.0048
1403	.5350	.0062
Ave.	.5262	.0068

At this time, however, there was rising concern over the tendency toward fragmentation of the media. Accordingly, the last two cold-flow tests were devoted to studying the more expensive, but much harder, aluminum-oxide spheres as media. Test C-6 served as baseline, and also included a brief parametric study. The study showed the pressure drop through the clean filter was independent of the rate of media circulation; dependence on approach velocity is illustrated by Figure 67. Pressure drop with the nearly

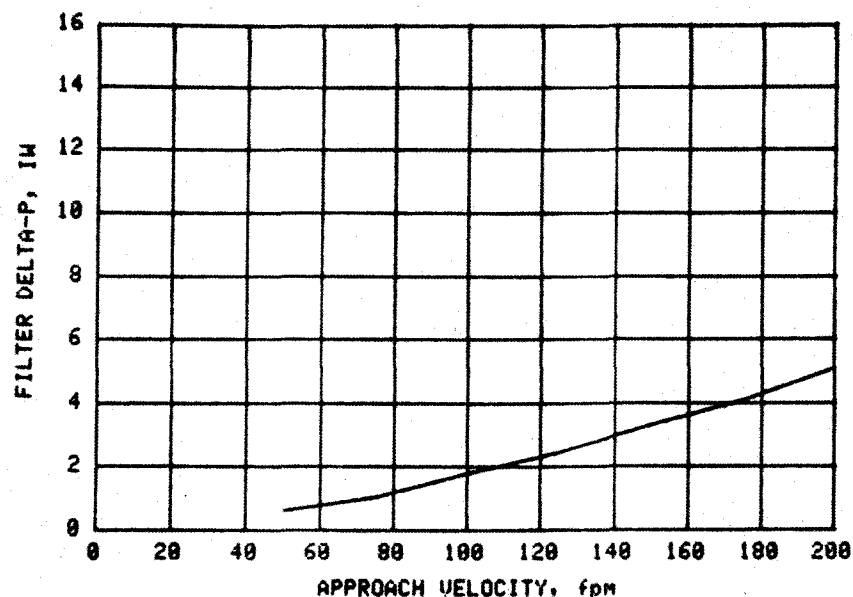


Figure 67 GBF Pressure Drop with 5-7 Mesh Al_2O_3 as Media

spherical media (5-7 mesh) is seen to be about half that developed with the 7-8 mesh San Simeon sand (Figure 65).

Loadings were recorded with a media circulation rate of 13 lb/min and an approach velocity of 125 ft/min; the two readings taken showed outlet loadings for the clean media of 0.00015 and 0.0005 gr/scf.

Test C-7 was then conducted with Burgess #10 pigment added to the inlet air at 2.6 lb/hr. With an approach velocity of 125 ft/min and media circulated at 11 lb/min, the average pressure drop through the filter was 8.4 IW, or about 2-1/2 times that developed by the clean media. Loadings recorded during the test are shown in Table 27. A reasonable steady state was achieved quite early in this 35-hour test, but post-test inspection did show substantial deposits of pigment along both sides of the inlet panel, enough to reduce the openings in that panel by about 10%.*

* This edge effect persisted in all the tests reported here. Reduced media activity along the sides -- coupled with preferential gas flow because of the lower void fraction there -- made that region more prone to deposition, which further inhibited media movement; the effect would gradually propagate inward. Thus it is seen that quantitative results for a segment-type model cannot be transferred directly to a full annular filter.

TABLE 27
LOADINGS IN COLD-FLOW TEST C-7

Elapsed Time (min)	Inlet Loading (gr/scf)	Outlet Loading (gr/scf)
146	0.1869	0.0141
320	.4753	.0166
615	.3693	.0084
790	.2182	.0098
1172	.4323	.0139
1277	.4756	.0301
1620	.4828	.0284
1750	.5406	.0309
1950	.4674	.0138
2240	.5183	.0109
Ave.	.4167	.0177

Second Hot-Flow Tests

The second series of hot-flow tests included two further attempts to use inexpensive sand as media before shifting over to studies with aluminum-oxide spheres. The complete series is summarized in Table 28.

Tests H-11 and H-12, using sand as media, made it quite clear that fragmentation would be a continuing problem with this material. Even on oil combustion (H-11) the outlet loading was excessive, and substantial increase was experienced when Test H-12 was carried out, using coal as fuel. In the latter test, there was evidence that a reduced media circulation rate could improve cleanup to some extent, but not enough to meet desired levels.

In Test H-13, 5-7 mesh aluminum-oxide spheres were used as media. The test began with the media circulated at about 18 lb/min; particle removal was inadequate. The circulation rate was then reduced to the minimum that could be maintained with the system as configured, about 10-15 lb/min, but cleanup was still unsatisfactory. The pressure drop through the filter had increased from the initial 2 or 3 IW to about 5. In an effort to generate further increase, a schedule of intermittent circulation was adopted some 46 hours into the test. Figure 68 shows pressure drop and loadings recorded thereafter. Loadings were reduced--though still not sufficiently--and the pressure drop increased to around 17 IW. Subsequent resumption of continuous circulation resulted in increased loading, but pressure drop did not undergo any sustained reduction.

The reason for this behavior became evident in post-test inspection: there had been ash deposition to as much as an inch deep over the entire inlet louver panel, and the slots were almost totally plugged.

The inadequacy of filtering in Test H-13 led to a change in subsequent tests to 8-12 mesh Al_2O_3 . Also, prior to Test H-14, a system for returning media spilled through the inlet face was incorporated. Test H-14 began with the media circulated at 10 lb/min. At this rate, excessive spillage of media through the outlet louver was encountered.

TABLE 28
SECOND HOT-FLOW
GBF TESTS

Test	Media	Fuel	Duration (hr)	Media Circ. (lb/min)	Approach Velocity (ft/min)	GBF Delta-p (IW)	Inlet Loading (gr/scf)	Outlet Loading (gr/scf)	Description
H-11	7-8 mesh sand	oil	19	0	125	2	-	0.084	Background with sand media
H-12	7-8 mesh sand	coal	21	17	125	4-6	.2236 .3436 .3754	.1983 .2240 .4611	Check of cleanup with sand media
			7	12		11	.4298	.1069	
H-13	5-7 mesh Al ₂ O ₃	MSW	118	18 10-15 pulsed	125	2-3 5 16-18	.3412 .4342 ^(a) .2892 ^(b)	.1450 .1713 ^(a) .0647 ^(b)	Check of cleanup with Al ₂ O ₃ media
H-14	8-12 mesh Al ₂ O ₃	MSW	85	10 20	100	15-27 29-31	1.1596 ^(a) 2.0671 ^(b)	.0625 ^(a) .3246 ^(b)	Trial of finer media
H-15	8-12 mesh Al ₂ O ₃	MSW	60	10	100	5	.4062 ^(a)	.0897 ^(a)	Methods of front-face cleaning
H-16	8-12 mesh Al ₂ O ₃	MSW	57	5-7.5	100	6-15	.3199 .9181 1.0354 2.1802 1.9314 .9131	.0836 .0718 .0851 .0642 .0398 .0210	Cleanup with front-face cleaning

Notes: (a) Average of 6
(b) Average of 4

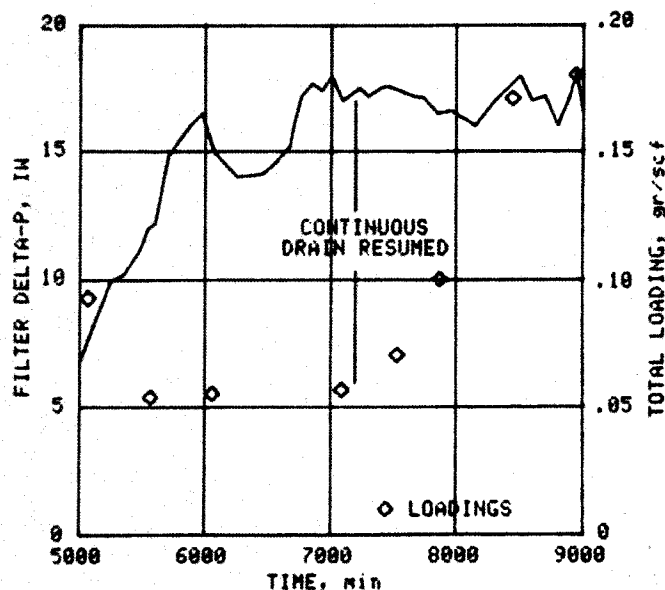


Figure 68 Pressure Drop and Loadings with Pulsed and Continuous Media Circulation, Test H-13

To reduce this spillage, the circulation rate was increased to 20 lb/min. Control of spillage was still inadequate, and outlet loadings rose drastically. Once again, post-test inspection revealed severe deposition on the inlet louver.

To ameliorate the spillage problem, the filter was fitted with a new outlet louver panel, in which the louver slots had been rolled down to provide an opening width of 0.062 ± 0.007 inch. And, in Test H-15, several methods for periodically removing deposited ash from the front face

were tried out. These included air blasts in various directions, and a rain of media from a region about 2" in front of the panel. The two most successful were then employed in Test H-16. These were a series of four vertically aligned air jets directed normal to the center of the right half, and a similar series directed obliquely at the left half. Selection was made--during Test H-15--by allowing the pressure drop to build to about 12 IW and then employing one or another of the methods and observing their effectiveness in reducing that value.

In Test H-16, minor modifications in the circulation system permitted slowing media circulation to a value generally between 5 and 7.5 lb/min; this made possible the development of a pressure drop through the filter that was for most of the test between 8 and 9 IW. No effect of this increased pressure drop was evident until the latter half of the test, and only the final outlet loading (0.021 gr/scf) was at a satisfactory level. However, about 40% of the particulate collected by the sampling probe was now being identified as alkali salts that would exist as vapors at the GBF inlet temperature of 1250 F. Thus there existed a strong probability that further reductions in outlet loadings could be achieved by using precipitating additives; further investigation of that approach was included as a part of Task CP-6 (Section 8).

Cleaning of the front face had been adequate where the air blasts impinged directly (Figure 69), with somewhat better results for the head-on blast than for the oblique one. Some areas between air jets had not been cleaned adequately, and further study of methods of front-face cleaning seemed in order. For reasons of schedule, the air-jet approach was incorporated in the design of the Pilot Plant GBF along with the narrow-louver outlet panel, but testing in this general area continued, as described below.

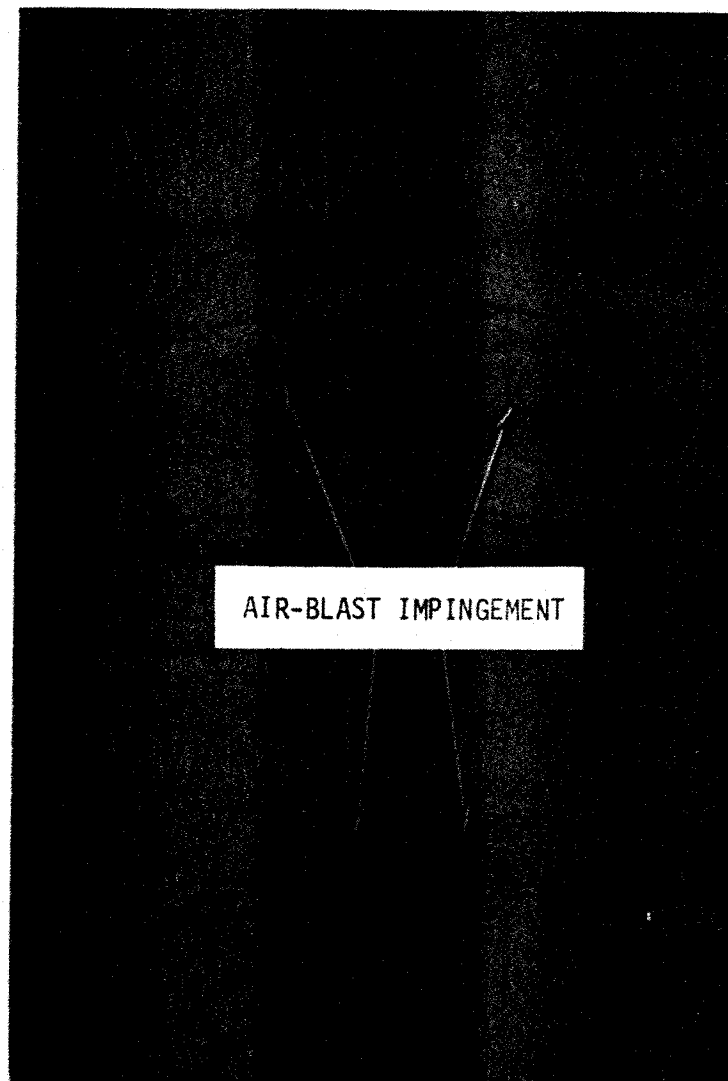


Figure 69 Inlet Louver Panel after Test H-16

C. FRONT-FACE CLEANING

The methods for cleaning the front face of the GBF tried out up to this point involved intermittent action. It would, of course, be eminently more satisfactory if cleaning could be done on a continuous basis, thus avoiding any buildup of deposits in the first place. The idea of encouraging enough spillage of media through the front-face panel to scour off deposits as fast as they were formed thus seemed promising, and this investigation was therefore designed to explore that possibility.

Testing was carried out in three phases: a problem definition study (cold), a development of hardware concepts and design (cold), and a series of verification tests (hot). The model used was the 31-degree segment representative of the annular Pilot Plant GBF; the inlet louver panel, however, was changed from the "sunshade" screen to a slotted design having 1-inch-long louvers sloped at an angle of 70° to the horizontal, providing a 1/4-inch-wide slot.

The setup used for all cold-flow testing is shown in Figure 70 (in the photograph at the right, the inlet plenum has been removed).

Problem Definition Study

This phase of the program included calibration, an investigation of the effect of flow rates on spillage, and testing to select an appropriate material to inject into the air stream as simulated flyash. Calibration results are plotted in Figure 71. The easily measured pressure drop in the lift pipe is seen to be a good indicator of the rate at which media is being circulated; the single point for which air was blown through at 140 lb/min shows that this parameter has no significant effect on the calibration.

The plot of Figure 72 shows the effect of rates on the amount of front-face spillage that is developed. As might be expected, the more media activity that is developed (i.e., the higher the rate of circulation) the greater the spillage that results. The retarding effect of air flow is also evident. Visual observation during these tests gave indication of a rather substantial edge effect. In the corners where the panel met the side walls of the GBF segment, the media activity--and hence the spillage--was very slight. This inability to represent completely the characteristics of a full annulus by a single segment would have to be borne in mind when interpreting test results.

In selecting the "ash" to be injected into the air stream, the main criterion is that it would have to be somewhat troublesome; i.e.,

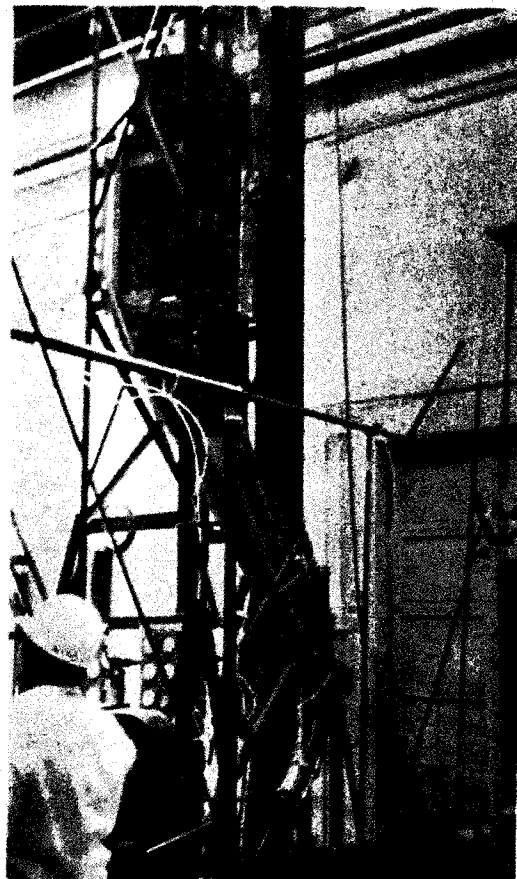
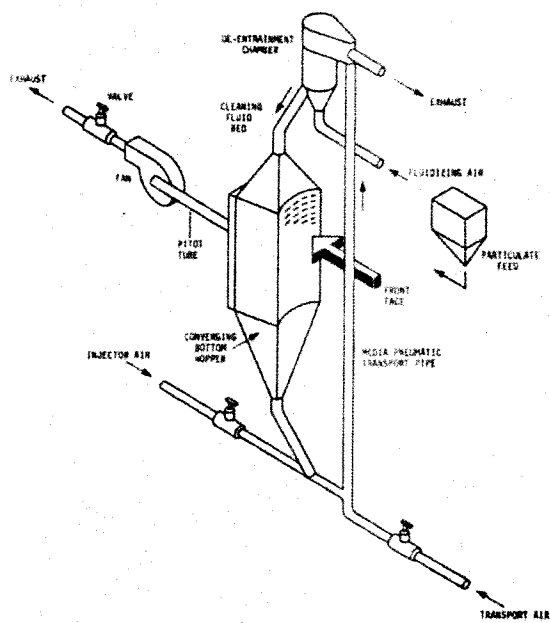
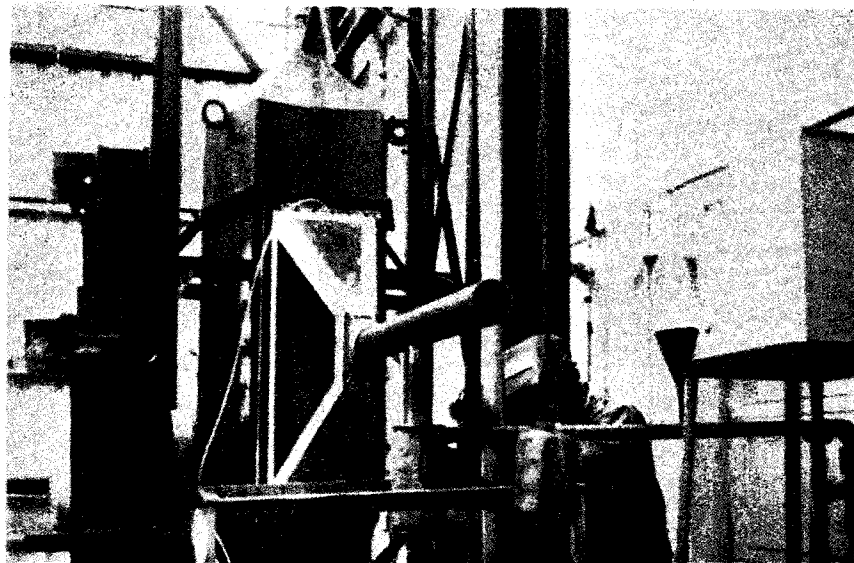


Figure 70 Model Setup for Front-Face Cleaning Tests

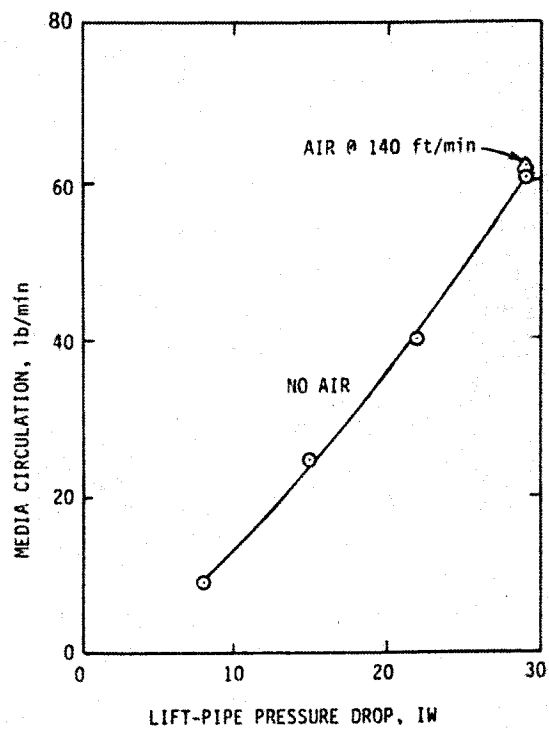


Figure 71 Lift-Pipe Calibration

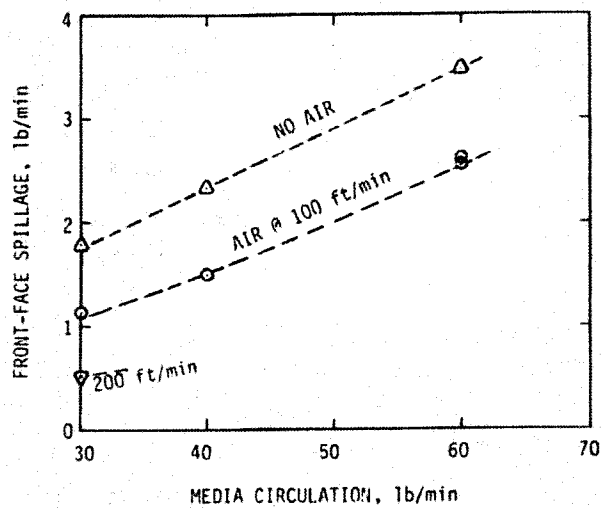


Figure 72 Rate Effects on Front-Face Spillage

prone to deposition. Two candidates were considered. The first was actual ash collected by a Dry Scrubber from the exhaust gas of a wood-fired boiler in Snoqualmie Falls, Washington; the second was a processed kaolin, Burgess #10 pigment. Test results for the two are shown in Figure 73; the materials were injected into the air stream at such a rate as to give a nominal inlet loading of 1 gr/scf. Comparison with

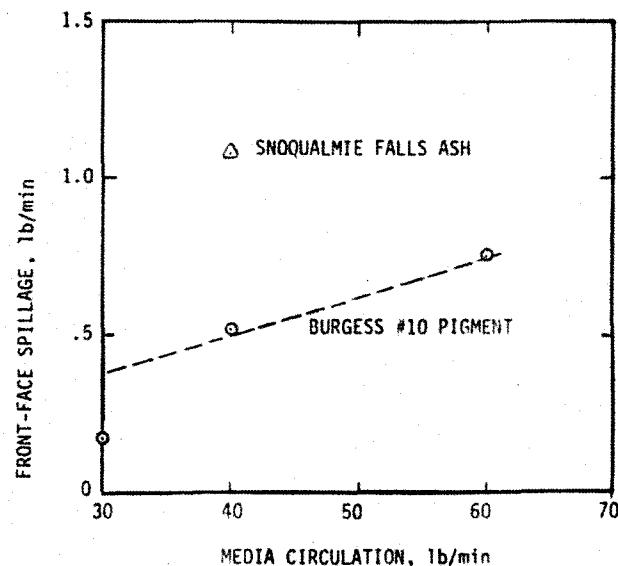


Figure 73 Front-Face Spillage with Dust Injection and Air at 100 ft/min

Figure 72 shows that the true ash--at least at low temperature--has only a minor effect on the rate of spillage out the front face. The clay pigment, on the other hand, reduced the spillage rate by more than half. It was also much more prone to deposition and was therefore used--except for a single instance--in the design-development tests.

Design Development

Seven different configurations of the inlet panel were tested in the process of arriving at an acceptable one. The testing effort was focused on the media spillage phenomenon at the front face as a natural and important mechanism in preventing deposition and consequent plugging. Accordingly, the tests were planned to gather additional data, both quantitative and qualitative, on spillage as it is influenced by operating parameters and louver-panel geometry. A slight change was made in the test geometry in that the outside louver column on each side was taped over so that the edge effect that had been observed would not be a significant factor in the comparative tests. This reduced the effective front-panel area by about 30%.

The test program included a quasi-baseline test (without dust injection), using the original louver panel with some slot openings

reduced to promote maximum spillage from the upper portions of the panel. Following that, a revised type of louver panel, produced by Duus Perforated Metal Co., was adopted for structural reasons. In contrast to the original louver type, which was shown in Figure 60, the Duus panel has the louvers so aligned as to incorporate continuous metal columns between louvers; this arrangement, with the appropriate nomenclature, is shown in Figure 74.

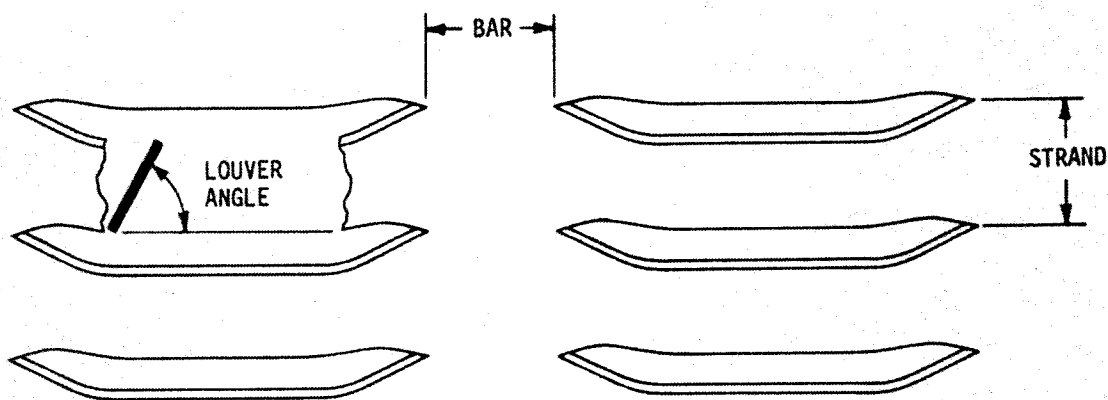


Figure 74 Duus Louver

Three of the panels tested were modifications of this basic geometry, developed by milling off portions of the louver, both on the inside and on the outside, as shown in Figure 75. The two other types were the "sunshade" (Figure 60, p. 89) and a smooth panel with oblong slots of the dimensions shown in Figure 75.

Test results are given in Table 29. Except for the final entry in the table, the tests were nominally four hours long (at 60 lb/min, the media completes a circulation cycle in about one hour). All tests showed significant reductions in media spillage when dust was injected, along with varying degrees of plugging in the openings; but the panel with oblong slots retained the best spillage rate by a substantial margin, even after 14 hours of testing, and it underwent only minor plugging. Results for this final geometry are compared in Figure 76 with the curves that were drawn in Figures 72 and 73 for the original configuration.

During operation with media circulation, spillage occurred from each of the openings of all panels, but at different rates and with differing media movement. Figure 77 illustrates the mechanisms for retention and release of the individual spheres. With the louvered panels, flow had to change direction from down to almost vertically

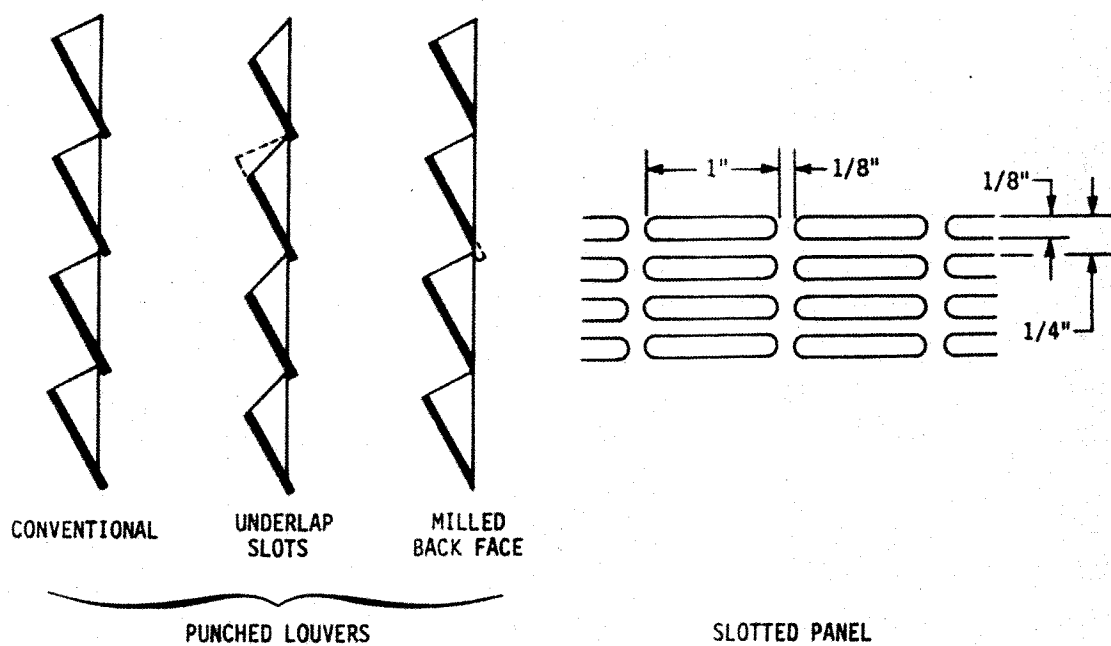


Figure 75 Panel Configurations

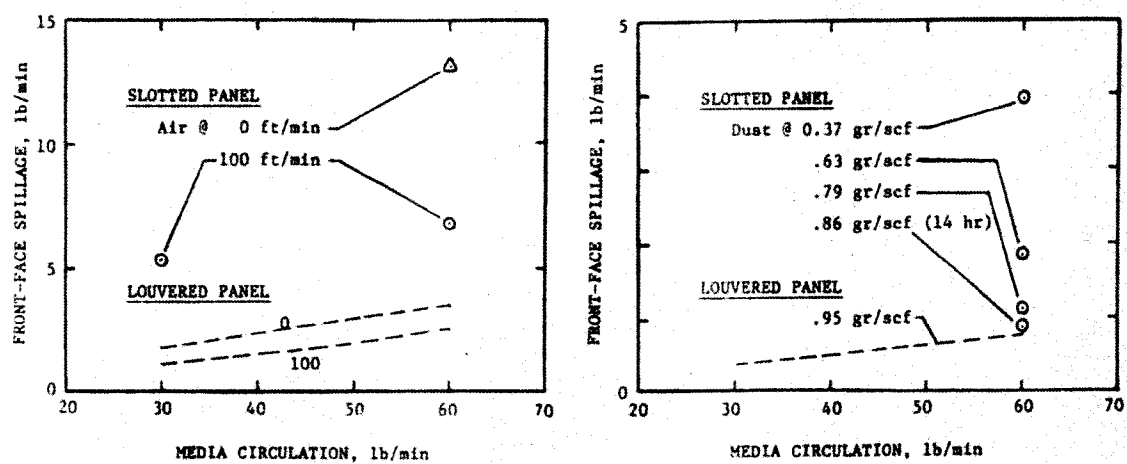


Figure 76 Comparative Results for Slotted and Louvered Panels

TABLE 29
LOUVER-PANEL EVALUATION RESULTS

Louver	Approach Velocity (lb/min)	Media Circ. (lb/min)	Dust	Inlet Loading (gr/scf)	Average F.F. Spillage (lb/min)
A	0	30	None	-	2.1
	100	30	None	-	1.4
	100	60	None	-	3.2
	200	30	None	-	.63
B	0	30	None	-	5.4
	0	60	None	-	12.4
	100	30	None	-	3.05
	100	60	None	-	6.05
	200	30	None	-	1.40
	200	60	None	-	2.75
	100	60	#10 pigment	1.11	(a)
	100	60	#10 pigment	.32	.99
	100	60	SF ash	1.00	1.47
	100	60			
C	0	60	None	-	5.0
	100	30	None	-	.9
	100	60	None	-	2.1
	100	60	#10 pigment	.31	.43
D	0	60	None	-	15.7
	100	30	None	-	2.4
	100	60	None	-	5.23
	100	60	#10 pigment	.63	.75
	100	60	#10 pigment	.49	.92
	100	60	#10 pigment	.28	2.65
E	0	60	None	-	30.5
	100	30	None	-	5.43
	100	60	None	-	14.17
	100	60	#10 pigment	.88	.80
F	0	60	None	-	12.0
	100	30	None	-	4.35
	100	60	None	-	4.60
	100	60	#10 pigment	.93	.60
	100	60	#10 pigment	.67	1.86
	100	60	#10 pigment	.32	4.58
G	0	60	None	-	13.13
	100	30	None	-	5.35
	100	60	None	-	6.8
	100	60	#10 pigment	.79	1.12
	100	60	#10 pigment	.63	1.85
	100	60	#10 pigment	.37	3.94
	100	60	#10 pigment	.86	.84 (b)

Notes: (a) Front face plugged in 18 min.
(b) After 14 hrs.

LOUVER DESCRIPTIONS

A Regular panel with some slot openings reduced (counting from top to bottom) as follows:

1 to 9 0.300"
14 to 22 .275"
27 to 35 .250"
40 to 48 .225"

B Duus louver with 5/8" bar, 5/8" strand, 3/16" gap, 80° louver angle.

C Duus louver with 3/4" bar, 3/4" strand, 1/4" gap, 70° louver angle. Two columns as is, two columns milled for 1/8" underlap slot.

D Same as C, but all columns with 1/8" underlap slot, and back face of two columns milled flush with panel surface.

E "Sunshade" panel.

F Modified from D. All back faces ground flush, two columns with 0.25" underlap slots, two with 0.21" underlap slots.

G Smooth panel with 1/8" x 1" slots.

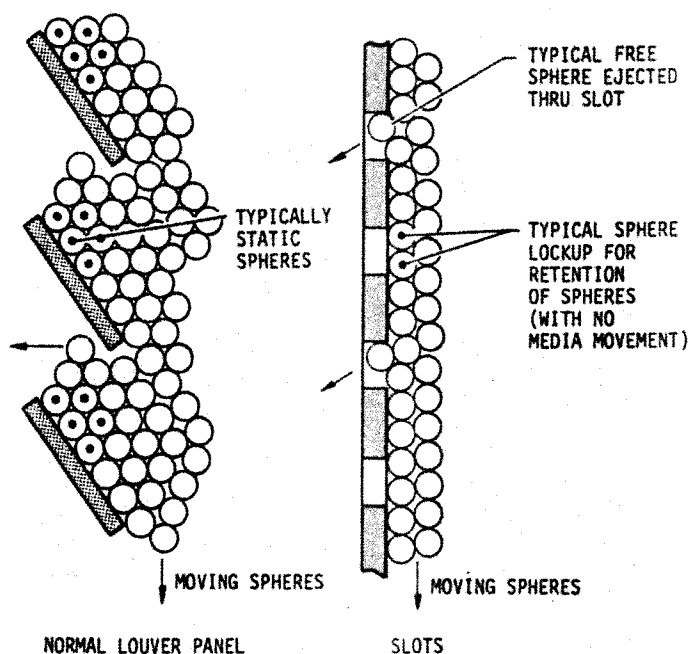


Figure 77 Media Retention and Flow

upward before release would occur, and a stagnant region was developed at the upper part of the louver surfaces. In operation, such a region would accumulate ash and eventually block all local movement of media. Each of the louvered panels showed this tendency, with the steeper (80°) louvers being somewhat more free-flowing than the less steep (70°). Making the back faces of the panels flush also increased spillage.

Stagnant areas are eliminated with the simple slotted panel. The width of the opening (about 1.6 times the diameter of the media spheres)

was found to be sufficiently small to stop spillage in the absence of media circulation, and sufficiently large to facilitate it when operating with circulation. The spillage rate can in fact be controlled by adjusting circulation rate. There is also a horizontal component of motion associated with release of the spheres and that, coupled with the effect of the air stream, tends to wipe clean the surfaces of the panel between openings.

Hot-Flow Verification

In order to evaluate the slotted panel with actual combustion gas in a hot environment, it was installed in the hot model GBF and operated in conjunction with a company-funded wood-burning test program. This program included eight test series and encompassed 513 hours of hot operation; all were run with the GBF on-line for the full test duration. The fuel used was wood waste, and various additives were fed with it for the control of alkali salts in the exhaust. Nominal test conditions are listed in Table 30.

TABLE 30
WOOD-WASTE VERIFICATION TESTS

Test	Approach Velocity (ft/min)	GBF Temp. (F)	Media Circ. (lb/min)	Time (hr)	Loading (gr/scf)
V100	100	1500	35	57.8	>1.5
V101	↓	↓	40	26.1	>1.0
V101A			40	52.5	>1.0
V102			50	60.8	>1.0
V103			50	34.7	>1.0
V103A			50	57.9	>1.0
V104	↓	↓	50	75.8	0.76
V105			40	148.2	0.65

No front-face deposition problems were experienced in any of the tests. Particulate loadings into the GBF varied from a measured 0.65 gr/scf in test V105 to a calculated 1.6 gr/scf in test V101. The highest loadings were generated with Burgess #10 pigment as an additive, selected in the cold-flow tests as a worst-case additive because of its deposition-prone character. Calculated loading values for tests V101 through V103A were all above 1 gr/scf. The relatively high loadings, although they caused no problems on external surfaces, did have a tendency to cause deposition on the inner surface; this was controlled by increasing media circulation from the initial 35 lb/min to 50 lb/min.

Figure 78 is typical of the condition of the front face after completion of the test program. A few very hard ceramic-like deposits were formed during the first 100 hours of the wood-burning test; these bridged the openings in the inlet face at approximately 50 locations. They were found to consist of small particulate matter cemented together with a material rich in potassium.

The deposits did not grow in either number or size during the subsequent 500 hours, a phenomenon that may be ascribed to higher recycle rates and resultant improved suppression of potassium-salt vapors.

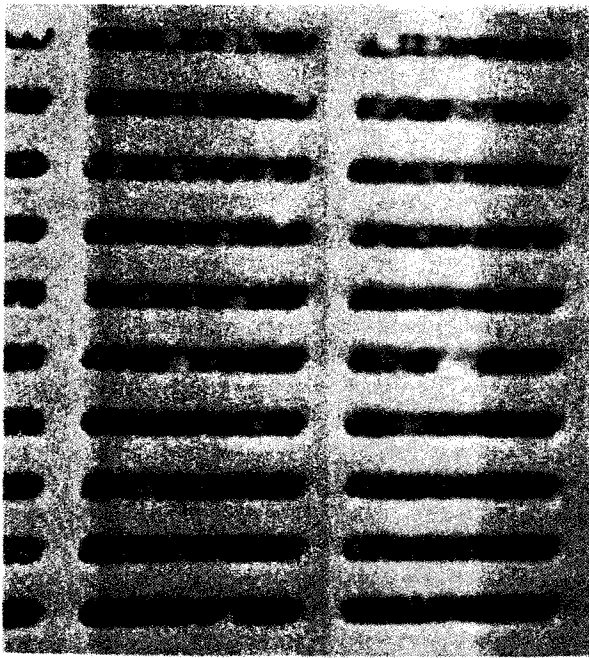


Figure 78 Slotted Louver Panel after 513 hours of Hot Operations with Wood Combustion

(As mentioned earlier, this very successful panel design was not incorporated in the design of the Pilot Plant GBF for reasons of schedule).

D. DESIGN OF THE PILOT PLANT GBF

A detailed three-volume report on all aspects of the design of the GBF was submitted earlier (Reference 4). The material that follows is a digest of that report.

Performance Objectives

The granular filter has two gas-filtration objectives. One is to meet emission standards for particulates and the other is to protect the turbine from erosion and deposition. The particulate-emission requirement

is 0.1 lb/million Btu of fuel fired; the erosion/deposition requirement is a turbine-inlet loading no greater than 0.001 grains of particles greater than 5 microns per actual cubic foot. To put the requirements on a uniform basis, the EPA standard of 0.1 lb/million Btu converts to 0.0208 gr/scf on solid waste and 0.0196 gr/scf on coal. These are total-loading figures at exit from the filter. Loading measurements in the exhaust stack may differ because of moisture content and dilution by bypass air.

In order to establish the component-efficiency goal for the GBF, an analysis was made of the loading distribution at the GBF inlet for the solid-waste and coal design points. The results of this analysis are presented in Figures 79 and 80 as cumulative loading greater than stated size in gr/scf. The particle size is plotted over the range of 0.1 to 100 microns. The 0.1-micron value is sufficiently near zero to permit plotting total loading at that point. Particles with diameters over 100 microns are not considered since they are collected by the cyclones (Sep 1 and 2) at efficiencies of 100 percent. This analysis was performed by an analysis technique based on a modeling theory by Leith and Licht (Ref. 6). The combustor outlet distribution

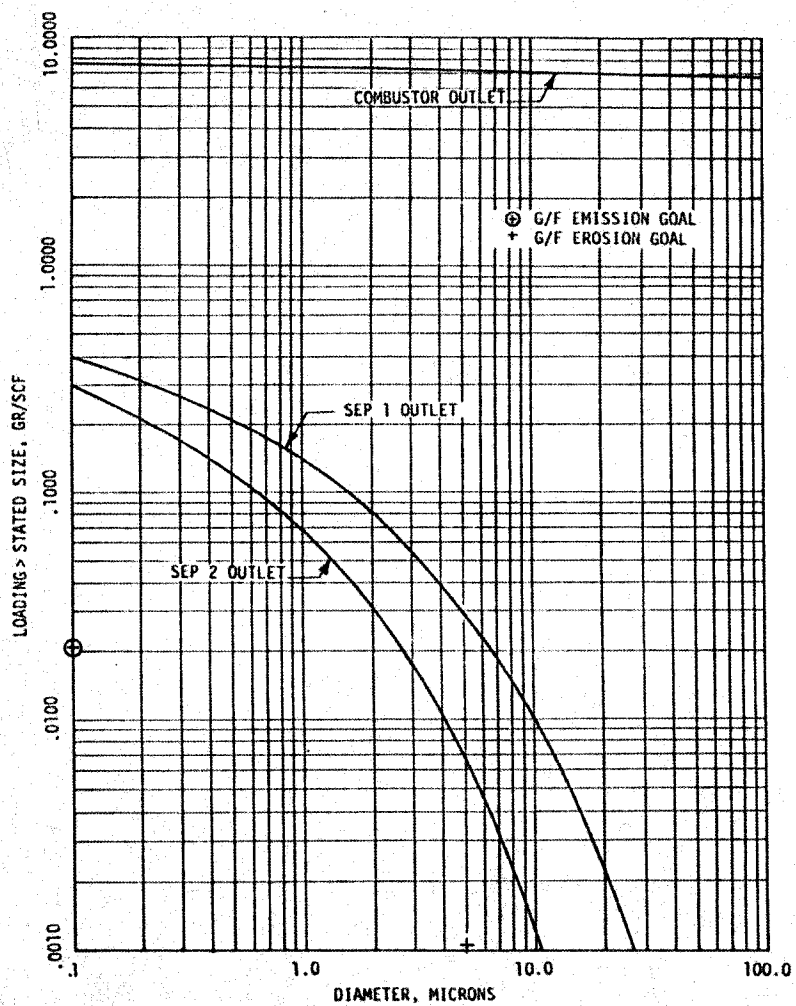


Figure 79 Particle Loading for Solid-Waste Operation

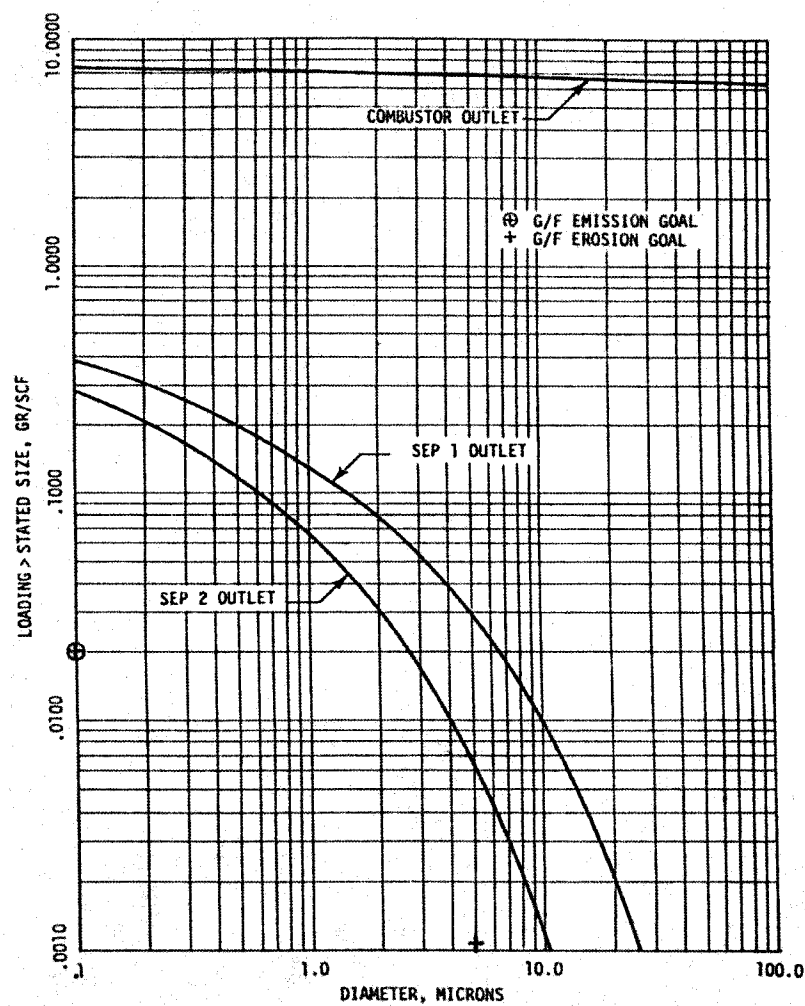


Figure 80 Particle Loading for Coal Operation

was generated by calculating the total loading from the combustor assuming a stable bed height, and calculating the particulate flow from the design-point solids-input flow and composition. It was assumed that the cumulative loading distribution is a straight line on a log-log graph and that the loading at 100 microns is 0.877 of the value at 0.1 micron. This latter figure was arrived at by matching the technique to recent test results on coal and limestone with two stages of cyclones but no granular filter.

The collection-efficiency goals for the granular filter were calculated from the inlet and outlet loadings, and indicate a minimum collection efficiency of 92.9 percent on solid waste and 93.0 percent on coal to meet a particulate emission level of 0.1 lb/million Btu (front half of the EPA train). To meet the erosion goal of 0.001 gr/scf for particles greater than 5 microns, a collection-efficiency goal of 86.2 percent is required on solid waste and 86.4 percent on coal.

A summary of the GBF design-point conditions is presented in Table 31. This includes temperatures, pressures, and flows. The temperature drop from combustor outlet to GBF inlet is caused by heat

TABLE 31 GBF DESIGN-POINT CONDITIONS		
	MSW	Fuel Coal
Power (kW)	845	1000
Temperatures (F)		
Combustor Out	1500	1600
GBF In	1483	1583
GBF Out	1444	1543
Turbine Inlet	1409	1478
Pressures (psia)		
Combustor Out	54.5	58.6
GBF In	52.3	56.4
GBF Out	51.3	55.4
Gas Flows (lb/min)		
Combustor Out	1200	1250
GBF In	1178	1226
GBF Out	1178	1226
Particulate Flow (lb/min)		
Combustor Out	17.5	17.3
GBF In	0.654	0.652
GBF Out	0.047	0.046
Fuel Flow (lb/min)	102.2	42.7
Heat Release (10^6 Btu/hr)	28.04	27.51
GBF Media Flow (lb/min)	360	360

loss from vessels and piping. Across the GBF the temperature loss is a combination of vessel heat loss and loss due to media circulation by relatively cool air (compressor discharge). The temperature drop from GBF outlet to turbine inlet is due mostly to bypass-air dilution of the hot gas. The pressure loss from combustor outlet to GBF inlet is due to piping and two stages of cyclones. The GBF pressure drop is carried as 1 psi, which should be more than adequate for the design chosen.

The difference in gas flow between the combustor and GBF inlet is due to ash-system bleeds from the cyclones. No mass-flow change is assumed

across the GBF, since the chosen design uses seal legs in the circulation system to maintain gas leakage near zero.

The particulate flows reflect the same rates previously discussed in the section on loading estimates for the inlet and outlet of the GBF. The outlet flow assumes the system is just meeting the emission standard of 0.1 lb/million Btu (front half of the EPA train). The media circulation rate of 360 lb/min should be adequate since it results in a particulate-to-media ratio of 0.0017, while dry-scrubber experience is in the range of 0.0050 to 0.0075. Figure 81 summarizes the nominal mass flows of the GBF operating on solid waste.

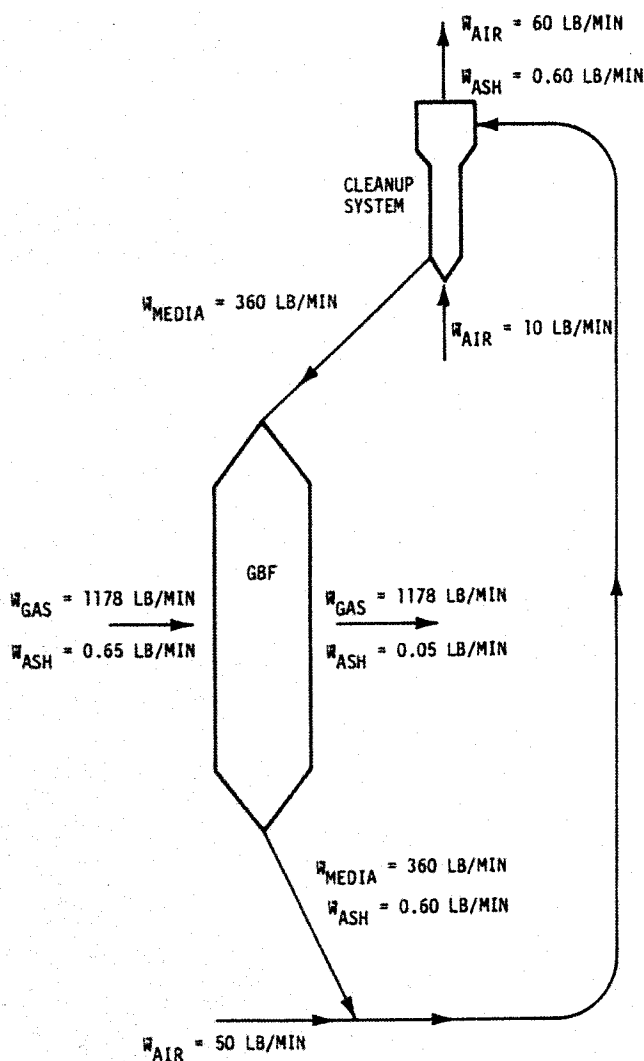


Figure 81 Nominal Flows in GBF on Solid Waste

Selection of Filter Media

One of the principal attributes of filter media is the granule size. Results of the model tests showed that the most promising choice is the smallest available size that can be retained by an outlet louver of practical design. At present, limitations on louver fabrication techniques appear to place a lower limit of about 0.060 in. on the nominal dimension for the slot opening. Accordingly, granules which will pass through a U.S. Mesh No. 12 sieve (0.066" openings) are excluded.

The deficiencies of natural materials in the CPU-400 environment were revealed in the model tests. Accordingly, a decision was made to employ manufactured media in initial CPU-400 testing. A rather clear choice for this purpose is an alumina-based granule. This oxide is very stable physically and chemically over the entire temperature range (i.e., inert), very

hard (i.e., attrition-resistant), thermally shock-resistant, and commercially available. Equivalent candidate materials manufactured by Diamonite Products Manufacturing Company of Shreve, Ohio and Ferro Corp., of East Liverpool, Ohio were tentative choices. The material, a high-alumina ceramic trademarked "Aluma-Sand," was designed as a grinding product. It is available in various sizes and shapes. For filter purposes, a spherical shape and a standard size denoted 8-12 mesh were selected.

Mechanical Design

Figure 82 is a sectional view of the granular filter. Hot, dirty gas enters at the top into the interior of the annular bed of downward-moving media. The cleaned gas, having traversed the media bed by way of inner and outer louvered panels, leaves the granular filter vessel from a port on its upper sidewall and flows to the vessel that originally contained the third-stage separator. From there it flows to the turbine inlet through pre-existing piping.

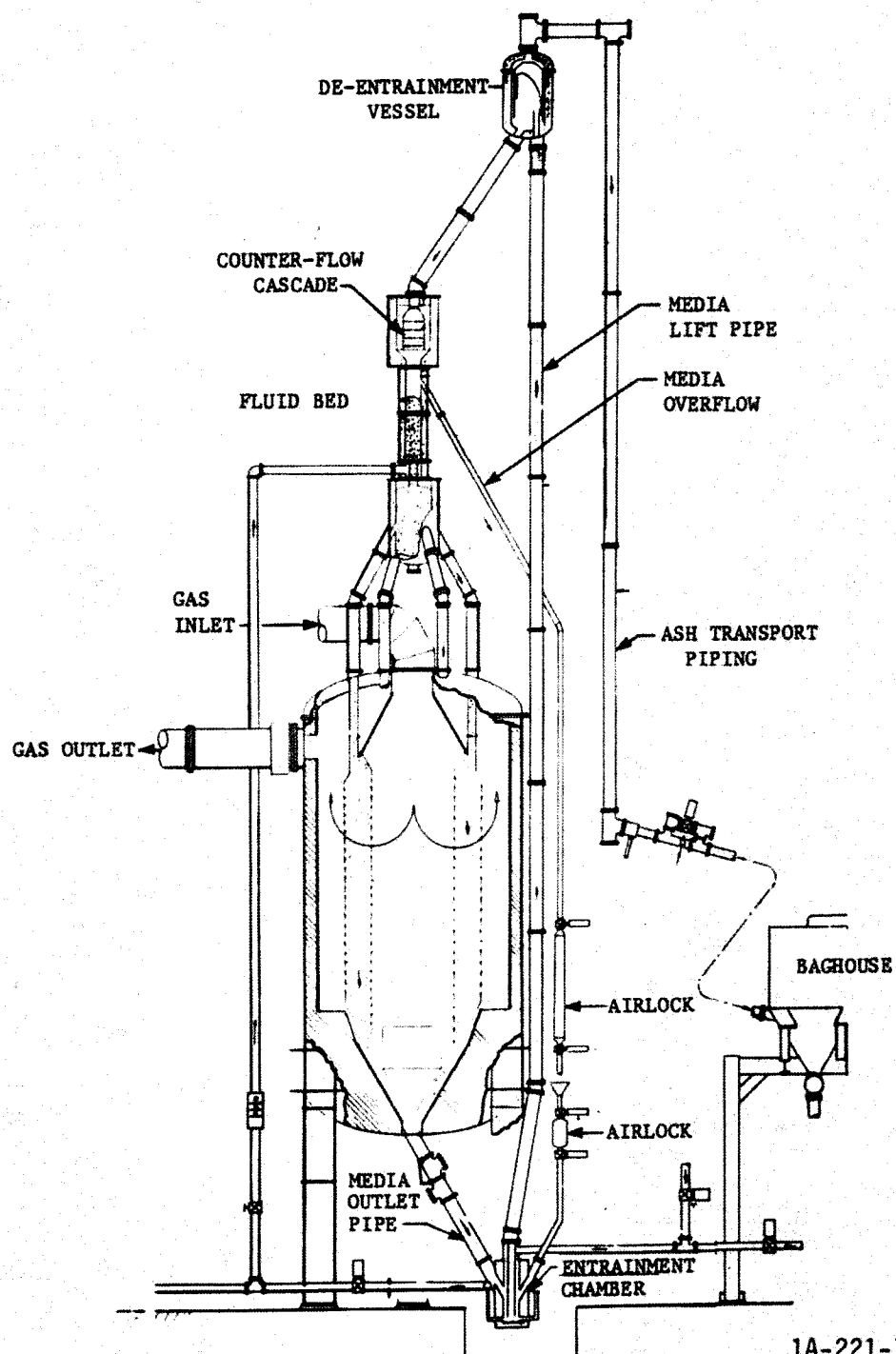
Both the inlet and outlet piping contain tied expansion joints with low lateral spring constants, three in each pipe run. High-pressure sampling ports are included in both inlet and outlet piping. A structural-steel support frame and flexible spring hangers are included to support the piping weight but allow thermal expansion. The GBF pressure vessel is supported on six tubular legs, with ten feet of clearance to accommodate the media-circulation system below the lower flange.

Filter areas, flows and velocities are summarized in Table 32.

Internal Arrangement

The top port leads to a 59½-inch-diameter inlet plenum from which the gas passes through the inlet louver into the 20-inch-thick annulus of 8-12 mesh alumina filter media. The cleaned gas leaves via the outlet and plenum to the gas-outlet in the vessel wall.

The cleaned media enters the pressure vessel via six ports and downcomers into the upper media plenum. The media then flows downward through the annular filter element. The media exits via a lower cone leading to the outlet boss. Any media or ash falling off the inlet (inner) face mixes with the dirty media and leaves the filter either outside of or through a media flow-control cone. No media should be able to pass through the outlet louver, since the outlet louver openings are smaller than the media. Should some media pass the louver, however, it will fall to the bottom of the outlet plenum, since the terminal velocity of the media is higher than the maximum plenum velocity. An annular opening is provided to allow any such spillage to rejoin the main media flow.



1A-221-717A

Figure 82 Moving-Bed Granular Filter

TABLE 32
AREA, FLOW, AND VELOCITY SUMMARY

ITEM	DIMENSIONS	AREA (ft ²)
Inlet & Outlet Pipes	20" dia	2.182
Inlet Plenum	4' 4-3/4" dia	15.18
Filter Inlet	4' 4-3/4" dia x 13' high	179.53
Filter Outlet	7' 11-1/4" dia x 10' high	249.36
Mean		214.45
Outlet Plenum	7' 11-1/4" ID x 11'5" OD	52.09

	DESIGN POINTS	
	MSW	COAL
Filter Gas Flow (lb/min)	1178	1226
Filter Inlet Temperature (F)	1483	1583
Filter Inlet Pressure (psig)	37.6	41.7
Volumetric Flow (acfm)	16,360	16,410

Velocities		
Inlet & Outlet Pipes (ft/sec)	125	125
Inlet Plenum, max (ft/sec)	18	18
Inlet Face, superficial (ft/min)	91.1	91.4
Outlet Face, superficial (ft/min)	65.6	65.8
Mean Superficial (ft/min)	76.3	76.5
Outlet Plenum, max (ft/sec)	5.15	5.17

The pressure vessel has a two-layer refractory lining: hard facing backed up with insulating refractory. The lower portion has a mass refractory pour that supports the filter internals. The filter inlet and outlet panels are supported independently from the lower refractory cone. They rest on a series of pin-guided sliding feet. This allows the panels to expand independently while maintaining concentricity. The panels expand vertically upward from the planes of their support feet; differential expansion is taken up by inner and outer slip joints where the panels meet the filter hood.

Pressure Vessel

Pressure-vessel stress calculations were based on the ASME Unfired Pressure Vessel Code, Section 8. The vessel was hydrostatically proof-tested, and State of California approval was obtained for design calculations, manufacture, and test. Insulation is a two-part castable-refractory system with internal metal ties securing the refractory to the vessel. The inner layer is a hard, abrasion-resistant, high-temperature, high-density refractory. The outer layer is a softer low-density refractory. Based on vendor data and CPC analyses with 1600 F GBF temperature, the following temperatures will prevail:

	Temperature, F	
	<u>Side Wall</u>	<u>Top Dome</u>
Hot Gas	1600	1600
Between Refractory Layers	1325	1307
Vessel	241	228

The analytical model used to obtain these temperatures has previously proven to give good or conservatively high results on CPC combustor and separator vessels. These temperatures give low heat losses and a good margin of safety since allowable stresses were based on a temperature limit of 650 F maximum.

Seismic and Wind Considerations

The pressure vessel, with internals and media, must meet the wind- or seismic-load requirements of the Uniform Building Code, Section 23 (it is not required that the item continue to operate, but only that it withstand the loads without structural failure). CPC is in the highest seismic zone, and seismic loads exceed wind loads. The basic seismic requirement is 0.25g horizontally in any direction. This corresponds to a 75,000-lb load horizontally through the center of gravity.

These considerations affect the design as follows:

- The pressure vessel must withstand the loads transmitted to it by the internals when hot and pressurized.
- The support skirt and legs must transmit loads to the foundation.
- The foundation must transmit the loads to the soil, and the mass of the foundation must react the overturning moment from horizontal loading. CPC designed the foundation to accomplish this, based on core borings of the soil.

The total piping system must withstand forces caused by:

- Piping and insulation weight
- Pressure
- Expansion

Not only must the pipe itself withstand these loads, but it must keep to acceptable limits the loads transmitted to vessels. Also, if the pipe is not capable of supporting itself, then pipe supports must be provided that do not aggravate piping loads.

In similar applications by others, good results have been had with a two-layer refractory lining similar to that in the granular-filter pressure vessel. The high gas velocities require that the hot-face lining be reinforced with a stainless-steel hex mesh (Keene "Lance Grid"). The granular filter piping was designed accordingly, with the following results:

	Temperature, F
Gas	1600
Between Refractory Layers	1417
Pipe Wall	210

For a straight spool, the pipe weighs 250 lb/ft. The individual pipe spools are limited to a length of 90 inches to permit access for application of insulation.

A first check was made to determine whether pipe expansion could be handled by the pipe elasticity alone. The piping stresses proved adequately low, but input moments were too high to the GBF pressure vessel. It is not possible to use simple bellows expansion joints in high-pressure piping, because the effective piston area of the bellows results in extremely high axial loads (38,500 lb) due to internal pressure. The alternate is to use tied expansion joints where the pressure loads are transmitted past the bellows by tierods and the expansion of the piping is taken up in lateral deflection of the bellows. The right-angle turns in the GBF piping allowed this scheme to be used.

In addition to allowing for expansion, the length of each expansion joint may be varied ± 0.5 inch by adjusting tierods. This allows some adjustment for manufacturing and assembly tolerances. The spool lengths were determined after locating the various vessel flanges in space after their installation, using surveying methods. The spool pieces were manufactured to these dimensions to minimize accumulation of tolerances.

Internals

The internals of the GBF are made from Type-330 stainless steel. The mean coefficient of expansion from 70 to 1600 F is 10.0×10^{-6} in./in./F. The actual expansion over this same temperature range would be 0.0153 in./in. or approximately a 1.5% increase in any linear dimension.

There are no mechanical connections between the inner panel, the outer panel, and the filter hood. Not only must these expand, but they will expand at different rates because of differences in heating rates.

The expansion from 70 F to 1600 F will be as follows:

<u>Component</u>	<u>Direction</u>	<u>Dimension, (in.)</u>	<u>Expansion (in.)</u>
Inner Panel	Axial	168	2.52
	Radial	26.875	0.40
Outer Panel	Axial	132	1.98
	Radial	47.625	0.71
Filter Hood	Axial	100	1.50

Radial expansion of the hood will be the same as that of the panels at their respective radii.

The effect of the three components going from 70 F to 1600 F is as follows:

- The 5-in. (cold) lap at the joint between the panels and hood will increase to 9.02 in. for the inner panel and 8.48 in. for the outer panel.
- The support feet of the inner panel will slide out radially 0.40 in; of the outer panel 0.71 in. As a result, the active filter thickness will increase 0.31 in.

During the preheat of the filter, the inner panel will heat up before the outer panel. The media will have to be circulated slowly to preheat the media and filter hood, and to allow free media movement at the lap joint, permitting unrestricted differential expansion. During cooldown of the filter, the media will have to be circulated slowly to drain media from the lap joint, allowing differential contractions between panel and hood; and to remove media from between panels as distance between panels decreases 0.31 in., thereby to prevent deformation of panels.

The volume of media to fill the filter changes as it goes from cold to hot. In addition to circulating during heatup or cooldown media can be added or withdrawn from the system to compensate.

Hydrostatic and Pressure Forces

Solids in a bin impose sidewall loads that are a function of density and angle of internal friction of the solids. The stress calculations were run using assumed values for these properties that later proved conservative; i.e., assumed and subsequently measured values were as follows:

<u>Parameter</u>	<u>Assumed</u>	<u>Measured</u>
Density	150 lb/ft ³	132 lb/ft ³
Angle of Internal Friction	36°	42°
Angle of Repose	-	17 - 28°

Calculated stresses were limited to a maximum of 2800 psi, based on use of Rolled Alloys Type-330 stainless steel (RA330) with mill anneal, and one percent creep in 10,000 hours. The 10,000 hours were further defined as 500 hours at 1600 F and 9500 hours at 1400 F. The 500 hours at 1600 F was to represent the GBF checkout on coal with sulfur suppression; the 9500 hours represent running on solid waste, in which fluid-bed temperature is limited by agglomeration of the bed material.

Materials

Various austenitic stainless steels (300 series) and chrome-nickel alloys were reviewed on the following bases:

- Cost
- Creep Strength
- Hot Corrosion
- Availability in Wrought Structural Shapes
- Availability in Small Quantities, i.e., less than mill run.

The field was narrowed to Rolled Alloys 330 and Inconel 601. While 601 had a small technical advantage, it was not available in needed structural shapes in less than mill run, or approximately 2000 linear feet of each shape. Since RA330 was technically adequate, the design was based on this alloy. RA330 is essentially 35% Ni, 19% Cr.

Media Circulation and Cleanup

The design of the pneumatic transport and cleanup system has the following features.

- The entire system operates at either high or ambient temperature and pressure.
- The media drains from the bottom of the GBF down a seal leg under a packed plug-flow condition.
- The media enters the lift-engagement pot from the seal leg; this pot uses a small controlled quantity of air flowing up through the media to vary its angle of

repose and thereby vary the media's proximity to the existing lift-air path.

- Air required to power the pneumatic lift system is provided by a bleed from the compressor outlet.
- Media cleanup is accomplished in five stages:
 1. The majority of the ash is removed in the pneumatic lift pipe while the media is being transported to the upper lift-disengagement vessel.
 2. The media is allowed to impact in the lift-disengagement vessel on a curved baffle to absorb lift energy and further dislodge ash.
 3. The media rolls down a slanted pipe with a counter-current of air as in a ball mill.
 4. The media falls through a series of impact baffles and into a fluidized bed.
 5. The fluidized bed provides final media cleanup, pressure isolation between the transport system and the GBF, and total-system media-inventory control. The fluidizing air provides the air used for counterflow both at the impact baffle and in the slanted pipe. This ash-laden air, along with the ash-laden lift air, is vented from the lift-disengagement vessel to the baghouse for final ash collection and disposal.
- The media flows from the fluid bed into a distribution vessel and then into six symmetrically placed seal legs that return the media to the GBF, thereby completing one circuit around the circulation and cleanup system.
- An auxiliary loop on the system provides for media addition or removal to maintain media level during heatup and cooldown transients as well as in normal operation.

The level control uses the upper fluid bed as follows: if media level is too high, it spills over into the drain line and can be withdrawn through an airlock; if measured fluid-bed differential pressure is too low, the media can be added through the filling hopper and airlock into the lift-engagement vessel.*

* Experience later showed this to be an inadequate method of media-inventory control, and the design was altered accordingly.

Process Control

Putting aside for the moment the matter of front-face cleaning, the only aspect of GBF operation that is subject to control is the circulation of the media. In order to hold a calibration between pressure drop in the lift pipe and media circulation rate, the amount of lift air (bled from the turbine compressor) is maintained constant, and independent of pressure transients of the system. The setpoint for this airflow is established by the computer (default mode), but it can be changed by the operator through the operator-interface console, if desired. Control is mechanized in computer software as a two-mode controller, the output signal from which goes to the positioner of a proportional valve through a manual loading station. The arrangement is shown schematically in Figure 83.

Media circulation is modulated to maintain the desired pressure drop across the GBF, modulation being accomplished by the adjustment of engager airflow through a proportional valve. The loop consists of a three-mode controller, a differential pressure transmitter, a proportional valve, and the valve positioner. The setpoint for this controller is supervised by a two-mode loop implemented in computer software; the supervisory-loop setpoint is established by computer software (default mode), but can be changed by the operator if desired.

Front-Face Cleaning

During model tests, the necessity for periodic removal of ash deposited on the front face of the GBF became obvious. Various techniques were evaluated in the model; the most effective up to the time of completing the design of the Pilot Plant GBF was the use of periodic short air blasts impinging directly on the panel. In the Pilot Plant GBF, front-face cleaning is accomplished with a system having the following features:

1. Eight vertical 1½-in.-diameter manifolds are mounted on the horizontal reinforcement bars of the inlet panel.
2. Each manifold has 24 1/4-inch-diameter nozzles, directed against the panel, each covering one square foot of panel area.
3. Each manifold is externally connected to a 100-psi pressure tank, from which a timer-controlled valve provides blowdown air flow to each manifold. Initially, the timing was set for 15-minute intervals.
4. Some of the material dislodged by this front-face cleaning will be forced into the filter bed, to be collected

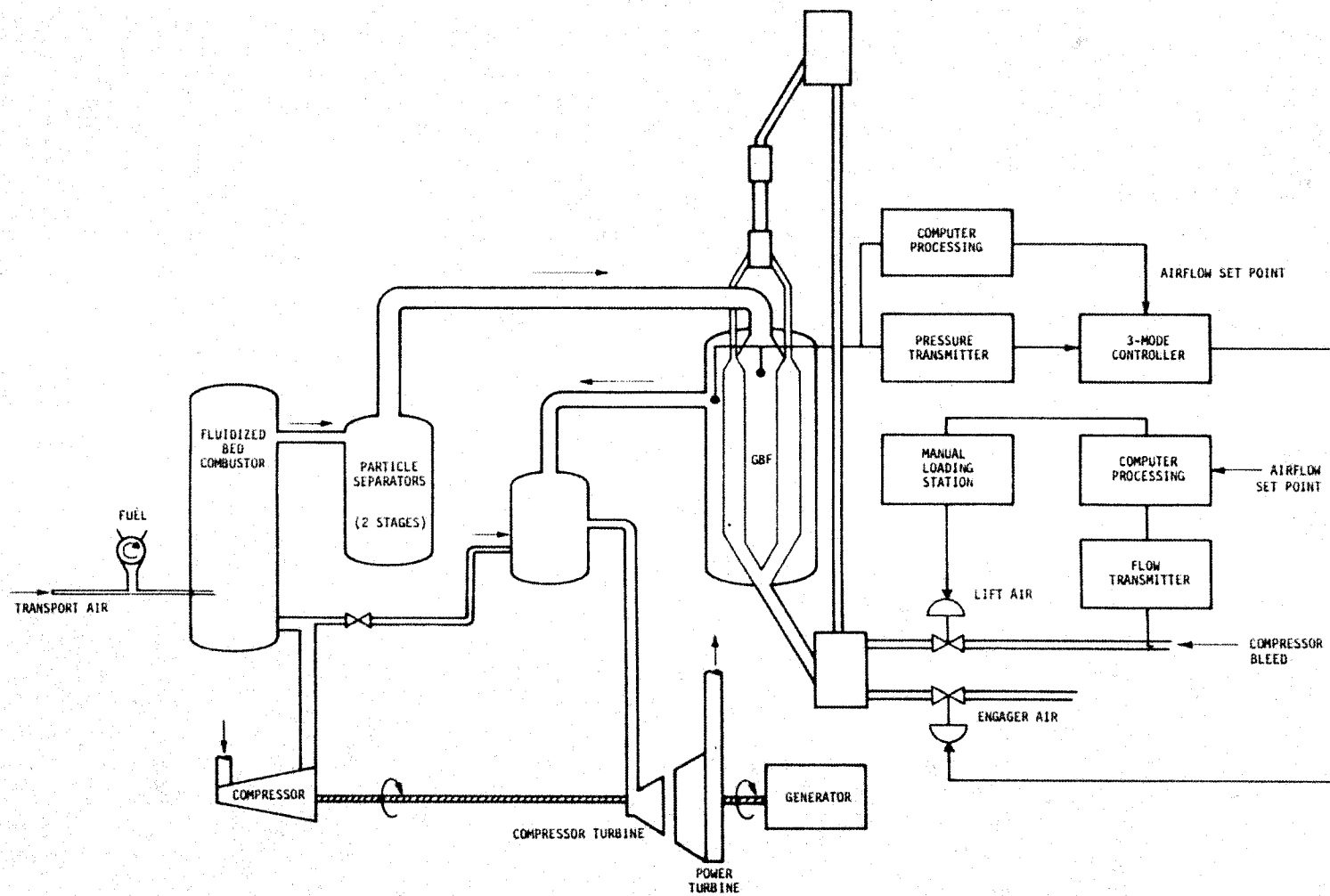


Figure 83 GBF Control System

there by the media; the major fraction, however, will fall to the bottom of the inlet plenum, and be removed with the media.

Particle Sampling

Two probe assemblies penetrate the piping to provide particle sampling upstream and downstream of the GBF; their operation is illustrated by the schematic of Figure 84.

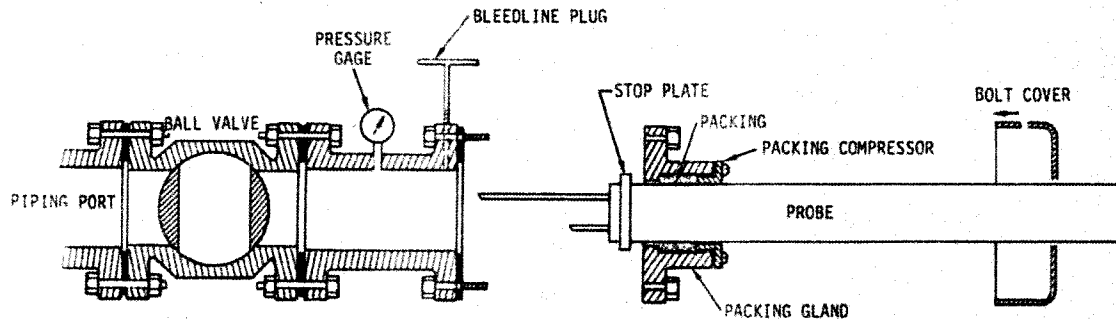


Figure 84 High-Pressure Sampling Probe

With the ball valve closed, the probe assembly is inserted in the pipe spool on the atmospheric side of the valve, and the mating flanges are bolted together. The bolt cover is then brought forward over the mating flanges, which requires that the bleedline plug be removed and reinserted through the bolt cover. This prevents any inadvertent disassembly while the probe is in a pressurized environment. Likewise, the stop plate on the probe prevents its withdrawal while the system is pressurized. Once the bolt cover has been secured, the ball valve is opened and the probe is advanced into the hot-gas stream. If the bleedline plug is removed for disassembly with the valve still open, the resultant continuous bleed gives immediate warning.

E. INSTALLATION AND CHECKOUT

The granular filter was installed during the latter half of 1975. Figure 85 shows the pressure vessel being lowered through the roof of the building that houses the Pilot Plant, and Figure 86 is a view of the louver panels after their emplacement inside the vessel. The relatively light members that make up the support structure for the panels were chosen to avoid major differences in heatup rate, which could cause severe thermal stresses, and to minimize obstructions to gas flow.

Figure 87 shows the upper media-distribution cone prior to its installation; it is shown primarily to give an indication of scale. Figure 88 is the completed installation, with the access platforms in place.



Figure 85 Granular-Filter Pressure Vessel
During Installation

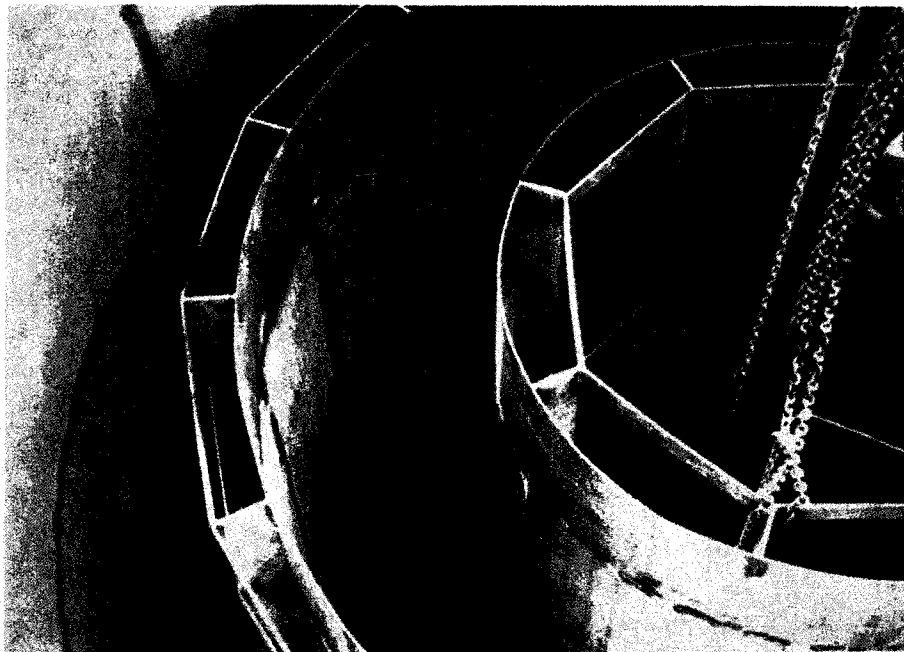


Figure 86 Inner and Outer Louver Panels in Place in GBF Vessel

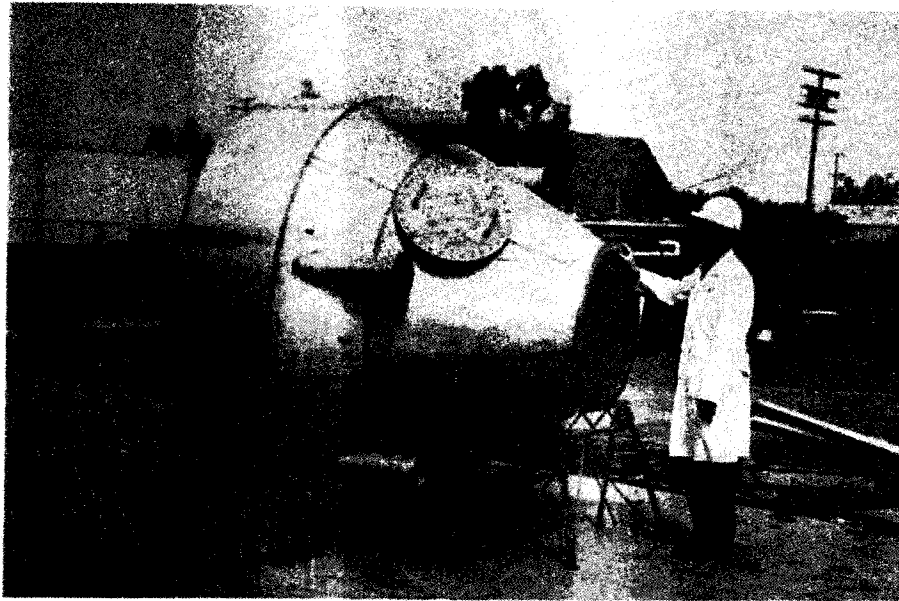


Figure 87 GBF Upper Distribution Cone

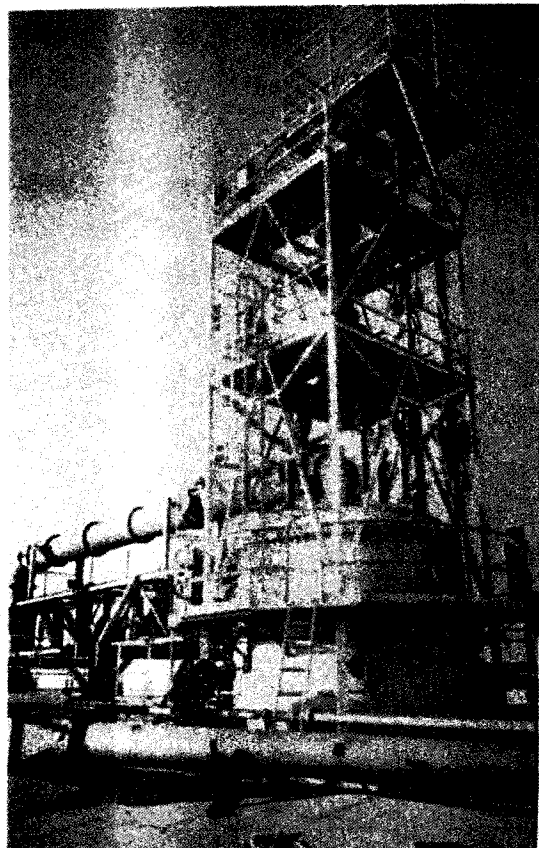
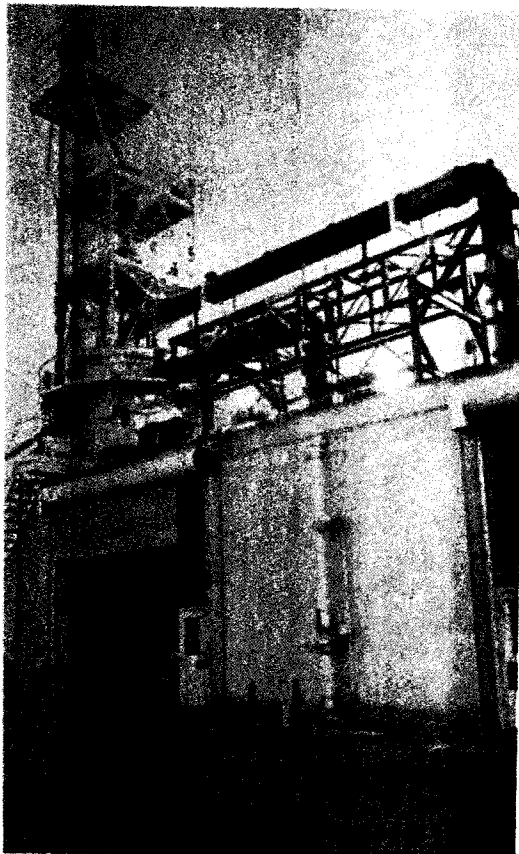


Figure 88 Completed GBF Installation with Media-Circulation System

Test History

Only one run of real significance was completed, since that run was terminated by structural failure of the inner louver panel, which rendered the filter inoperable. That run was a system preheat that covered about 33 hours,* begun at ET (elapsed time) of 821 minutes on the control-computer clock, with a setpoint for combustor-bed temperature at 1420 F. A time history of gas temperatures in and out of the granular filter vessel is shown in Figure 89. Several increases in bed-temperature setpoint are noted; they were made in an effort to increase the granular-filter heating rate.

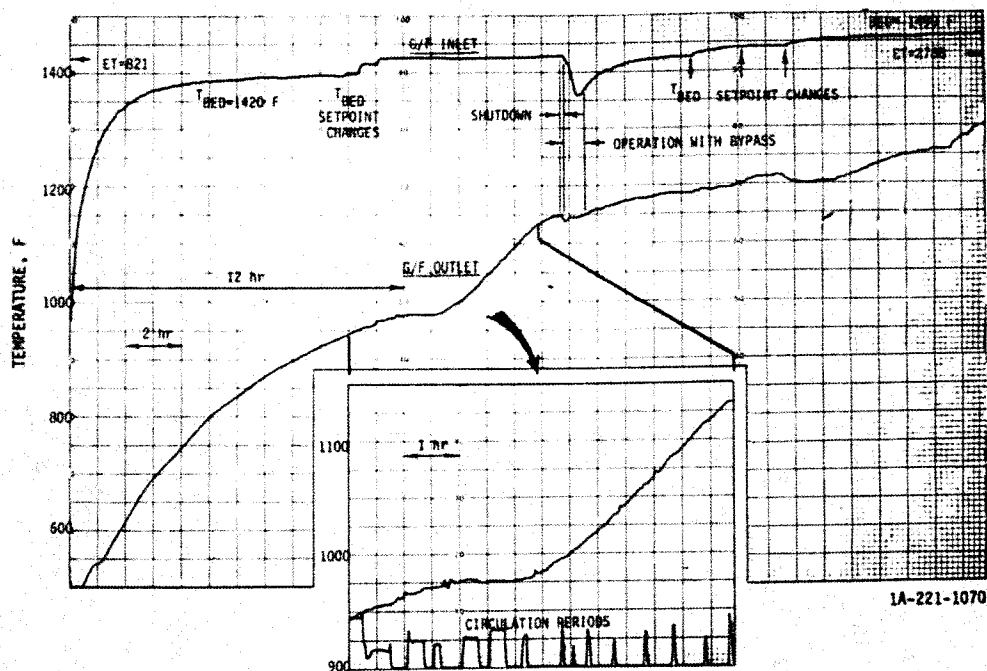


Figure 89 Granular-Filter Heatup on Fuel Oil

* Design Modifications (Part H of this Section) have been made that will substantially reduce the time required for heatup.

Beginning at ET = 1466, circulation of the granular-filter media was stopped for 18 minutes--again with the intent of increasing the heating rate--and was subsequently resumed on an intermittent basis, as indicated in the expanded-scale inset in Figure 89. The change in operational mode was followed by a renewed rising trend in outlet-gas temperature. A four-minute shutdown at ET = 1881, followed by 23 minutes of operation with some of the combustion air being bypassed to the combustor freeboard, showed that the high thermal inertia of the system converts very evident changes in inlet temperature to almost imperceptible perturbations in outlet temperature.

The pressure drop across the GBF and that of the circulation-system fluid bed are plotted in Figure 90. Pressure drop across the filter bed probably provides the best clues as to the progress of the structural collapse. This delta-P was more or less level during the second half of the run, but then underwent two downswings near the end. These are best illustrated by the stretched--and vertically compressed--plot shown in the inset. The faired-in lines show that delta-P had become quite stable at about 5.7 Iwd. Then, at about ET = 2671, it entered a decreasing trend, which accelerated sharply at 2703. These trends in all probability relate to the level of media in the GBF. The buckling of the inner panel was such as to add greatly to the contained volume between the two panels, and the contained media was grossly insufficient to fill the space.

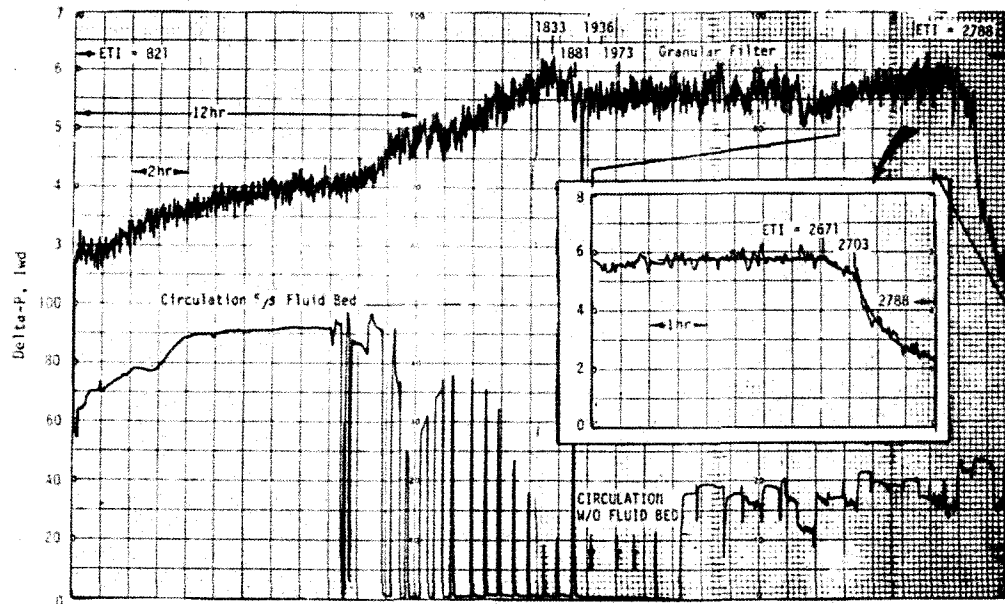


Figure 90 GBF and Fluid-Bed Pressure Drops

The inset curve in Figure 90 may be interpreted as follows: at or before 2671, beginning buckles permitted the top of the media to approach the top openings in the louver panels, either permitting end-effect paths of reduced resistance for the hot gas near the top or permitting some of the hot gas to escape upward through the fill legs. At 2703, the media level actually fell below the top louvers, and unobstructed passage began, resulting in the steeper drop in delta-P.

The circulation-system fluid-bed delta-P, also shown in Figure 90, is a good indicator of continuous or intermittent circulation during the first two-thirds of the test. This reading did not return to zero during later periods of non-circulation because of hot-gas leakage permitted by the very low media level. The onset of leakage at this time was confirmed by temperature increases in the fill legs.

GBF Effectiveness

This operation was conducted on fuel oil rather than coal (use of oil for initial heatup is established procedure), so that no actual measurements of particulate emissions were made. Visual observation, however, showed the stack to be the cleanest ever attained during oil-fired heatup operations. Though not unexpected, this result gives evidence that the granular filter was indeed filtering particulate from the hot exhaust gas.

Controls of Media Flow

Termination and subsequent resumption of media flow through the circulation system was accomplished without difficulty. (The trace showing the periods of circulation in the large inset on Figure 89 is actually a graph--to no particular scale--of the lift-pipe delta-P). Prior to the 32.7-hr run, and during filling of the granular filter, it was found that the circulation rate could be successfully modulated between zero and 300 lb/min by variations in the airflow to the pneumatic-transport lift pipe.

Pressure Seals

There are two distinct gas flows in the granular-filter system: hot combustion gas through the filter bed and transport and fluidizing air to activate the media circulation system and move collected particulate to the baghouse. Seals between the flows are dependent upon the media contained in the distribution vessel and fill legs at the top, and the outlet dipleg at the bottom. (See schematic, Figure 82). No hard evidence existed to the effect that the canted dipleg would successfully provide the necessary sealing, but temperature and pressure measurements showed that it was not only functioning as desired but could seal against a pressure difference of almost 200 IW (operational values will be substantially less). At the top of the vessel,

the distribution vessel and fill legs also effected the desired seal as long as sufficient media was present in the system to keep them filled (see Fill-and-Drain System, below).

Media Distribution

Post-test inspection revealed the media had established a "high-water" mark in the upper cone where the fill legs deliver media from the distribution vessel, above. This mark, seen in Figure 91, had a uniform "star" pattern that indicated very good symmetrical distribution of the media arriving through each of the six fill legs. Uniformity of fill-leg temperatures provided additional confirmation of the good distribution achieved.

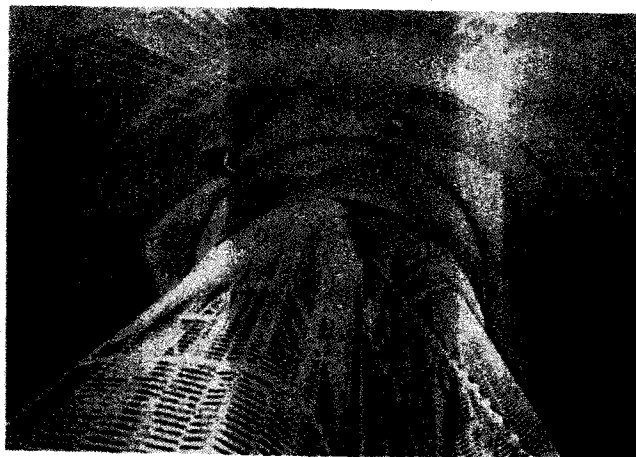


Figure 91 Fill Pattern in GBF Inlet Cone

GBF Pressure Drop

Pressure drop across the filter bed was quite steady at between $5\frac{1}{2}$ and 6 Iwd following its initial transient. This result is in good agreement with calculations used to arrive at a design value for bed thickness.

Fill-and-Drain System

The as-designed fill-and-drain system constituted a problem area. Difficulties with making airlock valves dependably operational for control of media flow had been experienced previously. These same difficulties were present in the operations reported here. They were, in fact, present in such degree that the valves ultimately had to be removed to accommodate filling or draining. Their removal, of course, obviated adding or withdrawing media during pressurized operation or when media was being circulated. The fill-and-drain system was identified as an area where some redesign was required, because there are volumetric changes during heating and cooling--as well as possible elutriation of fractured media during operation--that must be accommodated.

F. FAILURE ANALYSIS

An in-depth analysis of the failure and an extensive redesign effort followed the collapse of the filter panel. These activities are reported in detail in Reference 5; a summary account is given here and in Subsection G, following.

Review of Loads

A review of media-induced loads was conducted by Dr. John Carson of Jenike & Johanson, Inc., of No. Billerica, Massachusetts; the nominal normal-pressure profile estimated by Dr. Carson is presented in Figure 92 along with the loading, calculated by the Janssen equation, that was used as the basis for the design.

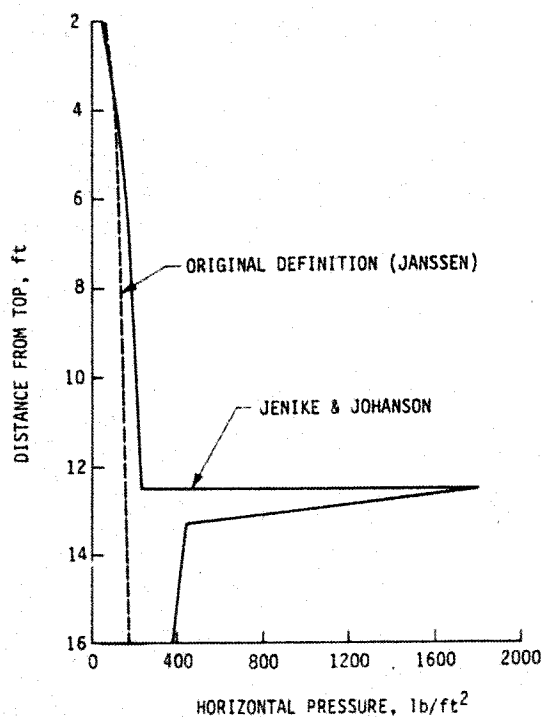


Figure 92 Pressure Loads on Inner Louver Panel

design--is the possibility of imbalance. Dr. Carson's estimate was that the loads might vary locally, and for periods of time up to several hours, by 40 percent from their nominal values. Extreme cases would be represented by increased and reduced loads existing simultaneously in opposed or adjacent quadrants.

The Jenike and Johanson predictions, it should be noted, were based on measurements made in circular (as opposed to annular) bins with smooth (as opposed to louvered) walls, containing fine powdery (as opposed to hard spherical) materials.

The two curves differ by a factor that reaches 1.4 in the straight top portion of the filter, and about 2.5 in the lower conical section, the levels used in design being the lower ones in each case. In addition to this, a much greater difference is evident in the region of the transition, where a load is indicated by the Jenike and Johanson approach that goes to over 11 times the level predicted by the Janssen equation. The precise vertical location of the load spike cannot be stated with certainty, according to Dr. Carson; it could lie anywhere within an 18-inch band extending from 12 inches above the top of the conical section to 6 inches below it.

An additional aspect of loading--not foreseen in the

Review of Stress Analysis

The stress analysis conducted in support of the granular-filter design was reviewed in detail. The philosophy adopted for that analysis was that the louver panels and their supporting structure should each have full and independent capability to carry the pressure loads. (As has been stated, these were predicted by the Janssen equation, or "sliding-wedge" method; they were calculated on the assumption that the media-containing annulus was uniform over its full height). The supporting structure was intended to have the capability to carry the vertical load imposed by the moving media and by dead weight, and the louver panels were to have the capability to carry vertical loads into the supporting structure.

Gas-flow pressure was added to media pressure in analyzing the outer panel and its supports; for the inner panel, the gas-flow pressure, being opposite to the media pressure and much smaller, was neglected.

Buckling of the individual louver panels under the pressure loads imposed by the media was checked by standard formulas, and a safety factor against buckling of 1.92 was calculated. Some assumptions were required with regard to the appropriate material properties, because of the special geometry of the louvered material (test information was not then available). Those assumptions have since been checked against experimentally determined values and, although some discrepancies were shown, they represented largely compensating errors; so the calculated factor of safety is a quite reasonable value for the loads anticipated.

Since the possibility of unsymmetrical loading was not considered, the stresses in the various elements comprising the structure could be --and were--calculated by quite standard methods. These calculations showed no stresses in excess of 3100 psi.

There was, however, a vital omission. Some of the analysis was conducted while the design was still in an evolutionary state, and one potential stress-producing situation was not checked out for the as-built design. That had to do with the frictional force that can develop at the foot of the longeron, resisting expansion or contraction during thermal transients.

In the final design, the first array of rib straps was $4\frac{1}{2}$ inches above the longeron foot. If one assumes at the foot a force of the magnitude implied by a coefficient of friction of 1.0, and if the longeron is analyzed as a cantilever beam with its base at the first strap array, the indicated calculation shows a bending stress in the longeron of 6975 psi. Coupled with axial compression, this gives a maximum combined stress of 9298 psi. If the loads were indeed considerably higher than assumed, that stress would be increased accordingly. Bending in the longerons would, in turn, put additional upsetting

moments into the rib straps of the lowest array, and in all probability induce buckling.

With those straps ceasing to provide support, the bending stress in the longeron would rise still higher, and additional loading would be imposed on the next array of straps. Buckling of the straps in the lowest row would thus appear to have been the first step in collapse, followed quickly by the general collapse. Whether the first buckling was set in motion by excessive friction forces resisting thermal expansion or simply by media-induced pressure loads higher than anticipated cannot be ascertained; it was very likely a combination of both factors.

G. STRUCTURAL REDESIGN

No final decisions had been reached at the time of contract termination with regard to appropriate redesign of the louver-panel support structure. A design was generated, however, using very conservative assumptions throughout, and it will be instructive to look at the geometry that would result.

Because a damaged louver panel could, if the occasion demanded, be replaced at a relatively low cost, whereas repair of the supporting structure could be very expensive, the redesign was approached on the basis that the supporting structure be conservatively designed to be capable of carrying all imposed loads, whether or not the louver panels retained any structural integrity. Conservatism was introduced from both sides; i.e., the allowable stress was reduced, and worst-case loading was assumed as a present condition for the full intended lifetime.

Allowable Stress

At granular-filter operational temperature, creep strength of the material becomes the controlling criterion. For RA 330, the stress for one percent creep in 10,000 hours at 1500 F is 2300 psi. For the most part (exceptions noted below) the allowable stress for the redesign of the louver panels and their supporting structure was taken as 80% of this value.

Loads

Media-pressure and media-friction loads were taken to be those predicted by Jenike and Johanson (Figure 92). Three loading conditions were investigated:

1. Nominal loads applied symmetrically.
2. 140% of nominal loads applied in two opposite quadrants, with 60% of nominal loads in the remaining two quadrants.

3. 140% of nominal loads applied to one side of the cylinder and 60% of nominal to the other side, with linear transition over a 45-degree arc between the two loadings.

Sliding-friction forces at the base of the longerons were assumed equal to 0.75 times the vertical load, and applied radially. It was assumed that these forces could be generated in reaction to thermal expansion or contraction of unknown direction, rather than simply in reaction to the pressure loads. Thus, on the inner panel, with pressures applied radially inward, the friction forces were similarly oriented; for the outer panel, by the same token, they were applied radially outward.

Dead weight of the structure was automatically included, a feature of the selected method of analysis.

Configuration

The revised design of the support structure for the louver panel is depicted in Figure 93. Revised assumptions with regard to load produced some marked changes in the overall design. The greatly increased pressure loading along with a reduction in allowable stress could reasonably be expected to result in a much more massive structure than the original. Perhaps a more profound change, though, was dictated by the assumption of major imbalance in loading (load condition No. 3, above). To resist this kind of loading, the entire cylindrical structure has to function in the manner of a cantilever beam. That

can be accomplished only by provision for shear transfer from longeron to longeron; hence the use of diagonal lacing to replace the rib straps of the original design.

Sizing of the members was such as to keep maximum stresses below the allowable level of 1840 psi. The method by which stresses were calculated (see "Analysis" below) presumes complete moment-transfer capability at all structural joints. Experience with heavy steel construction indicates that such moment transfer is not readily accomplished in a joint in which converging members are merely welded one to another; one-inch gusset plates were therefore added to assure the integrity of the joints.

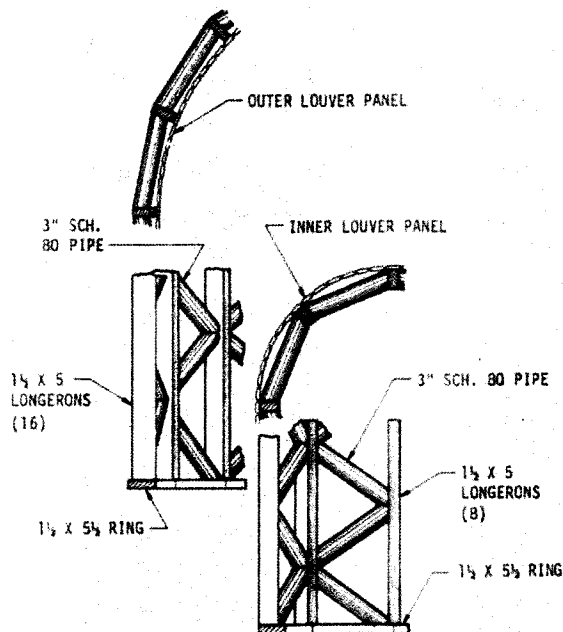


Figure 93 Redesign of Louver-Panel Support Structures

Analysis

As stated earlier, a guiding principle of the design was that the supporting structure would be capable of carrying all applied loads; it was therefore analyzed in the absence of the louver panels themselves. The manner in which the loads distribute themselves through this complex three-dimensional array is not readily predicted by any simple means, and that fact ruled out any simple "slide-rule" analysis of individual members. Rather, the entire structure would have to be analyzed as a unit.

To accomplish this, a well-established computer program (ANSYS, for Engineering ANalysis SYStem) was selected. This program is so constituted as to treat a single set of simultaneous equations (some with as many as 80 terms) that includes all concentrated loads, pressures, material properties, and element dimensions.

A series of runs was made, simultaneously iterating to determine the friction forces to be applied at the base of the longeron and arriving at final sizes for the elements that would keep maximum combined (axial and bending) stresses below the allowable. Results, after final sizing, were as follows:

<u>Element Type</u>	<u>Maximum Combined Stress (psi)</u>	
	<u>Outer Panel</u>	<u>Inner Panel</u>
Bottom Ring	1675	1590
Longeron	1296	1627
Diagonal	1549	1804

The inner-panel louver screens, increased by four standard gauges from those of the original design, are shown quite safe against buckling. Simple stress analysis as an arch, however, shows them to develop stresses of 2120 or 2697 psi, depending upon whether the edges are assumed fixed or hinged. Either value, of course, is in excess of the allowable level of 1840 psi used for the supporting structure. They are, however, still below the 10,000-hour stress to rupture for RA 330 (2800 psi). Moreover, they are basically compressive stresses, for which stress to rupture is not a totally suitable standard of comparison.

There are other mollifying factors as well. First, these high stresses occur only in the immediate region of the presumed spike, and it cannot be considered certain that a spike of the predicted magnitude will actually develop (annular shape, louvered walls, and media characteristics all represent departures from the conditions on which the prediction is based). Second, if serious distortion should occur, it is entirely feasible to replace damaged panels.

Whether so massive a structure as is indicated by this redesign effort is really necessary remains in question. Additional subscale testing, particularly to pin down more precisely the magnitude of media-induced loads, seems in order.

H. OTHER MODIFICATIONS

Media Inventory Control

In the original configuration, the inventory of media in the filter was to be controlled by adding or withdrawing media through gate-valve airlocks. In spite of vendor assurances that the valves would function properly in the intended environment, the small-diameter, hard media spheres consistently jammed into valve clearances, freezing the valves.

To circumvent the gate-valve problems, a design has been prepared for a valveless pressurized reservoir integral with the circulation system, as shown by the schematic of Figure 94. In steady-state operation, the media flows by gravity from the de-entrainment chamber to the cleaning chamber;

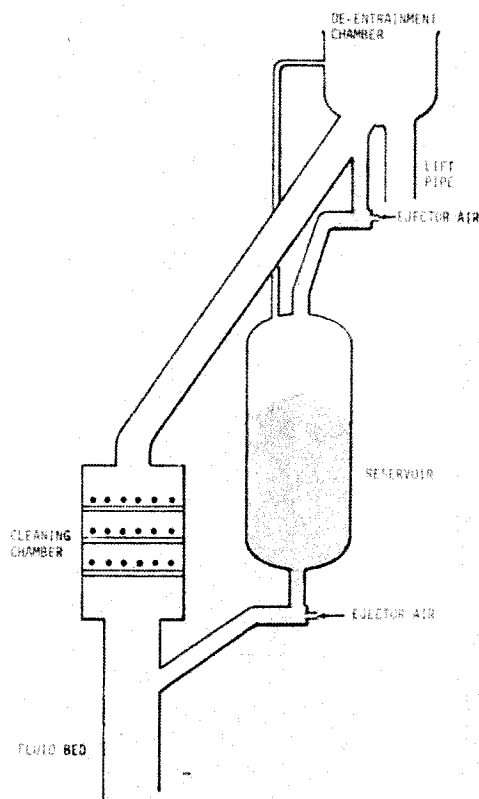


Figure 94. Media Inventory Reservoir

the angle of repose of the media is such that it blocks the pipe leading to the reservoir. When the circulation-system inventory is to be reduced, ejector air is blown into the entry pipe, clearing it and allowing media from the circulation system to enter the reservoir. Below the reservoir, an identical arrangement is used to control additions of media to the circulation system. An equalizer line to the deentrainment chamber maintain the reservoir at system pressure. The reservoir will be filled to a predetermined level (based on the calculated transient swings during heatup) prior to the start of operations.

Model granular filter experience and cold-rig testing have shown the on-off bridging-ejector system to be both simple and reliable. The reservoir will have a capacity of 33 cu ft, allowing sufficient excess media not only to accommodate volume change, but also to make up projected attrition losses during at least 120 hours of continuous operation.

Modifications to Increase Gas Flow

Analysis of data from the 33-hour run indicates that the gas flow through the granular filter during this run was about 200 lb/min. This is 100 lb/min less than the 300 lb/min that was expected, and resulted in a very slow heatup. The reason for this flow difference was that more flow was being by-passed through the Ruston compressor (in reverse direction) than had been anticipated. The bypass valve is modulated to maintain a positive pressure difference (compressor outlet greater than turbine inlet) across the cooling-air passages of the Ruston turbine, to prevent products of combustion from entering the passages and the Ruston compressor. Dumping air in this manner also lowers the blower load by lowering the blower outlet pressure; and the operating condition during the 33-hr run was near maximum pressure that the motor could handle without a circuit-breaker trip. About half of the system pressure drop was being taken across the turbine section of the Ruston unit, and this suggested that gas flow through the granular filter could be increased by dumping hot gas through a vent placed between the granular filter and the turbine.

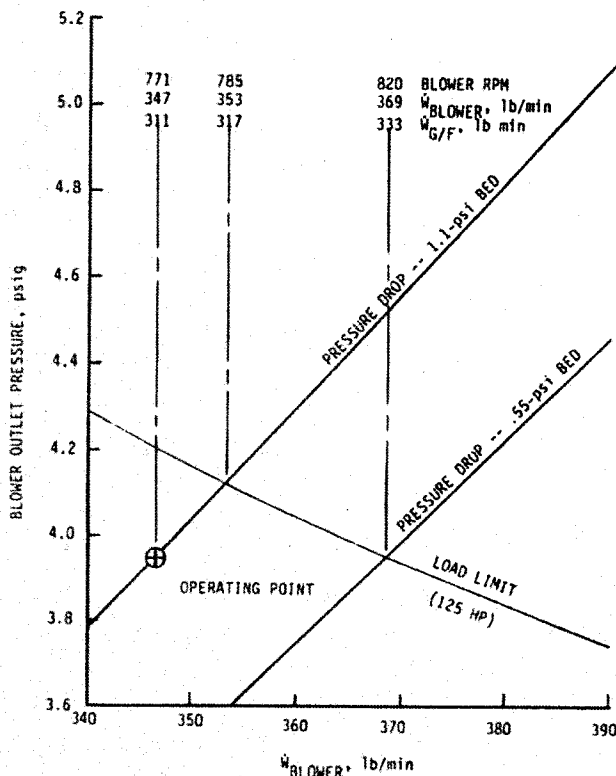


Figure 95 Mode-6 Vent

Results of a study of these factors are presented in Figure 95, and indicate that probably the best initial vent-system choice is to operate the blower with the present low-speed sheaves (771 rpm) to give a granular-filter flow of 311 lb/min. This configuration is predicted to operate at 3.96 psig blower outlet pressure, which is 94 percent of the load-limit pressure (4.2 psig) used for 771 rpm. Figure 95 presents blower outlet pressure as a function of blower flow. Two pressure-drop characteristics for the bed are shown: 1.1 psid and 0.55 psid. The 0.55 psid was investigated to show the effects of a half-depth bed. The load-limit characteristic was generated by using 4.2 psig and 347 lb/min as limiting conditions at 771 rpm and varying outlet pressure

inversely with flow (which, at constant efficiency, will give constant power). The pressure-drop characteristics were generated by assuming a turbine flow of 50 lb/min, calculated to give a turbine-inlet pressure at 1200 F of 0.094. Enough flow was then assumed to pass through the bypass valve to generate an equal pressure at the cooling-air passages and compressor. The flow required to do this is calculated as 36 lb/min.

Figure 95 indicates that slight increases in granular filter flow could be accomplished by speeding up the blower and operating at the load limit. These increases are so small (2 or 7 percent, depending on bed depth) that they do not appear to merit consideration.

SECTION 8

CORROSION, EROSION, & DEPOSITION STUDIES (TASK CP-6)

A. PURPOSE

As discussed in Section 4, operation of the Pilot Plant was severely hampered by problems with deposition inside the turbine, and also in the particle separators. In the turbine, deposits grew quickly to the point of critically reducing flow area, and the tendency to agglomeration created larger particles that introduced severe erosion. The same "sticky" nature of the flyash caused frequent plugging of small inertial separators and fouling of the residue-removal system.

Turbine-blade deposits were found to be rich in aluminum, and a similar phenomenon, the formation of aluminum-rich clinkers in the separator vessels, had often caused trouble in earlier model tests.

The composition of the ash was also found (Section 7) to limit somewhat the effectiveness of the granular filter in removing particulates before turbine entry, in that certain alkali salts were found to exist as vapors at the temperature at which the gas entered the filter.

It had thus become evident that purely mechanical means of hot-gas cleanup would not suffice to make the Pilot Plant a workable, environmentally safe system. It would be necessary to work with the chemistry of the system, by using additives during the combustion process. Task CP-6 was outlined with this in mind. It included a set of laboratory-scale screening tests, to select the nature and quantities of additives to be used, and followed with testing of the additives in a model combustor system.

No specific problems with corrosion had been encountered in Pilot Plant operation up to this point. Many of the hot-gas constituents, however, do have corrosive potential. Exposures of alloy specimens were therefore included as a part of the program.

B. CHEMICAL CONSIDERATIONS

Aluminum

The presence of aluminum in the products of combustion causes problems not only in the turbine, but in the combustor bed and particle separators as well. Slag from the model combustor typically shows a high concentration of aluminum. The deposits of metallic aluminum apparently originate from thin aluminum-foil coatings on packaging

materials; These form molten aluminum spheres about 10 microns in diameter, each with an aluminum-oxide layer at the surface. The oxide layer tends to protect the sphere from further oxidation, but is not strong enough mechanically to prevent splashing and coalescing when the droplets impact on a surface. The coalescing of the liquid aluminum and oxides forms an aluminum-rich clinker material, in the Pilot Plant usually found in the first-stage collector.

To reduce these deposits, a more complete oxidation of the aluminum before impaction and coalescence is indicated. Chemical oxidation of aluminum may be accelerated by HCl. A possible mechanism would be penetration of the protective oxide layer by HCl (more effectively than by oxygen): at the metal-oxide interface, HCl could react with aluminum metal to form vapors of aluminum chloride and hydrogen, which could fracture the oxide film from the inside. Such a mechanism may have been in effect in those model runs in which no aluminum clinkering was observed; the feed perhaps contained high concentrations of plastics (chlorides).

Physical dilution with ash particles at the point of impact would also be beneficial; this may be accomplished by using a high recycle rate of solids.

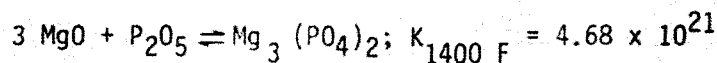
Bed Agglomeration

The number of potential low-melting eutectics is too great--and they are too varied and complex--for detailed evaluations. Generally, high sodium chloride, sodium sulfate, potassium chloride, and potassium sulfate tend to form low-melting eutectic salt, particularly with phosphates, borates, and lead compounds. Much of the sodium and potassium in solid waste is derived from bottle glass, which is usually a soda-lime glass containing chiefly sodium silicate and calcium silicate. Analysis of typical bed clinkers has indicated low-melting materials of this sort.

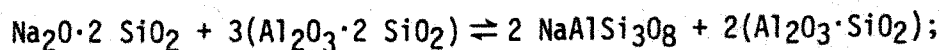
Combustion additives to increase the melting points of the glass constituents would be ZrO, Al₂O₃, MgO, and possibly additional CaO. The first of these, ZrO, is ruled out by its high cost. Clay (aluminum silicate) should be more cost-effective than Al₂O₃. Dolomite or talc may be more appropriate than pure MgO on a cost basis. Iron oxide is an unknown: it could influence the melting and sticking either way.

The solution to the bed-agglomeration problem depends on:

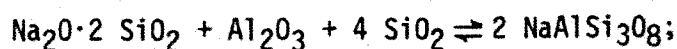
1. Converting KCl and K₂SO₄ (NaCl, Na₂SO₄) to high-melting solid feldspars.
2. Converting phosphates to non-sticky magnesium orthophosphate according to the favorable reaction,



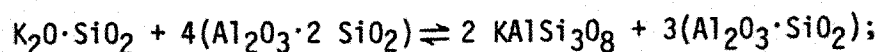
3. Converting sticky glass melts to feldspars by reactions like the following:



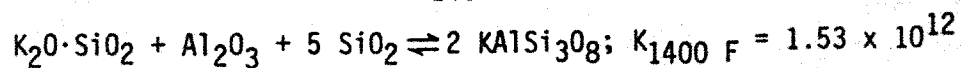
$$K_{1400 \text{ F}} = 2.85 \times 10^{46}$$



$$K_{1400 \text{ F}} = 7.20 \times 10^4$$



$$K_{1400 \text{ F}} = 5.93 \times 10^{67}$$



The feldspars thus formed may, however, be reacted with SO_2 and HCl to form sticky alkali salts.

4. Coating the glass and alkali-salt particles with higher-melting, non-sticky oxides such as MgO and CaO . Finely divided powders of pure Al_2O_3 (or clay) and MgO should be the most effective additives to prevent bed sticking. Enough must be added to coat each particle or effective particle agglomerate. Since the dust coatings will be dissolved by the glass particles, constant makeup materials will be required.

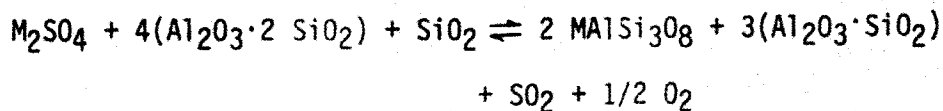
Downstream Deposits and Hot Corrosion

The chemical problems of fouling deposits and hot corrosion are interrelated with the aluminum and bed-agglomeration problems just discussed. The most predictable and effective reduction in deposits and corrosion will be accomplished by low-temperature (1350 F) operation of the combustor; this is the technique used in commercial fluid-bed incineration. The bed in this situation becomes essentially solid Na_2SO_4 , pure enough to be high-melting. The vapor phase is then saturated with Na_2SO_4 , but at a low level. Condensation occurs only as temperature decreases, and the vapors condense directly to solid particles that nucleate on small dust particles. To avoid sintering in the bed, chlorine input is limited to that which is carried over as NaCl vapor and HCl . Clay is also added to react with NaCl vapors.

At CPC, fouling deposits downstream of the combustor have been found to contain significant concentrations of sodium and potassium salts (chlorides, sulfates, and phosphates) which probably serve as bonding agents for other materials.

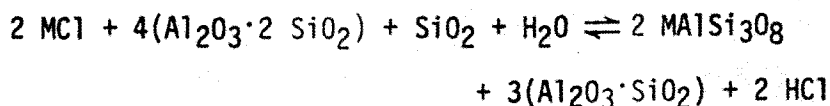
Sodium and potassium salts can be reacted with clay ($\text{Al}_2\text{O}_3 \cdot 2 \text{SiO}_2$) to form feldspars according to the following reactions (for M, read

either Na or K):



$$K_{1400 \text{ F}} = 1.17 \times 10^{59} \text{ for Na}$$

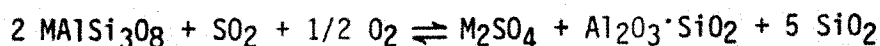
$$K_{1400 \text{ F}} = 1.32 \times 10^{61} \text{ for K}$$



$$K_{1400 \text{ F}} = 9.20 \times 10^{62} \text{ for Na}$$

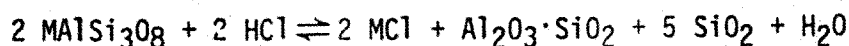
$$K_{1400 \text{ F}} = 3.94 \times 10^{63} \text{ for K}$$

The feldspar particles should be removed from the system as solids by tangential collectors before impacting on surfaces that tend to collect them. The conversion of feldspar to forms of aluminum silicate more stable than clay can reverse the feldspar reaction if the SO_2 and HCl are not adequately suppressed. Possible feldspar reverse reactions are as follows:



$$K_{1400 \text{ F}} = 7.79 \times 10^{-4} \text{ for Na}$$

$$K_{1400 \text{ F}} = 6.90 \times 10^{-6} \text{ for K}$$



($\text{Al}_2\text{O}_3 \cdot \text{SiO}_2$ = Andalusite)

$$K_{1400 \text{ F}} = 9.92 \times 10^{-8} \text{ for Na}$$

$$K_{1400 \text{ F}} = 2.32 \times 10^{-8} \text{ for K}$$

The addition of lime to the reaction provides an overall equilibrium condition in which SO_2 is negligible. However, in the actual cases, SO_2 persists because of kinetic limitations. The continuing presence of SO_2 allows the equilibrium conversion of feldspar to stable aluminum silicate (andalusite) and alkali sulfates. This reaction, however, could be kinetically limited or blocked by development of CaO coating on the feldspar particles.

Prevention

Bed agglomeration, fouling deposits, and corrosion are all

interrelated, with essentially the same approach being required to solve each problem:

1. Low (and constant) temperature of combustor operation.
2. Minimum afterburning.
3. Phosphates tied up as $3 \text{ MgO} \cdot \text{P}_2\text{O}_5$.
4. Sodium and potassium tied up as feldspars.
5. Flyash and bed particles coated with non-sticky oxide particles (CaO and MgO).
6. Chlorine released as HCl .

The additives indicated are MgO and $\text{Al}_2\text{O}_3 \cdot 2 \text{ SiO}_2$, plus CaO , all added as micron-size powders.

C. ADDITIVE SCREENING

Prior to testing with additives in the Model Combustor, a series of bench-scale tests was carried out to establish appropriate combustion temperature and additive concentrations. Small plates ($1/2'' \times 1/2'' \times 1/8''$) of type-316 stainless steel were used as specimens. These were coated with ash mixed with additives in predetermined concentrations and heated in a crucible furnace. After heating, a portion of the ash was dissolved in 50 ml of de-ionized water for specific-ion analysis: an Orion Research Model 407A specific-ion meter was used to identify concentrations of Na^+ , K^+ , and $\text{SO}_4^{=}$.

Ash from previous solid-waste combustion was used as the corrosion medium. A pre-test analysis of the ash showed a composition that included 2.5% Na^+ , 0.8% K^+ , and 10.4% $\text{SO}_4^{=}$. In an initial test using the ash without additives, a specimen was fired at 1550 F for 16 hours. No evidence of corrosion was found on the test specimen after cooldown, and a rerun at 1600 F for 40 hours still produced no detectable corrosion. The ash sample was then modified by adding 10% by weight of reagent-grade sodium sulfate, and it was this modified ash that was used for the screening tests.

Additives Used

The screening tests are described in terms of the additives used and their concentrations. A particular mole ratio specifies the concentration of each additive, identified by letter as follows:

- "A" Calcium oxide (CaO) was added for suppressing sulfur, if any, in the ash sample. Throughout the test, the amount of CaO used in each sample provided a calcium-to-sulfur mole ratio of 1. The CaO used was reagent grade.
- "B" Magnesium oxide (MgO) was added to each sample to react with phosphorous in order to increase the melting temperature of the alkali salts. The MgO used was industrial grade.

Magnesium-to-phosphorous mole ratio was varied downward from a starting value of 3.0.

"C" Clay ($\text{Al}_2\text{O}_3 \cdot 2\text{SiO}_2$), was added to each sample to react with alkali salts. The clay used was Burgess #10 pigment. Concentration is indicated by the aluminum-to-alkali mole ratio starting at 3.0.

Results

Table 33 lists the significant results of the screening tests in terms of the amount of water-soluble ions that were reacted by the various additive combinations. Values were determined by comparing the after-firing analysis with the analysis of the initial modified ash.

TABLE 33		
PERCENT REDUCTIONS OF WATER-SOLUBLE IONS		
Ion	1400 F	1500 F
	Ash only	
Na^+	0	0
K^+	0	0
SO_4^-	0	0
	Ash+1.0A,1.5B,1.5C	
Na^+	97	98
K^+	82	95
SO_4^-	73	(a)
	Ash+1.0A,1.5B,1.2C	
Na^+	-	77
K^+	-	41
SO_4^-	-	82
	Ash+1.0A,1.2B,1.5C	
Na^+	-	93
K^+	-	27
SO_4^-	-	85
	Ash+1.0A,1.2B,1.2C	
Na^+	-	81
K^+	-	38
SO_4^-	-	66

Notes: (a) Measurement faulty

A = CaO by Ca/S mol ratio
 B = MgO by Mg/P mol ratio
 C = Clay by Al/alkali mol ratio

In initial tests at 1600 F, the water-soluble ions were in large measure eliminated by the firing alone, independently of the amount of additive used; it was concluded that at this temperature they are carried off as vapor-phase sulfates rather than being chemically tied up by the additives. The remaining tests were therefore limited to temperatures of 1400 and 1500 F. At both temperatures, with additives "B" and "C" at mole ratios of 1.5, there was good suppression of the alkali ions. Further tests at 1500 F with reduced additive concentrations led to poorer alkali reaction, and the basic conditions selected for extended testing in actual combustion were a temperature of 1500 F using additives "B" and "C" at mole ratios of 1.5.

D. THE MODEL COMBUSTOR

The model-combustor system (Model No. 3) used for testing is shown in Figure 96. It is a low-pressure system with a combustor area 1/18 the size of that in the Pilot Plant. Air is supplied by

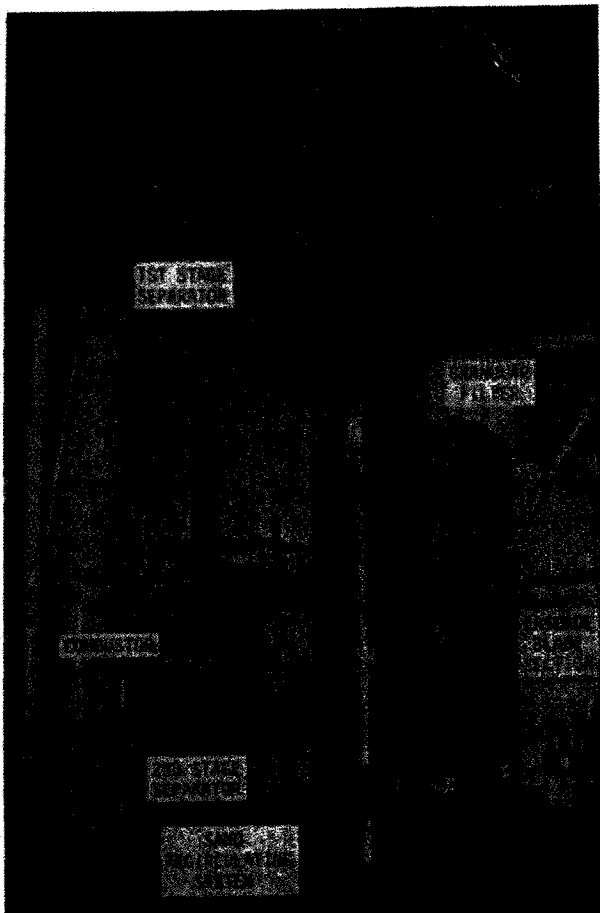


Figure 96 Model Combustor System

a low-pressure blower and the particle-laden products of combustion traverse two or more stages of particle separators before exhausting to the atmosphere. A schematic of the system configuration used in testing with MSW is shown in Figure 97.

The combustor (Figure 98) consists of a carbon-steel shell, insulated by six inches of Kaowool ceramic fibers and protected from erosion by a stainless-steel liner. It has a bed area of 2.2 sq ft and a 13.5-ft freeboard. Together with its support equipment, this combustor provides a versatile test bed in which fluidizing velocities up to 15 fps and bed depths up to four feet can be obtained. Excess oxygen and fluid-bed and freeboard temperatures can be varied over a wide range.

Exhaust gases from the combustor enter the first-stage separator, a 16-inch cyclone with a dipleg to the combustor for the return of elutriated fines to the bed. A 6-inch cyclone provides a second stage of exhaust-gas cleanup. The third stage is the granular filter, in which fines not separable by cyclones are collected on the surfaces of the granular media. Removal is then completed by a media cleanup system that is external to the hot-gas flow. When the granular filter is on line, the bleed to atmosphere from the second stage is controlled so as to give an approach velocity of 100 ft/min at the granular filter.

E. MODEL-COMBUSTOR TESTS

The test series in the Model Combustor consisted of three individual runs (see Table 34) and totalled 201.6 hours. Tests CP6M-1 and -2 were conducted with the two additives fed with the fuel; additionally, in CP6M-1, fines collected by the first-stage separator were

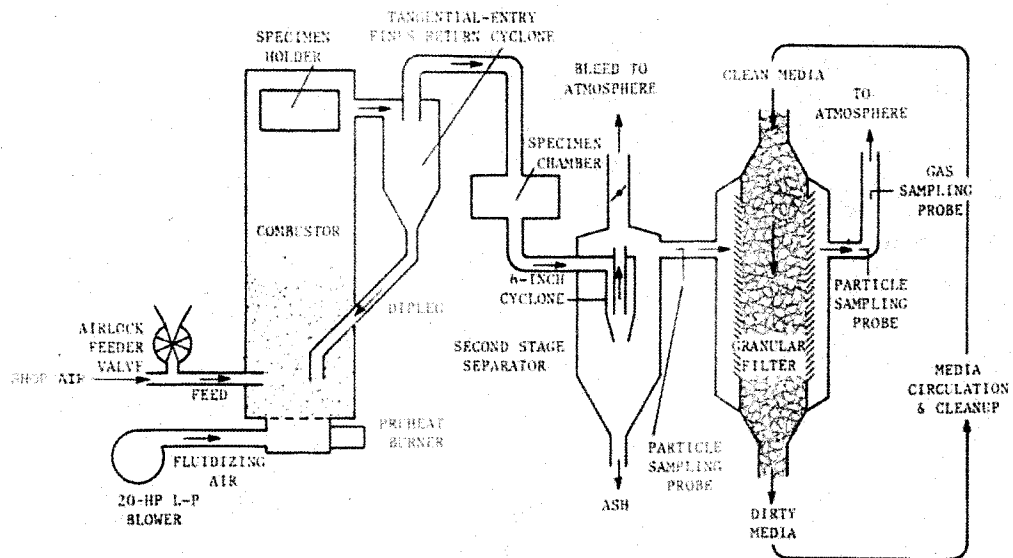


Figure 97 Model Combustor Flow Schematic

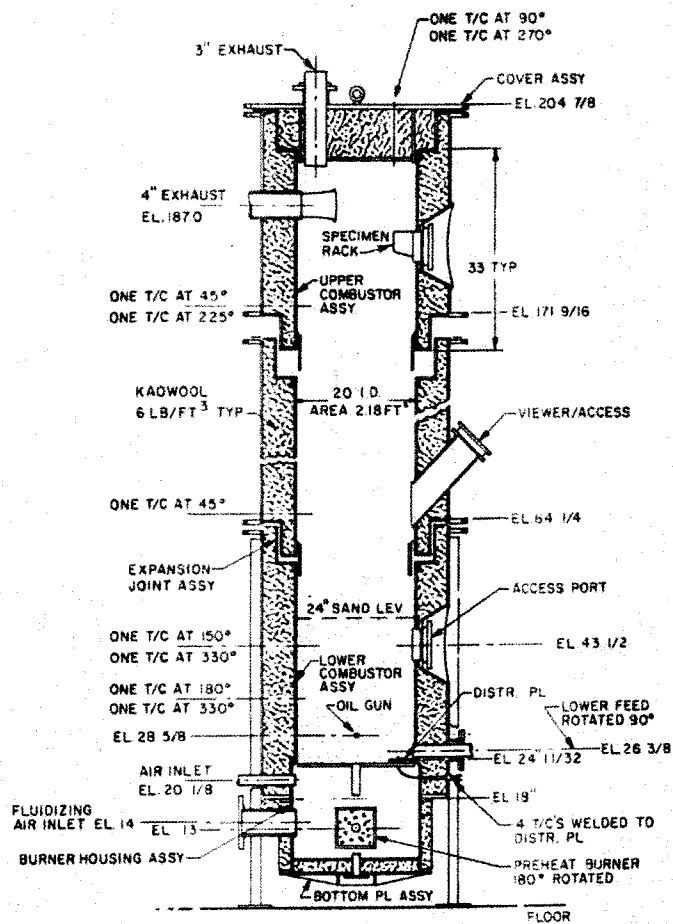


Figure 98 Model No. 3 Combustor

TABLE 34
SUMMARY OF CONDITIONS FOR
TEST SERIES CP6M

Test	CP6M-1	CP6M-2	CP6M-3
Duration	68.2	65.8	67.6
Type of Fuel	----- Municipal Solid Waste -----		
Fuel Feedrate, lb/min	2.07	2.11	1.96
Additive (55.1% Burgess No. 10 pigment, 44.9% MgO)	Yes	Yes	No
Bed Material	Virgin Gopher Sand	Used Bed from CP6M-1	Used Bed from CP6M-2
Bed Temperature, F			
Average	1438	1420	1430
Maximum	1520	1585	1520
Minimum	1190	1180	1240
Freeboard Temperature, F			
Average	1494	1497	1482
Maximum	1575	1665	1585
Minimum	1300	1325	1280
Air Superficial Velocity, fps	6.22	6.11	6.02
Air Flowrate, lb/min	19.9	19.2	19.2
Fines Recycle	Yes	No	No
HCl, ppm			
Average	103	21.0	14.5
SO ₂ , ppm			
Average	12.1	14.0	10.0
Maximum	76.7	49.3	43.0
Minimum	0	0	0
NO _x , ppm			
Average	75.2	124	83.2
Maximum	476	279	132
Minimum	0	0	0
O ₂ , %			
Average	12.5	14.1	11.0
Maximum	18.6	21.0	17.9
Minimum	6.3	6.2	7.8
CO ₂ , %			
Average	6.1	7.3	7.8
Maximum	14.0	15.1	14.5
Minimum	0	0.4	0.8
CH _x , ppm			
Average	21.7	14.0	9.6
Maximum	99.3	100	94.8
Minimum	0	2.0	2.1
Average loading at granular-filter inlet, gr/SDCF	4.258	1.661	0.417

returned to the combustor bed to retard the formation of aluminum clinkers in the system by physical dilution. Test CP6M-3 was conducted as a baseline test, without any chemical additives or recycling of first-stage fines.* Alloy specimens were exposed in the combustor freeboard during each of the three tests.

Fouling

Summarized results for the aluminum clinker and fouling deposits are shown in Table 35. Comparison of the CP6M-2 and CP6M-3 data shows that the clay additive alone cannot completely eliminate the aluminum-

clinker problem. However, the positive effect of clay is clearly demonstrated by the clinker weights and HCl concentrations; CP6M-2 data show an 88 percent reduction in weight of the aluminum clinker and a 45 percent increase in HCl concentration when compared with the baseline (CP6M-3) data.

TABLE 35 SUMMARY OF ALUMINUM-SLAG CLINKER AND ASH DEPOSITS FOR TEST SERIES CP6M			
	CP6M-1	CP6M-2	CP6M-3
Aluminum-slag clinker formed in first-stage separator, grams	0	7.0	57.0
Second-stage-separator ash deposits, lb	0	2.0	3.0
Additive (55.1% Burgess No. 10 pigment, 44.9% MgO) to MSW wt. ratio, lb/lb	0.022	0.028	0
Fines recycling	YES	NO	NO
Concentration of HCl** in the exhaust gas, ppm by vol.	103	21.0	14.5

** The HCl concentration in the exhaust gas was determined by the Volhard titration method on the periodically collected exhaust-gas condensates from the on-line gas-analysis system.

The CP6M-1 data indicate that clay additive plus fines recycling is capable of completely eliminating aluminum-clinker formation. This may be explained by the increased concentration of solids fines, which dilute the liquid drops of aluminum and form agglomerates of solid particles whose size remains in the free-flowing regime (30-100 microns). Also,

the much higher HCl concentration (about five times that of CP6M-2) shows that the fines recirculation benefits the clay and alkali-chloride reactions, in addition to its dilution effects. This is probably due to better mixing and contact of the two compounds when fines are being recycled.

* This order of testing, with the baseline run last, was adopted to minimize any residual fouling potential from a previous test, i.e., presumed best conditions were run first and presumed worst, last.

Fouling deposits other than the aluminum slag which occur in the CPU-400 system downstream of the combustor bed have been found to contain significant concentrations of sodium and potassium salts, which probably serve as bonding agents for other materials.

A study of the data for second-stage deposits in Table 35 reveals that additives alone without fines recycling can only reduce the deposits 33 percent from baseline values, while additives plus fines recycling can virtually eliminate the deposit problem.

Figure 99 shows the appearance of the second-stage separator tube following each of the three tests. Note that there was only a very light coating of ash on the outside of the separator tube after test CP6M-1, and that the ash deposits increased for the two subsequent tests, with test CP6M-3 showing the most severe deposition.

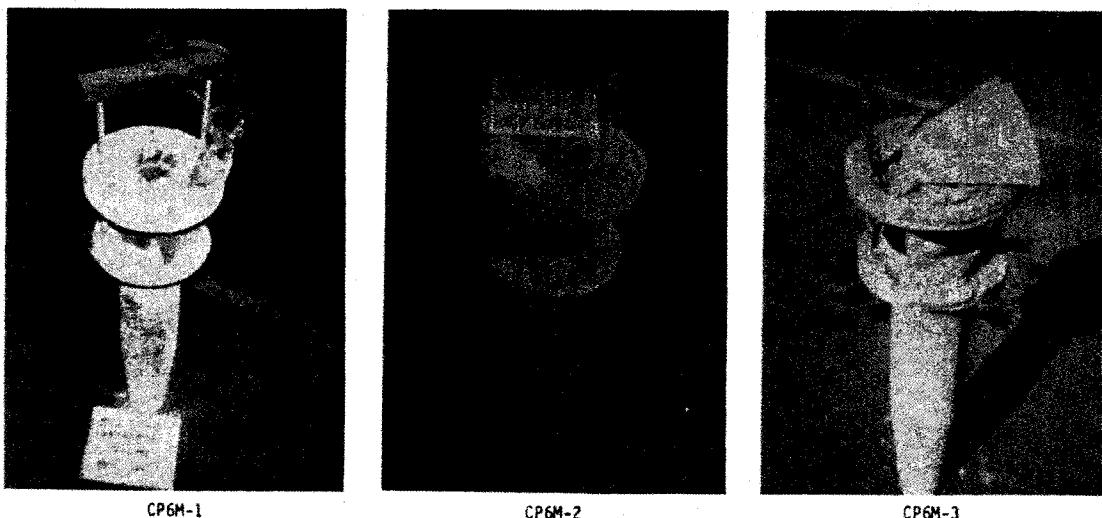


Figure 99 Deposition in Second-Stage Separator for Test Series CP6M

Corrosion

Alloy specimens were installed in the combustor freeboard to measure the severity of corrosion attack; nominal compositions are listed in Table 36. Seven selected alloy specimens for each test were analyzed by scanning electron microscope at an outside laboratory; results are summarized in Table 37. A study of Table 37 reveals that corrosion levels were very slight, and were roughly of the same order of magnitude in all three tests (thus substantially unaffected by the presence or absence of fines recycling and/or additives). The higher penetrations for test CP6M-2 are believed to be due to high-temperature excursions during that test.

TABLE 36
CORROSION SPECIMEN MATERIALS

Alloy	Ni	Co	Cr	Fe	Al	W	Ti	Mo	Cd	C	Zr
Nimonic 80A	75.64		19.5		1.3		2.5			0.06	
Inconel 600	76.42		15.5	8						0.08	
Inconel 601	61.5		23	24.1	1.35					0.05	
Inconel 690	60.47		30	9.5						0.03	
FSX 414	10	52.25	29	1		7.5				0.25	
Inco 713C	74.28		12.5		6.1	0.8	4.1		2	0.12	0.10
IN 738	62.68	8.5	16	0.5	3.4	2.6	3.4	1.75	0.9	0.17	0.1

TABLE 37
RESULTS OF ANALYSIS OF SELECTED ALLOYS
BY SCANNING ELECTRON MICROSCOPE

Test ID	CP6M-1	CP6M-2	CP6M-3
Freeboard Temp. F			
Average	1494	1497	1482
Maximum	1575	1665	1585
Minimum	1300	1325	1280
Additive (55.1% Burgess No. 10 pigment, 44.9% MgO) to MSW wt. ratio, lb/lb	0.022	0.028	0
Alloy	Penetration in Microns		
Nimonic 80A	5	15	15
Inconel 600	5	20	10
Inconel 601	13	12	None
Inconel 690	10	14	8
FSX 414	10	13	10
Inco 713C	3	7	None
IN 738	5	4	6
Average of the seven alloys	7.29	12.14	7.00

TABLE 38
CONDENSIBLES FROM VAPOR-
COLLECTION TUBE FOR TEST SERIES CP6M

Sample ID and Sampling Period	Length of Exposure (Hour)	K (ppm by Vol)	Cl (ppm by Vol)	SO ₄ (ppm by Vol)
CP6M-1 ET 1489 - 2110 min	6.9	0.068	277	0.22
CP6M-2 ET 3642 - 4063 min	7.0	0.100	353	0.15
CP6M-2 ET4934 - 5294 min	7.0	0.033	152	0.18
CP6M-3 ET 794 - 1277 min	7.4	0.040	205	0.04
CP6M-3 ET 2130 - 2555 min	7.0	0.063	226	0.32
CP6M-3 ET 3674 - 4104 min	7.0	0.031	207	0.13
Average of CP6M-1		0.068	277	0.22
Average of CP6M-2		0.066	253	0.17
Average of CP6M-3		0.045	213	0.16

- NOTES: 1. Condensible figures are reported as vapor concentrations in the hot gases in the combustor freeboard. The values were computed from results of specific-ion analysis of the vapor-tube washings.
2. Data for Na are not reported, as some of the values were unreasonably high, implying Na contamination of washings by lab.

Based on the above discussion, it is concluded that hot corrosion is not a significant problem when burning MSW with a freeboard temperature of around 1500 F.

A water-cooled vapor-collection tube was installed in the combustor freeboard and was periodically removed and washed with de-ionized water. The resulting solutions were analyzed with the specific-ion meter to determine the concentration of alkali-salt vapors in the freeboard during each test. Results are given in Table 38. Note that the condensible corrosives were similar for the three tests, which correlates with the similar corrosion levels that were observed.

The above discussion implies that the alkali-

salt reactions in the combustor were completed to a similar extent in all three tests (probably due to the enormous amount of SiO₂ in the bed and the significant amount of Al₂O₃ in the MSW ash.

Analysis of Solids

Samples of post-test bed materials and ash collected at different locations were analyzed, with the results summarized in Table 39. Note that the soluble-to-total alkali ratios for solids at different locations were roughly the same for tests CP6M-2 and -3, while those for test CP6M-1 were as low as 11 percent of the CP6M-3 values. This once again demonstrates the beneficial effect of additives plus fines recycling. In addition, it also discloses that alkali salts were still in reactions downstream of the combustor.

The composition of MSW fuel varies from moment to moment, so it is virtually impossible to select "representative" samples. The best

TABLE 39
SOLIDS ANALYSES FOR TEST
SERIES CP6M

	Weight Percent										
	Post-Test Bed Material			1st-Stage Ash		2nd-Stage Ash			G/F Front-Face Ash		
	CP6M-1	CP6M-2	CP6M-3	CP6M-2	CP6M-3	CP6M-1	CP6M-2	CP6M-3	CP6M-1	CP6M-2	CP6M-3
P	0.05	0.06	0.09	0.29	0.29	0.36	0.36	0.36	0.27	0.40	0.54
Si	40.06	34.22	36.55	26.75	29.13	25.62	15.13	13.48	19.64	15.81	12.66
Fe	1.70	7.04	2.62	2.75	2.58	3.19	1.69	2.22	5.25	3.08	2.64
Al	1.29	3.14	1.48	7.20	5.63	8.75	10.41	9.71	7.61	9.12	8.33
Ti	0.13	0.05	0.17	0.80	0.80	0.91	1.90	2.61	0.75	1.63	1.93
Ca	2.36	2.86	4.07	6.55	6.64	5.49	7.20	9.90	8.64	6.74	8.35
Mg	0.57	0.74	0.77	2.79	0.90	2.89	9.60	1.72	4.03	7.54	3.17
K	0.84	9.96	1.32	1.72	2.05	1.76	1.49	3.19	1.25	1.76	3.09
(Total)											
K+ (Soluble)	0.01	0.04	0.04	0.03	0.03	0.04	0.23	0.65	0.18	0.64	1.15
Na	2.16	2.29	3.35	4.46	4.92	3.57	2.70	4.88	2.32	2.76	4.36
(Total)											
Na+ (Soluble)	0.11	0.18	0.21	0.10	0.15	0.18	0.62	1.18	0.49	1.30	2.07
S	0.11	0.30	0.34	0.38	0.49	0.82	2.40	6.14	3.95	4.77	7.70
Cl	N/D	N/D	*N/D	0.10	0.14	0.13	0.71	0.35	0.16	0.16	0.16
Loss on Ignition	N/D	N/D	N/D	0.34	0.11	0.27	4.07	1.01	8.90	0.70	2.62
Ratio of Water Sol. K to Total K (%)	1.58	4.14	2.89	1.69	1.58	2.21	15.4	20.4	14.0	36.2	37.1
Ratio of Water Sol. Na to Total Na (%)	5.12	7.77	6.28	2.14	3.09	5.13	22.7	24.2	21.4	47.0	47.4

*N/D=Not Determined

measure of overall uniformity of fuel in the three tests is the composition of the ash generated. There are variations depending also upon the point in the system where the sample was taken. To eliminate these, the averages for the three locations* are listed in Table 40, along with "typical" compositions from References 7 and 8, and an average of 11 CPC samples from earlier testing. The differences from one test to another are seen to be generally less than their departures from "typical," or than the differences among the three "typical" samples.

TABLE 40
COMPARISON OF ASH COMPOSITIONS

Element	Weight Percent					
	CP6M-1	CP6M-2	CP6M-3	Union Electric (Ref.7)	Incineration Conference (Ref.8)	11 CPC Samples
P	0.32	0.35	0.40	0.78	0.65	0.50
Si	23.13	19.23	18.42	23.51	24.75	>16.35
Fe	4.22	2.51	2.48	5.43	1.82	3.71
Al	8.18	8.91	7.89	5.87	3.28	>11.00
Ti	.83	1.44	1.78	.50	2.52	.71
Ca	7.06	6.83	8.30	8.68	10.58	> 7.11
Mg	3.46	6.64	1.93	.77	5.61	1.17
K	1.50	1.66	2.78	1.29	2.91	2.54
Na	2.94	3.31	4.72	6.36	3.19	3.83
S	2.38	2.52	4.78	.58	.04	-
Cl	.14	.32	.22	(a)	(a)	-

Conclusions

The following conclusions may be drawn from the three test runs in the Model Combustor:

- Bed agglomeration is not a problem at a fluid-bed temperature of 1430 F with a superficial velocity of 6 fps.
- Corrosion is not a significant problem at a freeboard temperature of 1500 F, whether additives (magnesium oxide and Burgess No. 10 pigment) are used or not.

* Two locations in the case of CP6M-1, since the material separated in the first stage was all returned to the bed.

- Additives alone help only little to reduce formation of sticky ash deposits; but additives plus fines recycle are very effective.
- Additives lead to a reduction in the formation of aluminum clinkers; additives with fines recycle eliminate this phenomenon.

SECTION 9

SYSTEMS STUDIES (TASK SS-10)

A. BACKGROUND

The EPA in late 1975 awarded Contract 68-03-2370 to Gilbert Associates, Inc., of Reading, Pennsylvania to perform a CPU-400 Systems Study and Preliminary Design. The purpose of this contract was twofold. Initially, the contractor would conduct a systems study to evaluate various turbine/hot-gas system configurations in order to determine which available gas turbines are best suited for large-scale systems. System cost, performance, and reliability would be evaluated for each turbine/hot-gas system combination to determine which offered the lowest life-cycle costs for the disposal of solid waste and sewage sludge.

The second, closely related, purpose of the contract is to produce a preliminary design for a large-scale solid-waste-fired gas-turbine system. The preliminary design is to be in sufficient detail to allow capital costs to be estimated to within 10 percent, and will provide communities and their consultants a basis for comparing projected system economics with those of other solid-waste disposal systems. Also, in the event EPA decides to fund a demonstration grant for the construction of the first large-scale system, the preliminary design will give all interested communities a common starting point for the preparation of their grant applications.

Task SS-10 was added to the contract effort described herein, with the objective of defining the operating characteristics and requirements of four gas-turbine modules for applications of the CPU-400 type. The studies were intended specifically to support the contract effort of Gilbert Associates, and are fully reported in Reference 9; the following material is a digest from that report.

B. BASIS OF STUDIES

This task evaluated four gas-turbine systems: three commercially available turbine/generator units and a system ("Components") made up of an industrial compressor and a turbine such as those built by Ingersoll-Rand Co. or Worthington Compressors, Inc. The advantage of the latter is that a unit can be built to operate at a low excess-air limit and thus dispose of large quantities of high-moisture wastes

such as sewage sludge without a mismatch in size between the compressor and turbine. The commercial units are limited when burning high-moisture fuels by surge margin (pressure ratio) since these are constant-speed machines.

Characteristics of the three commercial units selected are summarized in Table 41. These units were selected to give a wide range of sizes; they vary in airflow by a factor of eight. All of the units are single-shaft machines to ease the problem of load-shed speed control; this is acceptable since the output is electrical power. A further criterion used in the selection was that the units have an external combustor or be available in a regenerated version. This requirement was imposed to simplify the adaptation of the units to the external fluid-bed combustion system by taking advantage of the existing internal ducting that separates the compressor-outlet and turbine-inlet gas flows.

TABLE 41			
COMMERCIAL TURBINE CHARACTERISTICS			
(59 F, Sea Level)			
Manufacturer	Solar	Westinghouse	Brown-Boveri**
Model	Centaur	W-101	9
Pressure Ratio	8.7	6.5	7.75
Exhaust Flow (lb/min)	2300	7960	19290
Power Output (kW)	2600	8130	22700
Fuel Flow* (lb/min)	33.1	113.0	271.9

* Oil, LHV = 18150 Btu/lb

** Built under license in U.S.A. by Turbodyne

The compressor of the Components system was assumed to have an air-flow comparable with the Westinghouse W-101 and a pressure ratio of 9.0. This is the median size for the three commercial systems studied. Industrial units are essentially custom built, so there is flexibility in system sizing.

To analyze these systems, a cycle analysis was conducted to match the published performance data (pressure ratio, exhaust flow, power output and fuel consumption). To accomplish the match, assumptions were made with regard to compressor efficiency, turbine-cooling air-flow, combustor pressure drop, generator efficiency, and parasite losses. Turbine-inlet temperature and turbine efficiency were then varied to match fuel flow and power output, respectively.

The use of the commercial gas turbines in a CPU-400 application requires some modifications to increase capacity for high-moisture wastes. When high-moisture wastes are used, the mass addition in the combustor increases and the cycle pressure ratio increases. This results in moving the compressor operating point closer to the surge line (decreased surge margin). It was assumed that pressure ratio could increase 6 percent over the values of Table 41. To further increase system capacity, it was assumed the turbine nozzles could be increased in flow area by 10 percent.

C. STEADY-STATE OPERATING SOLUTIONS

The cycle used in this study is a simple Brayton cycle as shown in Figure 100. In those cases using commercial turbines, the turbine's combustor is replaced by a fluid-bed combustor and gas-cleanup system. A schematic of the computer model is shown in Figure 101, and a sample computer output in Figure 102; output nomenclature is shown in Table 42. Each module was analyzed for operation on solid waste and on solid waste plus sewage sludge, at two compressor-outlet temperatures (1300 and 1550 F).

The cycle parameters used are summarized in Table 43. The cold-bleed term accounts for feeder-valve leakage and air required for the pneumatic-transport system of the granular filter. Hot bleed is used to account for ash-system bleed required by cyclone separators. Cold-side pressure drop accounts for pressure drop between the compressor outlet and the top of the fluid-bed distributor plate (piping, valves, and distributor plate). Hot side pressure drop accounts for that between the combustor freeboard and the turbine inlet (piping, cyclones, and granular filter). Bed pressure drop is a constant since this is a characteristic of the fluid bed; the value used is representative of a static bed height of 3 ft. with a density of 91 lb/cu ft.

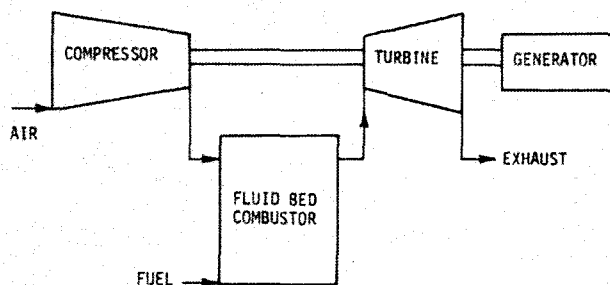


Figure 100 Simple-Cycle Gas Turbine

The CPU-400 cycle solutions are summarized in Table 44. The commercial units operated on the pressure-ratio limit (6% above Table 41 values) when sewage sludge is used. The Component system does not have this restriction and can operate on an excess-air limit. These cycles show that if



Figure 101 Cycle Schematic

CENTAUR SW 1550F FFR=906

325

8/16/75

ICON= 2 NSI= 0 NSC= 0 NCSSM= 0

DATE AND TIME 08/16 15:36

PAMB = 14.70 DPIN = 3.5 DPEXM = 2.0

COMPRESSOR P1= 14.57 T1= 519.00 PR= 8.5446 P2= 124.53 W2= 2310.0
 T2= 1026.83 T2C= 0.0 QCW= . ETAC= .850 HPC= 6733.2
 BLLEAK= .015 W02= 34.7 BLTCA= .0300 WTCA= 69.3

CPC COMB P6= 120.15 T6= 2010.00 W5= 2206.1 W6= 2355.7 WSC= 0.0
 RHOB= .630 MB= 3.0 TAB= 100. THETR= .95 THET= 2.670
 UO= 6.000 AB= 36.0 UFB= 6.810 AFB= 36.0 QCLO= 14936.
 OPC= .020 DPH= .050 RCAS= 1.50 FCAL= 1.000 RSUPP= .850
 WF1= 180.46 EPS1= .3000 ALP1= .2440 HHV1= 8643. AF1= 6.2939
 FC1= .5056 FM1= .0679 FO1= .4266 FS1= 0.0000 TF1= 519.00
 WF2= 0.00 EPS2= .9400 ALP2= .3650 HHV2= 11792. AF2= 8.7273
 FC2= .6209 FM2= .0837 FO2= .2954 FS2= 0.0000 TF2= 519.00
 XC02= .0490 XM20= .0758 XMIX= .7334 X02= .1418 XS02= 0.000000
 MW6= 28.71 WADD= 0.00 XCAC03= .5660 XMGC03= .4250 WRES= 30.82
 Y1= 1.0000 YCA0= 0.0000 YCAC03= 0.0000 YCAS04= 0.0000 YMG0= 0.0000
 WSUP= 0.00 TSUP= 519.0

INERTIAL P7= 114.14 T7= 1966.13 W7= 2332.1 W07= 23.6 BLH= .0100
 MW7= 28.71 QISLO= 29872.

TURBINE P9= 14.77 T9= 1286.83 W9= 2401.43 RKW= 3500. KW= 2618.
 HPOUT= 3619.49 HPT= 10404.76 ETAT= .856 SP= 68.002
 ETATH= .180 ETAGEN= .970 MECLO= .005 MW9= 28.72
 YC02= .0476 YM20= .0737 YMIX= .7350 Y02= .1437 YS02= 0.000000

WM STEAM HF= 68.0 TSSAT= 831.0 HS= 1196.7 SATPP= 59.6
 T10= 760.0 HSEVIN= 343.60 WS= 287.5 T9P1= 890.6
 TSSH= 831.0 SHPP= 455.8 ETATHC= .574
 STLO= .045 HCSSH= 1196.7

MAIN ITE= 3

TURBINE FLOW FACTOR= 906.00139

CENTAUR SW855 1550F

327

8/16/75

ICON= 1 NSI= 0 NSC= 0 NCSSM= 0

DATE AND TIME 08/16 15:40

PAMB = 14.70 DPIN = 3.5 DPEXM = 2.0

COMPRESSOR P1= 14.57 T1= 519.00 PR= 9.2198 P2= 134.36 W2= 2310.0
 T2= 1050.57 T2C= 0.0 QCW= . ETAC= .850 HPC= 7055.2
 BLLEAK= .015 W02= 34.7 BLTCA= .0300 WTCA= 69.3

CPC COMB P6= 129.79 T6= 2010.00 W5= 2206.1 W6= 2541.0 WSC= 0.0
 RHOB= .630 MB= 3.0 TAB= 100. THETR= .95 THET= 1.664
 UO= 6.000 AB= 33.4 UFB= 7.593 AFB= 33.4 QCLO= 14936.
 OPC= .020 DPH= .050 RCAS= 1.50 FCAL= 1.000 RSUPP= .850
 WF1= 234.27 EPS1= .3000 ALP1= .2440 HHV1= 8643. AF1= 6.2939
 FC1= .5056 FM1= .0679 FO1= .4266 FS1= 0.0000 TF1= 519.00
 WF2= 143.87 EPS2= .9400 ALP2= .3650 HHV2= 11792. AF2= 8.7273
 FC2= .6209 FM2= .0837 FO2= .2954 FS2= 0.0000 TF2= 519.00
 XC02= .0632 XM20= .1729 XMIX= .6578 X02= .1092 XS02= 0.000000
 MW6= 27.78 WADD= 0.00 XCAC03= .5660 XMGC03= .4250 WRES= 43.16
 Y1= 1.0000 YCA0= 0.0000 YCAC03= 0.0000 YCAS04= 0.0000 YMG0= 0.0000
 WSUP= 0.00 TSUP= 519.0

INERTIAL P7= 123.30 T7= 1971.86 W7= 2515.6 W07= 25.4 BLH= .0100
 MW7= 27.78 QISLO= 24872.

TURBINE P9= 14.77 T9= 1286.79 W9= 2544.92 RKW= 3500. KW= 3552.
 HPOUT= 4910.31 HPT= 12025.62 ETAT= .856 SP= 92.254
 ETATH= .178 ETAGEN= .970 MECLO= .005 MW9= 27.81
 YC02= .0586 YM20= .1044 YMIX= .6412 Y02= .1118 YS02= 0.000000

WM STEAM HF= 68.0 TSSAT= 831.0 HS= 1196.7 SATPP= 60.4
 T10= 760.0 HSEVIN= 343.60 WS= 327.9 T9P1= 891.4
 TSSH= 831.0 SHPP= 457.8 ETATHC= .504
 STLO= .045 HCSSH= 1196.7

MAIN ITE= 3

TURBINE FLOW FACTOR= 905.94854

Figure 102 Cycle-Analysis Output

TABLE 42
COMPUTER PROGRAM NOMENCLATURE

Identification	Definition	Identification	Definition
ICON	Iteration Control	XC02	CO ₂ Mole Fraction
NSI	Steam Injection if NSI = 1	XH2O	H ₂ O Mole Fraction
NSC	Combustor Steam Generation if NSC = 1	XMIX	N ₂ & A Mole Fraction
NCSSH	Steam Superheat in Combustor if NCSSH = 1	X02	O ₂ Mole Fraction
IRG	Regenerated if IRG = 1	MW6	Combustor Gas Molecular Weight
NPOLY	Polytropic Efficiency Used if NPOLY = 1	WADD	Additive Flow (lb/min)
ETACP	Polytropic Compressor Efficiency	XCAC03	CaCO ₃ Weight Fraction
ETATP	Polytropic Turbine Efficiency	XMGC03	MgCO ₃ Weight Fraction
PAMB	Ambient Pressure (psia)	WRES	Total Residue Flow (lb/min)
DPIN	Inlet Pressure Drop (IW)	YI	Inert Weight Fraction
DPEXH	Exhaust Pressure Drop (KW)	YCAO	CaO Weight Fraction
P1	Compressor Inlet Press. (psia)	YCAC03	CaCO ₃ Weight Fraction
T1	Compressor Inlet Temp. (R)	YCAS04	CaSO ₄ Weight Fraction
PR	Compressor Press. Ratio	YMGO	MgO Weight Fraction
P2	Compressor Outlet Press. (psia)	SWUP	Supplemental Air Flow (lb/min)
W2	Compressor Airflow (lb/min)	TSUP	Supplemental Air Temp. (R)
T2	Compressor Outlet Temp. (R)	P7	Turbine Inlet Press. (psia)
T2C	Intercooled Compressor Discharge Temp. (R)	T7	Turbine Inlet Temp. (R)
QCW	Intercooler Heat Extraction (Btu/min)	W7	Turbine Inlet Flow (lb/min)
ETAC	Compressor Efficiency	W07	Hot Gas Bleed (lb/min)
HPC	Compressor Power (HP)	BLH	Hot Bleed Fraction
BLLEAK	Compressor Bleed Fraction	MW7	Turbine Inlet Gas Molecular Weight
WD2	Compressor Bleed Flow (lb/min)	QISLO	Separator Heat Loss (Btu/min)
WTCA	Compressor Bleed Fraction for Turbine Cooling Air	P9	Turbine Outlet Press. (psia)
WTCA	Turbine Cooling Air Flow (lb/min)	T9	Turbine Outlet Temp. (R)
P6	Combustor Freeboard Press. (psia)	W9	Turbine Outlet Flow (lb/min)
T6	Combustor Freeboard Temp. (R)	RKW	Reference Output Power (kW)
W5	Combustor Inlet Air Flow (lb/min)	KW	Output Power (kW)
W6	Combustor Exhaust Gas Flow (lb/min)	HPOUT	Output Shaft Power (HP)
RHOB	Bed Density (psi/static ft)	HPT	Turbine Power (HP)
HB	Static Bed Height (ft)	ETAT	Turbine Efficiency
TAB	Overbed Temp. Increment (R), (T6-TBED)	SP	Specific Power (kW-sec/lb) (kW x 60)/W2
THETR	Reference Excess Air Fraction	ETATH	Thermal Efficiency, HHV
THET	Excess Air Fraction	ETAGEN	Generator
UO	Bed Superficial Velocity (ft/sec)	MECLO	Parasitic Loss, Fraction of Turbine Power
AB	Bed Area (ft ²)	MW9	Turbine Exhaust Gas Molecular Weight
UFB	Freeboard Velocity (ft/sec)	YC02	Exhaust CO ₂ Mole Fraction
AFB	Freeboard Area (ft ²)	YH2O	Exhaust H ₂ O Mole Fraction
QCLO	Combustor Heat Loss Factor (Btu/min)	YMIX	Exhaust N ₂ & A Mole Fraction
DPC	Cold Press. Drop, (P2-P5)/P2	Y02	Exhaust O ₂ Mole Fraction
RCAS	Ca/S Mole Ratio	YS02	Exhaust SO ₂ Mole Fraction
FCAL	Calcination Efficiency Factor (for CaCO ₃ only)	HFW	Feed Water Enthalpy (Btu/lb)
RSUPP	SO ₂ Suppression Efficiency Factor	TSSAT	Saturation Temp. (R)
WF1, WF2	Fuel Flow (lb/min) (includes moisture)	HS	Steam Enthalpy (Btu/lb)
EPS1, EPS2	Fuel Moisture Fraction	SATPP	Evaporator Pinch Point (R)
ALP1, ALP2	Inert Fraction, Dry Basis	T10	Stack Temp. (R)
HHV1, HHV2	Higher Heating Value, Dry/Inert Free	HSEVIN	Enthalpy of Water at TSSAT (Btu/lb)
AF1, AF2	Stoichiometric Air - Fuel Ratio, Dry/Inert Free	WS	Steam Flow (lb/min)
FC1, FC2	Carbon Weight Fraction, Dry	T9P1	Gas Temp. at Evaporator Pinch Point (R)
FH1, FH2	Hydrogen Weight Fraction, Dry	TSSH	Superheated Steam Temp. (R)
FO1, FO2	Oxygen Weight Fraction, Dry	SHPP	Superheater Outlet Pinch Point (R)
FS1, FS2	Sulfur Weight Fraction, Dry	ETATHC	Combined Cycle Efficiency HHV
TF1, TF2	Fuel Temp. (R)	STLO	Boiler Loss Fraction
		HCSSH	Combustor Superheat Steam Enthalpy (Btu/lb)

TABLE 43
CPU-400 CYCLE PARAMETERS

Ambient Conditions		
Temperature (F)		59
Pressure (psia)		14.7
Cold Bleed		1.5
Hot Bleed		1.0
Cold-slide Pressure Drop		2.0
Hot-slide Pressure Drop		5.0
	<u>Solid Waste</u>	<u>Sewage Sludge</u>
Fuel		
Moisture (%)	30.0	94.0
Ash (% dry basis)	24.4	36.5
Carbon (% dry, ash-free)	50.6	62.1
Hydrogen (% dry, ash-free)	6.8	8.4
Oxygen (% dry, ash-free)	42.7	29.5
HHV (Btu/lb)	8643	11792

TABLE 44
CPU-400 CYCLE SUMMARY

Turbine	Combustor Outlet Temp. (F)	Excess Air (%)	Fuel Flow		Power (kW)
			Solid Waste (lb/min)	Sewage Sludge (lb/min)	
Solar-Centaur	1300	395	134	0	1598
		146	237	319	3299
	1550	267	180	0	2618
		166	234	144	3552
Westinghouse W-101	1300	359	483	0	5758
		159	768	879	10057
	1550	246	641	0	8939
		182	756	307	10774
Brown-Boveri 9	1300	383	1035	0	14095
		138	1849	2516	27706
	1550	261	1387	0	21939
		157	1829	1178	29708
Components	1300	20	1590	2232	23830

solid waste only is used as a fuel the highest waste consumption and power output will occur at the higher temperatures. If sewage sludge is used in addition to solid waste, the highest consumption occurs at 1300 F while the highest power output occurs at 1550 F. The Component system is able to provide increased disposal capability and power output since it is limited only by excess air. This is made obvious by comparing the Westinghouse W-101 with the Component system, which has the same airflow but much different fuel flows and power output.

To show the effect of ambient temperature on the CPU-400 cycle, the solid-waste and sewage-sludge cycles were run at ambient temperatures from 0 F to 120 F, with the results summarized in Figures 103 and 104. This analysis indicates a 32-percent power increase at 0 F and a 25-percent decrease at 120 F for the commercial units. For the Component system the corresponding values are 25 and 20 percent, respectively. This is less variation than is seen in a normal gas turbine because of the variable ratio of solid waste to sewage sludge. On a hot day more sewage sludge (mostly water) is used to increase the pressure ratio and this results in a power boost. Pressure ratio and airflow for these runs were varied inversely with the absolute ambient temperature.

In order to assess the effect of using a waste-heat boiler, variations on the solid-waste and sewage-sludge cycles were run with different exhaust-pressure levels. The results are presented in Figure 105, and indicate a 2.3-percent power drop for the commercial units at 12 IW (typical value with boilers) when compared to the nominal exhaust-pressure condition (2 IW). The corresponding drop for the Component system is 1.7 percent.

D. SYSTEM OPERATION

The paragraphs to follow describe the operation of the hot-gas and turbine systems from cold start through steady-state operation to shutdown. Reference is made to the process schematic of Figure 106.

Startup

The first step for operation on the fluid-bed combustor is a system preheat. The fluid-bed material must be brought to a temperature compatible with good combustion efficiency, and the granular-filter media must be heated sufficiently to maintain zero-load turbine-inlet temperature during transition from the bypass combustor.

Preheating is accomplished by operating the turbine on the oil-fired bypass combustor while bleeding off some of the hot gas and passing it in reverse direction through granular filter, cyclone, and combustor bed. During the preheat mode the turbine is operated at zero electrical load and rated inlet temperature. Granular-filter media is circulated during the preheat to allow media volume to adjust for differential expansion of filter internals.

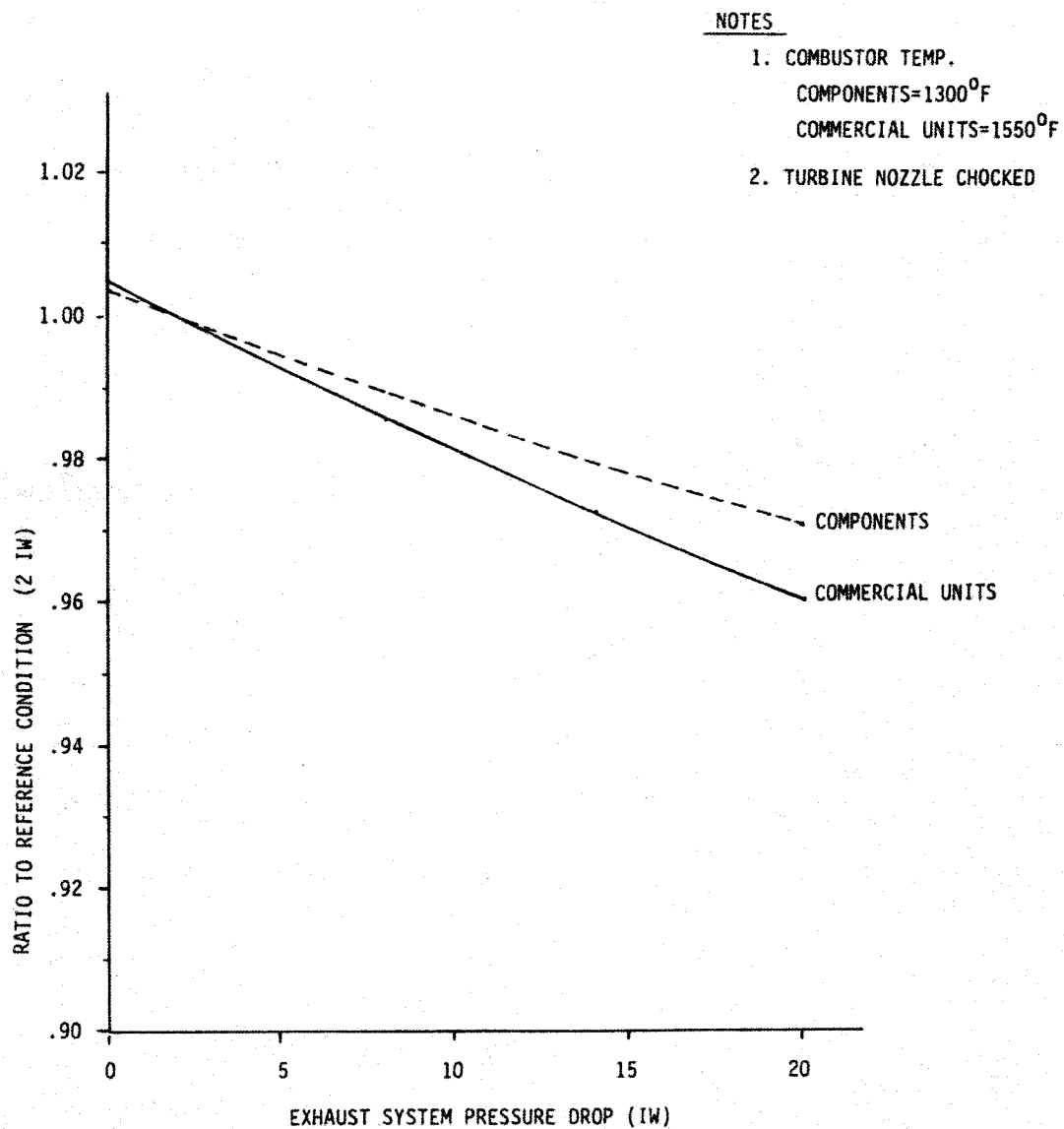


Figure 105 Effect of Exhaust Back Pressure

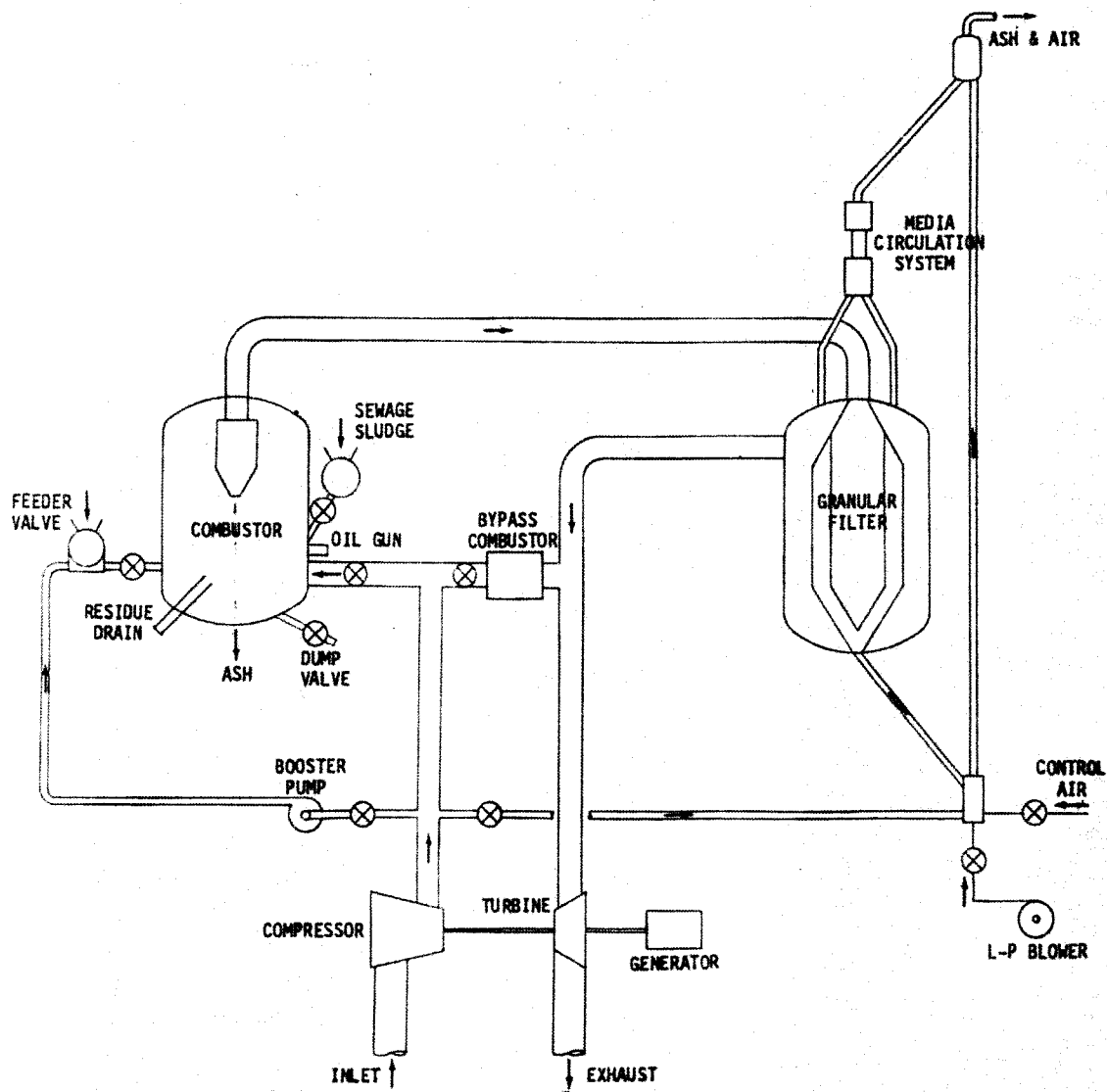


Figure 106 Process Schematic

Transition

At conclusion of the preheat, the system can proceed to fluid-bed operation. The first step is to change over from the bypass combustor to the fluid-bed combustor as the source of hot gas for the turbine. This is accomplished with the turbine at full rpm and zero load. When these conditions have been established, oil flow to the bypass combustor is terminated and the compressor output is directed to the combustor plenum. As soon as the bed is fluidized, oil flow to the fluid-bed oil guns is initiated and ash-system operation is started. After the system is stabilized on oil, flow of solid waste and sewage sludge is started and gradually increased, while oil flow is gradually decreased and then terminated.

Steady-State Operation

After transition, the system is in its normal operating mode at zero power. The control system then increases the load and maintains the setpoint. (Minor upsets, such as interruptions of fuel feed, can be compensated for by temporarily reverting to oil. Normal operation, however, does not involve supplying oil to the fluid bed; all energy is supplied by the solid waste and sewage sludge).

Shutdown

Shutdown can be accomplished simply by terminating fuel flow. The thermal inertia of the system is such that termination only results in the system's winding down to zero electrical load over an extended period of time, on the order of one-half hour. For a rapid emergency shutdown, the compressor-outlet air is bypassed directly to the turbine inlet (which leaves the system hot, permitting restart without preheating).

SECTION 10

CONCLUSIONS

The original broad objective of proving the feasibility of generating electrical power by burning municipal solid waste in a direct-fired gas turbine proved not to be attainable within the scope of this program. The promise of such a system remains attractive, however, and several positive advances were made toward its eventual attainment.

The solid-waste processing station that was designed and constructed fulfilled all design requirements for supplying a continuous flow of processed solid-waste fuel for Pilot Plant consumption. Because of limitations imposed by turbine deposition, the full intended use of the facility was not carried out, but sufficient operating experience was accumulated to engender confidence that it could have supported all the long-duration tests originally planned without difficulty.

The fluid-bed combustor was shown to be a highly efficient device for burning low-Btu fuel such as solid waste; combustion efficiency in excess of 99% was readily achieved. The effectiveness of the fluid bed in promoting mixing became evident when operation on a single feed line offered no difficulties as compared with operation on two. Gaseous emissions from solid-waste fuel were well within current environmental standards.

The complete energy-conversion process, from shredding to generator output, is highly amenable to computerized control. Procedures were successfully developed for smooth transition between operational modes, starting with the turbine operating on its own oil combustor and ending with steady-state operation on the fluid-bed combustor. Software underwent some evolution during the solid-waste testing and wood-waste testing, and reached a final highly effective state in the coal program, which included an uninterrupted 30-hour run. In continuous operation on coal, bed temperature was maintained within ± 10 F of the setpoint, and the turbine-inlet temperature within ± 4 F of its setpoint. An innovative system of controlling turbine speed by modulating the generator load proved very effective.

Removal of residue from the pressurized system posed some problems, owing primarily to the sticky nature of the ash when at system temperature. Both continuous-bleed orifices and airlocks were subject to plugging. The solution to this problem was eventually developed in the course of coal testing, and lay in quenching the ash-laden bleed gas to about 300 F while still in the pressurized regime and before the

sticky particles impacted interior surfaces. A water-cooled fluid bed accomplished the quenching; orifice plugging and downstream-of-orifice deposits were eliminated.

The sticky nature of the particulate in the hot gas also renders small (3 1/2-inch and 6-inch) inertial separators somewhat ineffective as cleanup devices, since they are susceptible to plugging. Cyclone separators alone, however, are inadequate for reducing exhaust loading sufficiently to permit long-term turbine operation, and some other device will be needed in order to provide a viable system. Based on subscale tests, a moving-bed granular filter shows promise for removing the preponderance of fine particulate inherent in the fluid-bed combustion process. A design was developed for the inlet screen of such a filter that effectively prevented buildup of deposition on the screen.

Corrosion of turbine materials was shown to impose no serious problems in operating with municipal solid waste.

Elemental aluminum is present in most solid wastes to a sufficient extent to cause serious deposition problems in the turbine; chemical additives were shown to have the capability of combining with the aluminum in solid compounds that can be removed in the filtration process. The additives also have the effect of converting to stable solids the alkali-metal salts that could pass through a granular filter in the vapor phase and condense to undesirable particulate downstream of the filter.

REFERENCES

1. Combustion Power Company, Inc. Final Report for Low Pressure Tests of the CPU-400 Pilot Plant. EPA Contract No. 68-03-0054 (unpublished). Menlo Park, California, 1974.
2. Combustion Power Company, Inc. Test Report for Weyerhaeuser Wood Waste Combustion Demonstration (unpublished). Menlo Park, California, 1974.
3. Combustion Power Company, Inc. Energy Conversion from Coal Utilizing CPU-400 Technology (FE-1536-30). ERDA Contract No. EX-76-C-01-1536. Menlo Park, California, 1977.
4. Combustion Power Company, Inc. PDU Granular Filter Design Report. Task GF-1 of EPA Contract No. 68-03-0143. Menlo Park, California, 1975.
5. Combustion Power Company, Inc. Structural Filter-Panel Failure and Redesign of the CPU-400 Pilot Plant Granular Filter. Prepared under Contract No. 68-03-0143 (unpublished). Menlo Park, California, 1976.
6. Leith, David, and William Licht. The Collection Efficiency of Cyclone Type Particle Collectors--a New Theoretical Approach. In: AIChE Symposium Series, Vol. 68, No. 126, 1972.
7. National Center for Resource Recovery, Inc. NCRR Bulletin, Vol. 5, No. 1. Washington, D.C. 1975. p.8.
8. Niesen, W.R., and A.F. Sarofim. Incinerator Air Pollution: Facts and Speculation. In: Proceedings of the 1970 National Incinerator Conference, Am. Soc. Mech. Engrs., Cincinnati, Ohio, 1970. p. 174.
9. Combustion Power Company, Inc. CPU-400 Systems Studies and Preliminary Design. Task SS-10 of EPA Contract No. 68-03-0143, (unpublished), Menlo Park, California, 1975.

CONVERSION TABLE

To convert	Into	Multiply by.....
in.	mm	25.40
in ²	mm ²	645.2
in ³	cc	16.39
ft	m	.3048
ft ²	m ²	.0929
ft ³	m ³	.02832
lb	kg	.4536
tons	kg	907.2
hp	hp (metric)	1.014
IW	mm Hg	1.868
psi (lb/in ²)	kg/m ²	703.1
gpm (gal/min)	l/sec	.06308
Btu/lb	kJ/kg	2.326
gr/ft ³	g/m ³	2.288
lb/10 ⁶ Btu	g/k-cal	1800
Temp, F	Temp, C	C=(F-32)/1.8

